SEDIMENTY

Glacigenní sedimenty

Původ glaciálního ledu

- Největší zdroj ledu: sníh
  - Snow to firn to ice
  - Influence of snow type and locale
- (Milankovic: Chladná léta podporují rust ledu)

Typy ledovců

- **Icesheet (ledový příkrov)**: large **continental ice mass** that does not cover the whole area within its borders
- **Icecap (ledový pokryv)**: **almost continental in size**, but nothing projects above ice
- **Icefields & valley glaciers (ledová pole a údolní ledovce)**: icefields found in high mountains, with **large valley glaciers** spilling from them
- **Mountain glaciers**: small ice masses, **cirque glaciers (karové ledovce)**

Kontinentální ledovec

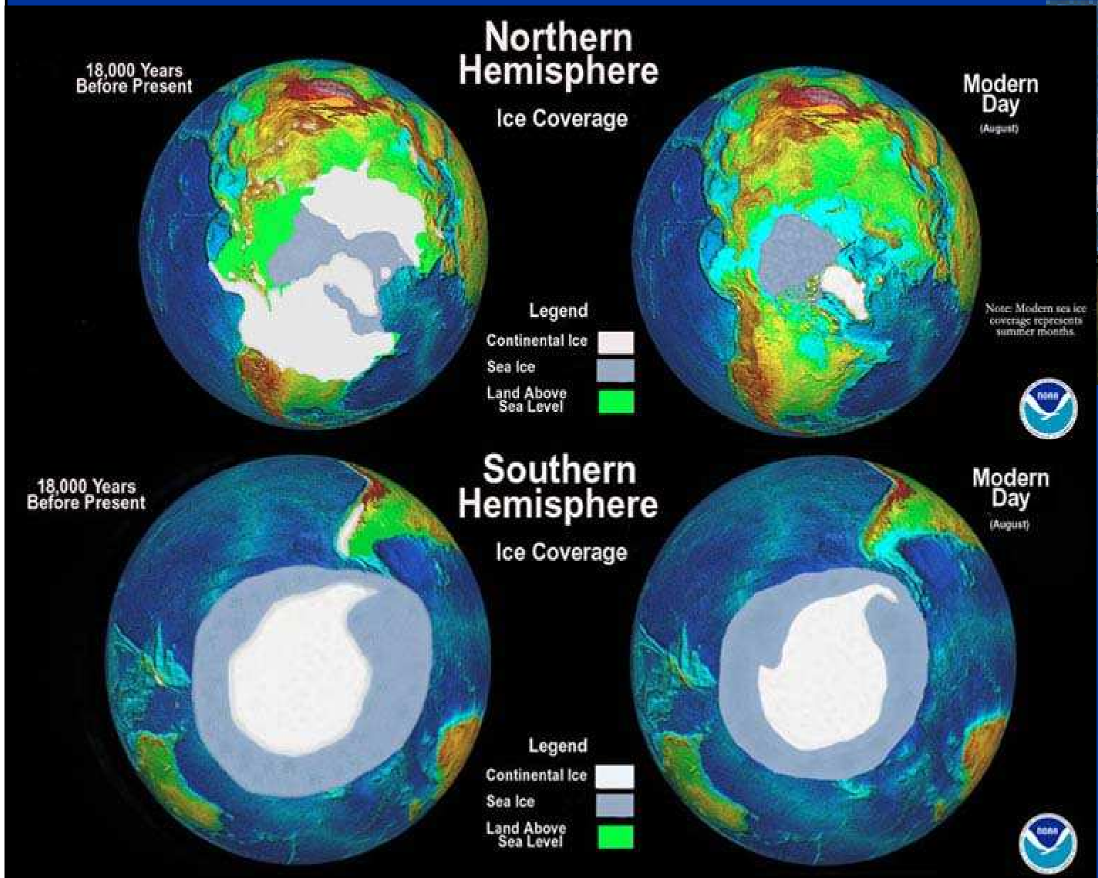

Kontinentální zalednění: morfologie

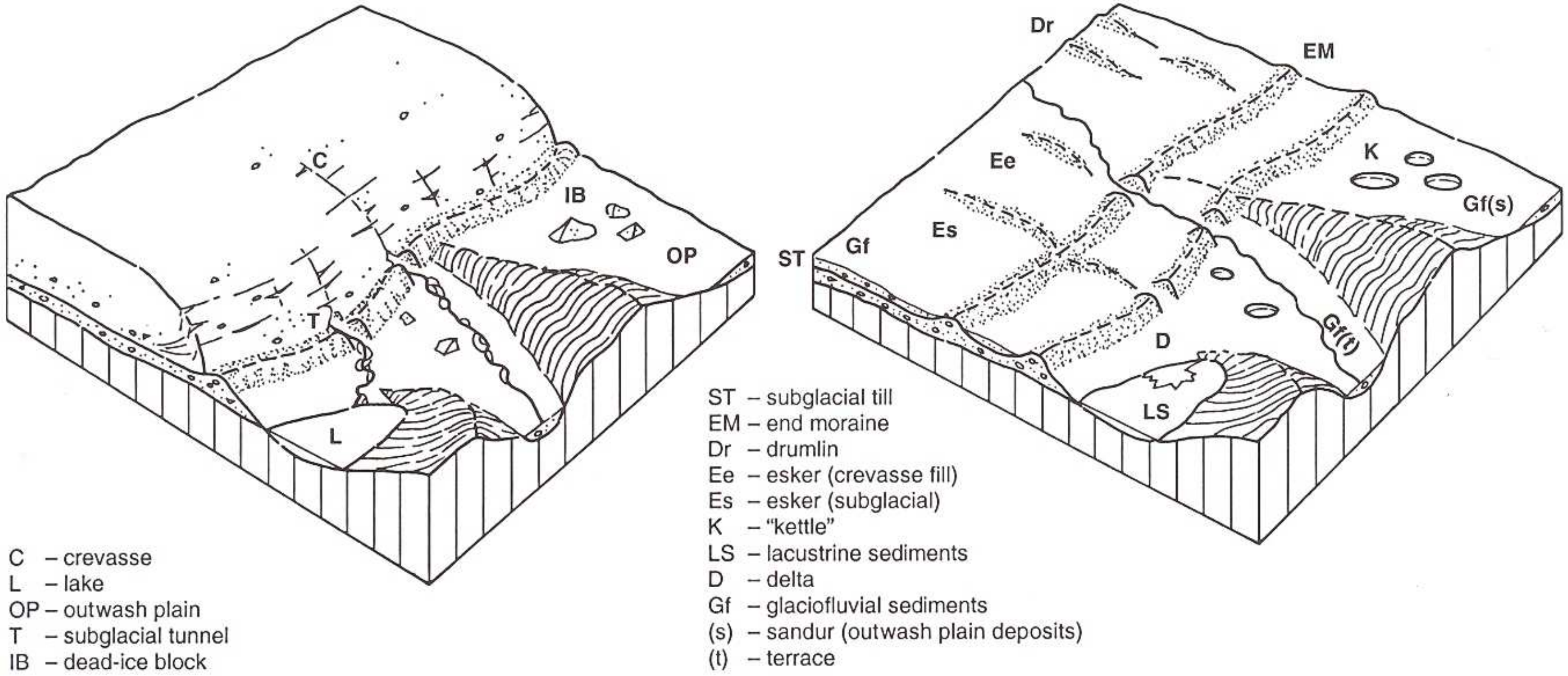

Figure 13. Block-diagram showing the topography of ice-sheet margin, proglacial environment and the resulting sediments (after FAIRBRIDGE 1968).

výplavová planina (sandur) – mírně ukloněná planina tvořená glaciofluviálními uloženinami v předpolí pevninského ledovce; vzniká splynutím plochých náplavových kuželů ledovcových toků

kotle (kettles) – okrouhlé deprese zpravidla vyplněné vodou; vznikají roztáním mrtvého ledu pohřbeného v gaciofluviálních sediementech

eskery = přímé nebo klikaté valy vznikající fluviální sedimentací v ledovcových tunelech

drumlin = oválný pahorek tvaru obrácené kávové lžičky; drumliny vznikaly při pohybu ledovce nahrnutím tillu

till = nevrstevnatá směs ledovcového materiálu obsahující všechny zrnitostní frakce od balvanů až po jíl

moréna = akumulace horninového materiálu deponovaná při okrajích ledovce

boční moréna, koncová (terminální) moréna, spodní moréna

Tvary kontinentálního zalednění

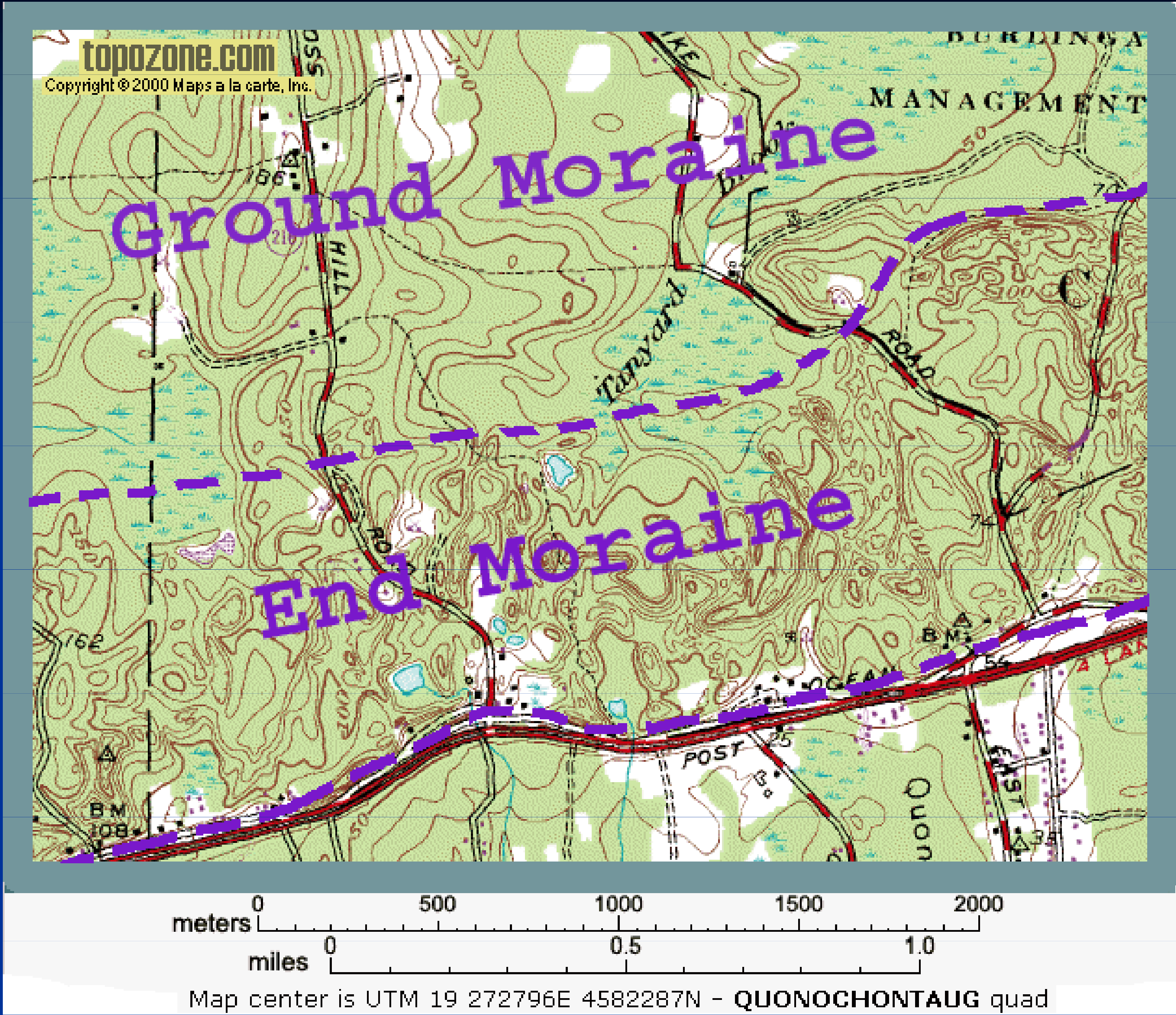
topozone.com
Copyright © 2000 Maps a la carte, Inc.
Ground Moraine
End Moraine
MANAGEMENT
Tanyard
ROAD
HILL
POST
Quon
EAST
OCEAN
B M
108
162
186
meters
0
500
1000
1500
2000
miles
0
0.5
1.0
Map center is UTM 19 272796E 4582287N - **QUONOCHONTAUG** quad

Kontinentální zalednění v ČR

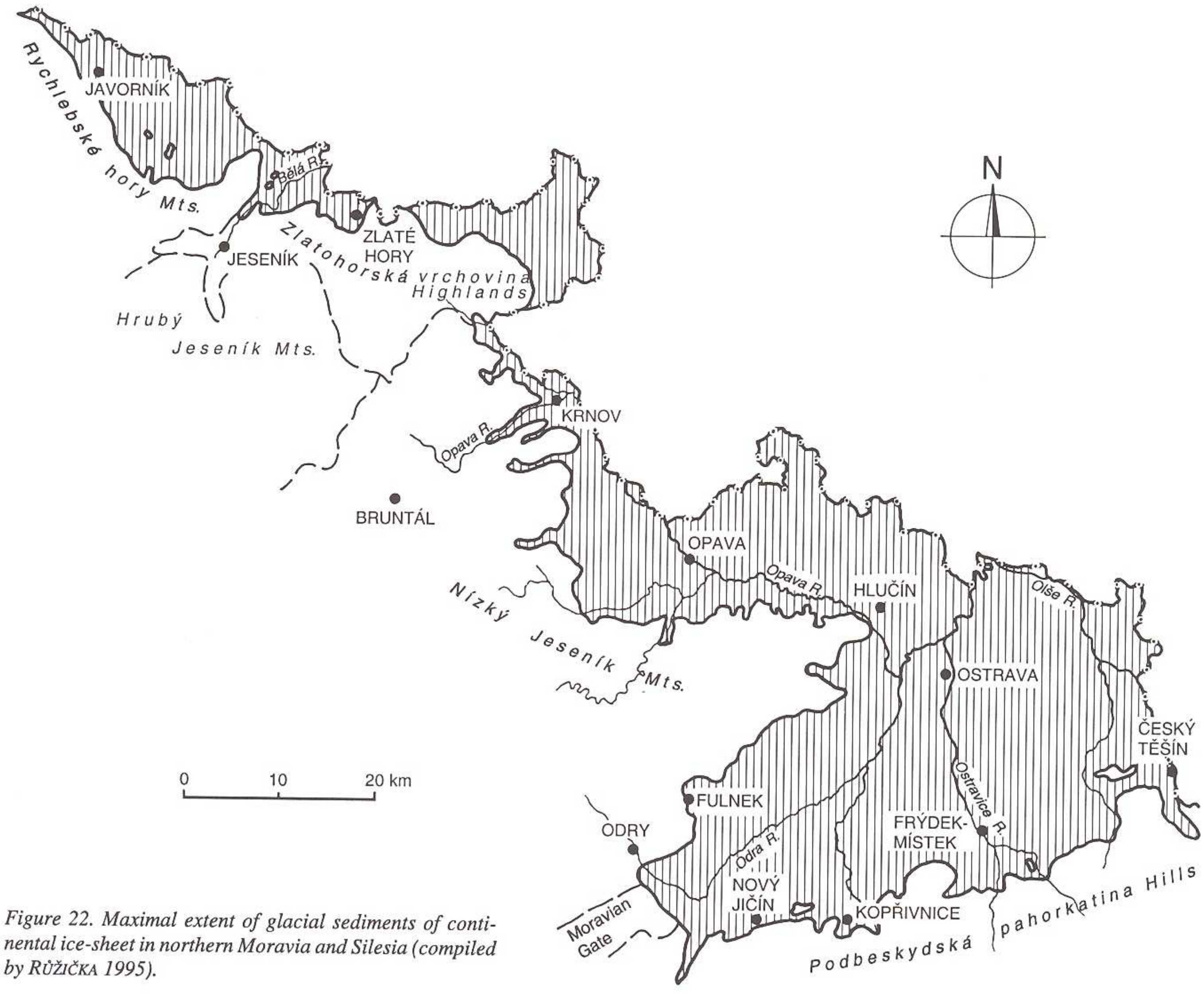

Figure 22. Maximal extent of glacial sediments of continental ice-sheet in northern Moravia and Silesia (compiled by Růžička 1995).

Kontinentální zalednění v ČR

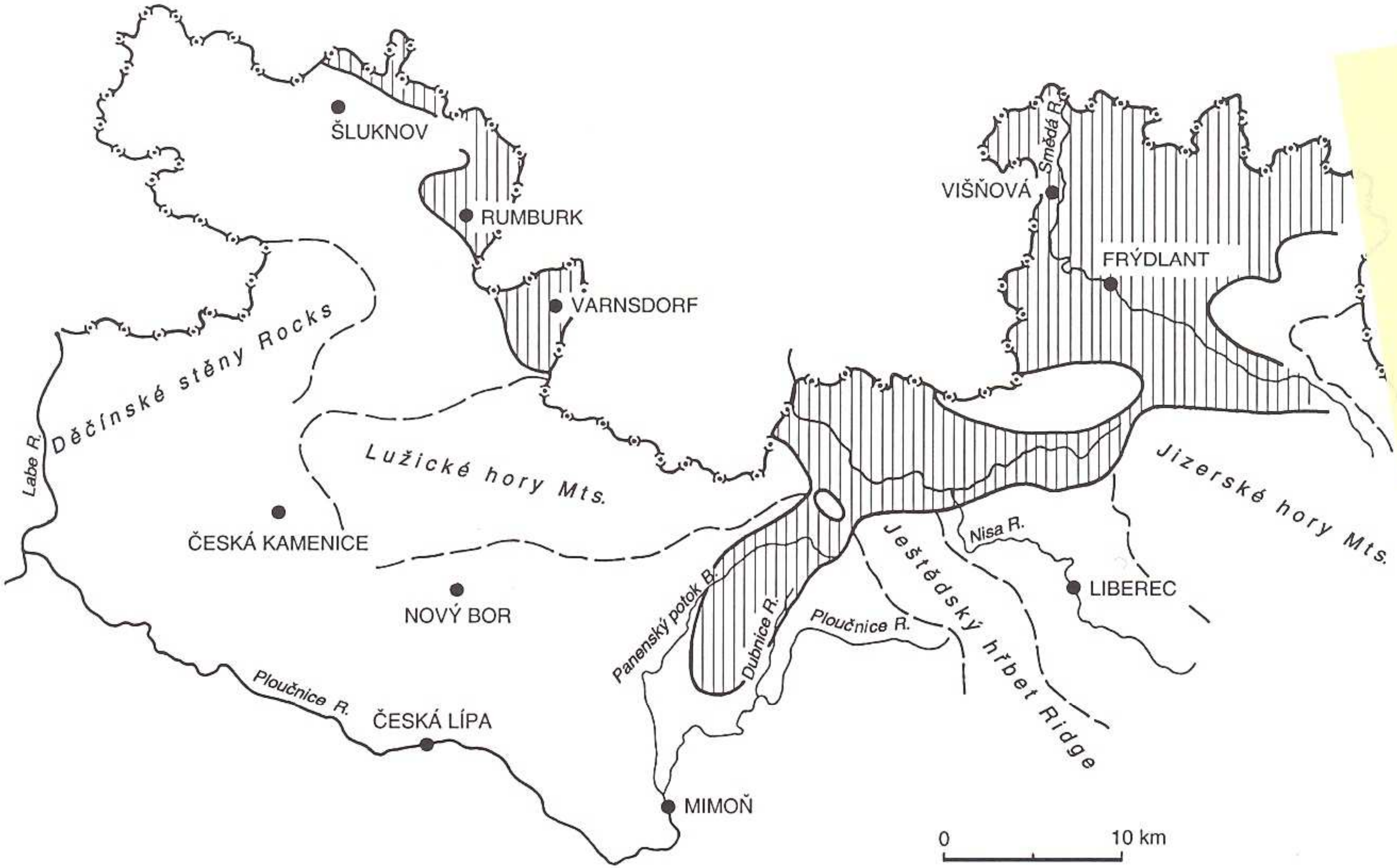

Figure 23. Maximal extent of glacial sediments of continental ice-sheet in northern Bohemia (after KRÁLÍK 1989, supplemented and modified by M. Růžička).

Horské zalednění: hlavní rysy

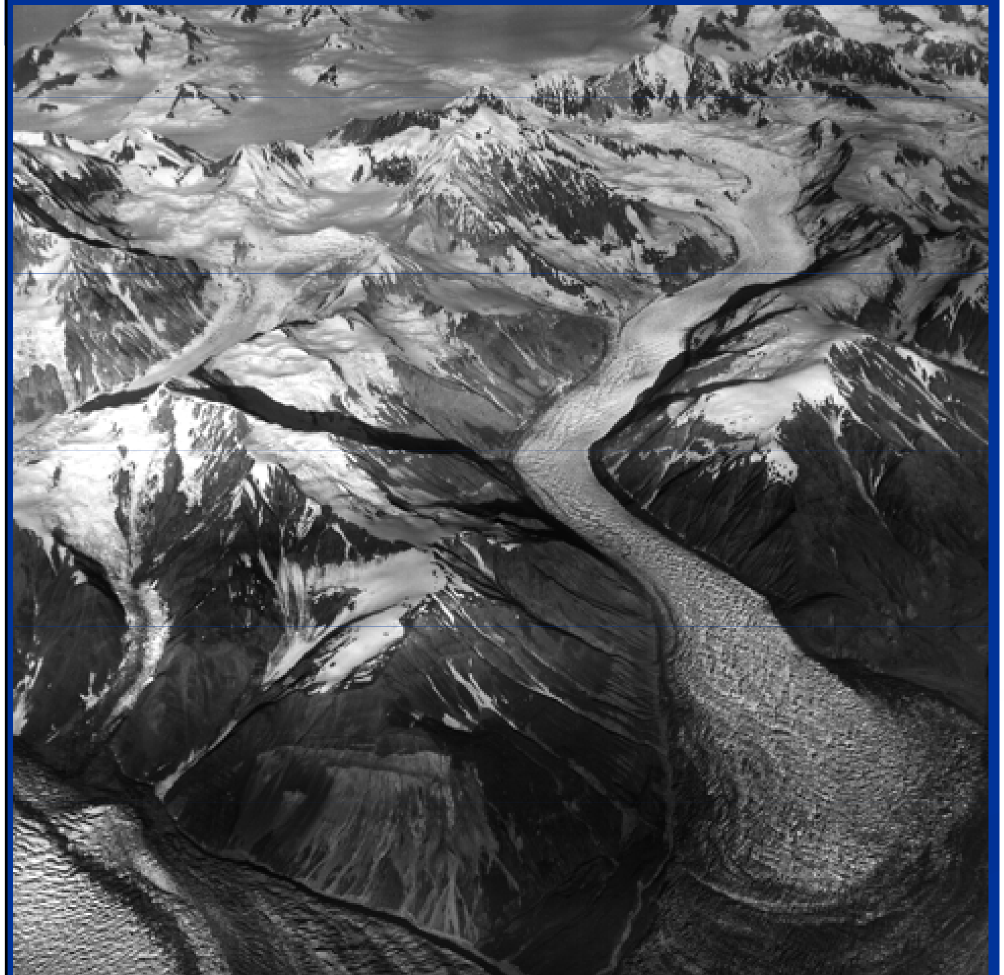

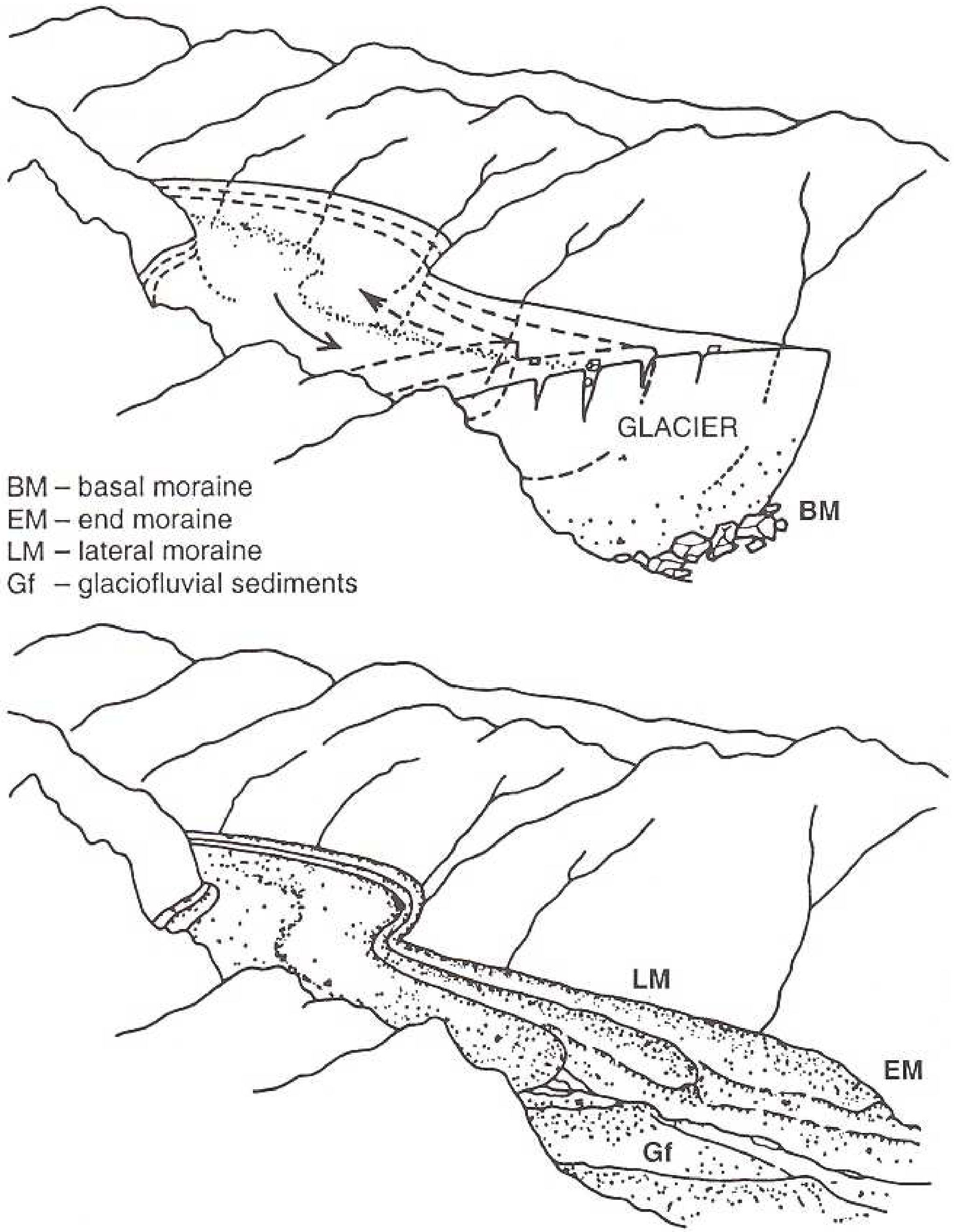

Figure 14. The morphology of a valley glacier and its deposits (schematic representation).

Horské zalednění

horn = ostrý vrchol který vznikl na kontaktu tří nebo více karů

kar = zdrojová oblast ledovce; amfiteatrální sníženina vzniklá přetvořením údolního uzávěru mrazovým zvětráváním a činností

ledovce

arête = úzký rozeklaný hřbet který vznikl protnutím svahů dvou karů

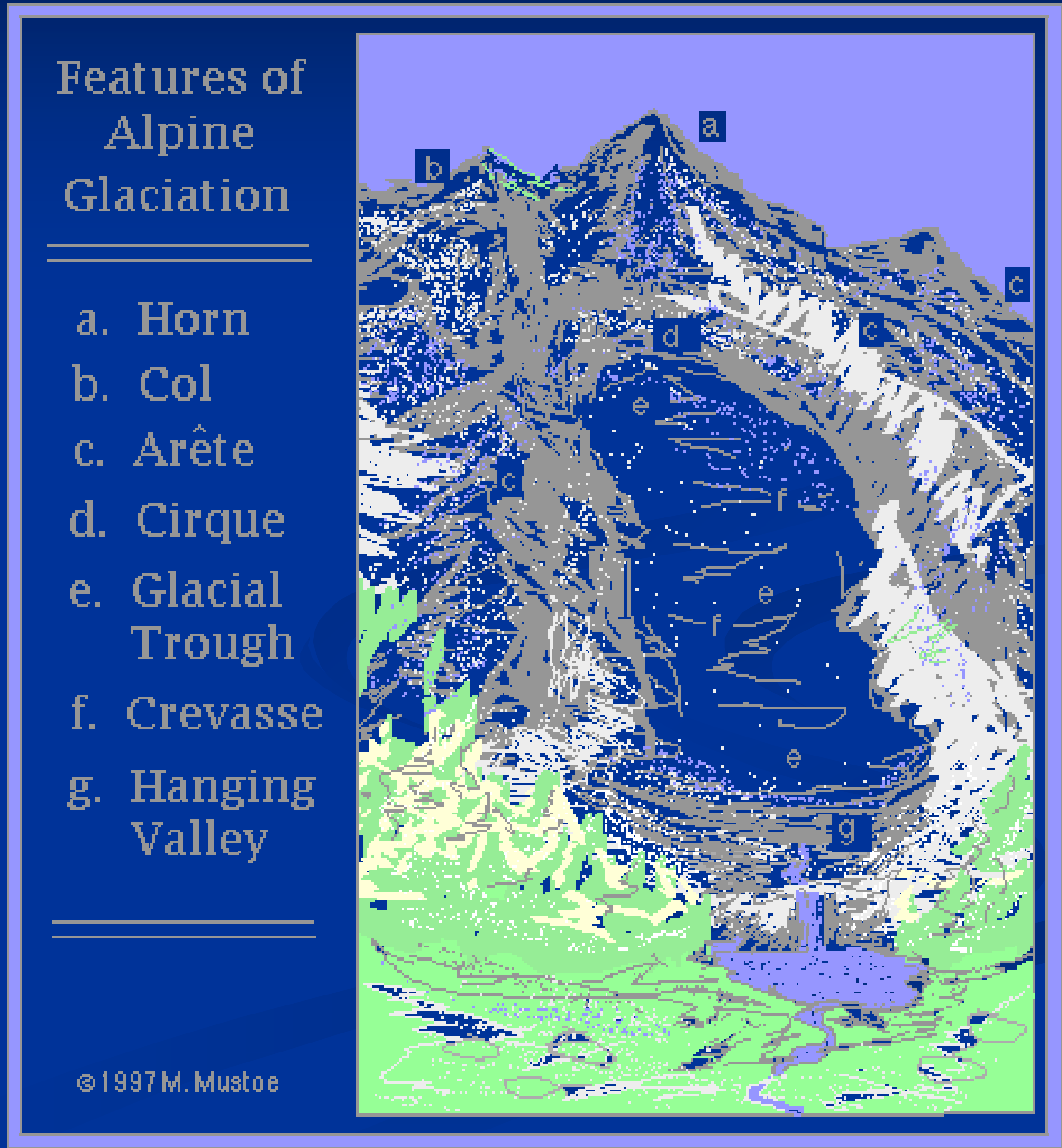

Tvary horského zalednění

Horn: Matterhorn

Údolí tvaru U

Morény

- Laguna Torre, morénové jezero

Morény

Alpine Glaciers

- Glacier fluctuations provide information about past climate change.
- Glacier fluctuations depend on ice movement and ice mass balance: increased net accumulation leads to glacier advancement.
- Ice mass balance depends on rates of snow accumulation and ablation (removal of snow via melting, evaporation, sublimation, avalanching or wind deflation).

Alpine Glaciers (cont.)

- The equilibrium-line altitude (ELA) marks the area where accumulation equals ablation.
- ELA responds to changes in winter precipitation, summer temperature, and wind's strength.
- Climate has a strong effect on modern ELA.

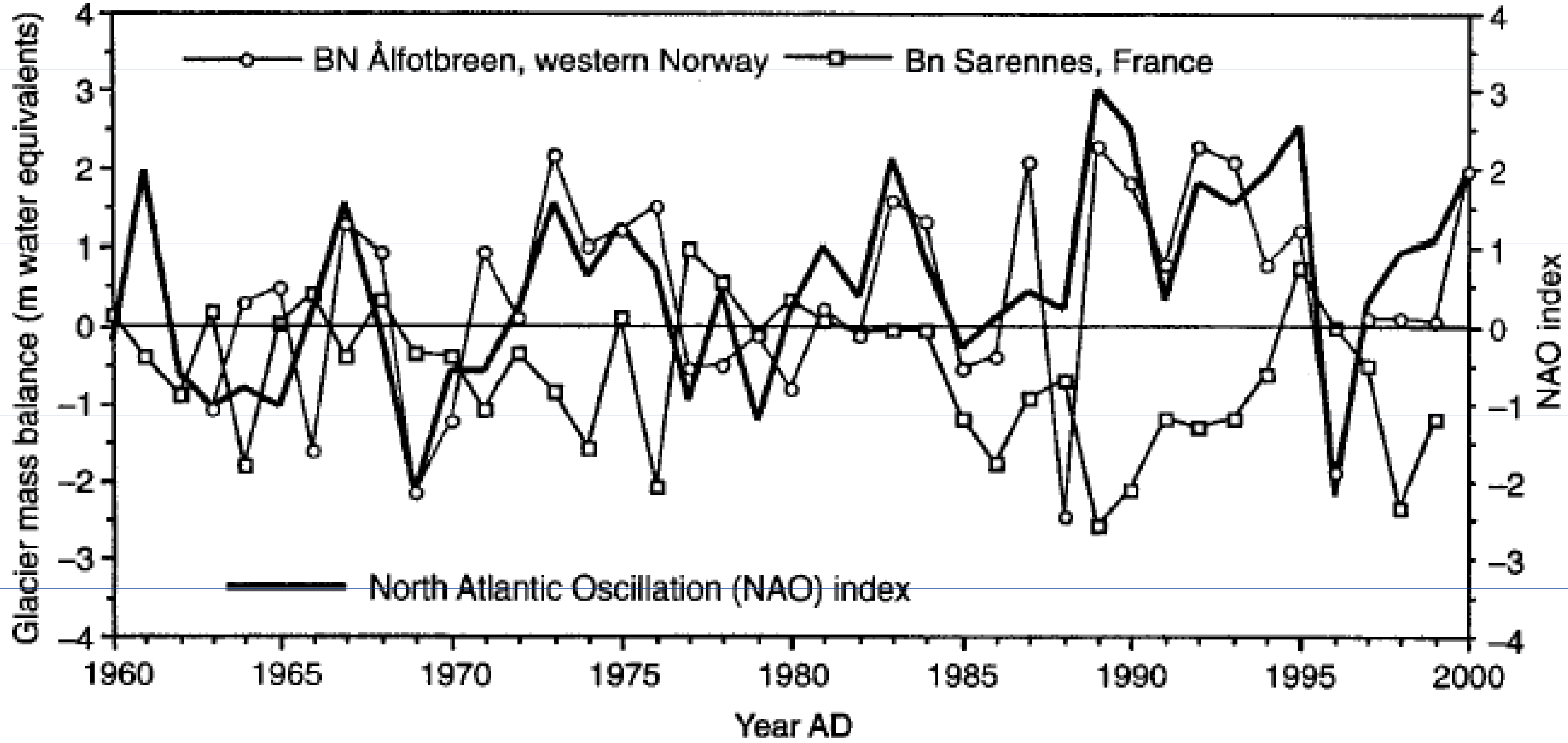

Figure 18.5 The annual net mass balance of Ålfotbreen, western Norway (data: Kjøllmoen 1998 with later updates), annual net mass balance of Sarennes Glacier in SE France (data: World Glacier Monitoring Service) and the North Atlantic Oscillation index (Jones *et al.*, 1996 with later updates).

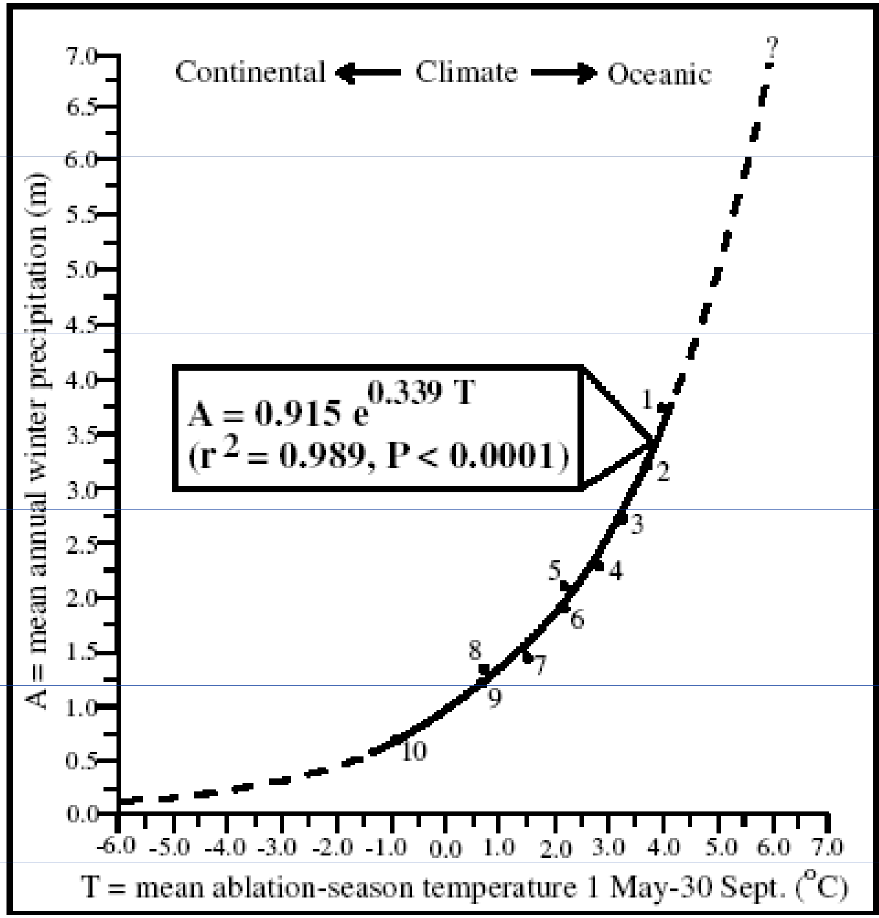

Figure 2 The non-linear (exponential) relationship between mean ablation-season temperature (1 May to 30 September) and winter precipitation (1 October to 30 April) at ELAs of 10 Norwegian glaciers: (1) Ålfotbreen; (2) Engabreen; (3) Folgefonna; (4) Nigardsbreen; (5) Tunsbergdalsbreen; (6) Hardangerjøkulen; (7) Storbreen; (8) Austre Memurubreen; (9) Hellstugubreen; (10) Gråsubreen. After Dahl *et al.* (1997).

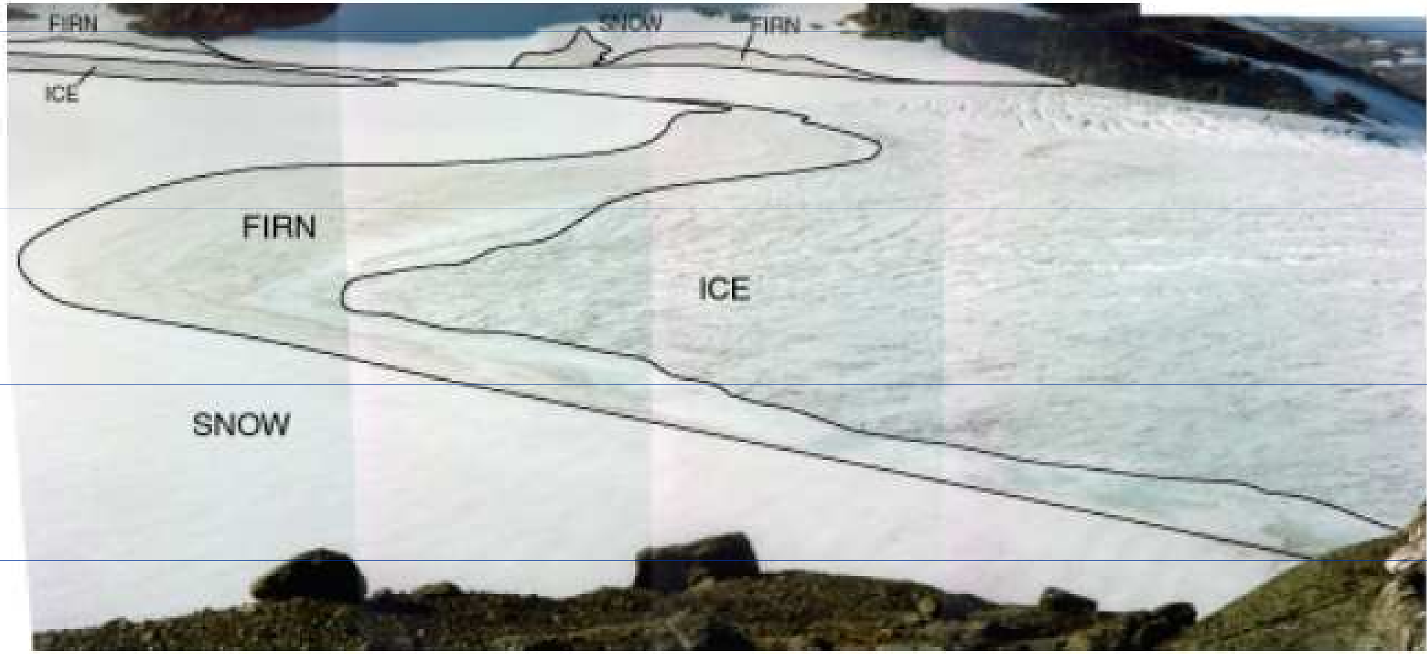

Figure 5: *A photography from August 1995 showing snow and firn line of Austre Okstindbreen at around 1250 metres elevation. The location and view direction of this photo is marked in Figure 3. The flow direction is to the right and crevasses can be seen. The firn line follows the same shape as the 1250-metre line. The snow line, which was located at 1250 metres in August 1995, was much higher at about 1300 metres in August 1994, i.e. the year represented by Figure 3.*

Reconstruction of paleo-ELA

- Paleo-ELA= maximum elevation of lateral moraines.
- Theoretically, deposition of lateral moraines only occurs in the ablation zone.

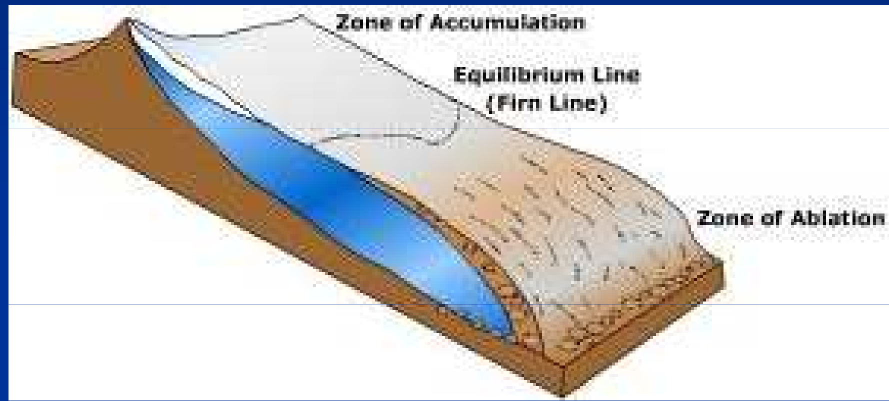

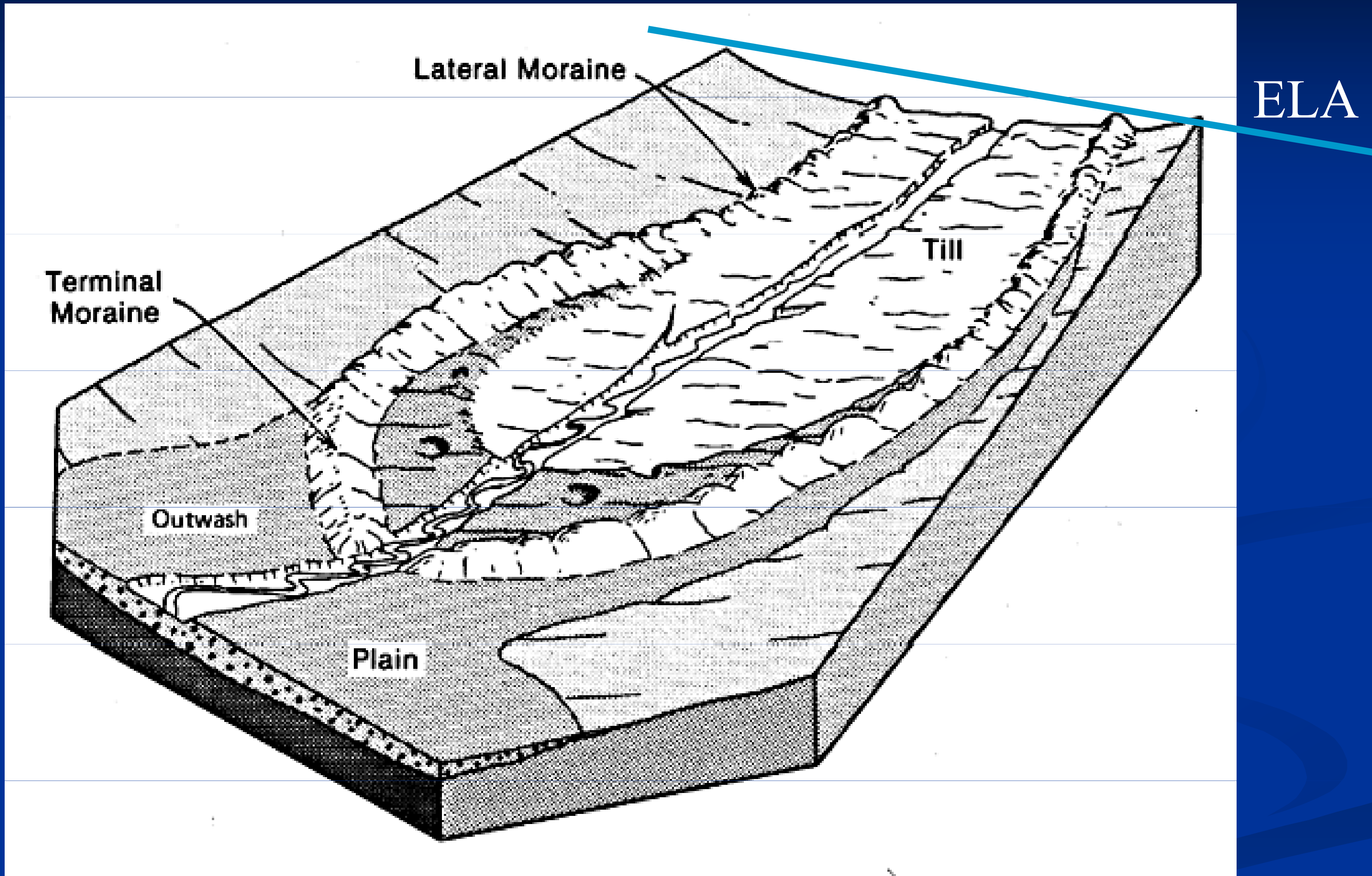
Lateral Moraine
ELA
Till
Terminal Moraine
Outwash
Plain

Photographs or field evidence are used to reconstruct lateral moraines and their maximum elevations.

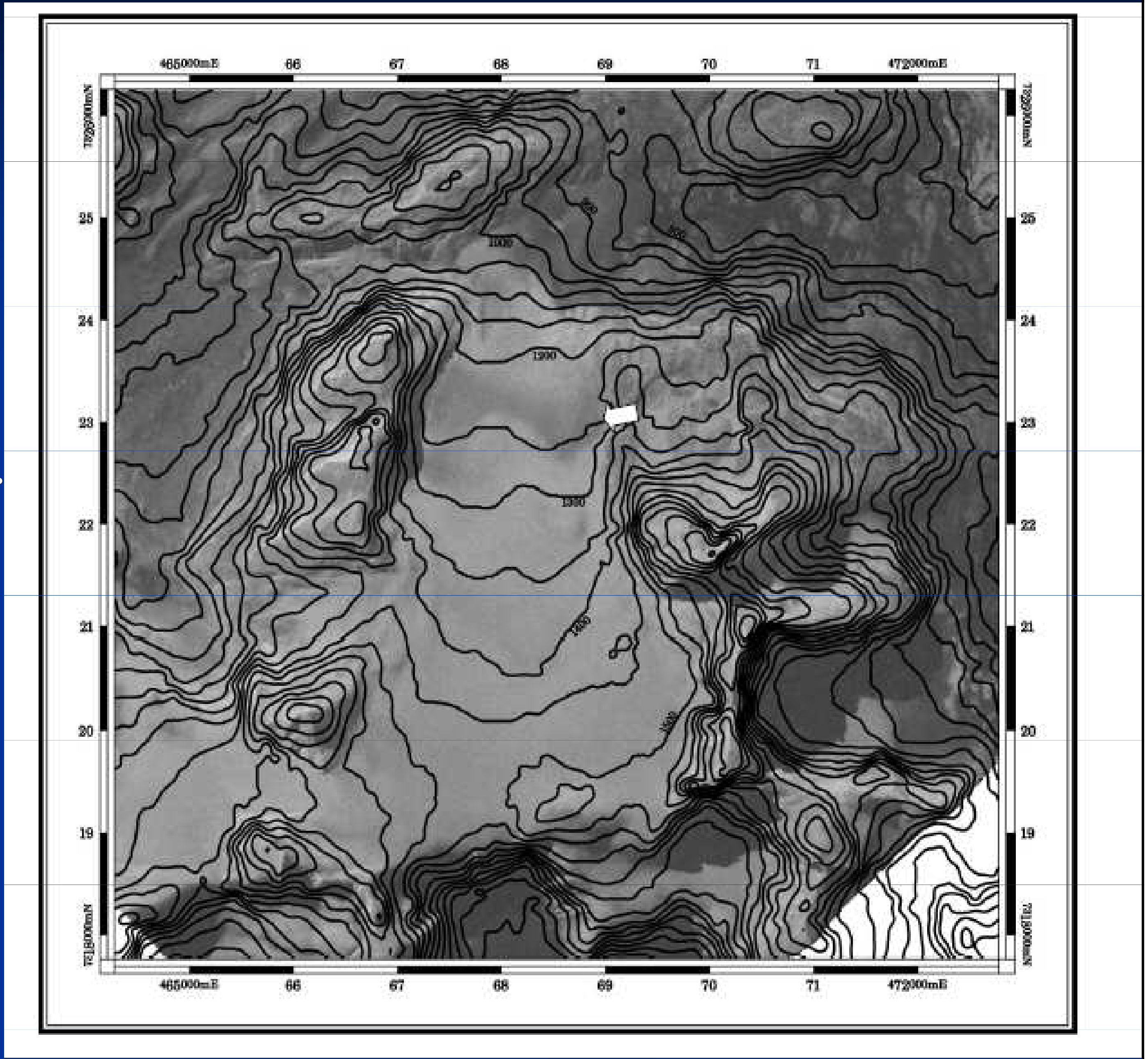

ELA- based paleoclimatic reconstructions

- ELAs provide information on temperature and precipitation.
- However, there is a time lag or response time (short for steep, fast-flowing glaciers).
- Response time is the time a glacier takes to adjust to a change in mass balance.
- Response time for alpine glaciers ranges from tens to hundreds of years.

Dating of moraines

- Radiocarbon ages. However, it takes some time for organic matter to accumulate on the moraines.
- Lichenometry. However, the reliability of this technique is uncertain.
- Cosmogenic isotopes. Relatively new technique.

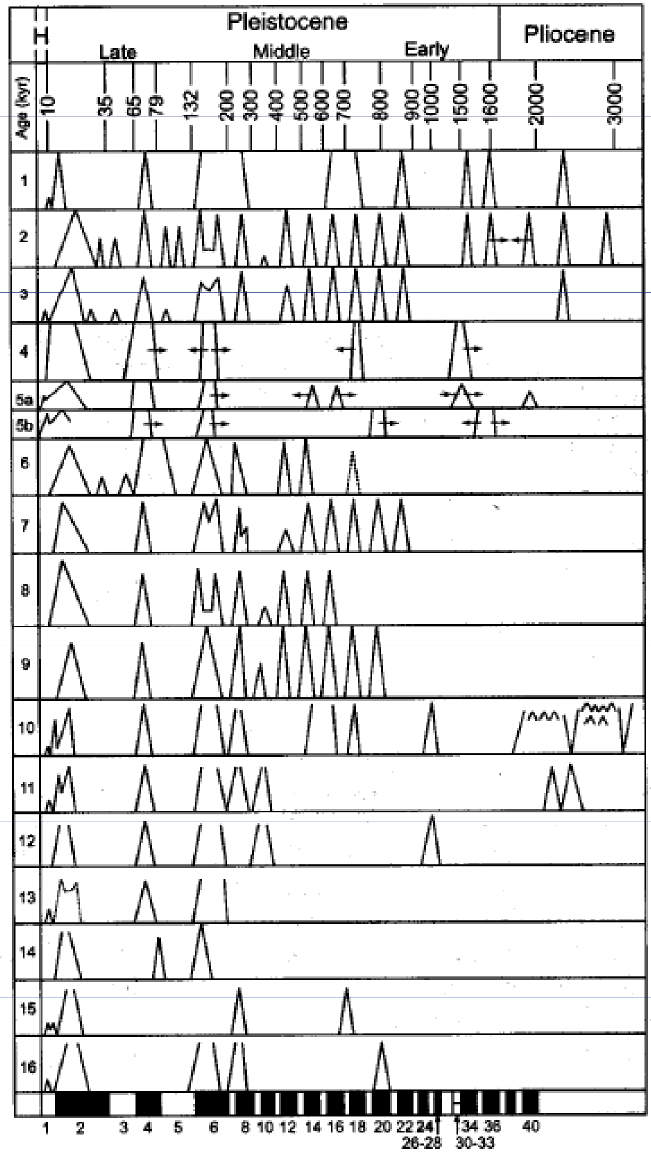

FIGURE 7.15 Summary diagram showing the principal episodes of glaciation in the northern and southern hemispheres over the past ~3 M years based on glacial geologic studies in the various regions indicated. Ice advances are indicated schematically by an upward pointing triangle, the relative dimensions of which signify the magnitude of each ice advance. Note that timescale (shown at top) is nonlinear; marine oxygen isotope stages are indicated at bottom with even-numbered stages (times of major ice accumulation on the continents) shaded (however, note that not all such stages are equal in magnitude — see section 6.3.2). Arrows indicate dating uncertainties; in spite of these, numerous episodes of globally significant ice advances are clearly identifiable. 1 = U.S. Cordilleran ice sheet; 2 = U.S. mountain glaciers; 3 = U.S. Laurentide ice sheet; 4 = Canadian Cordilleran ice sheet; 5 = Canadian Laurentide ice sheet (a = SW margin, b = NW margin); 6 = N.E. Russia; 7 = Poland/western (former) Soviet Union; 8 = N.W. Europe; 9 = European Alps; 10 = Southern Andes; 11 = New Zealand; 12 = Tasmania; 13 = Southern Ocean and sub-Antarctica; 14 = Antarctica (Ross Embayment); 15 = New Guinea; 16 = E. Africa (simplified from charts accompanying Bowen *et al.*, 1986; Clapperton, 1990).

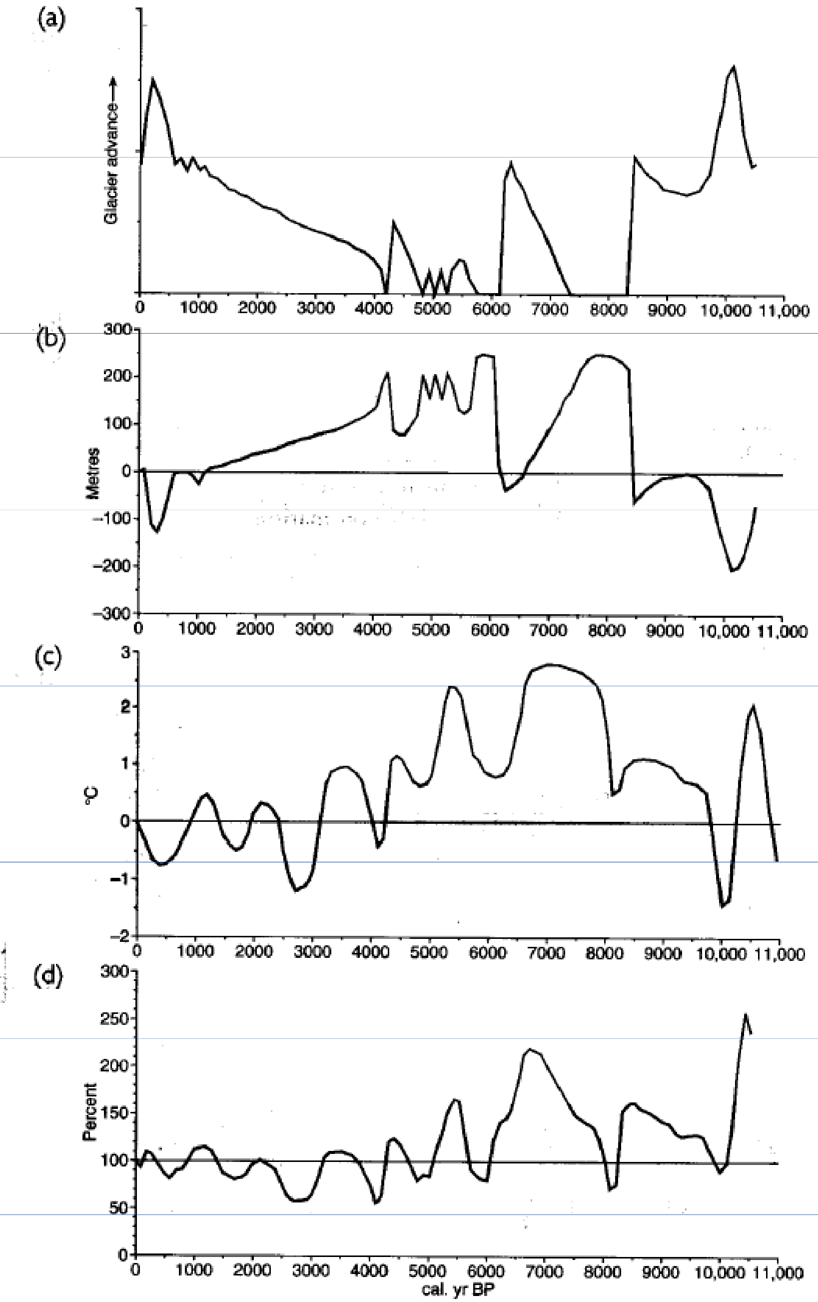

Figure 18.4 (a) Holocene glacier variations of Hardangerjøkulen (Dahl and Nesje, 1994); (b) Holocene equilibrium-line altitude (ELA) variations at Hardangerjøkulen (Dahl and Nesje, 1996); (c) Holocene July temperature variations based on chironomids (non-biting midges) from lake sediments at Finse north of Hardangerjøkulen (Velle, 1998). Due to poor age control in the upper part, the curve has been tuned towards a pine-tree curve for southern Norway (Lie *et al.*, unpublished); (d) Holocene variations in winter precipitation (in per cent, 100 per cent = 1961–1990 normal) in the Hardangerjøkulen area (Dahl *et al.*, unpublished data).

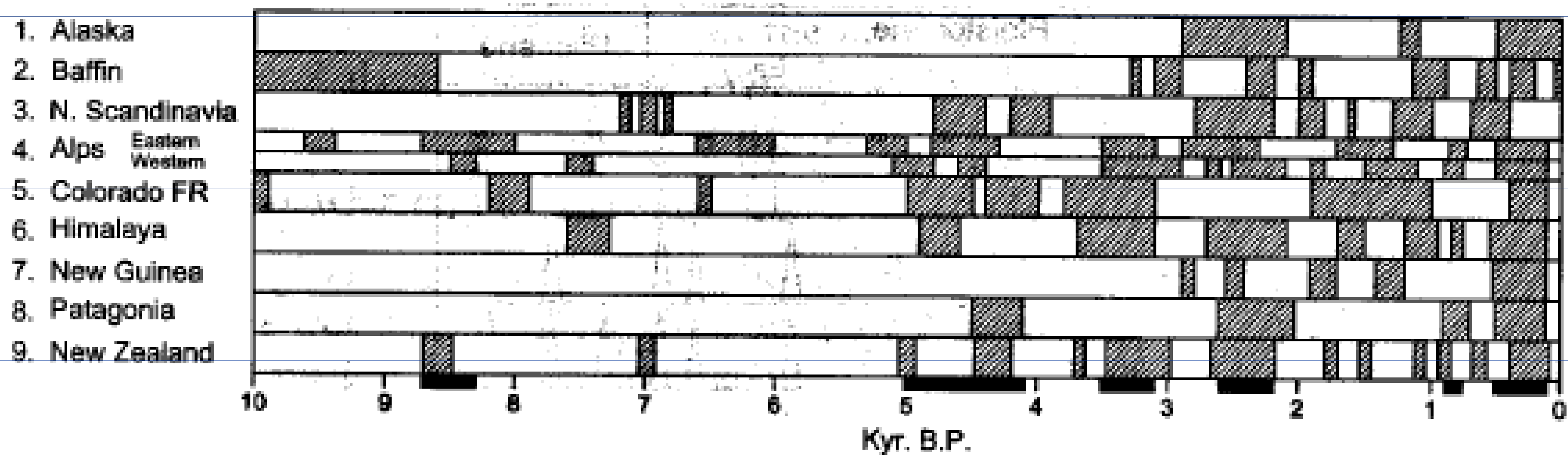

FIGURE 7.16 Summary of glacier expansion phases in different areas of the world during the Holocene. This compilation shows the complexity of the records and the difficulty of discerning worldwide synchronous episodes on this timescale (possible times of widespread advances are indicated by black bars at bottom of figure). This difficulty may be due to climatic fluctuations that are regional, not hemispheric or global in extent, or to poor dating, or to problems inherent in a discontinuous and incomplete data set. A general absence of glacier advances in the early to mid-Holocene is apparent, as is the onset of Neoglaciation after ~5000 yr B.P. (Grove, 1988).

Importance of records from alpine glacier

- Glacier fluctuations contribute information on how rapid climate change occurs and the the range of these changes.
- ELAs have changed considerably at many timescales: glacial/interglacial, millennial (Holocene), and seasonal.
- ELAs of most modern alpine glaciers have shifted upwards during the 20th century.

Horské zalednění v ČR

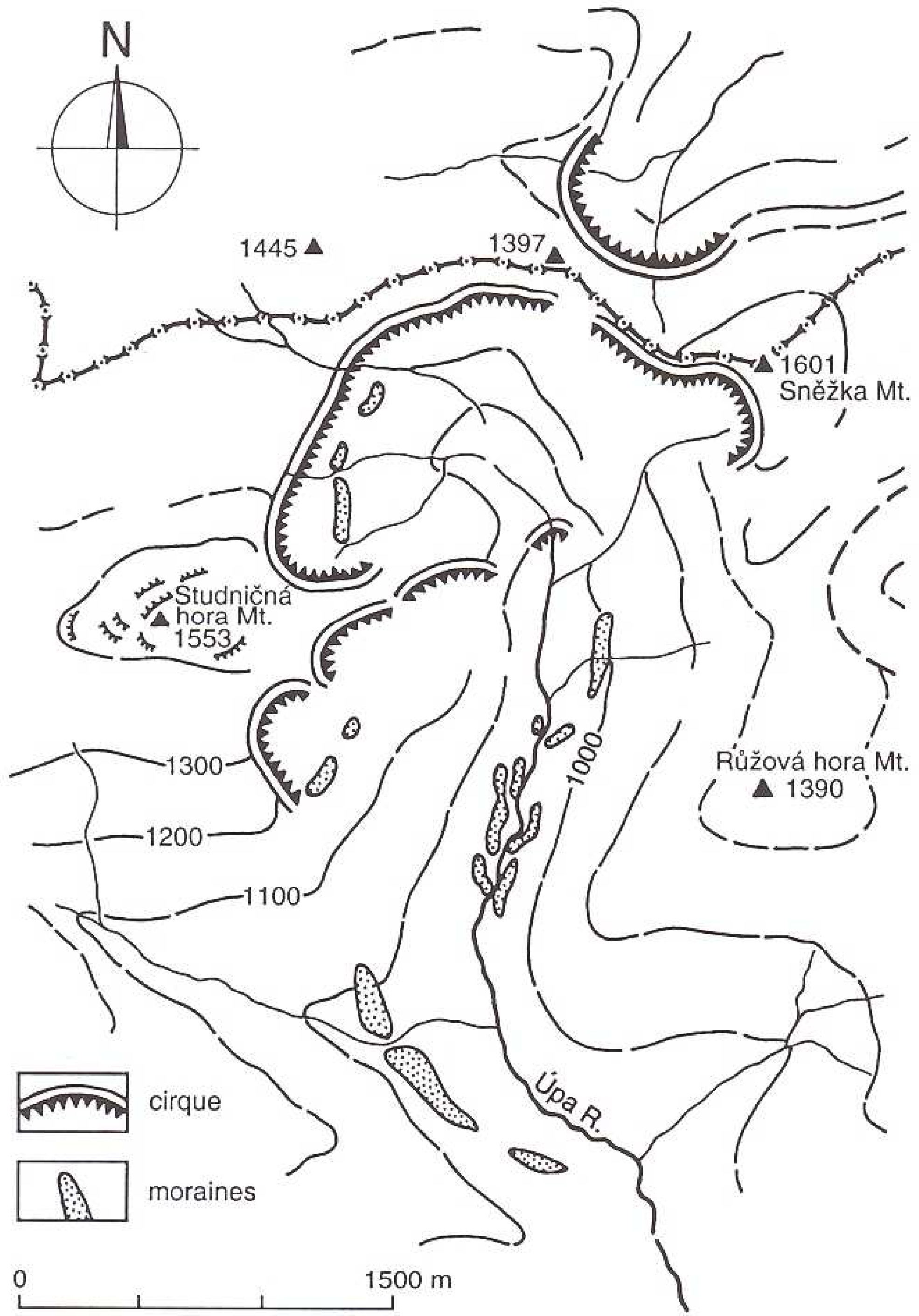

Figure 20. Cirques and valley glacier moraines in Úpa valley, Krkonoše Mts. (KUNSKÝ 1948, modified).

Glaciální transport

- **Subglaciální**

  -rounded & flattened

  -most materials comminuted to very small terminal grades if transported long distances
- **Englaciální**

  -can be transported long distances
- **Superglaciální**

  -broken down by freeze-thaw in angular blocky fragments

Glaciální depozice

- *till* = nevrstevnatá směs ledovcového materiálu obsahující všechny zrnitostní frakce od balvanů až po jíl
- bazální: basal or lodgement till

  -compact, generally fine-grained material
- englaciální: till or outwash
- superglaciální

  -ablační till

  --coarse-grained

  -outwash: generally sandy to coarse material

Facie glacigenních sedimentů

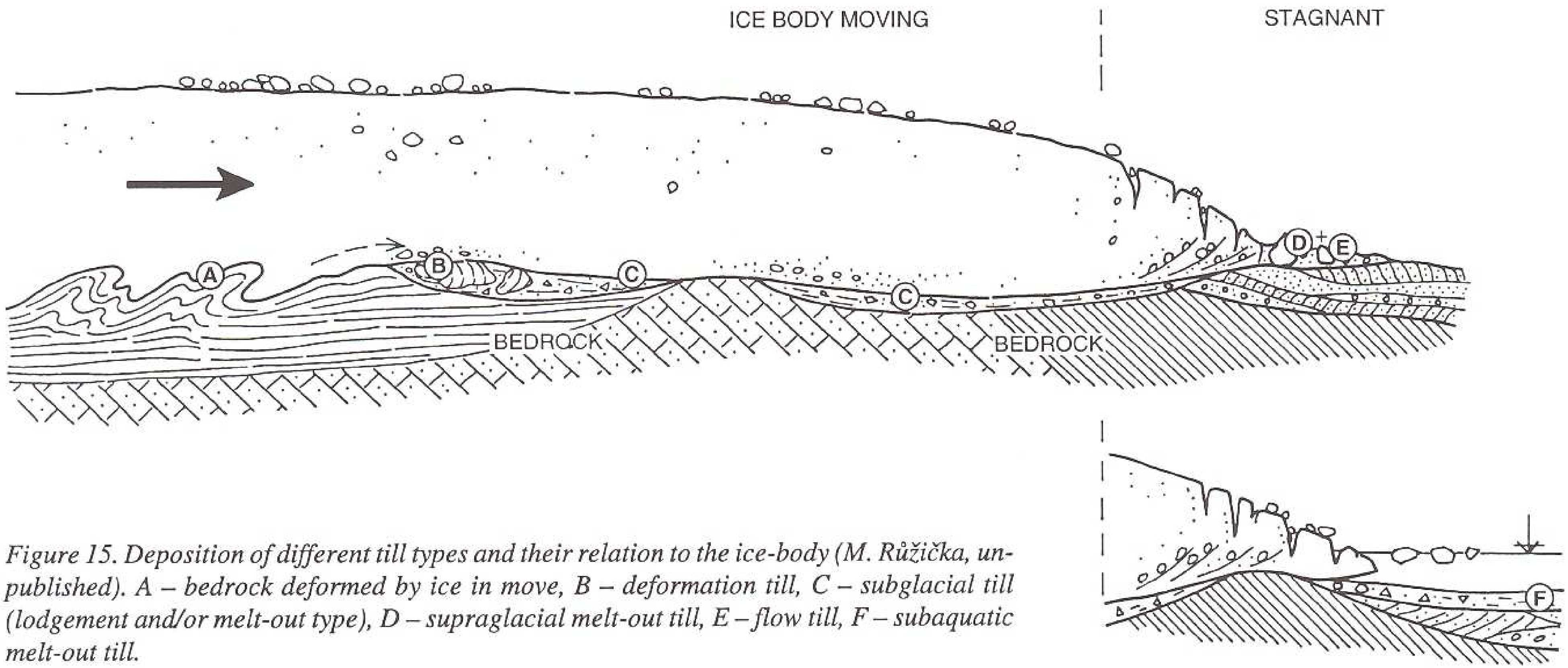

Figure 15. Deposition of different till types and their relation to the ice-body (M. Růžička, unpublished). A – bedrock deformed by ice in move, B – deformation till, C – subglacial till (lodgement and/or melt-out type), D – supraglacial melt-out till, E – flow till, F – subaquatic melt-out till.

Faciální model kontinentálních glacigenních sedimenů

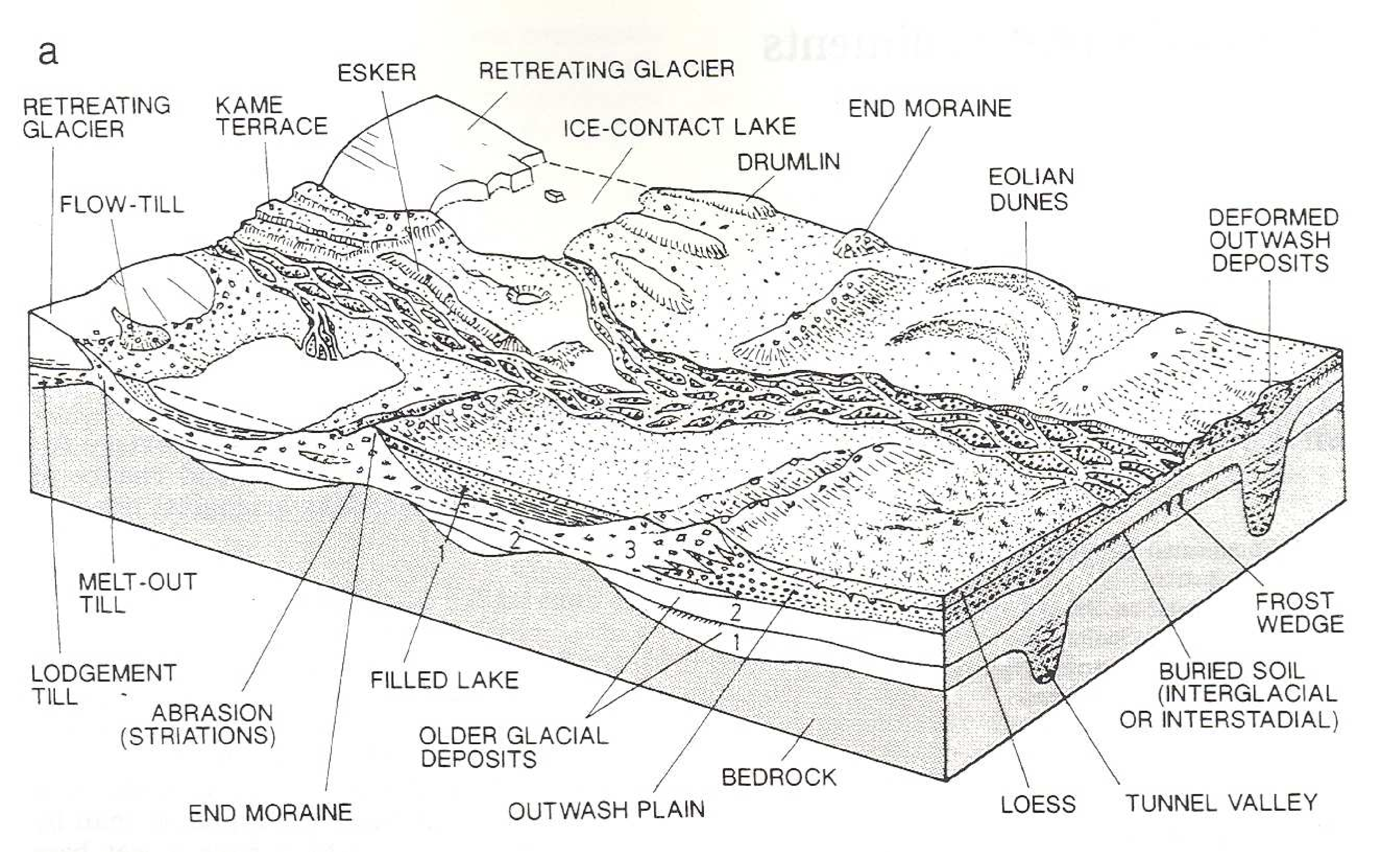

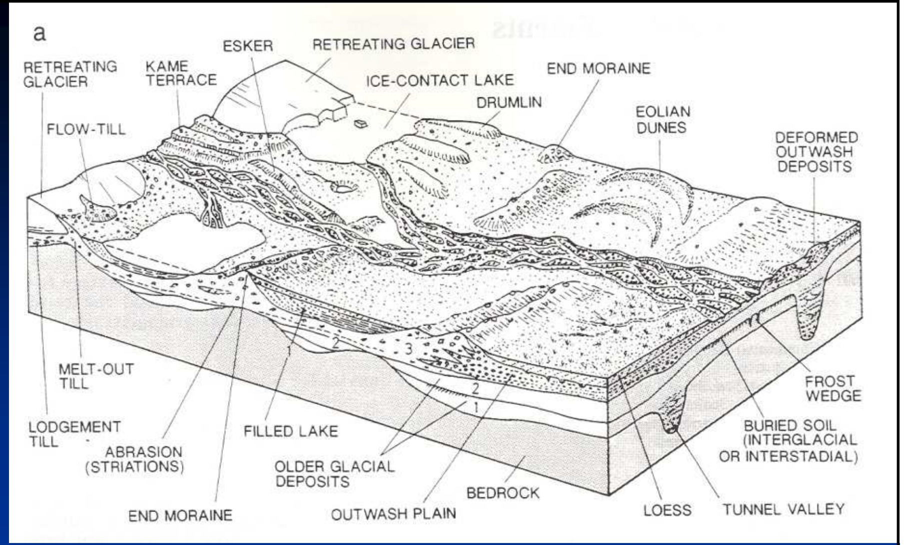
a
RETREATING GLACIER
KAME TERRACE
ESKER
RETREATING GLACIER
ICE-CONTACT LAKE
END MORAINE
DRUMLIN
EOLIAN DUNES
DEFORMED OUTWASH DEPOSITS
FLOW-TILL
MELT-OUT TILL
LODGEMENT TILL
ABRASION (STRIATIONS)
FILLED LAKE
OLDER GLACIAL DEPOSITS
FROST WEDGE
BURIED SOIL (INTERGLACIAL OR INTERSTADIAL)
BEDROCK
END MORAINE
OUTWASH PLAIN
LOESS
TUNNEL VALLEY

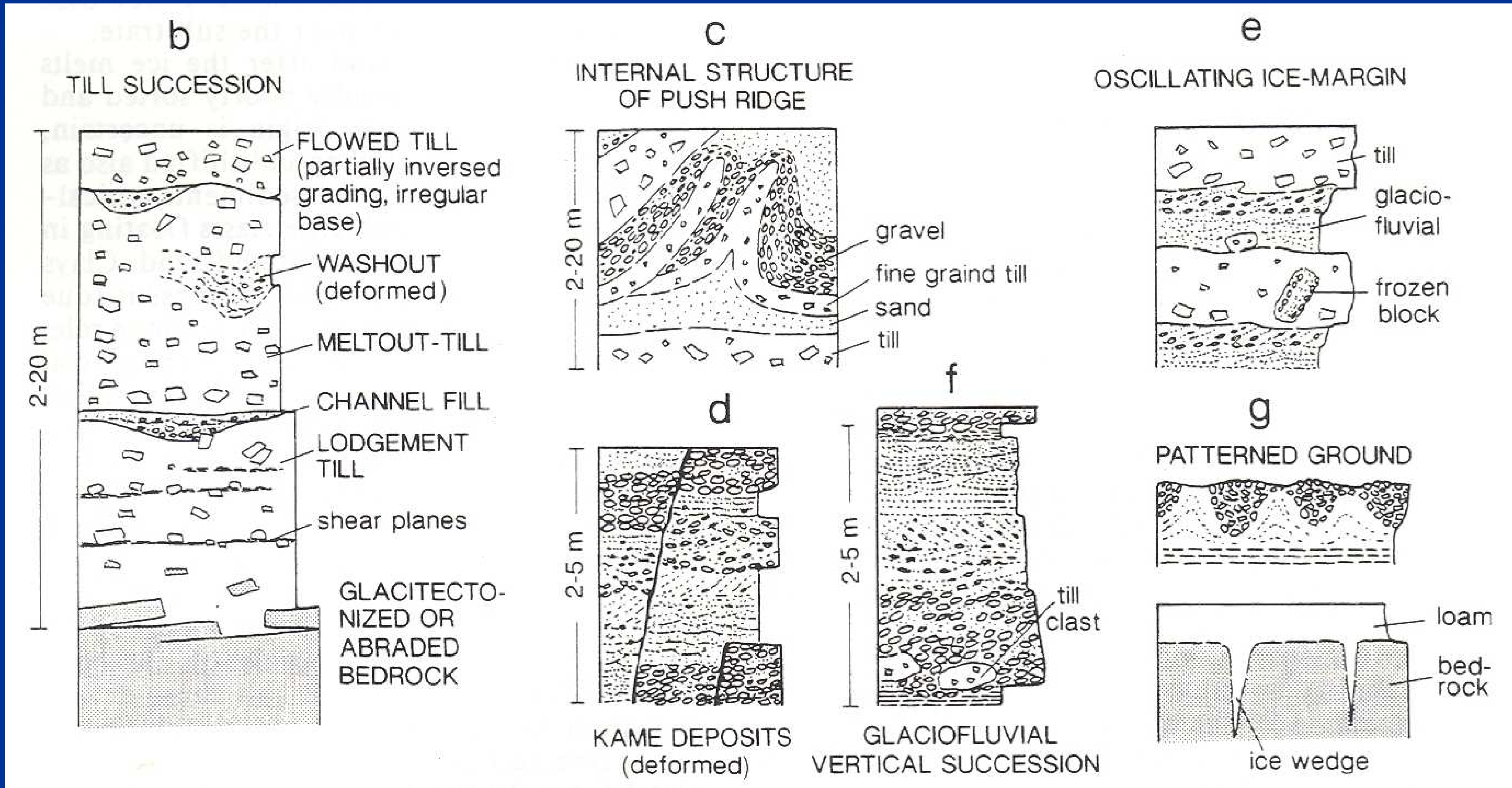
b
TILL SUCCESSION
2-20 m
FLOWED TILL (partially inversed grading, irregular base)
WASHOUT (deformed)
MELTOUT-TILL
CHANNEL FILL
LODGEMENT TILL
shear planes
GLACITECTO-NIZED OR ABRADED BEDROCK
c
INTERNAL STRUCTURE OF PUSH RIDGE
2-20 m
gravel
fine graind till
sand
till
d
2-5 m
KAME DEPOSITS (deformed)
f
2-5 m
till clast
GLACIOFLUVIAL VERTICAL SUCCESSION
e
OSCILLATING ICE-MARGIN
till
glacio-fluvial
frozen block
g
PATTERNED GROUND
loam
bed-rock
ice wedge

53. Morphologically distinct **rampart of an end-moraine;** older retreat stage of the last glaciation
Locality: Obří Důl valley, Krkonoše Mts.
Photo by: M. Růžička 1995

56. A detail of Plate 55, **till of an end-moraine**
Texture: sandy stone gravel with blocks
Structure: chaotic, no preferred orientation of clasts
Stratigraphy: retreat stage of the last glaciation – Uppe
Pleistocene
Locality: River Labe valley, Krkonoše Mts.
Photo by: M. Růžička 1999

55. Rampart of an end-moraine
Texture: sandy stone gravel with blocks, mostly angular clasts
Structure: chaotic
Stratigraphy: retreat stage of the last glaciation – Upper Pleistocene
Locality: River Labe valley, Krkonoše Mts.
Photo by: M. Růžička 1999

Souvky

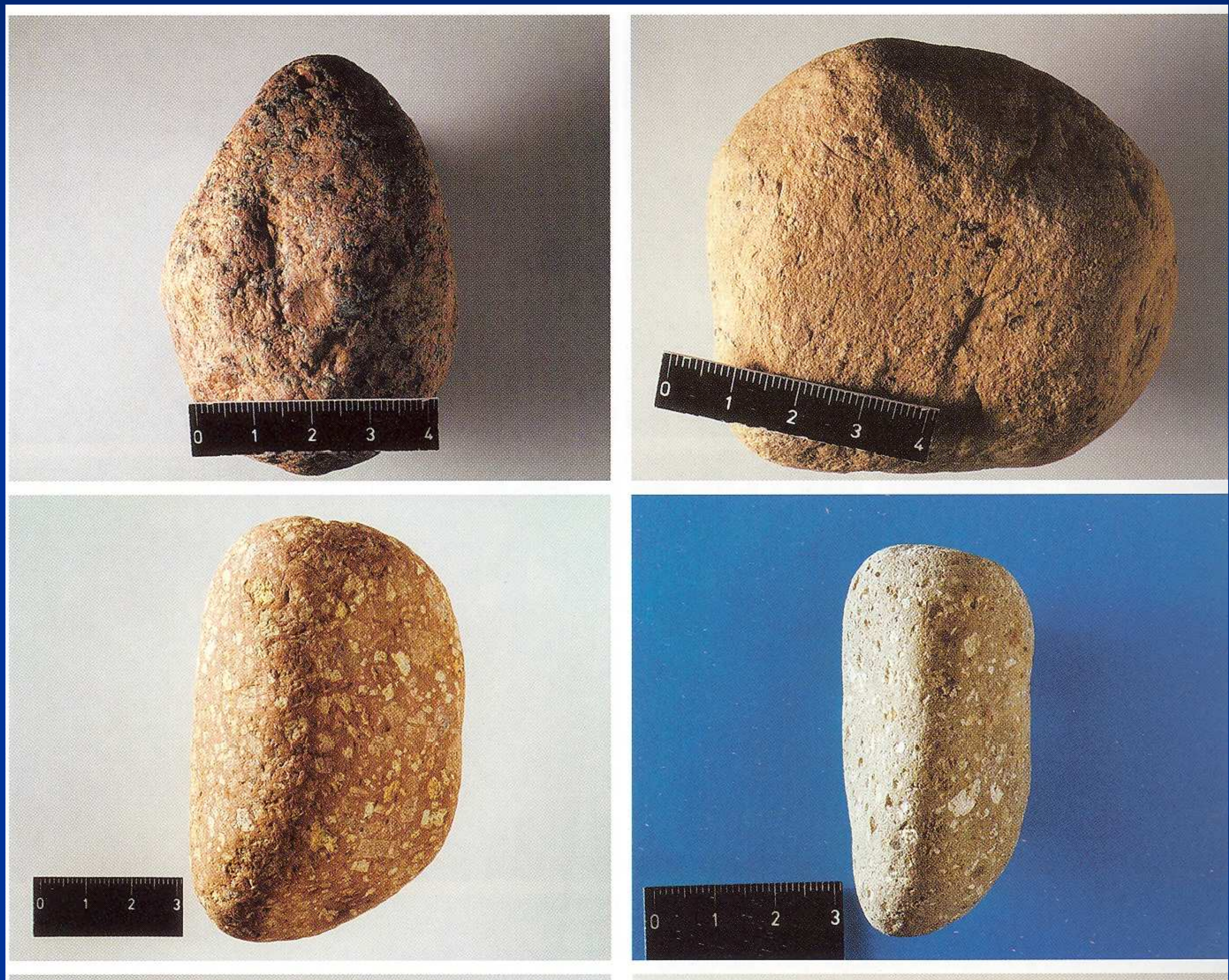

Till

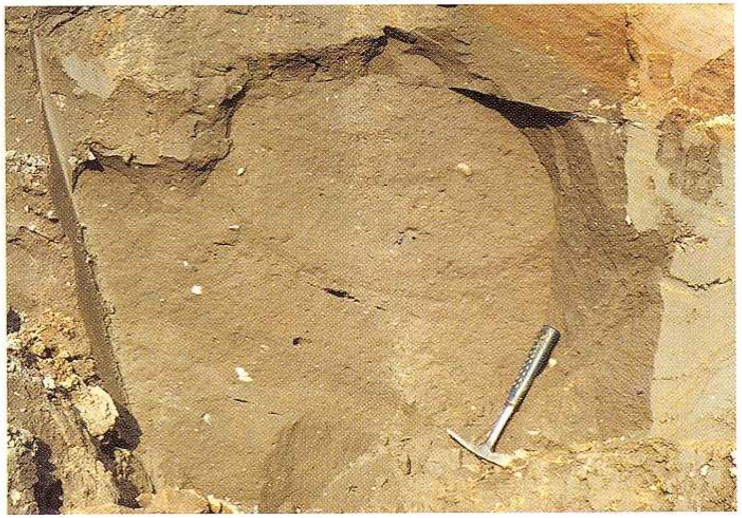

65. Lodgement till
Texture: clayey-silty sand, fine sand prevails, admixture of fine gravel clasts
Structure: massive, with signs of parallel stratification (deformed partly due to stresses exerted by younger ice advance); elongated pebbles show preferred orientation
Stratigraphy: Elsterian glaciation (the grey colouring is described as typical of Elsterian tills)
Locality: Kobeřice – open gypsum mine (Opava District)
Photo by: O. Holásek 1994

68. Lodgement till
The wavy base of the till layer is sloping down in the direction of the ice-sheet movement. The stratification at the base of the till suggests higher deposition rate in the lee-side of the underlying Pliocene sandy silts.
Texture: clayey-silty sand, mostly fine grained with admixture of gravel
Structure: massive with parallel stratification signs, distinct preferred orientation of elongated clasts
Comment: the surface of underlying sandy silt has been fragmented and loosened by the ice movement
Stratigraphy: Older Saalian (Palhanec) Glaciation
Locality: Chuchelná (Opava District)
Photo by: M. Růžička 1996

Glacimarinní sedimenty

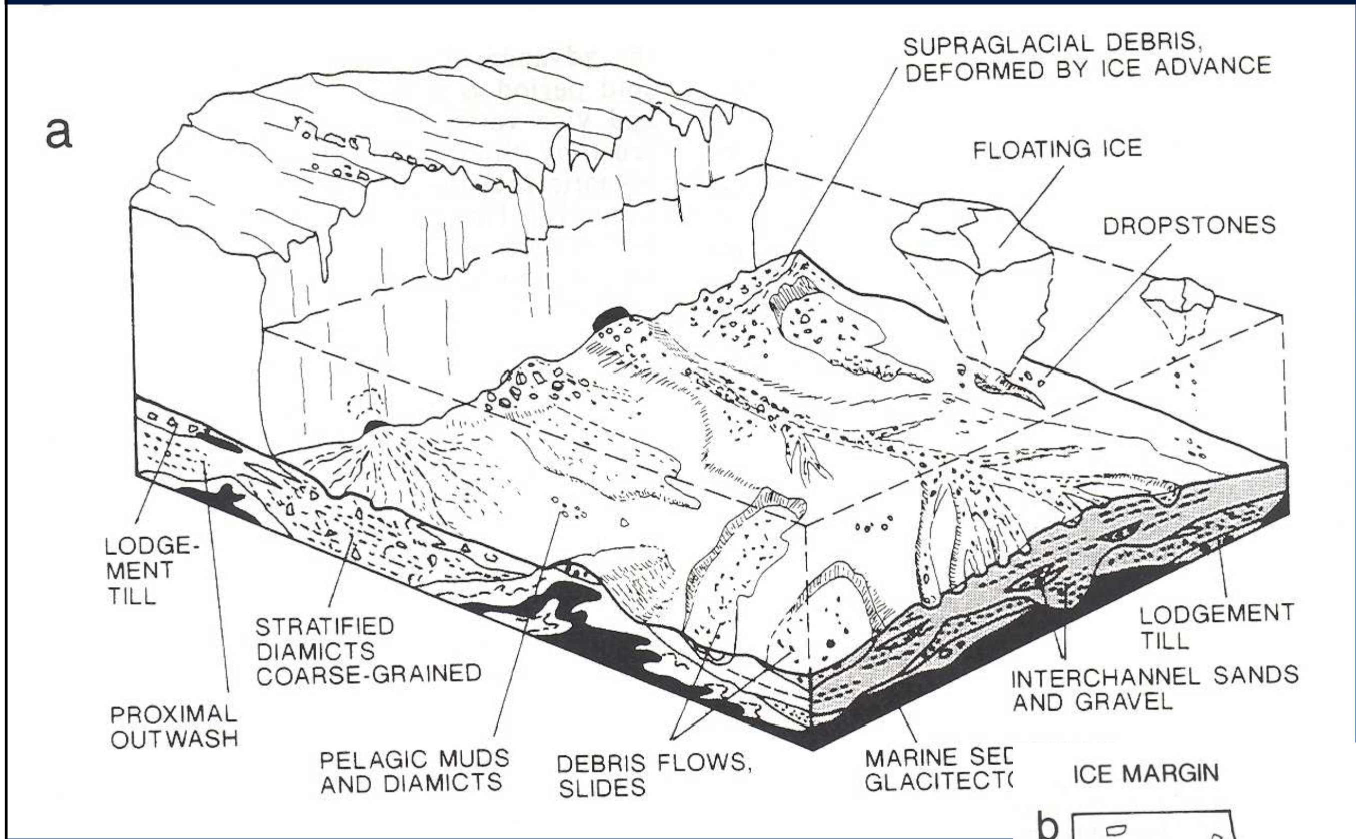

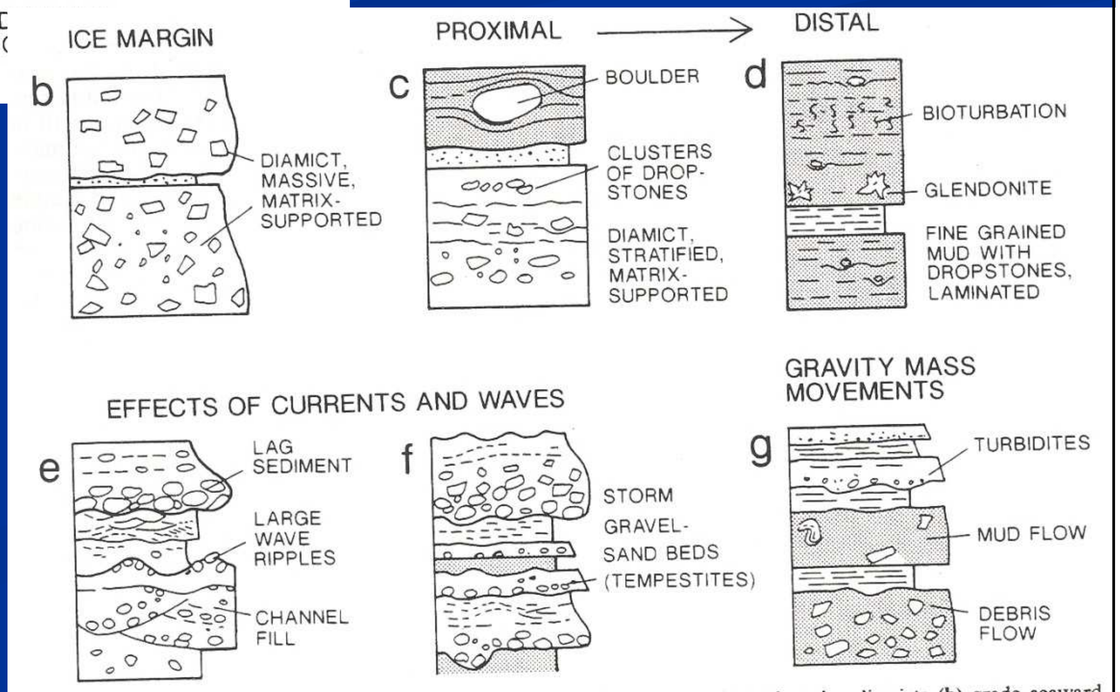

Kvartérní kontinentální zalednění na severní Moravě

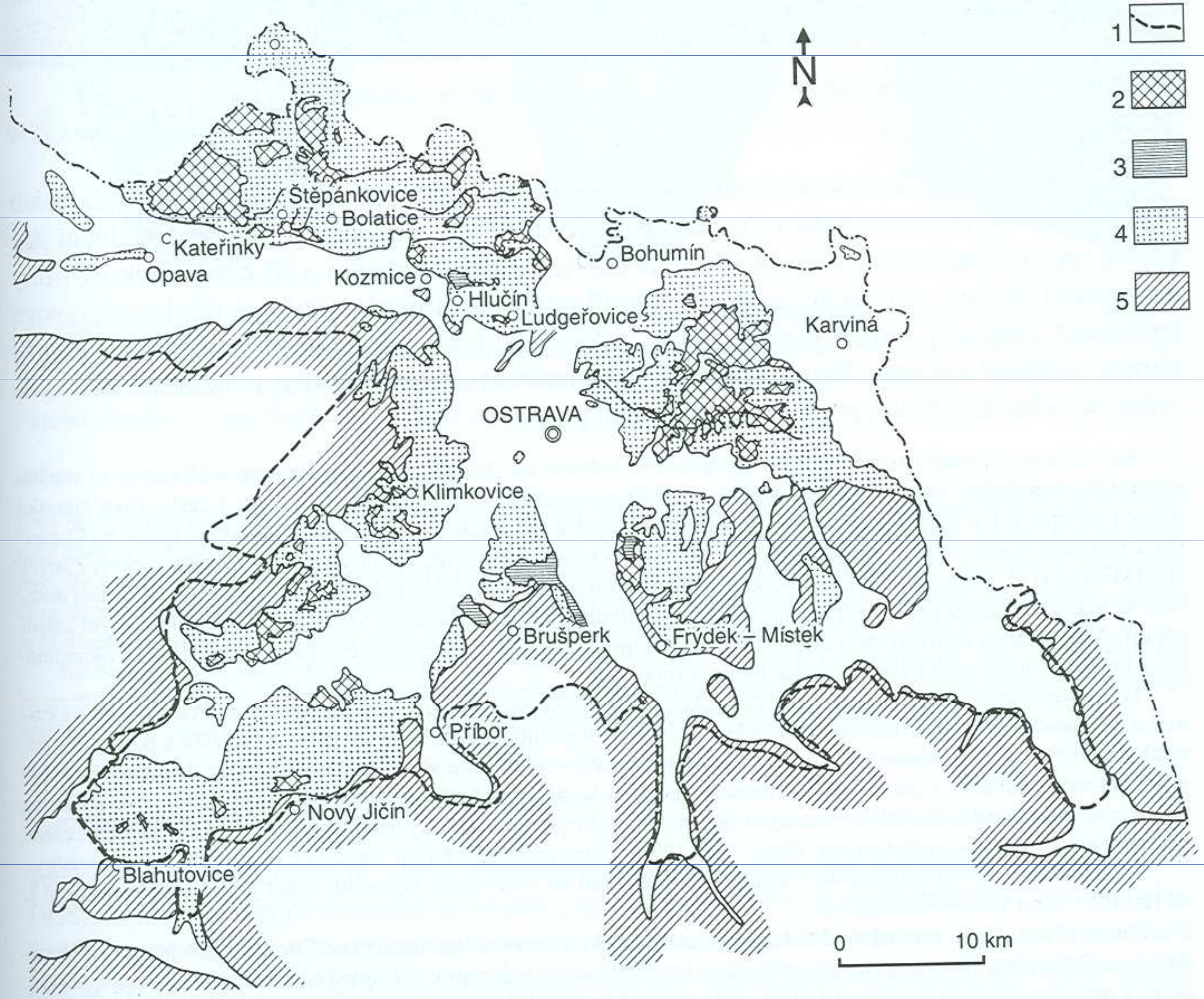

Obr. 264. Rozsah maximálního zalednění na severní Moravě a ve Slezsku. 1 – hranice největšího rozsahu saalského zalednění; 2 – souvkové hlíny; 3 – glacilakustrinní jíly a varvity; 4 – glacilakustrinní písky; 5 – horniny skalního podkladu (J. Macoun et al. 1965).

EOLICKÉ SEDIMENTY

Eolické sedimenty

- Písek, prach
- Ukládaná pod přímým vlivem činnosti větru (proudící vzduch) bez ovlivnění tekoucí nebo stojatou vodou
- tj. zachovávají si rysy typické pro eolické prostředí

Eolické prostředí

- Aridní prostředí (pouště a polopouště): cca 34% povrchu souše (recent)
- 20 – 45% plochy pouští je pokryto „písečnými moři“ (ergy)
- Od (sub)tropického pásma až po polární oblasti
- V geologické minulosti se plocha pouší měnila
- (pleitocén – plocha pouští větší, subtropické pámo posunuté k vyšším zeměpisným šířkám)

Recentní eolická prostředí

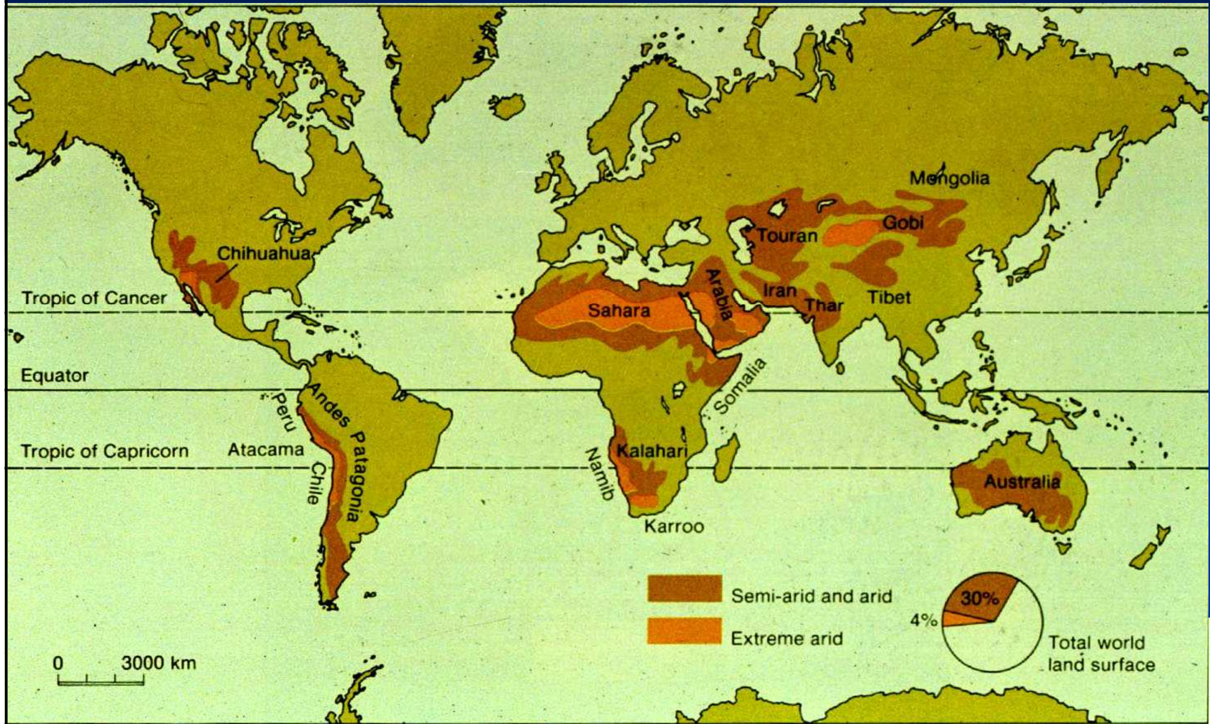

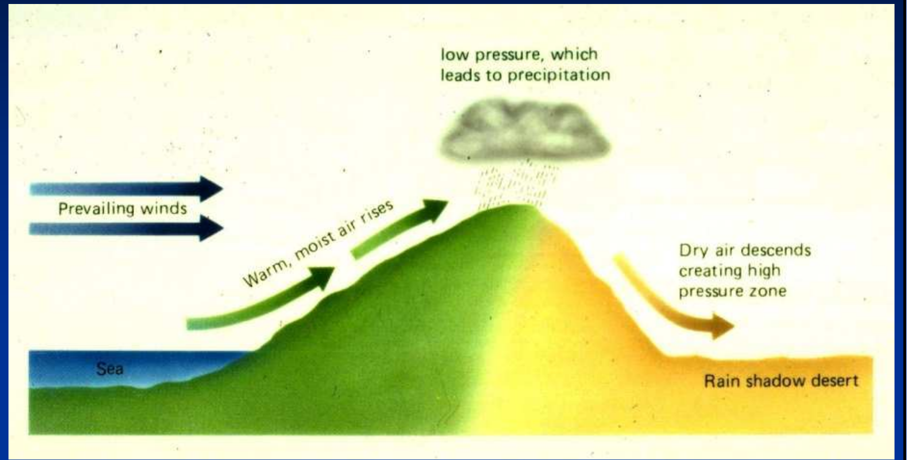

Srážkový stín

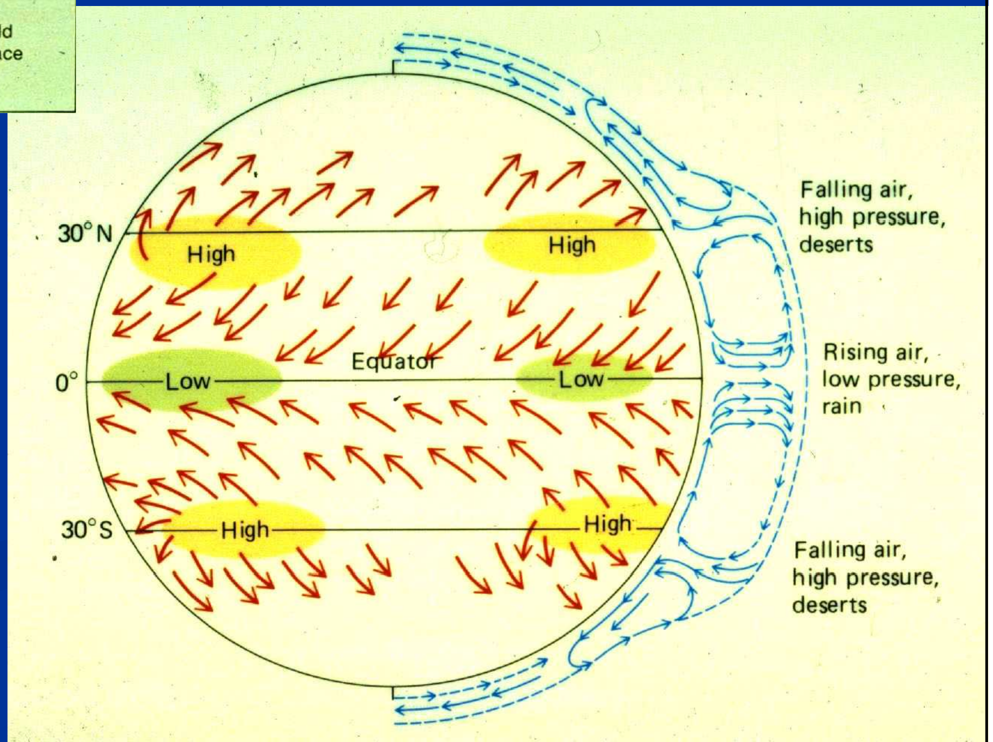

Why we get more deserts

In the subtropics-falling air is cold and dry,
Warm air rise and is moist- hits higher altitudes and
Causes precipitation as it cools

Globální distribuce recentních eolických sedimentů

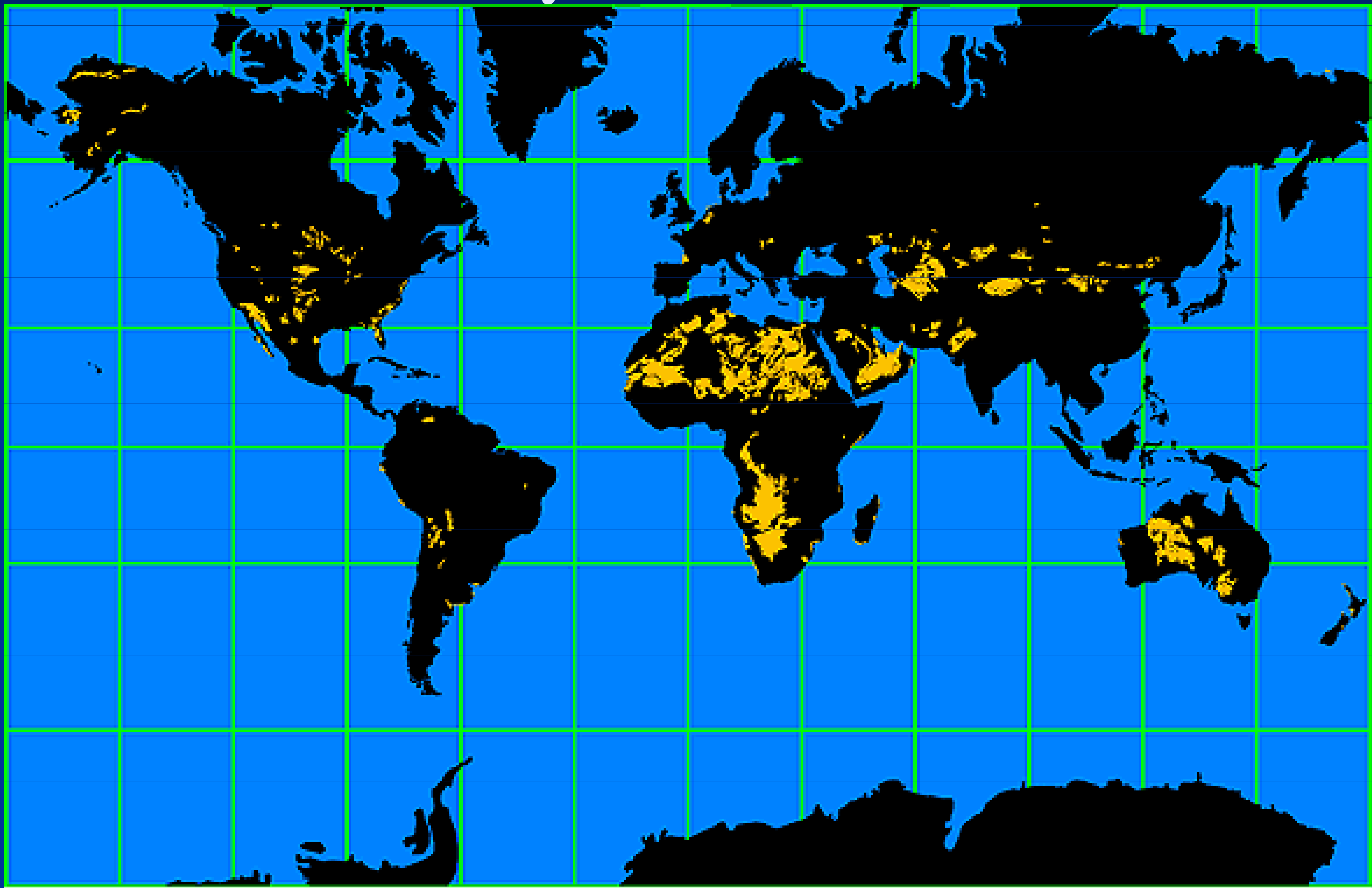

Větrná eroze a transport

- Odvalování, klouzání
- Saltace
- Suspenze

Závislé na velikosti částic

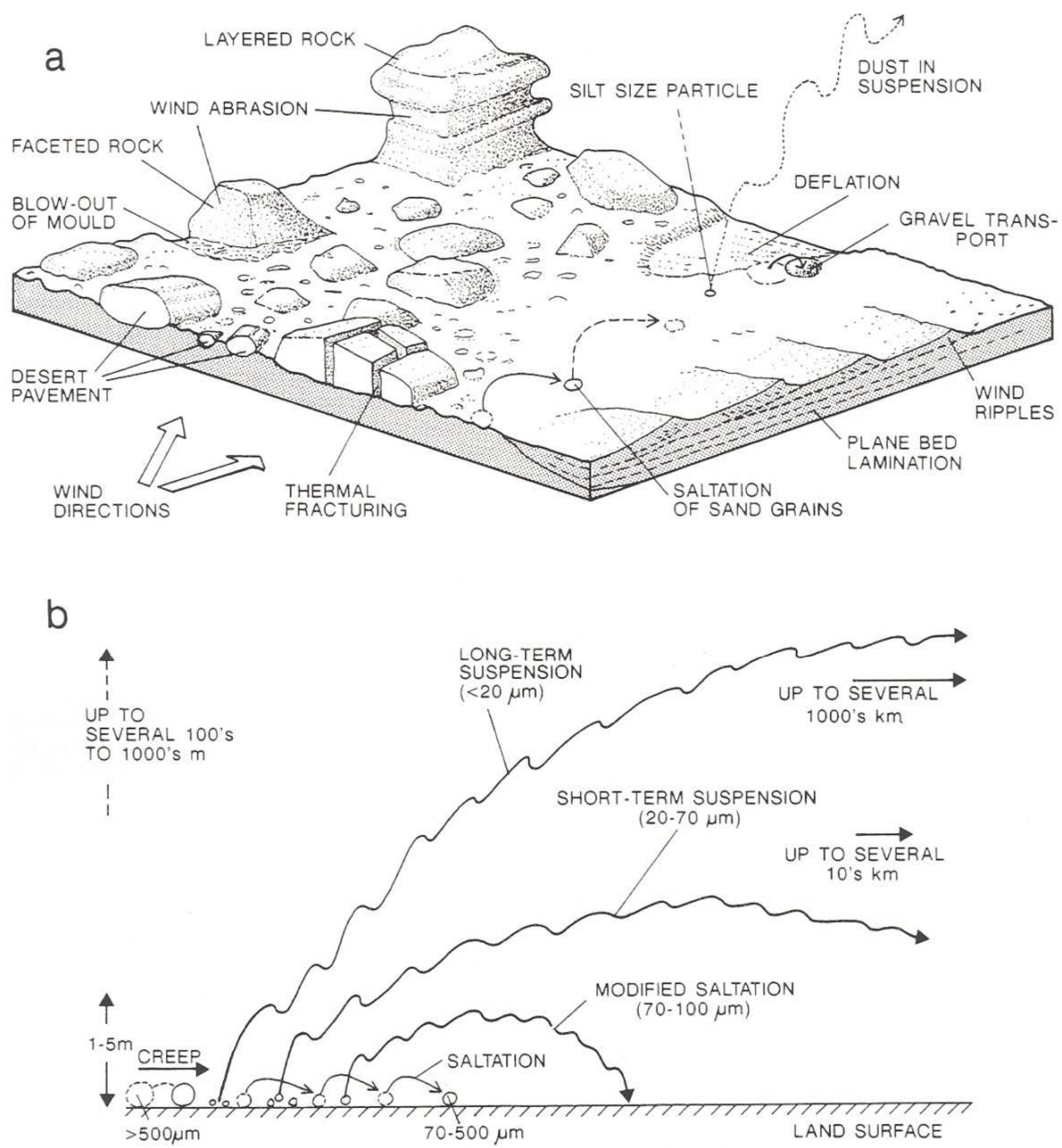

Fig. 2.20. **a** Various modes of eolian transport of silt, sand, and gravel, specific features of desert surfaces including deflation and wind abrasion, and bed forms on flat surface with limited sand accumulation (e.g., in interdune areas, as shown in Fig. 2.21). **b** Modes and distance of eolian particle transport by moderate storms (wind velocities of 10 to 20 cm/s) in relation to grain sizes. (After Pye 1987)

Fyzikální principy transportu hraniční vrstvy (boundary layer)

HRANIČNÍ VSTVA V NEWTONOVSKÝCH KAPALINÁCH (VZDUCH, VODA)

Hraniční vrstva: zóna zpomalení kapaliny v blízkosti kontaktu s pevnou látkou, se kterou je kapalina v relativním pohybu

Rychlostní profil proudící kapaliny na hraniční vrstvě

$$\tau = \eta \frac{dU}{dy}$$

τ = smykové napětí
η = kinematická viskozita

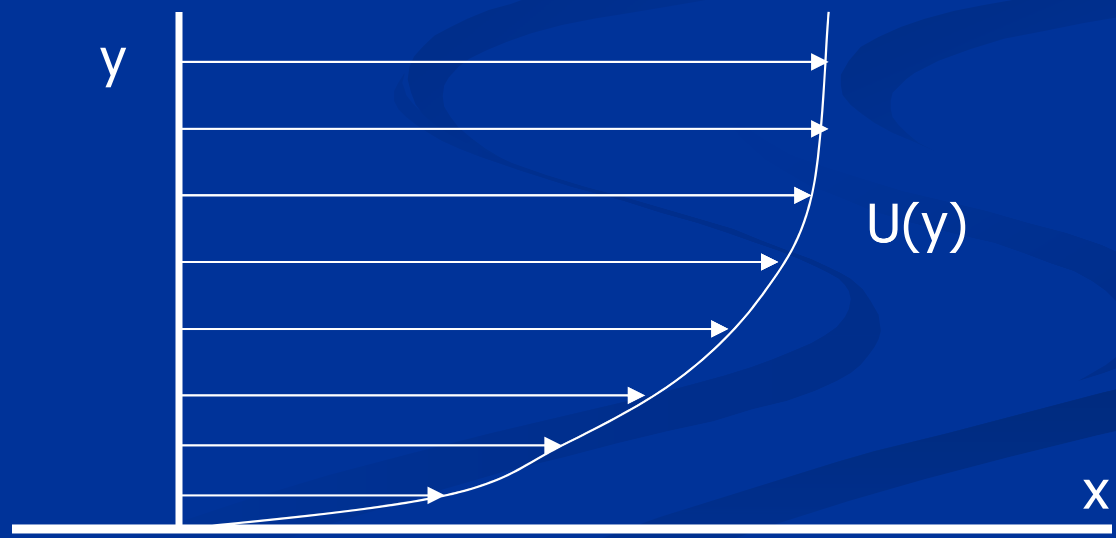

Proudění vzduchu

- Water and air are fluids
- But air is less dense (so higher velocities required)
- Suspension and saltation
- Prahová rychlost větru 1 cm nad povrchem
- $u = 0{,}06\sqrt{(\rho_s - \rho_f)gD}$

u = prahová rychlost

ρ_s = hustota částice

ρ_f = hustota fluida (vzduchu)

g = gravitační zrychlení

D = průměr částice

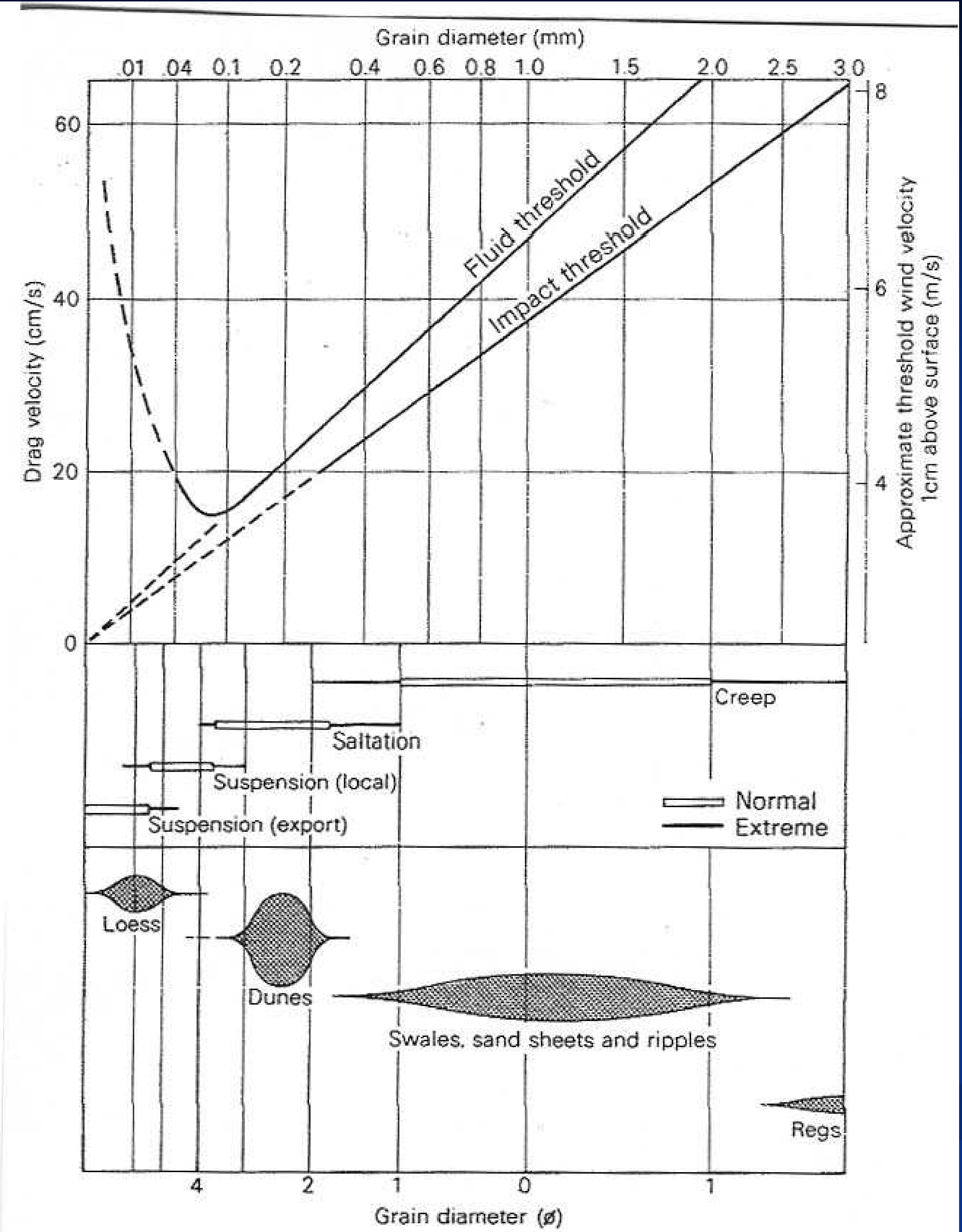

65. Relationships between grain size, fluid and impact threshold wind velocities, characteristic modes of aeolian transport, and resulting size-grading of aeolian sand formations. After Bagnold, 1941, and Folk, 1971a.

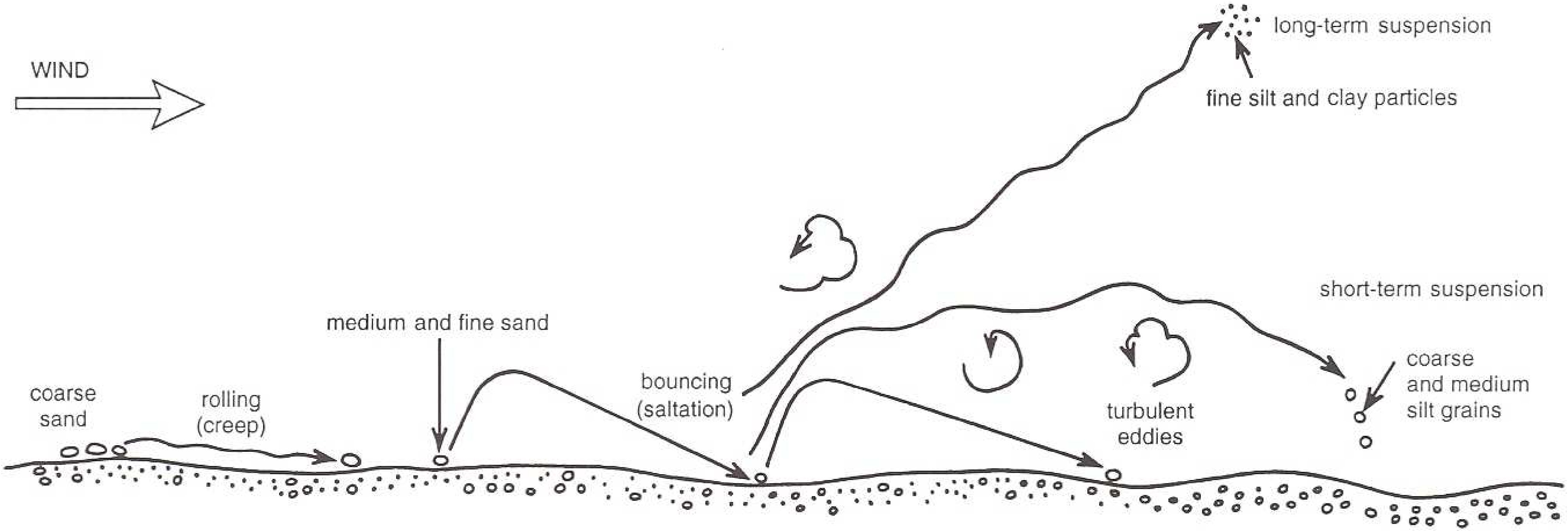

Figure 25. Schematic diagram showing the principal modes of aeolian transport and sedimentation (PYE and TSOAR 1987, modified).

Písčitá frakce
základní tvar povrchu: duna

SEPARACE TOKU

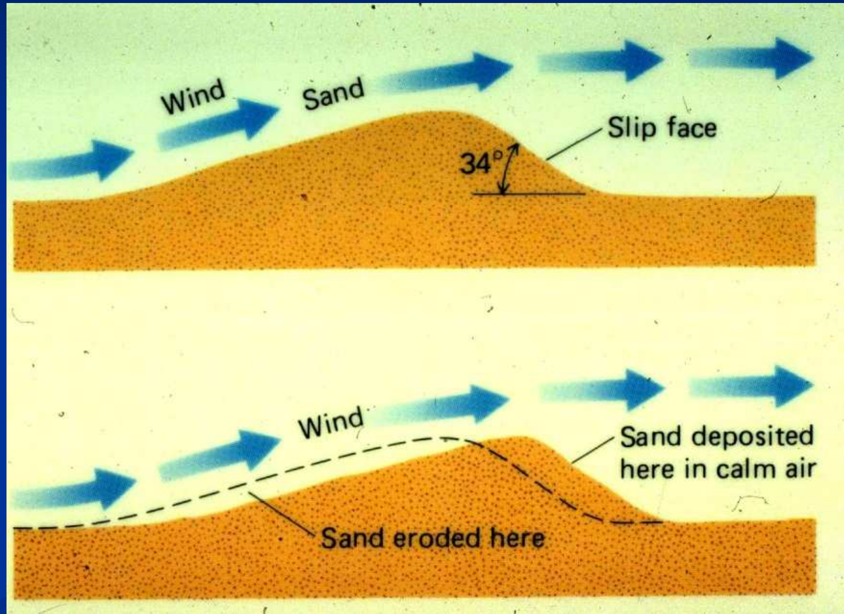

V hraniční vrstvě **částice ležící nejblíže podloží** (dnu) nebo přímo na dně mají **nejnižší kinetickou energii**
Tyto částice budou silně ovlivněny při změně rychlosti toku (zpomalení, zrychlení) nebo v místě změny sklonu dna

Zpomalení / ohyb dna směrem dolů -> tyto částice se zastaví nebo se dokonce začnou pohybovat pět, nahromaděná kapalina nutí hlavní tok téci výše ode dna a vyvine se zpětný proud – **separace proudu**

Proudnice se oddělí ode dna

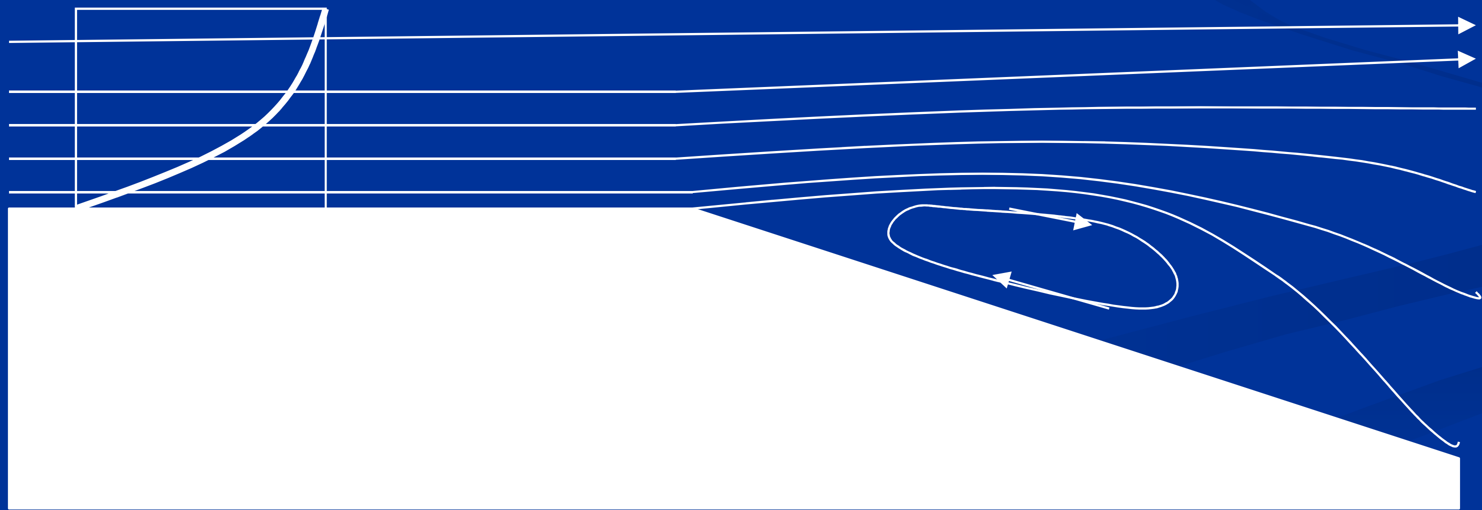

Nebraska sand hills

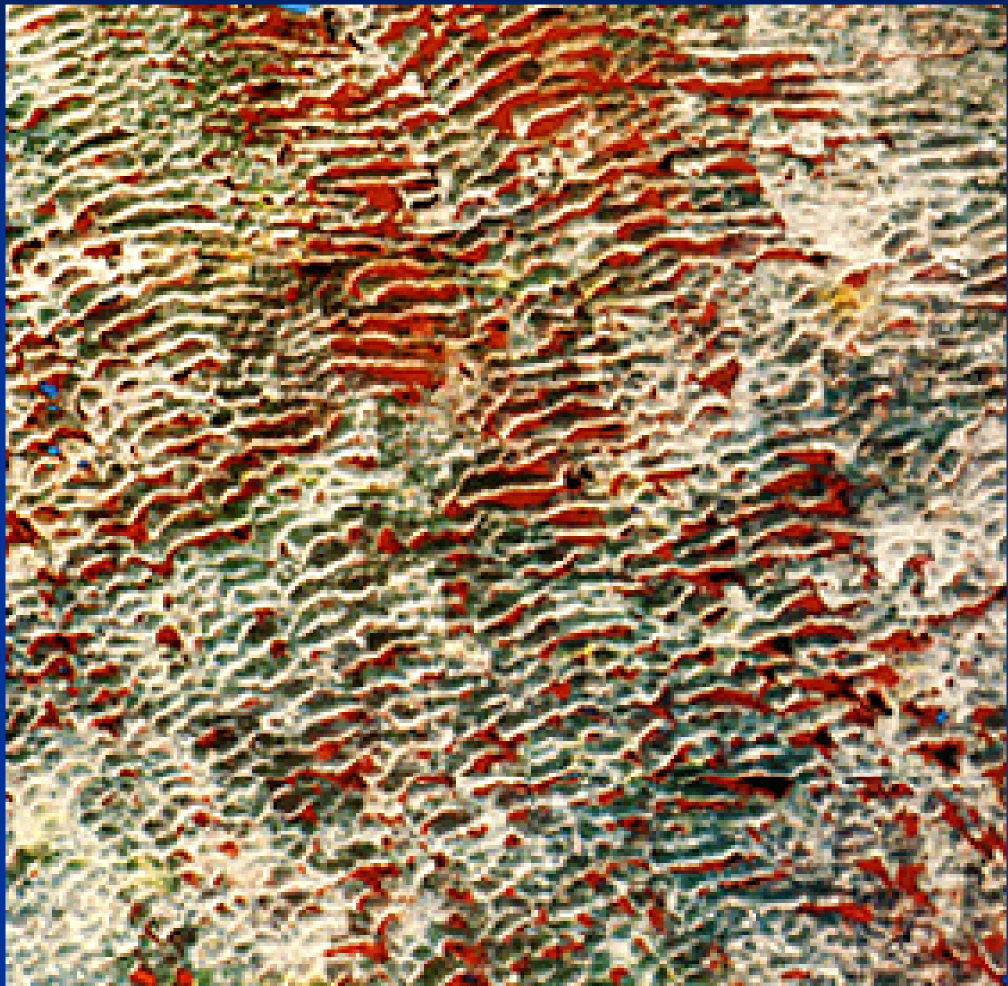

(NASA)

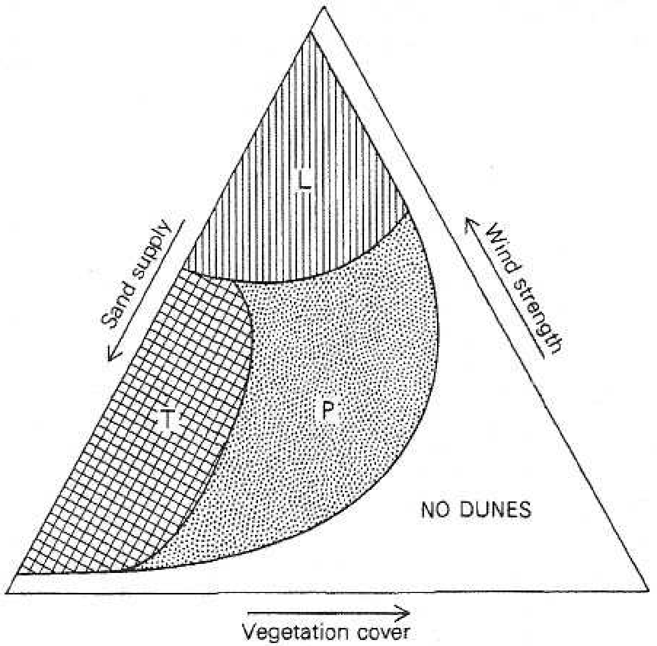

74. Relationships between dune form and the factors of sand supply, wind strength and vegetation in the Great Plains, United States. L = longitudinal, T = transverse, and P = parabolic forms. After Hack, 1941.

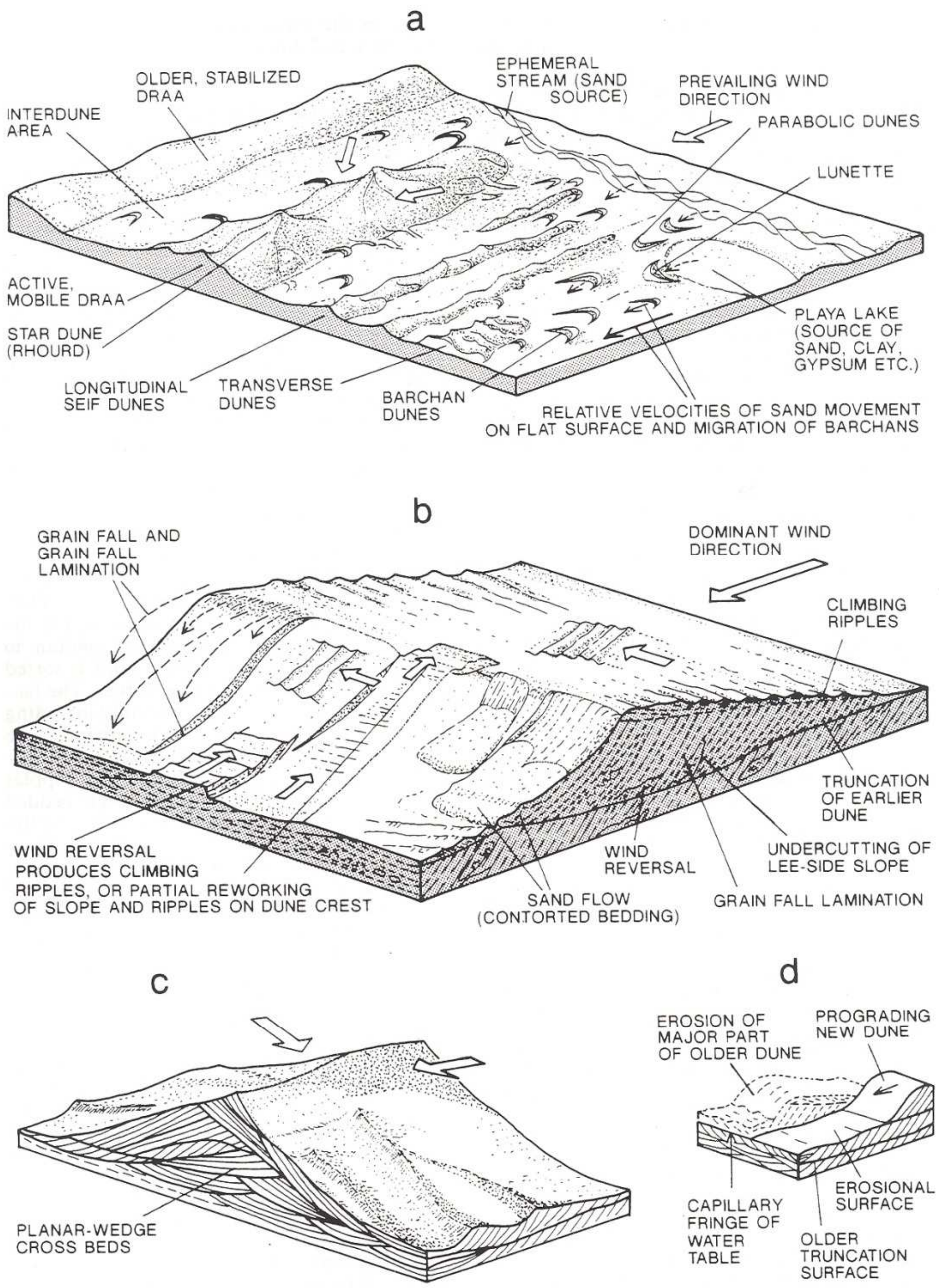

Texturní charakteristika:

Planární šikmé zvrstvení

Čeřinové zvrstvení (šplhavé čeřiny)

Laminární zvrstvení

Chaotické (zrnotoky na závětrné straně duny)

181. Sand dunes in the River Lužnice valley; height of dunes 3.5 m
Locality: Pískový vrch near Vlkov (Třeboň District)
Photo by: E. Růžičková 1997

184. A complex of **aeolian sands** forming a thick **sheet**
Texture: mostly medium grained sand with subordinate interlayers of well sorted coarse sand and/or fine gravel (pebbles < 5 mm)
Structure: stratified, parallel, thin bedded, lamination in places, laminae wavy or rippled
Locality: sand pit in Travčice near Terezín
Photo by: J. Kadlec 1997

Spraš

Definice

Yellowish-buff unstratified silt, sometimes calcareous, well sorted, with a modal grain size in the range 0.02-0.5 mm, and with pronounced vertical structure

Spraš

- Loess: wind-blown deposit comprised predominantly of silt-size particles (20-60 µm).
- Loess deposits cover ~10% of the surface of the planet. They are up to ~300 m in thickness in China.
- Loess deposits typically exhibit varying stages of soil development.

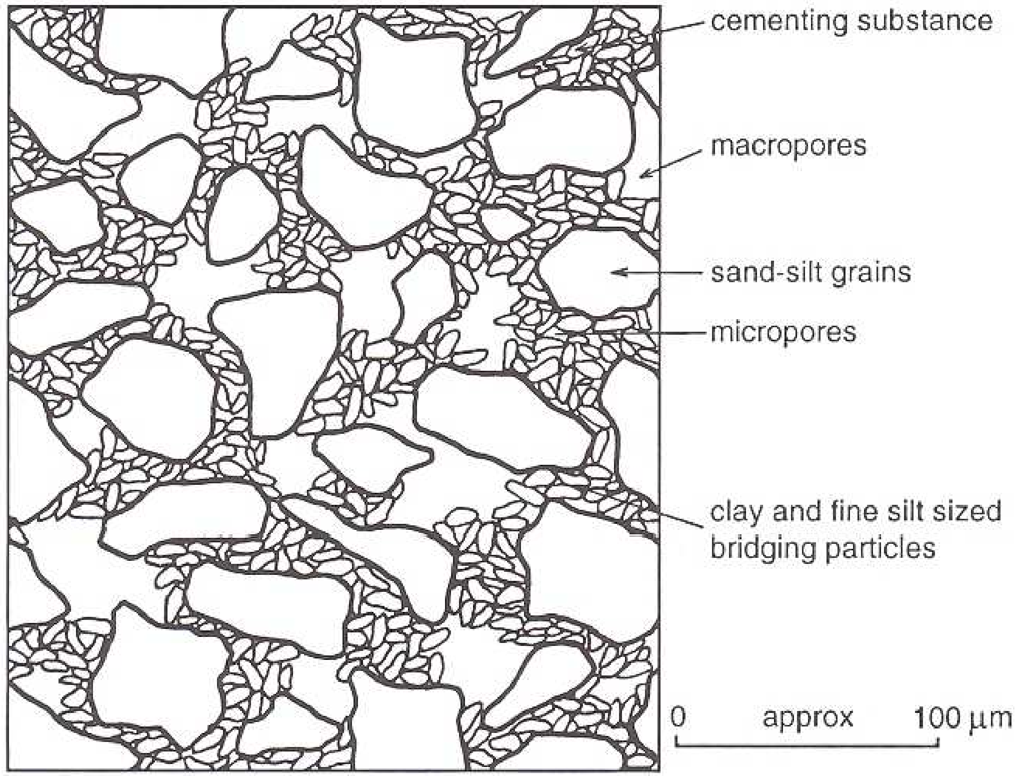

Figure 27. Microstructure of loess (after TAN 1988).

145. Loess, a detail of the Plate 144
Basal part of the chernozem fossil soil
Thin bedding to lamination parallel to the slope surface; typical prismatic jointing, the joint surfaces are sheathed with a white film of calcium carbonate
Locality: Praha-Sedlec
Photo by: A. Zeman 1997

146. Loess
A lee-side accumulation on a smooth south-eastern slope
Texture: calcareous silt
Structure: layering parallel to the slope in general, massive or thin bedded in individual layers
Stratigraphy: Upper Pleistocene
Locality: Kutná Hora-Sedlec
Photo by: A. Zeman 1997

166. Loess

Same as Plate 164, a position displaying a well marked parallel orientation of mica (🡐 the arrow is perpendicular to the lamination) and with a snail shell partly filled with the loess Magnification 26.9x, crossed polars

Globální distribuce sprašových sedimentů

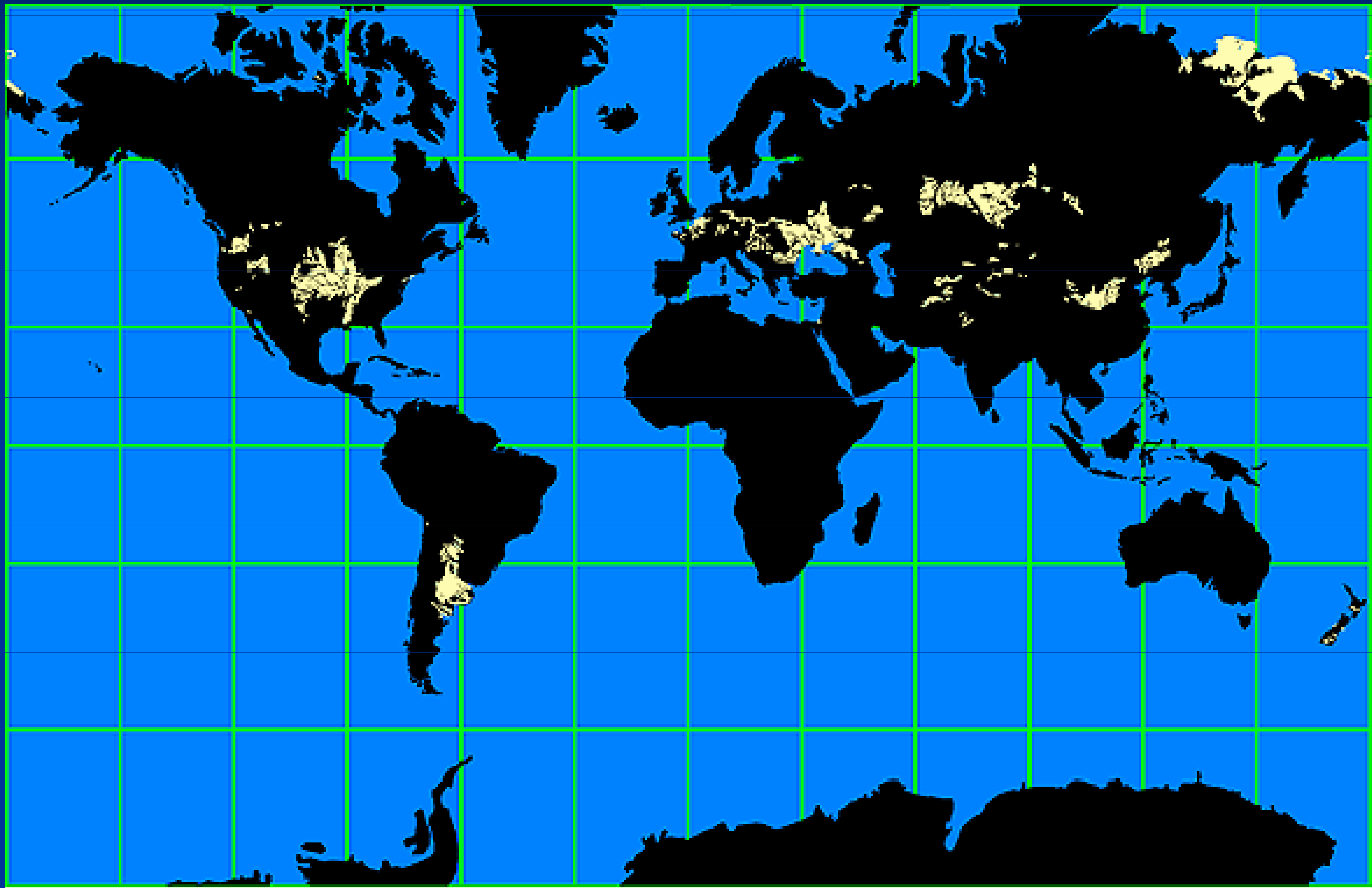

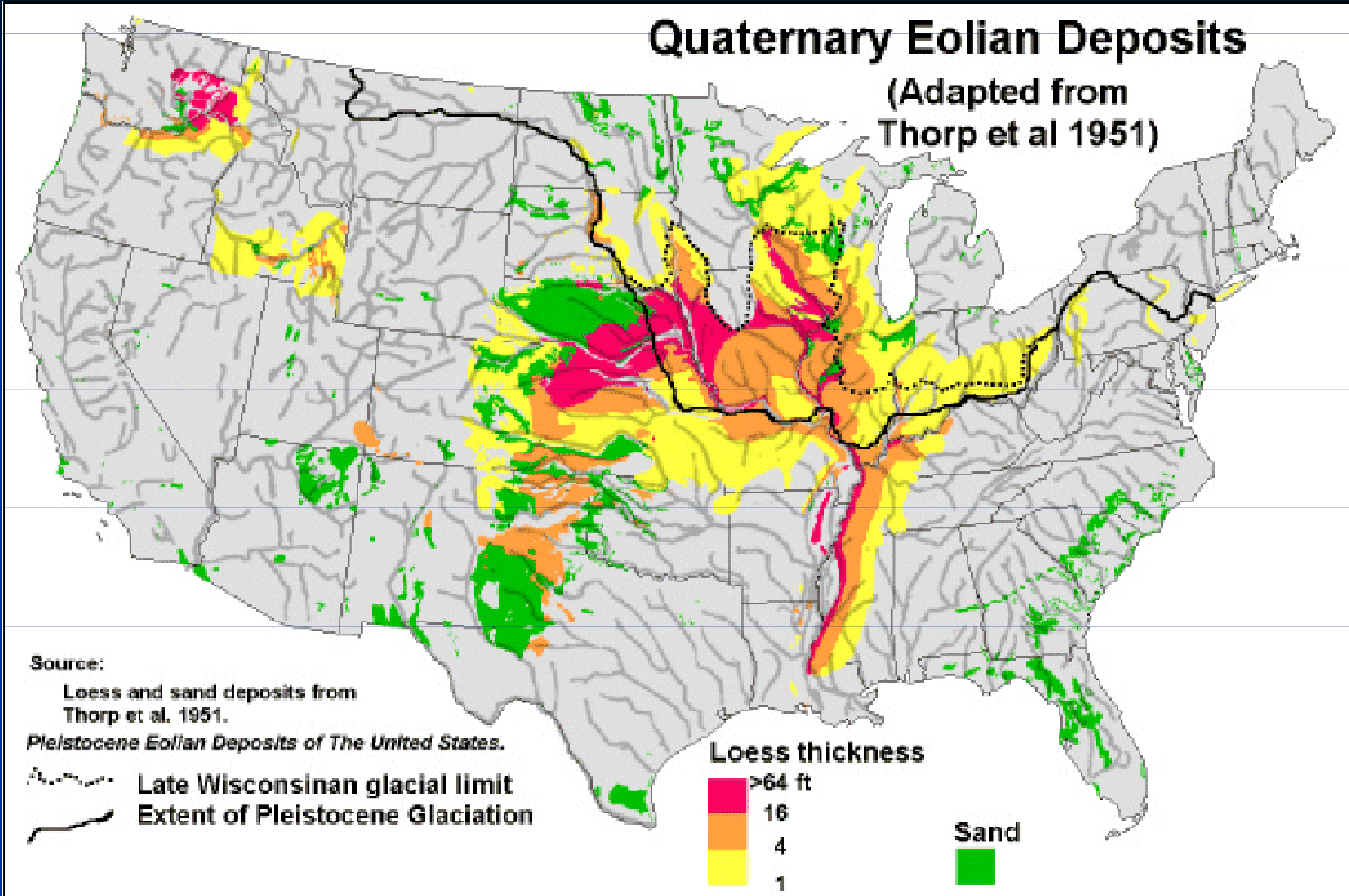
Quaternary Eolian Deposits
(Adapted from
Thorp et al 1951)
Source:
Loess and sand deposits from
Thorp et al. 1951.
Pleistocene Eolian Deposits of The United States.
Late Wisconsinan glacial limit
Extent of Pleistocene Glaciation
Loess thickness
>64 ft
16
4
1
Sand

Kvartérní produkce sedimentů prachové frakce

- Evidence of ice-driven response found in China
  - Plateaus of wind-blown silt
  - Deposited by strong winds and dry conditions
- Loess deposition post-date weathered soil at 2.75 mya
  - Onset of dry conditions at glacial inception
  - 100,000 year cycle over last 0.5 my

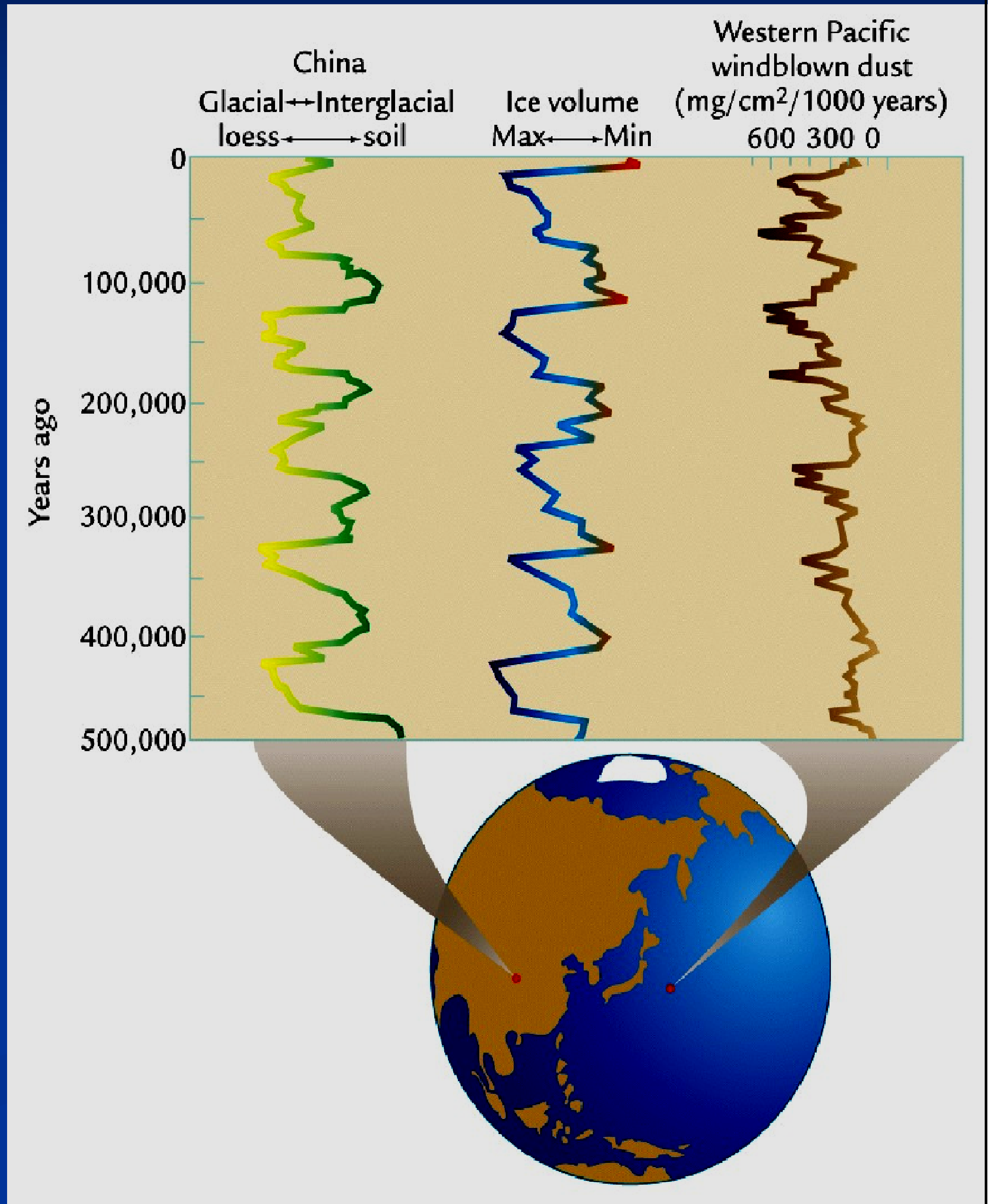

Vznik sprašĺ

- Related to four events:
  - Dust formation
  - Transport
  - Deposition
  - Post-depositional changes

Vznik sprašÍ

- Formation
  - Metamorphic rocks have silt-size minerals that are expelled during erosion.
  - Weathering and soil formation fracture coarse grains, creating silt particles.
  - Transformation of clay particles can produce silt-size minerals.
  - Glacial grinding, eolian abrasion, frost weathering, salt weathering.

Vznik spraší

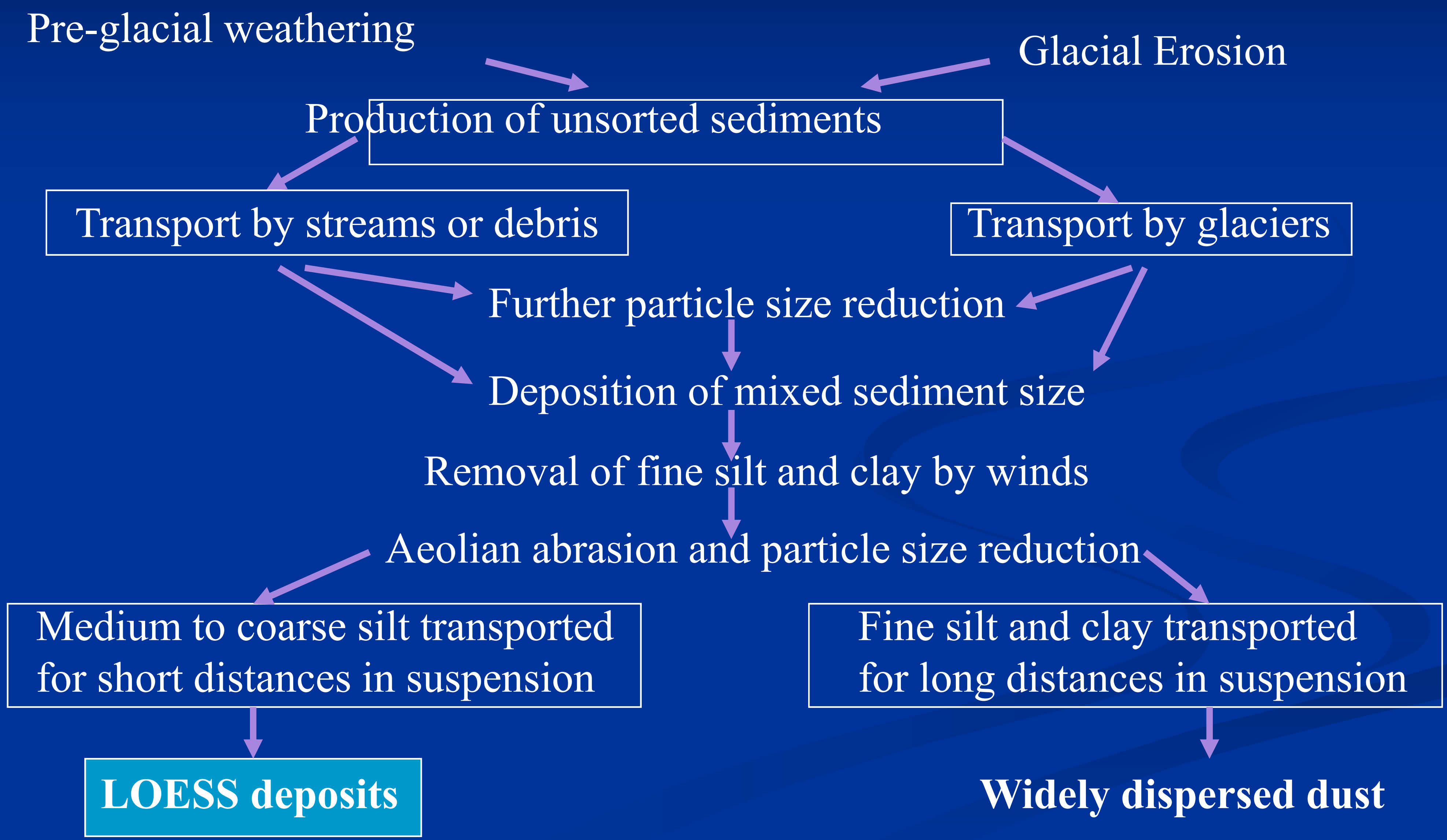

After Wright, 2001

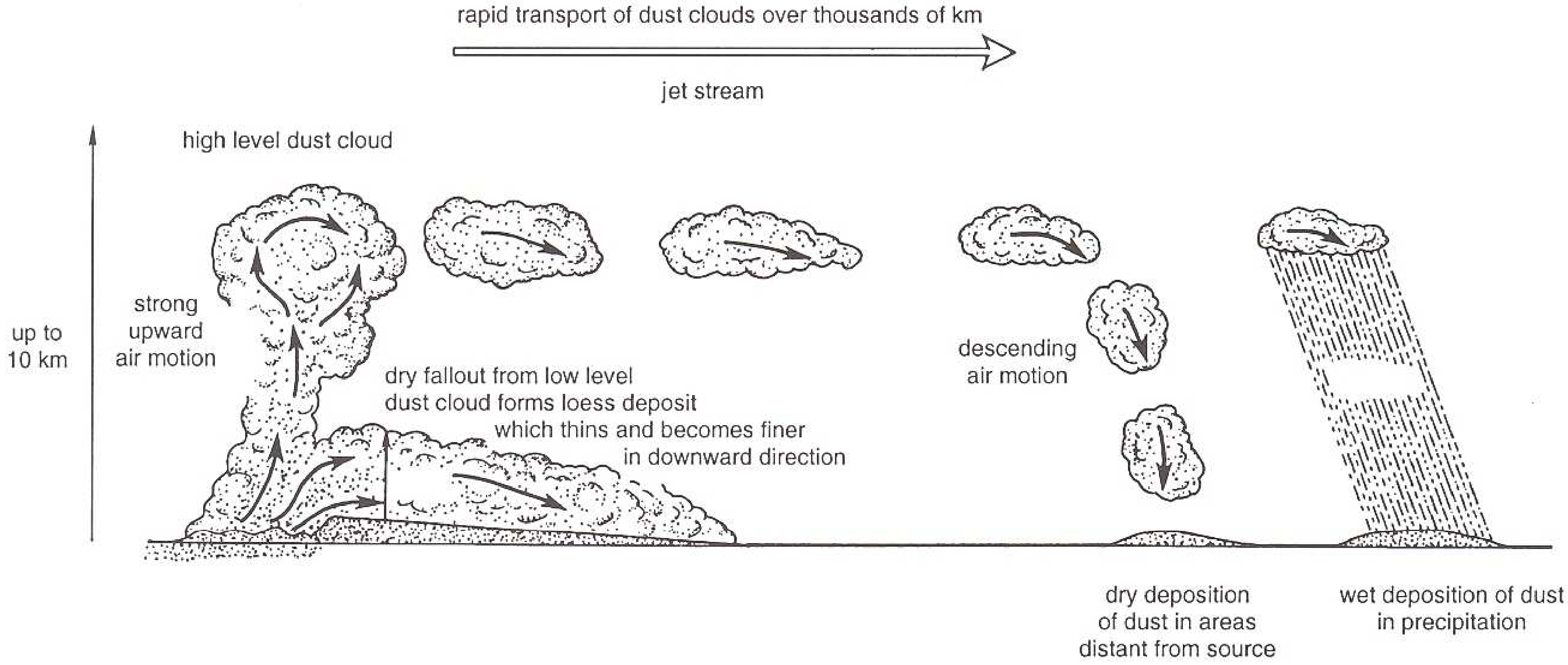

Figure 26. Diagram showing two transport models of aeolian silt (after PYE 1995).

Vznik spraší

- Transport/Deposition
  - Wind (streams?)
    - Strength
    - Direction
    - Vegetation
- Post-depositional changes
  - Soil formation
    - Temperature
    - Rainfall
    - Slope
    - Vegetation

Chronologie sprašových usazenin

- Stratigraphy
- Radiocarbon
- Magneto-stratigraphy
- Correlation (marine isotope record).

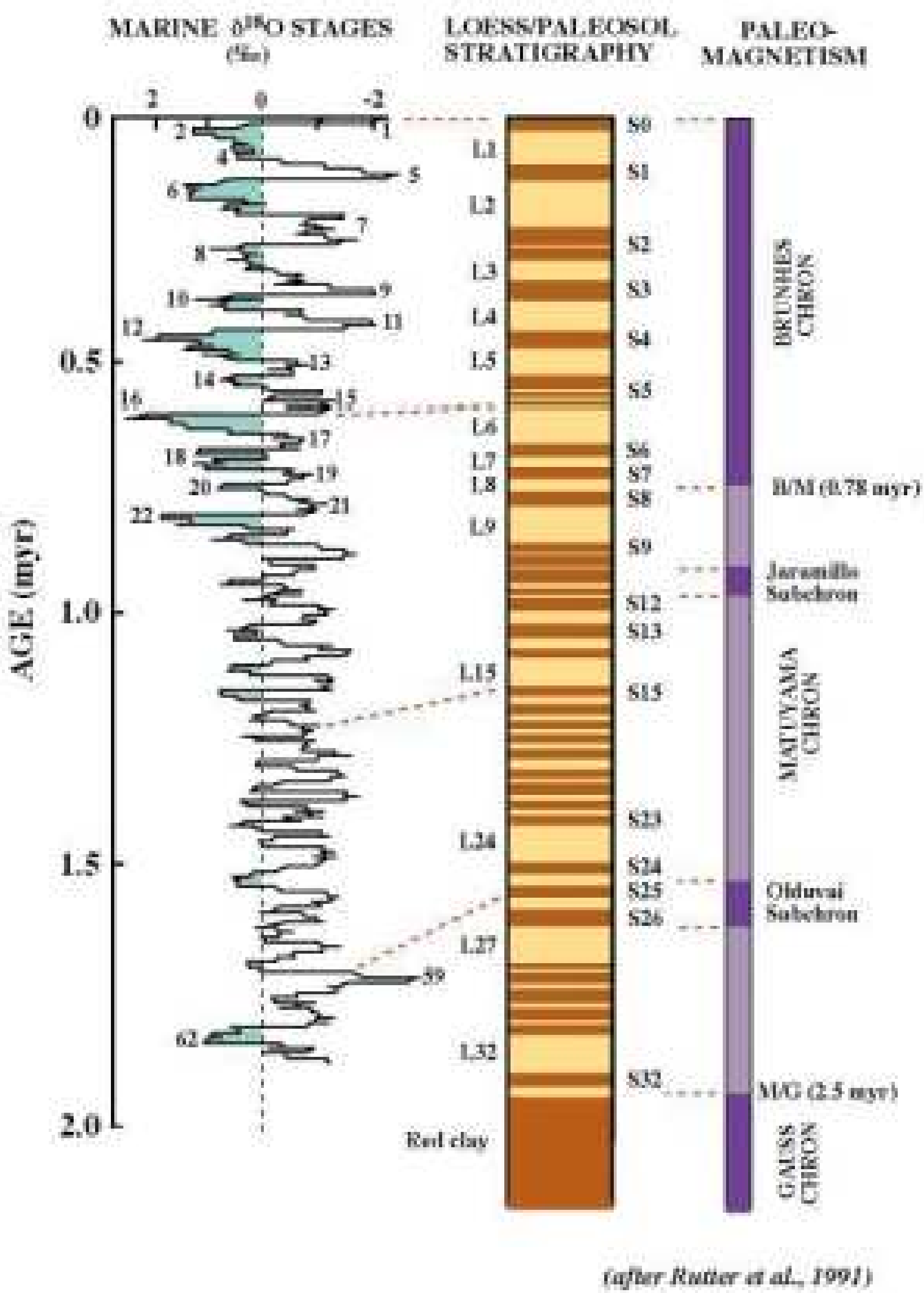

http://depts.washington.edu/uwpcc/images/loess_marine.gif

Paleoklimatologie spraší

- Grain size (wind direction/strength).
- Soil type (vegetation, rainfall).
- Magnetic susceptibility (source and post-depositional changes).
- Pollen (vegetation).
- Land snails (temperature, rainfall).

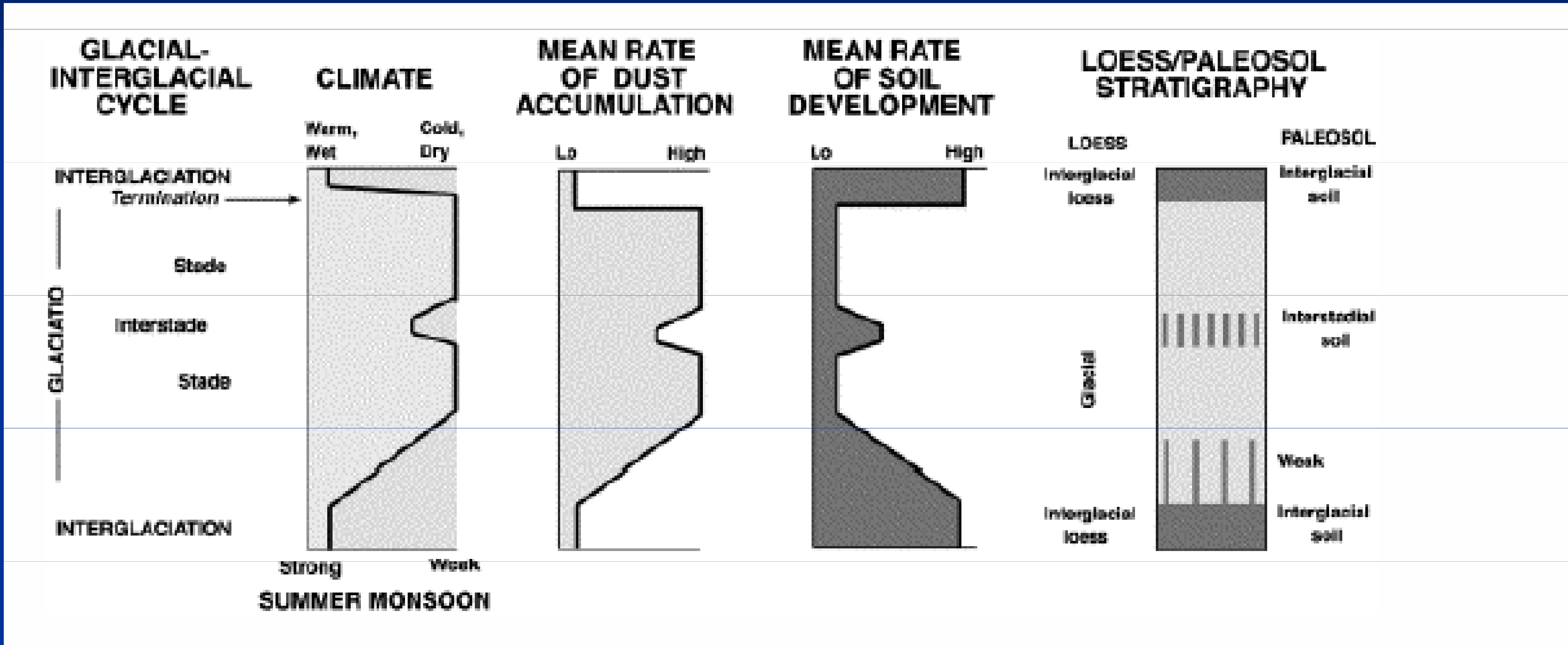

GLACIAL-INTERGLACIAL CYCLE
CLIMATE
MEAN RATE OF DUST ACCUMULATION
MEAN RATE OF SOIL DEVELOPMENT
LOESS/PALEOSOL STRATIGRAPHY
Warm, Wet
Cold, Dry
Lo
High
Lo
High
LOESS
PALEOSOL
INTERGLACIATION
Termination
Stade
Interstade
Stade
GLACIATIO
INTERGLACIATION
Interglacial loess
Interglacial soil
Interstadial soil
Glacial
Weak
Interglacial loess
Interglacial soil
Strong
Weak
SUMMER MONSOON

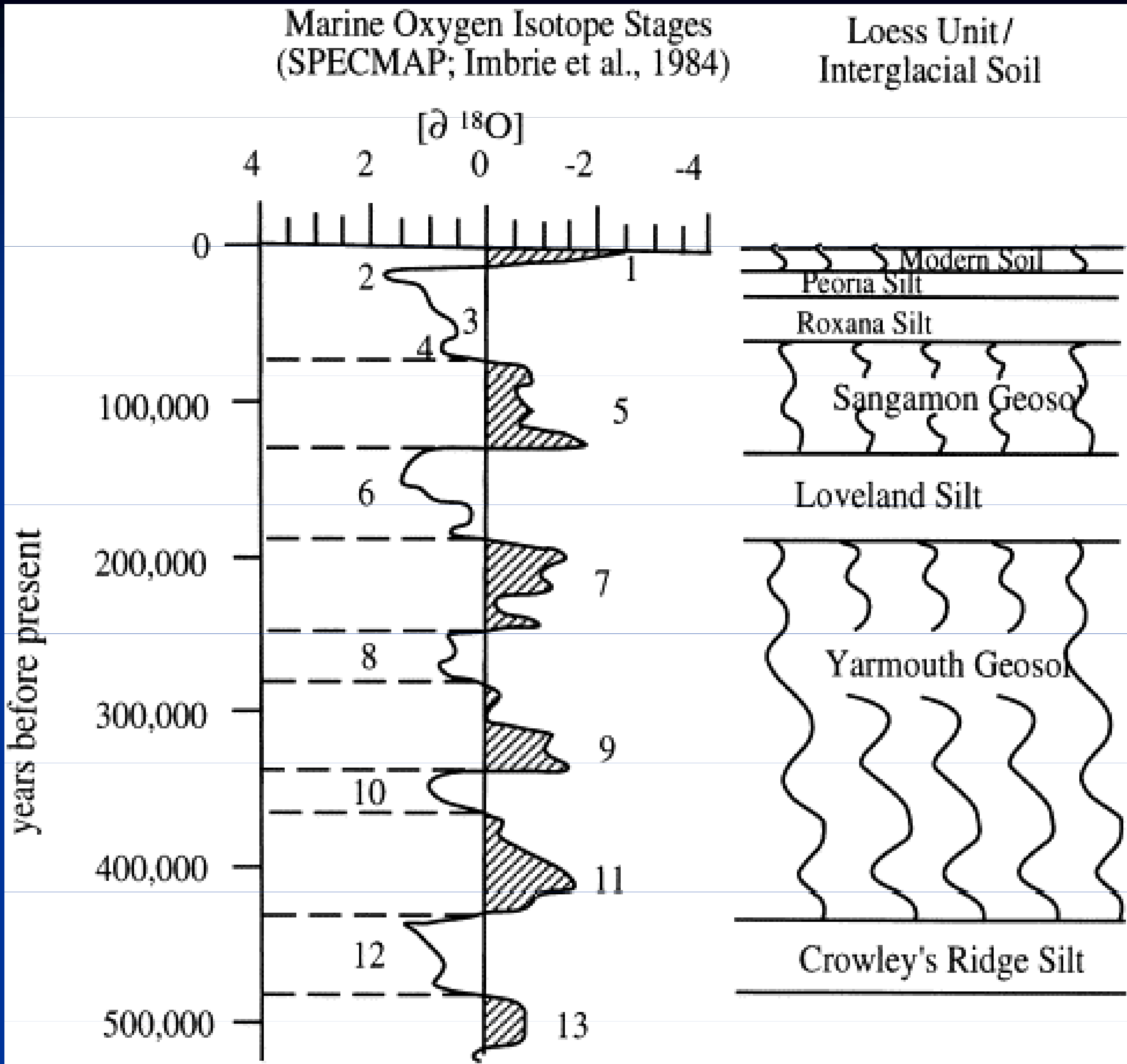

Loess–paleosol sequence at Thebes, Illinois

Grimley et al., 2003

Late Pleistocene -Holocene loess, Burzahom, Kashmir

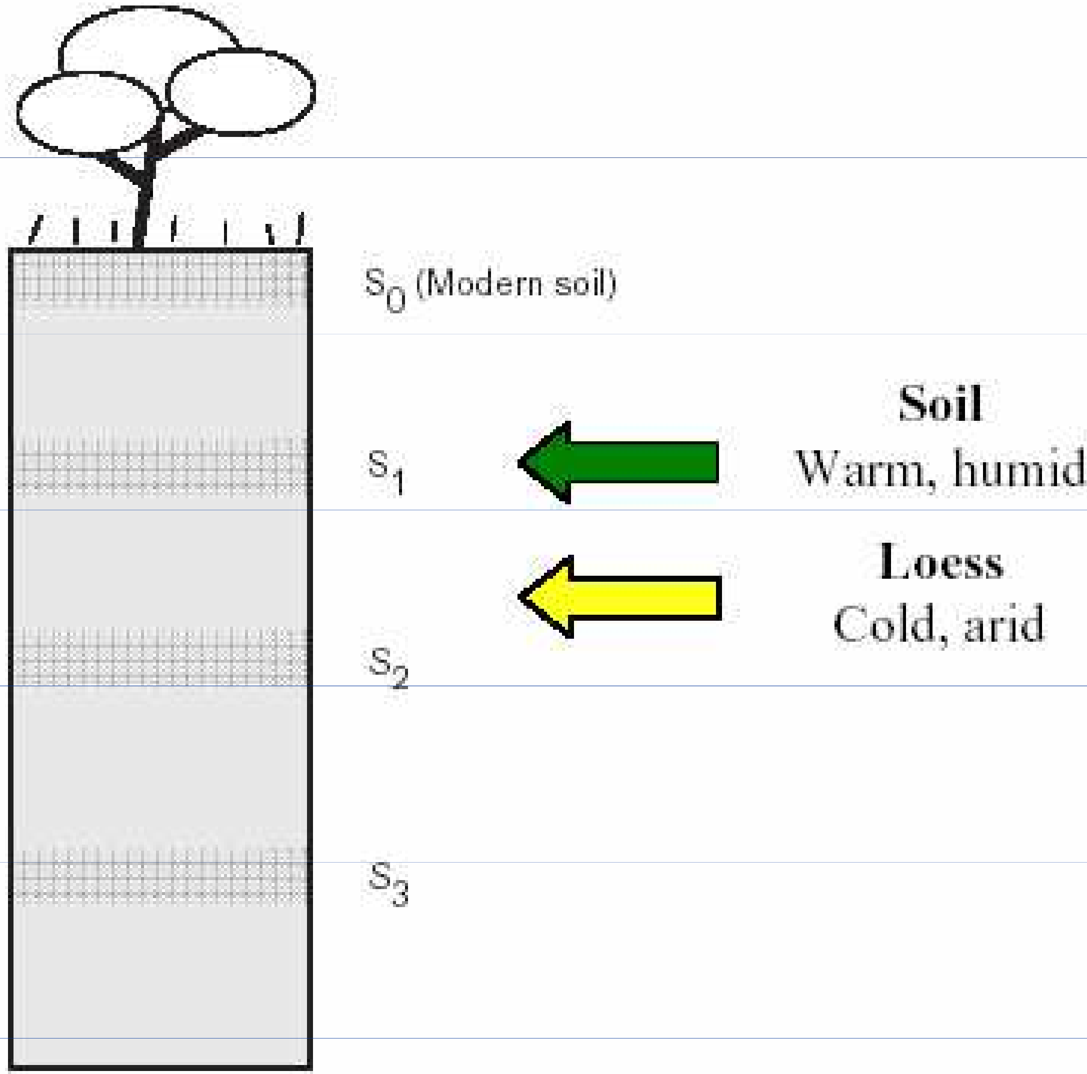

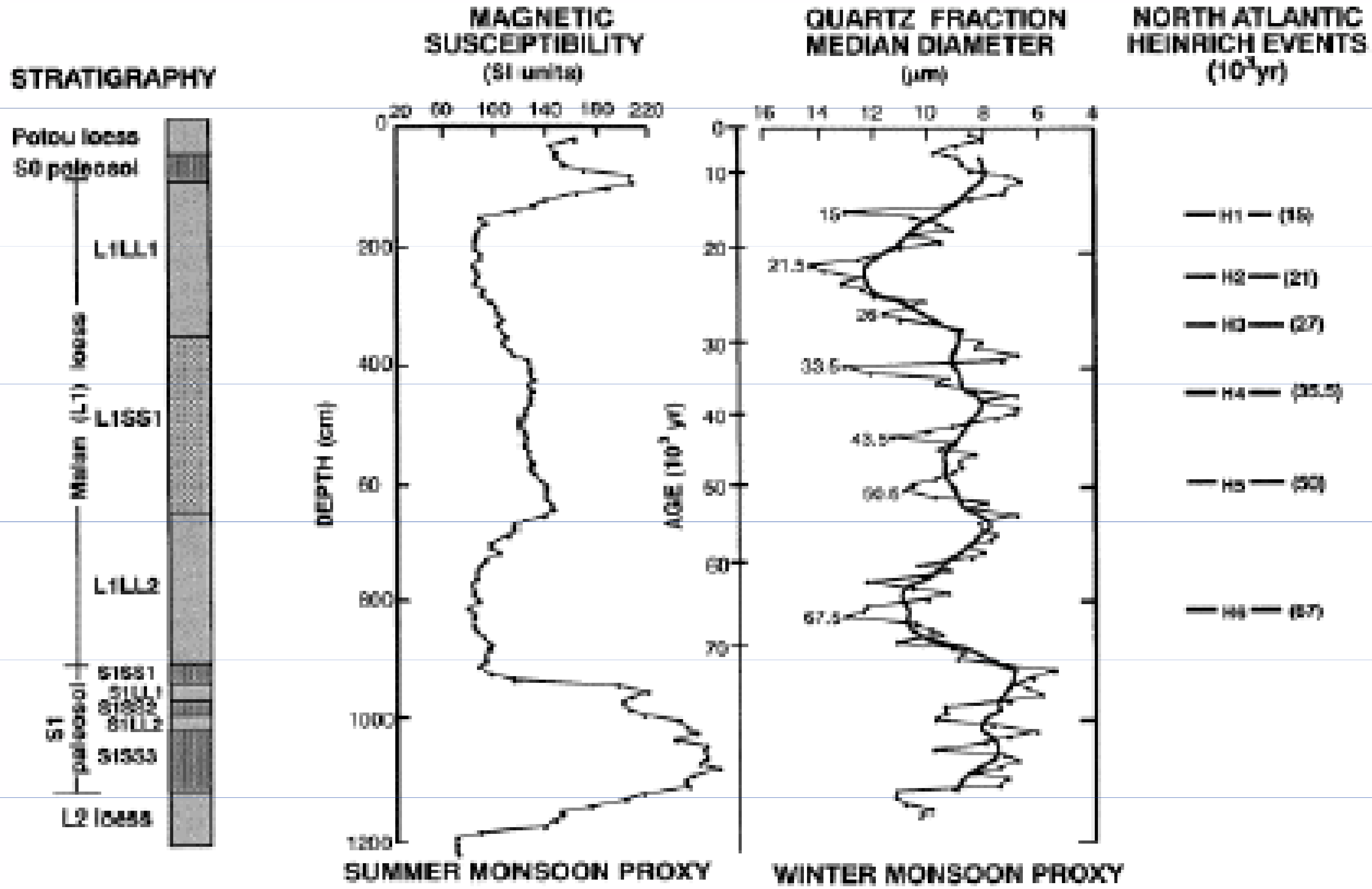
STRATIGRAPHY
Poiou loess
S0 paleosol
L1LL1
L1SS1
L1LL2
Malan (L1) loess
S1SS1
S1LL1
S1SS2
S1LL2
S1SS3
S1 paleosol
L2 loess
MAGNETIC SUSCEPTIBILITY
(SI units)
DEPTH (cm)
SUMMER MONSOON PROXY
QUARTZ FRACTION MEDIAN DIAMETER
(µm)
AGE (10^3 yr)
WINTER MONSOON PROXY
NORTH ATLANTIC HEINRICH EVENTS
(10^3yr)
H1 (15)
H2 (21)
H3 (27)
H4 (35.5)
H5 (50)
H6 (67)

Magnetická susceptibilita

- Spraš: relativně nízká MS
- Paleosol: relativně vysoká MS

Příčiny

- Relative enrichment of magnetic minerals due carbonate leaching. (BUT it only accounts for a small increase).
- Diluting effect by influx of weak magnetic minerals. (BUT believed to be insignificant).
- Pedogenic formation of magnetic minerals.
- Variable sources of magnetic minerals.
- Ultra-fine magnetic particles produced from decomposition of vegetation. (BUT its significance is unknown).
- Frequent fires in loess. (BUT no evidence of frequent fires).

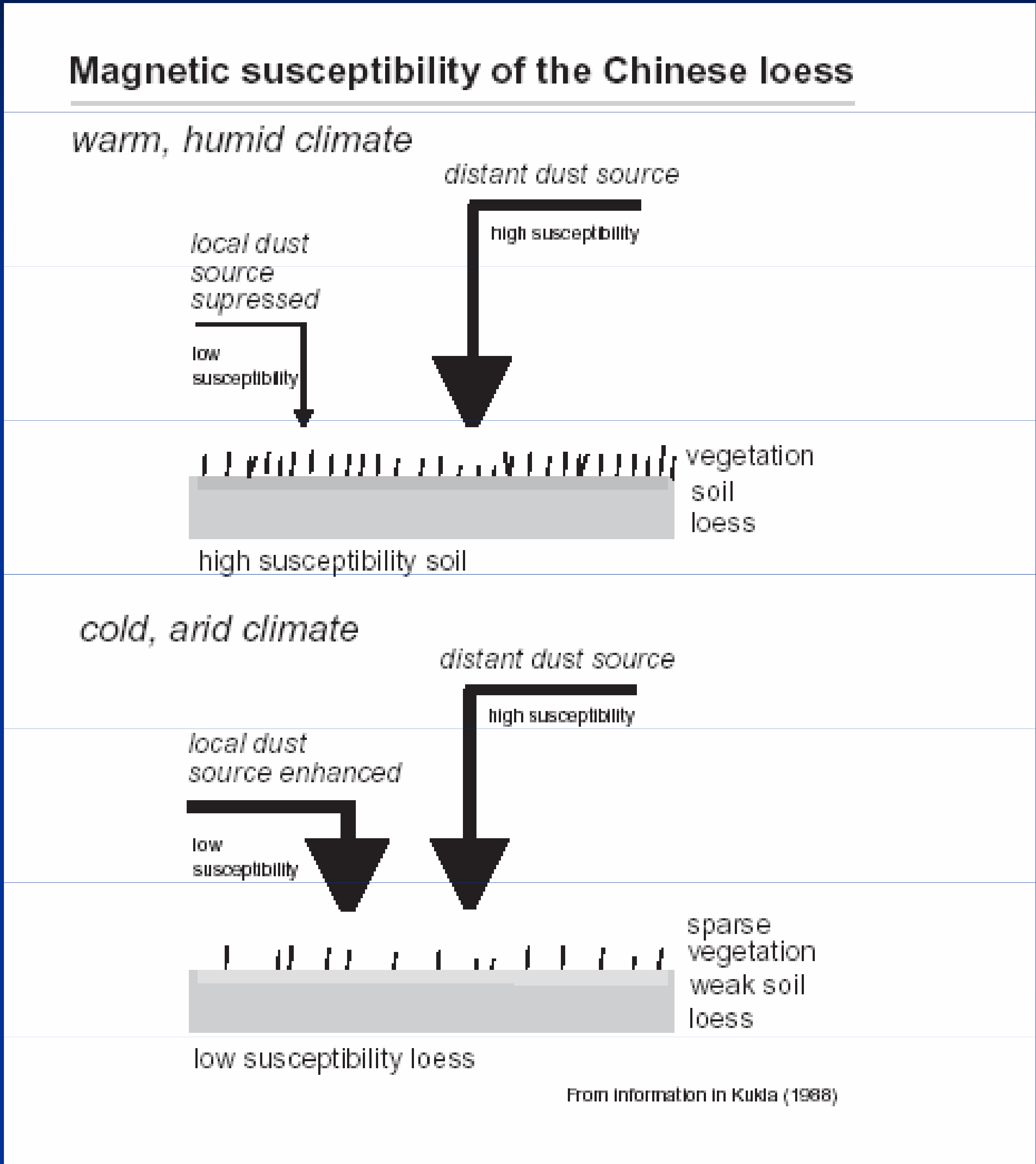

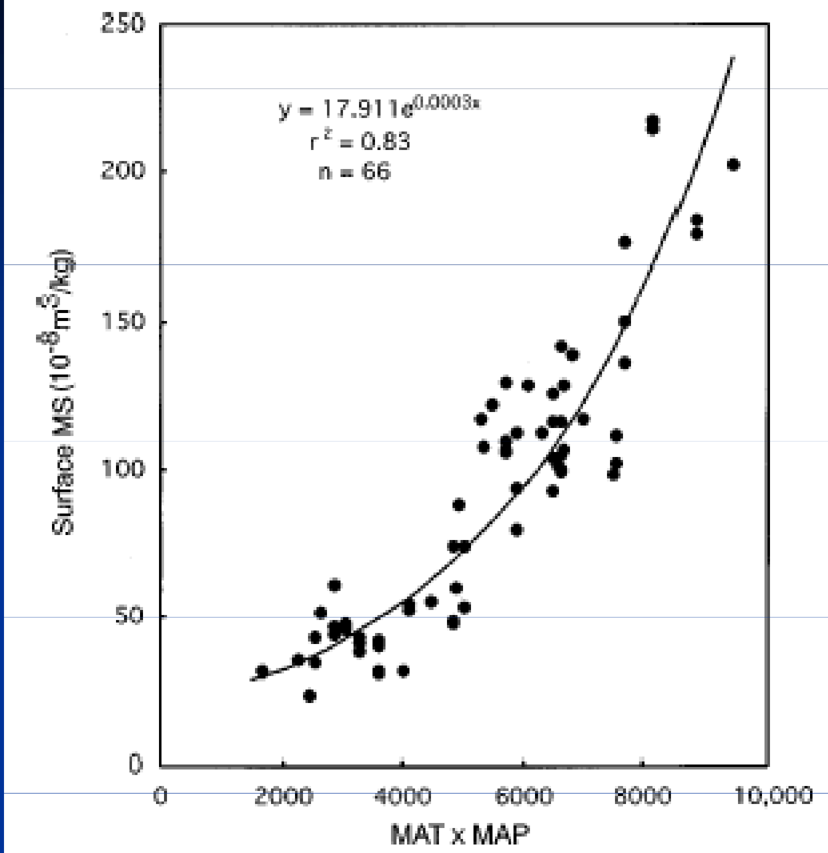

FIG. 8. Surface MS plotted as a function of MAT × MAP (°C mm).

Studies on modern soils show a positive relationship between magnetic susceptibility (MS)and mean annual temperature (MAT) and precipitation (MAP).

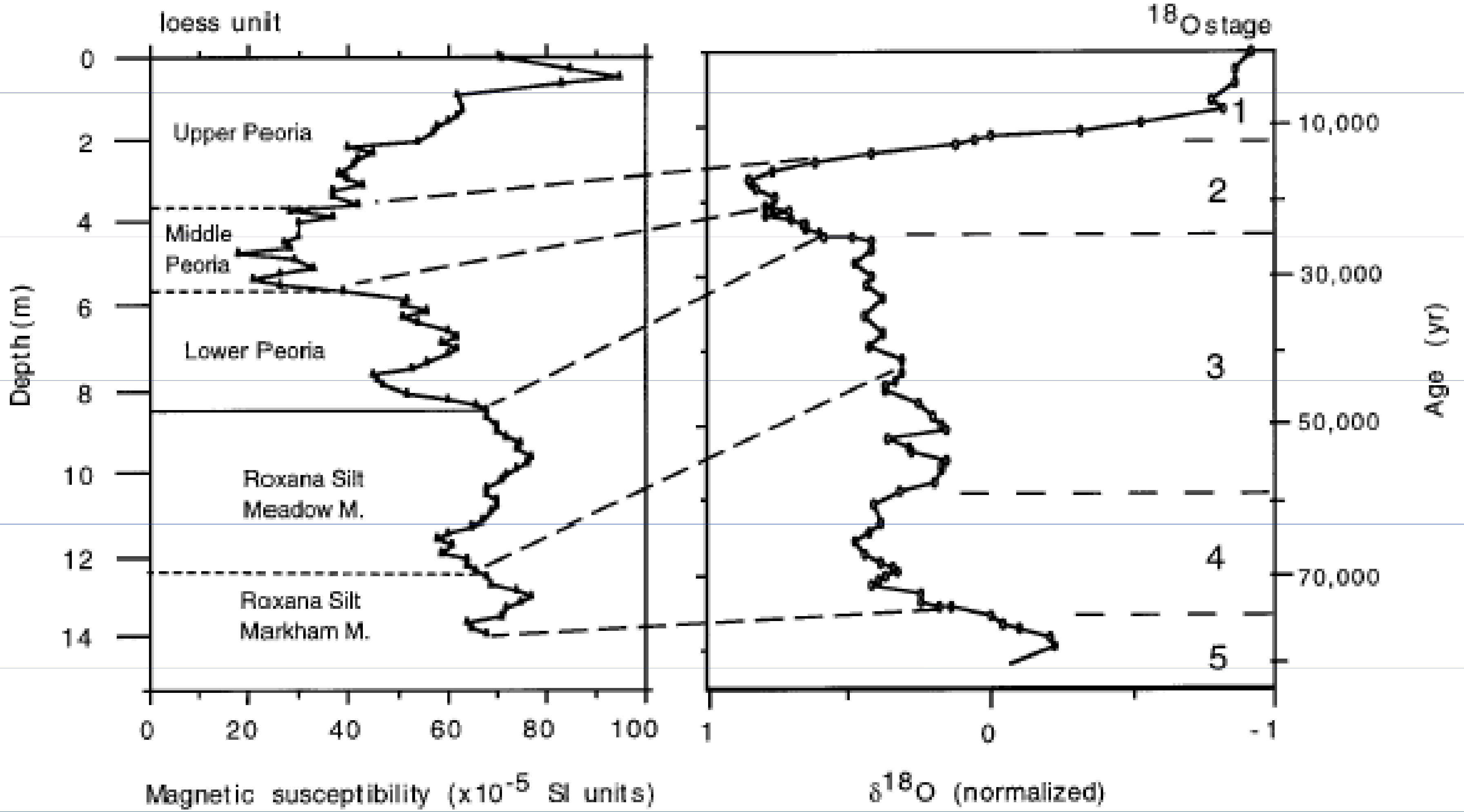

FIG. 7. Magnetic susceptibility from the G-56 core (left) and the oxygen isotope record from deep sea Indian Ocean sediments (right; from Martinson *et al.*, 1987). Correlations are based upon ages estimated from loess units (Fig. 6) in comparison with the high resolution orbitally tuned chronology devised by Martinson *et al.*, 1987.

LAKUSTRINNÍ SEDIMENTY

Jezerní systémy

Otevřené systémy

Oligotrofní, dobře prokysličené

- *Roční varvy*
- *turbidity*

Uzavřené systémy:

Eutrofní, špatně prokysličené

- *Organická hmota*
- *Evapority*
- *karbonáty*

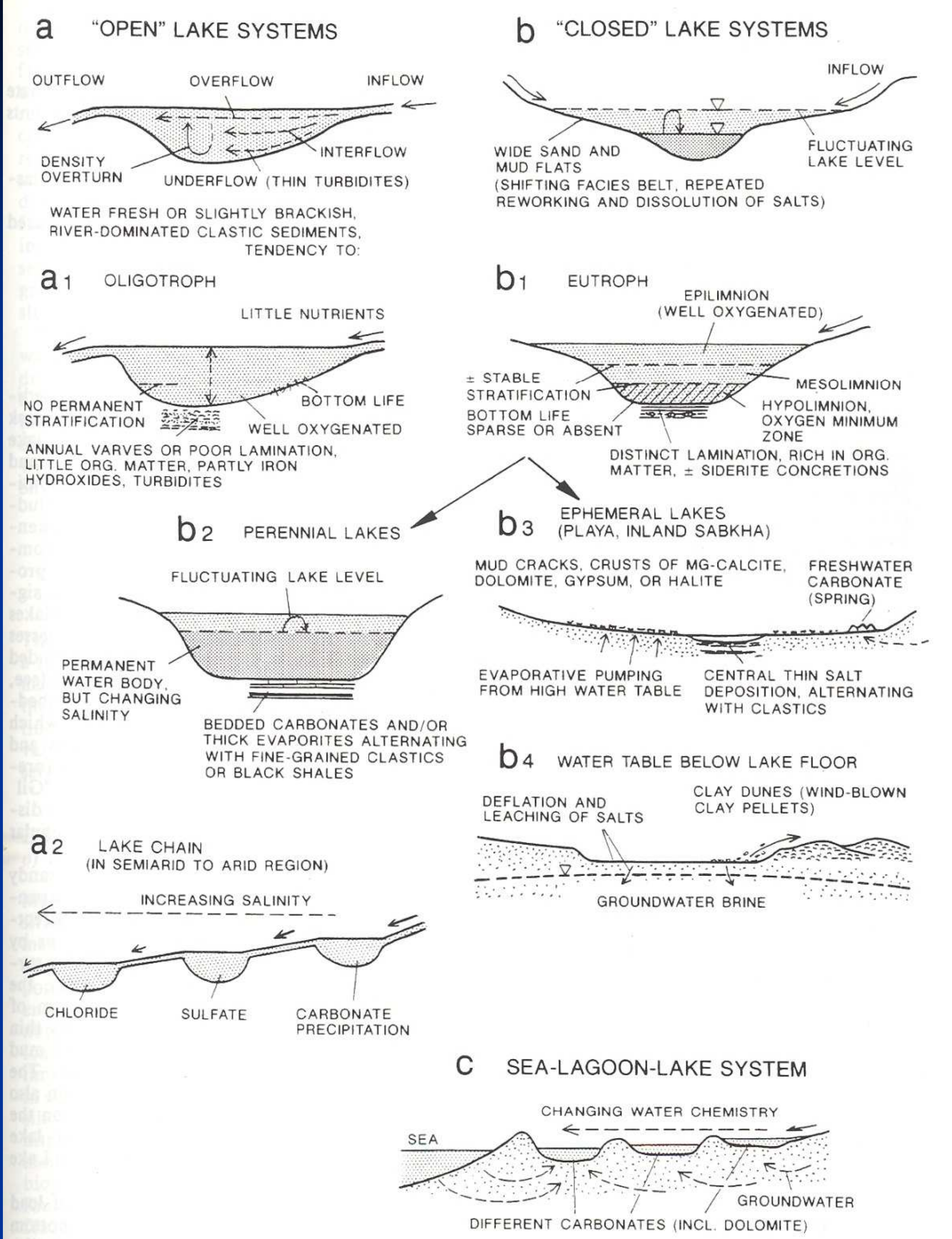

Otevřený jezerní systém postglaciální výplň jezera

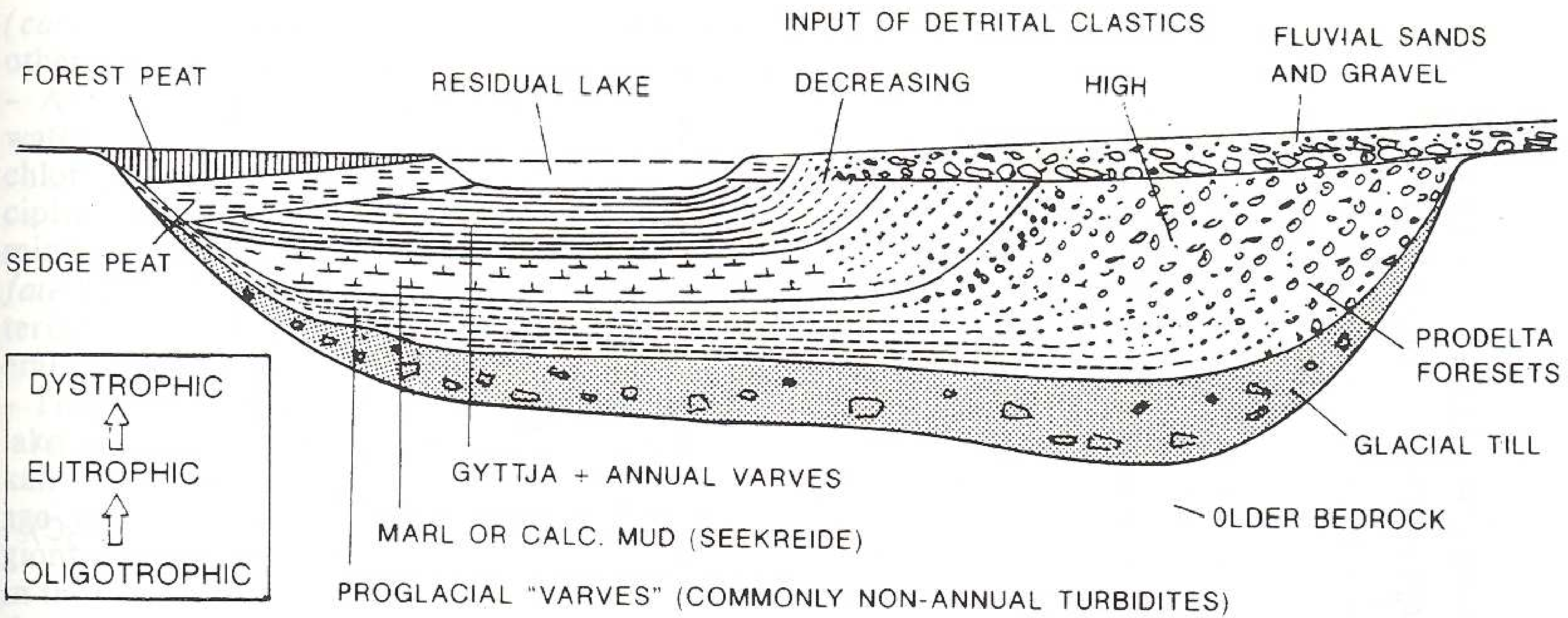

Fig. 2.29. Generalized scheme of the post-glacial sediment fill of a glacier-shaped lake. (After Dean 1981). It is assumed that the input of detrital clastics decreases with time and finally ends

Varvy

- The light-colored layer of silt and clay
  - formed during the spring and summer
  - and the dark layer made up of smaller particles
  - and organic matter formed during the winter
  - when the lake froze over
- Varved deposits
  - may also contain
  - gravel-sized particles,
  - known as dropstones,
  - released from melting ice

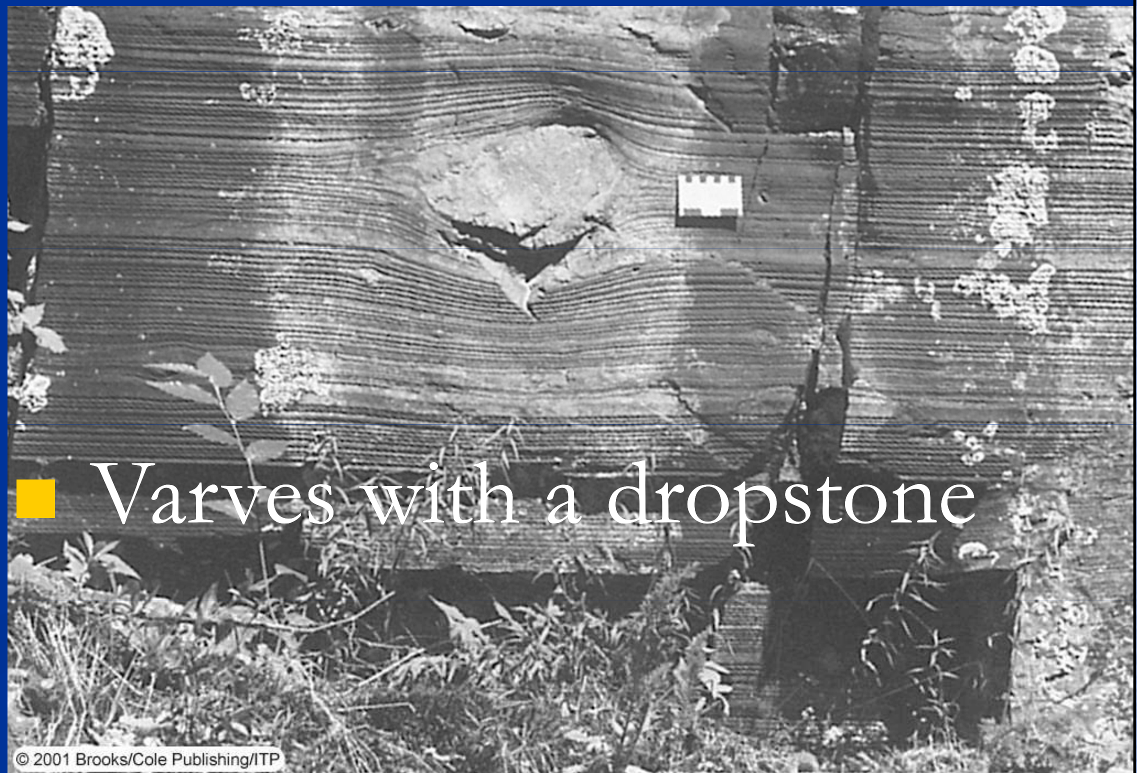

- Varves with a dropstone

STOKESŮV ZÁKON

$$u = \frac{1}{18} \frac{\rho_s - \rho_f}{\eta} g D^2$$

Zrnitostní frakce: silt – jíl

Silt klesá ke dnu rychleji

Jíl klesá ke dnu pomaleji

u = rychlost usazování

ρ_s = hustota pevné částice

ρ_f = hustota kapaliny

g = gravitační zrychlení

D = průměr částice

η = kinematická viskozita

OTHER NUMERICAL DATING TECHNIQUES

VARVE CHRONOLOGY

RTG densitometrie varvitů

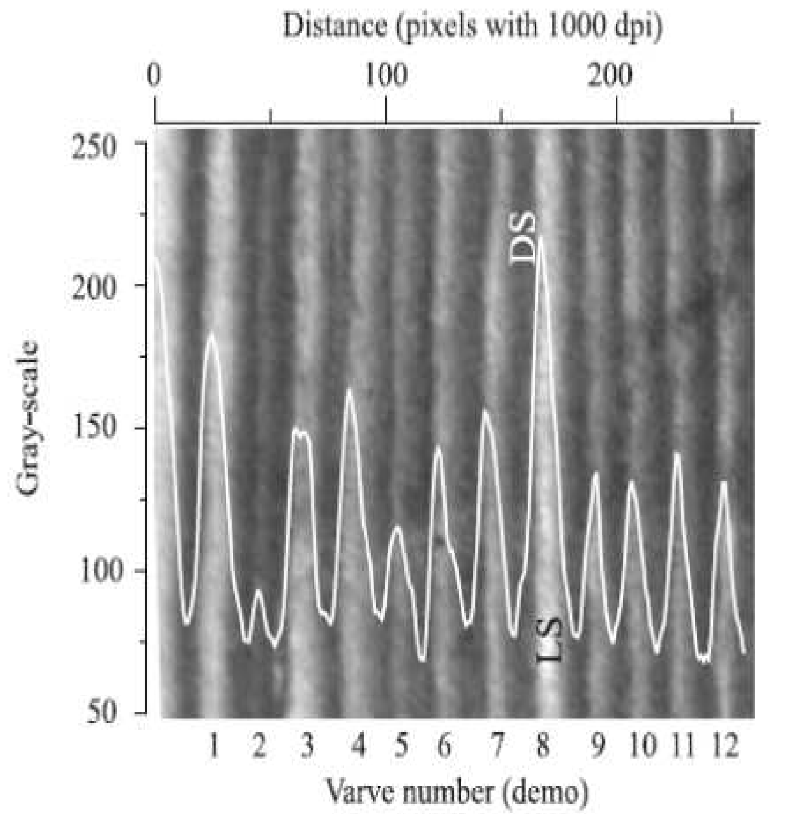

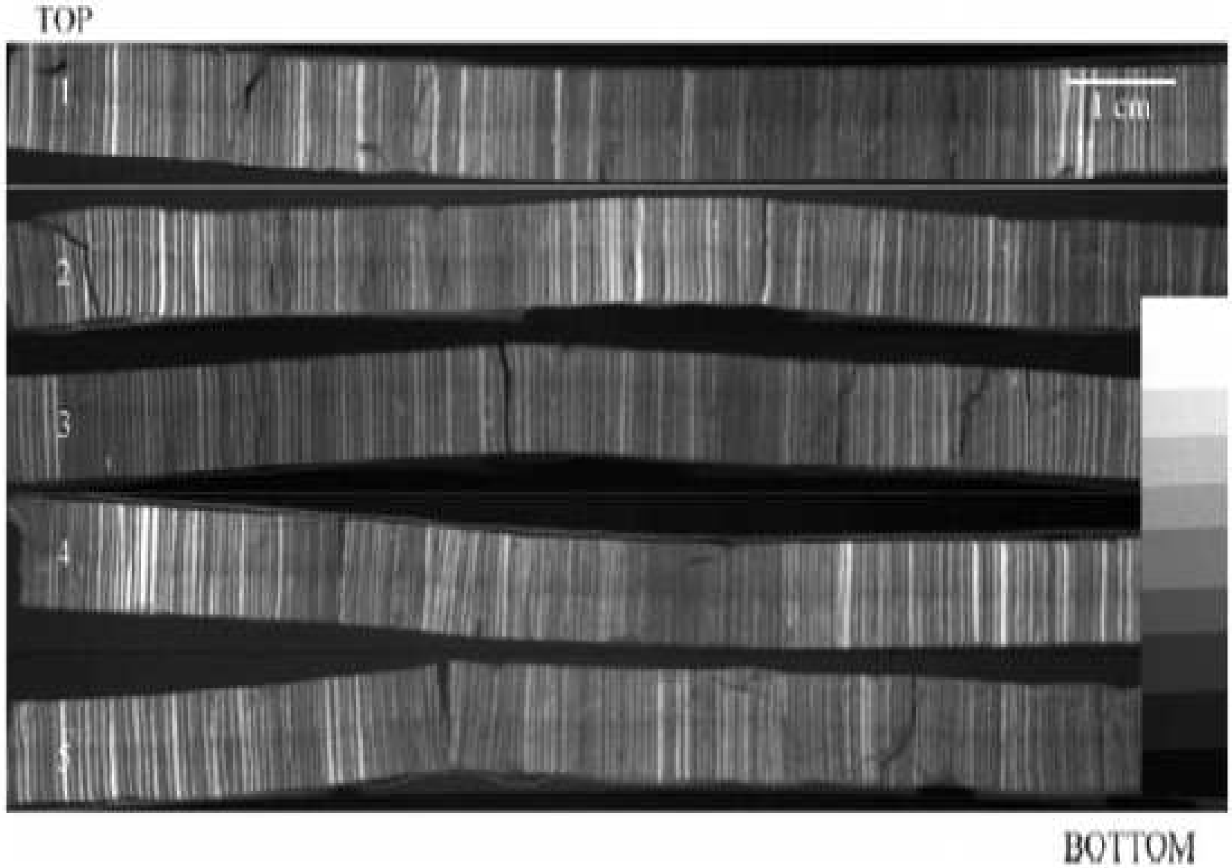

Figure 3. X-ray images of clastic-organic varves from Lake Nautajärvi representing the period from ca. AD 200 to 600 BC. Radiographs are taken from epoxy-embedded slabs of uniform 2-mm thickness. A calibration sample made of glass is seen in the right-hand corner.

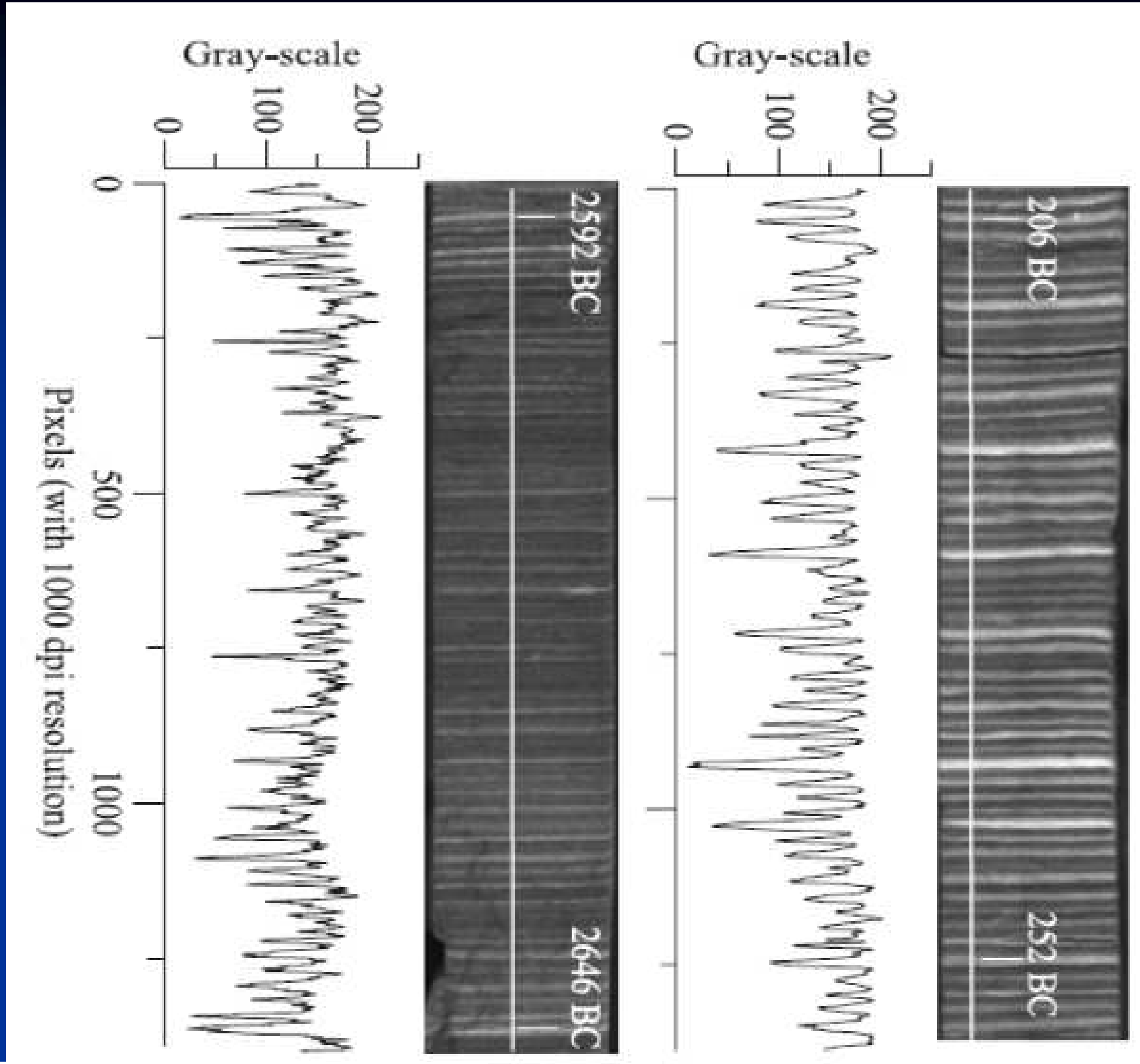

Figure 5. Two X-ray radiographs from 206 to 252 BC and 2592 to 2646 BC of Lake Nautajärvi sediment show that the visually striking components, mineral-rich and organic laminae, are far from perfect throughout the sequence for studies of automated line-scan image analysis. Therefore, it is also necessary to estimate the error in the varve chronology.

Chronologie varvitů

- Deglaciation in Scandinavia
  - Based primarily on varve chronologies.

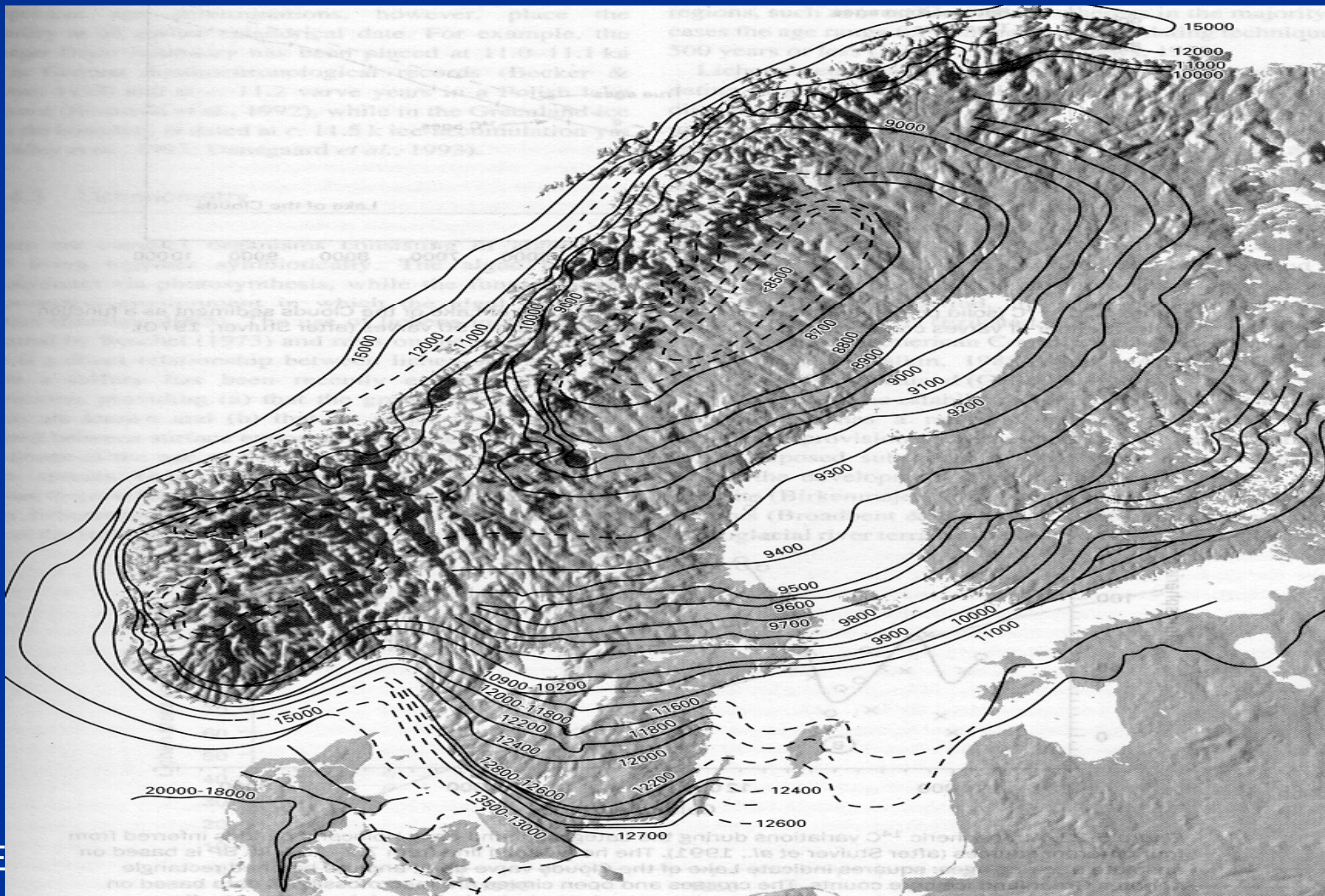

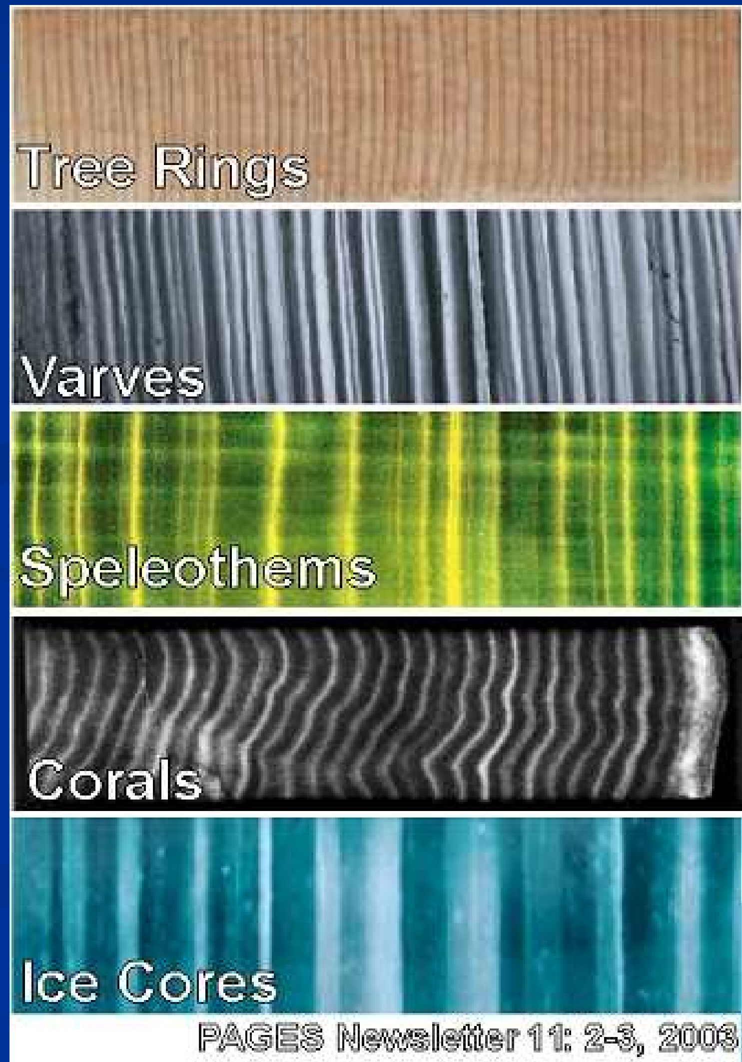
Tree Rings
Varves
Speleothems
Corals
Ice Cores
PAGES Newsletter 11: 2-3, 2003

Varvy a “varvovité“ sedimenty

- Více „varvů“ za jednu sezónu : ???
- Hustotní proudy !

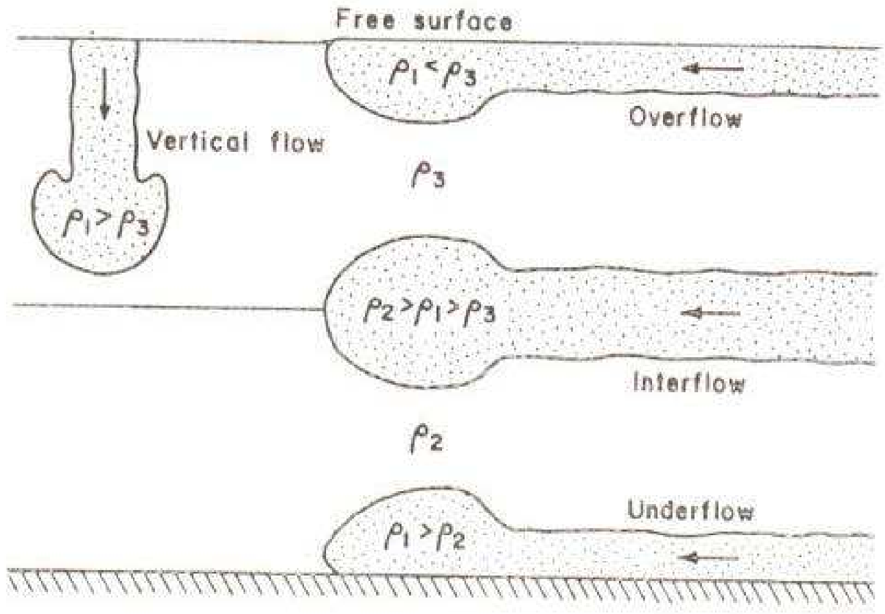

Fig. 1-25. Principal types of gravity current.

Hyperpyknické proudy

hlava – tělo – ocas

Rychlost šíření hyperpyknického proudu

$$U_h = k \left| \frac{(\rho_1 - \rho_2)g}{\rho_2} h_2 \right|^{1/2}$$

Rychlost nezávislá na velikosti zrna

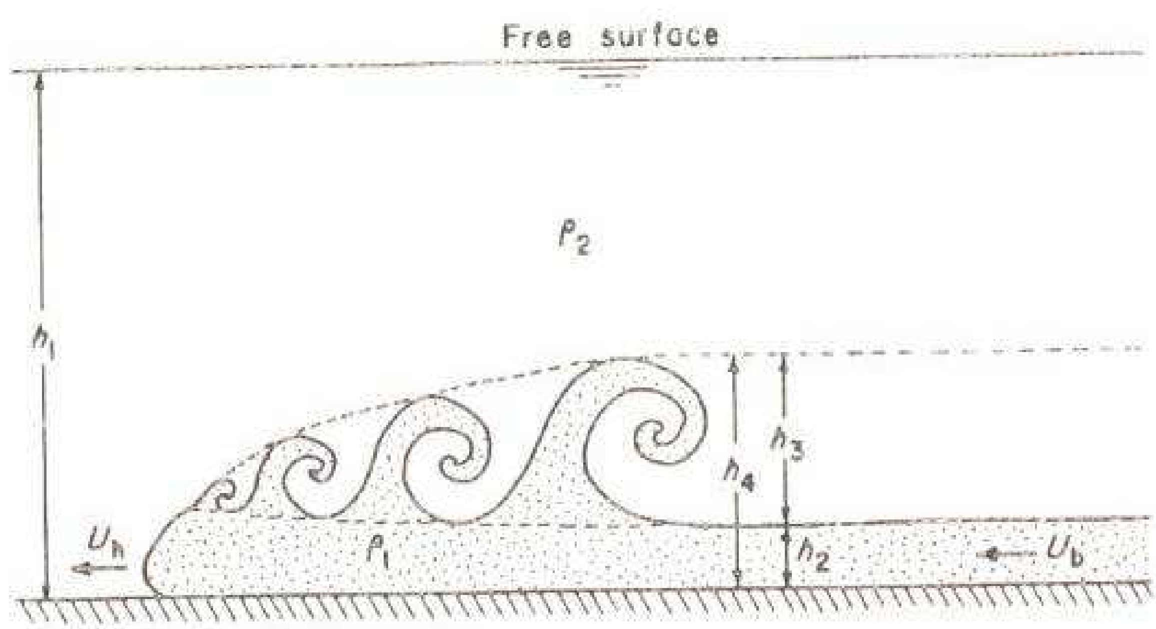

Fig. 1-31. Definition diagram for an underflowing gravity current.

- Turbidity: Jezera, která nezamrzají
- Varvity: jezera, která periodicky zamrzají, klimatický indikátor

Brněnská přehrada

Jezerní (přehradní) sedimentace

Svahová sedimentace

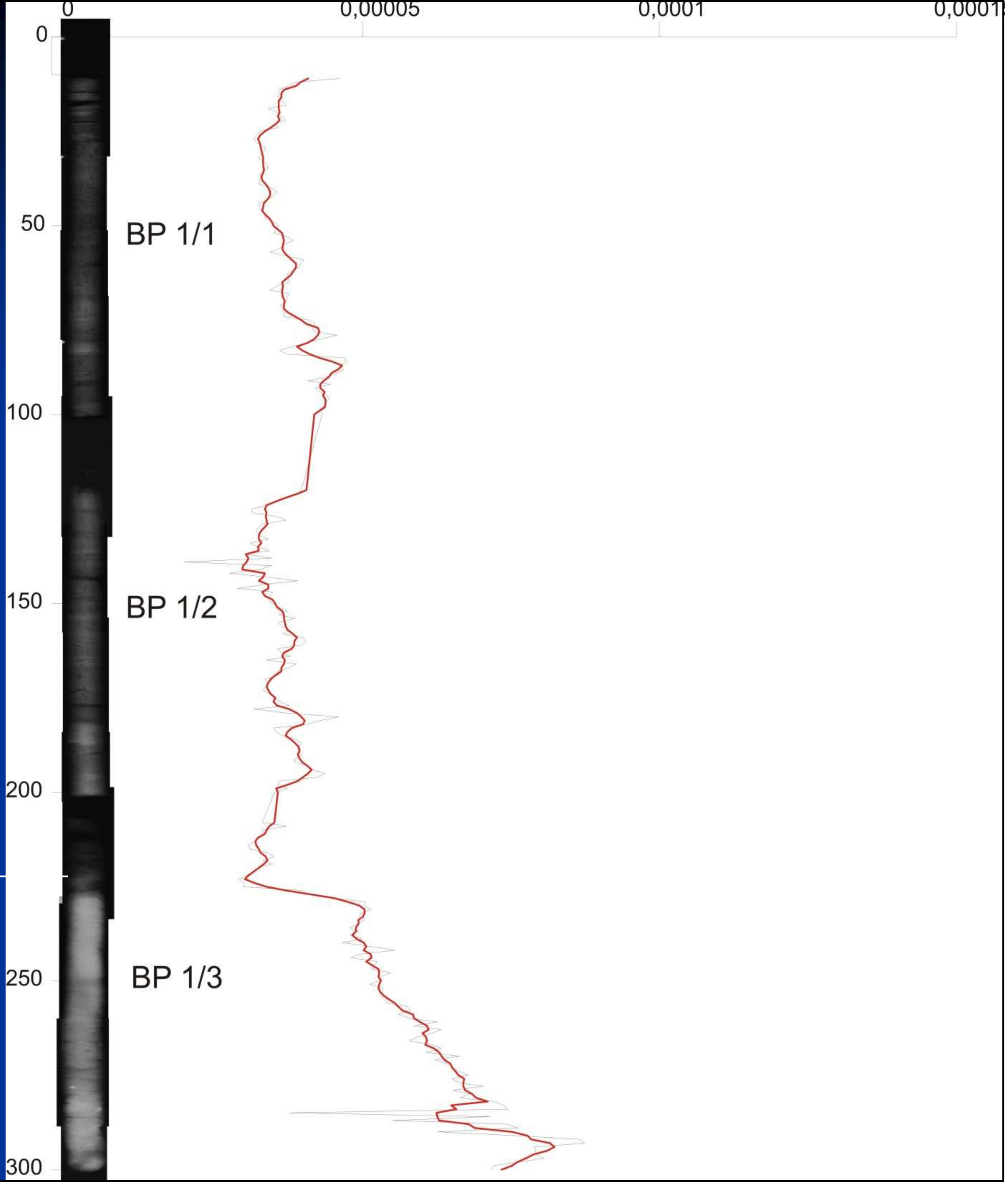

Mrtvé rameno Čerťák (U. Hradiště) povodňové vrstvy v sedimentch jezera

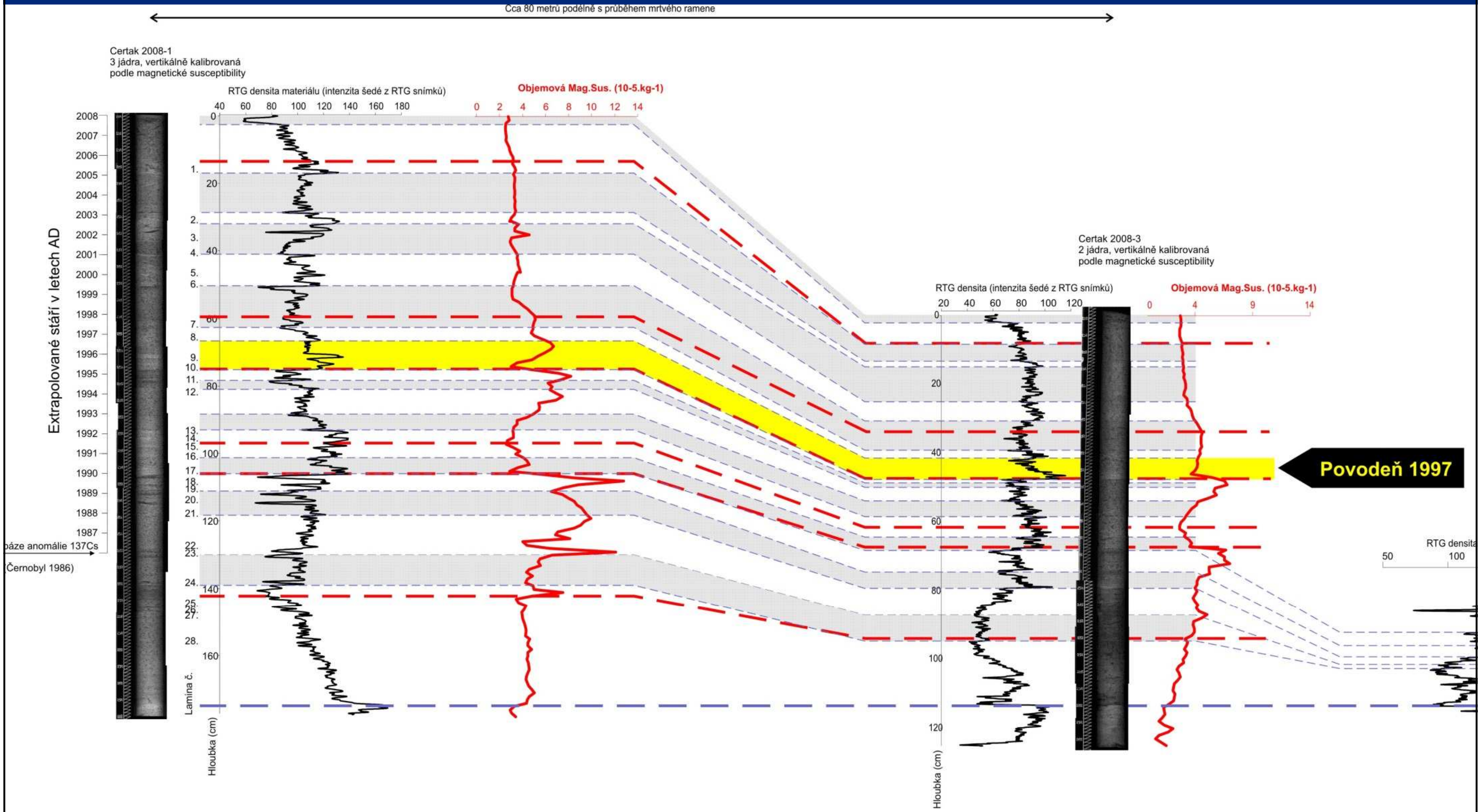

Korelace jezerních sedimentů se sprašemi jezero Bajkal, klimatické archívy

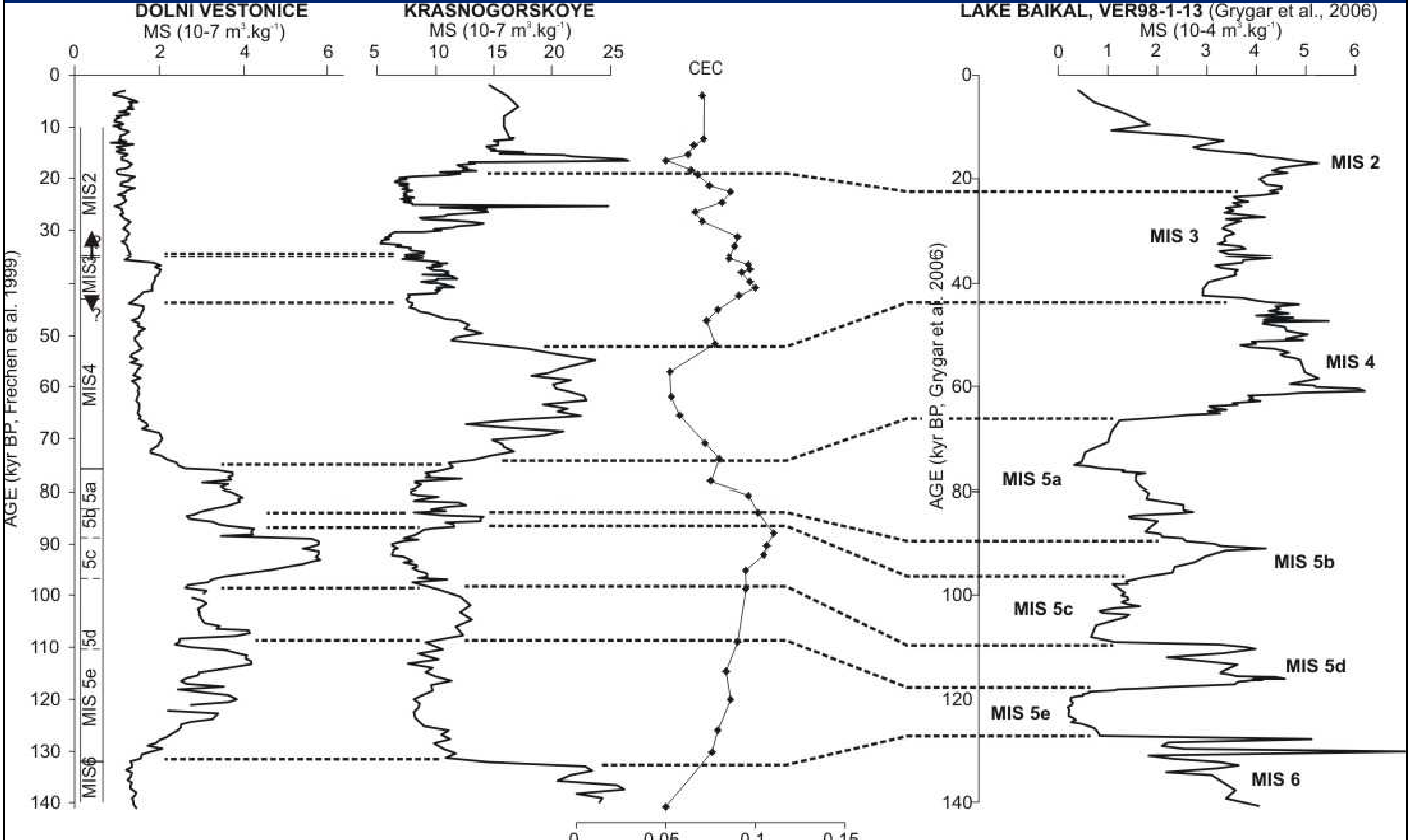

FLUVIÁLNÍ SEDIMENTY

SPÁDOVÁ KŘIVKA

A stream in balance with its surroundings is called a **graded stream**. Such a stream balances erosion, sediment transport, and sediment deposition along its length, and has a smooth concave-upward profile from beginning to end. Examples of two graded streams are shown below.

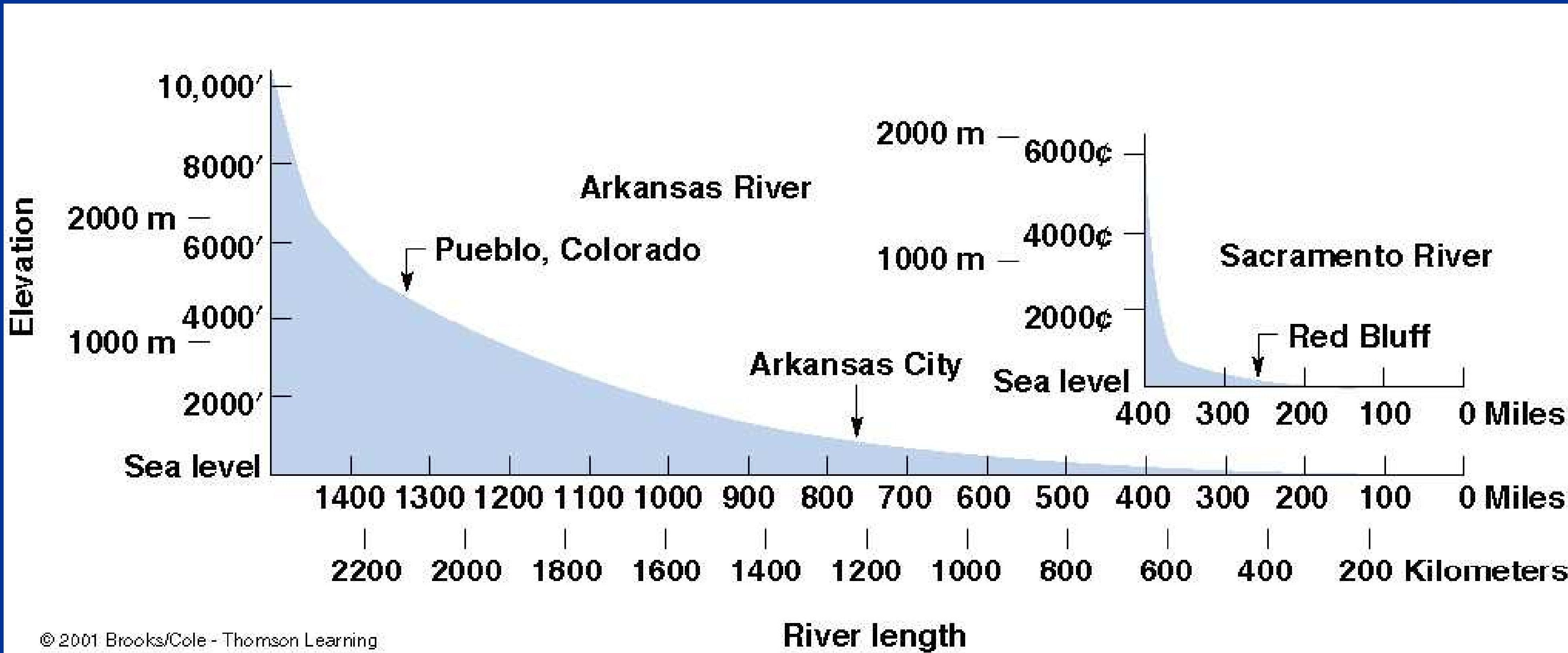

FLUVIÁLNÍ EROZE

Erosion by streams has shaped the land surface worldwide over geologic time. This spectacular gorge in Colorado is entirely a product of stream erosion acting over several millions of years.

The ability of a stream to erode relates to two things:

1. **Velocity** -- the speed of the water, generally measured in feet per second.
2. **Discharge** (průtok) - the total amount (volume) of water carried by the stream. Discharge is generally measured in cubic feet per second, or **cfs**.

PRŮTOK vs. NASYCENÍ SEDIMENTEM

This graph shows the connection between discharge and the amount of sediment a stream can carry (sediment derived from erosion of the stream's banks and channels).

A 10x increase in discharge corresponds to a nearly 100x increase in erosion and sediment load carried.

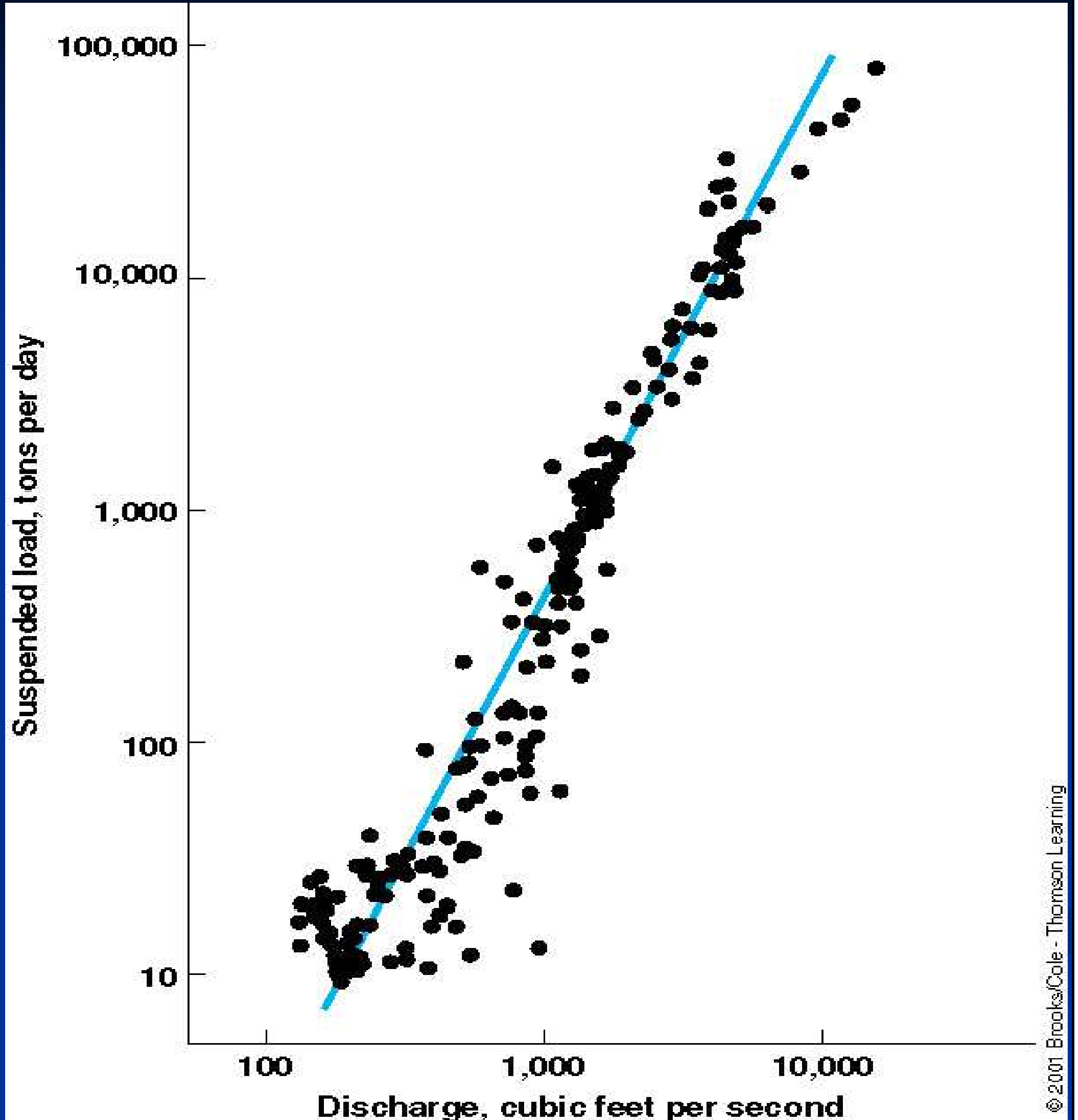

ŘÍČNÍ SYSTÉMY PODLE SPÁDU

- Aluviální systémy
- Divočící řeky
- Meandrující řeky
- Říční delty

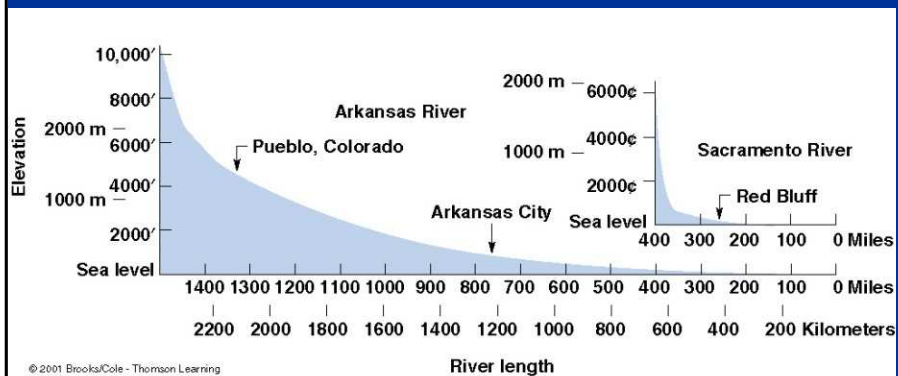

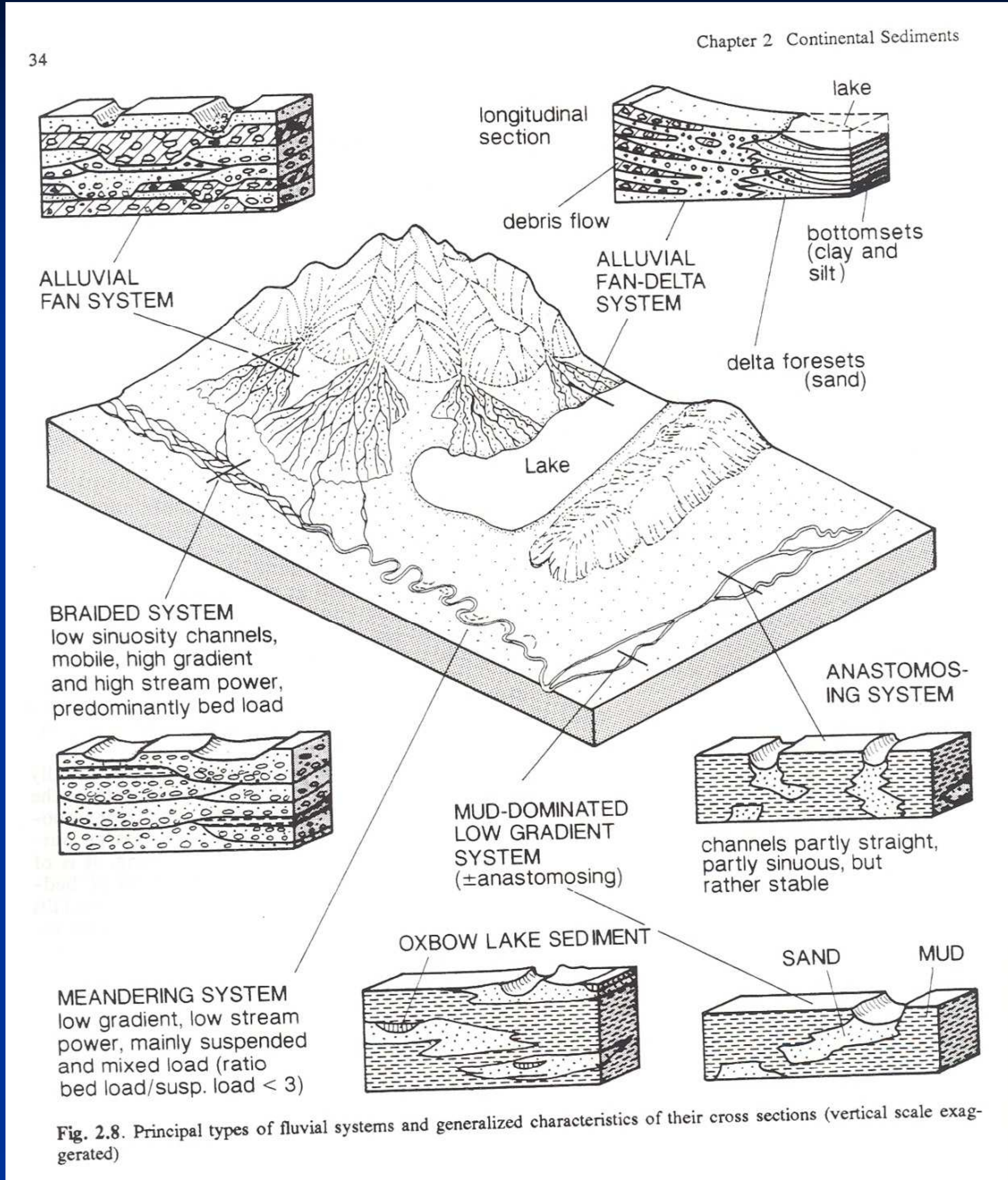

Fig. 2.8. Principal types of fluvial systems and generalized characteristics of their cross sections (vertical scale exaggerated)

In arid areas, like in the desert mountains next to Death Valley, CA in this photo, streams flow only intermittently after heavy rain storms. After heavy rains, water charges down the canyons as **flash floods**, carrying large amounts of sediment as **debris flows** (recall Chapter 7: Mass Wasting). As the debris flows slow down, this sediment is deposited to form **alluvial fans** -- broad sloping sheets of coarse sediment at the mouths of mountain canyons.

This air photo of the Missouri River beautifully shows the main **meandering channel** and the adjacent **floodplain** (the band of darker land along the channel).

Farms and fields produce the patchy appearance of the floodplain here. The fertile soil of floodplains is intensively farmed throughout the world. Intensive human use of floodplains is one of the problems we will consider later in this lesson.

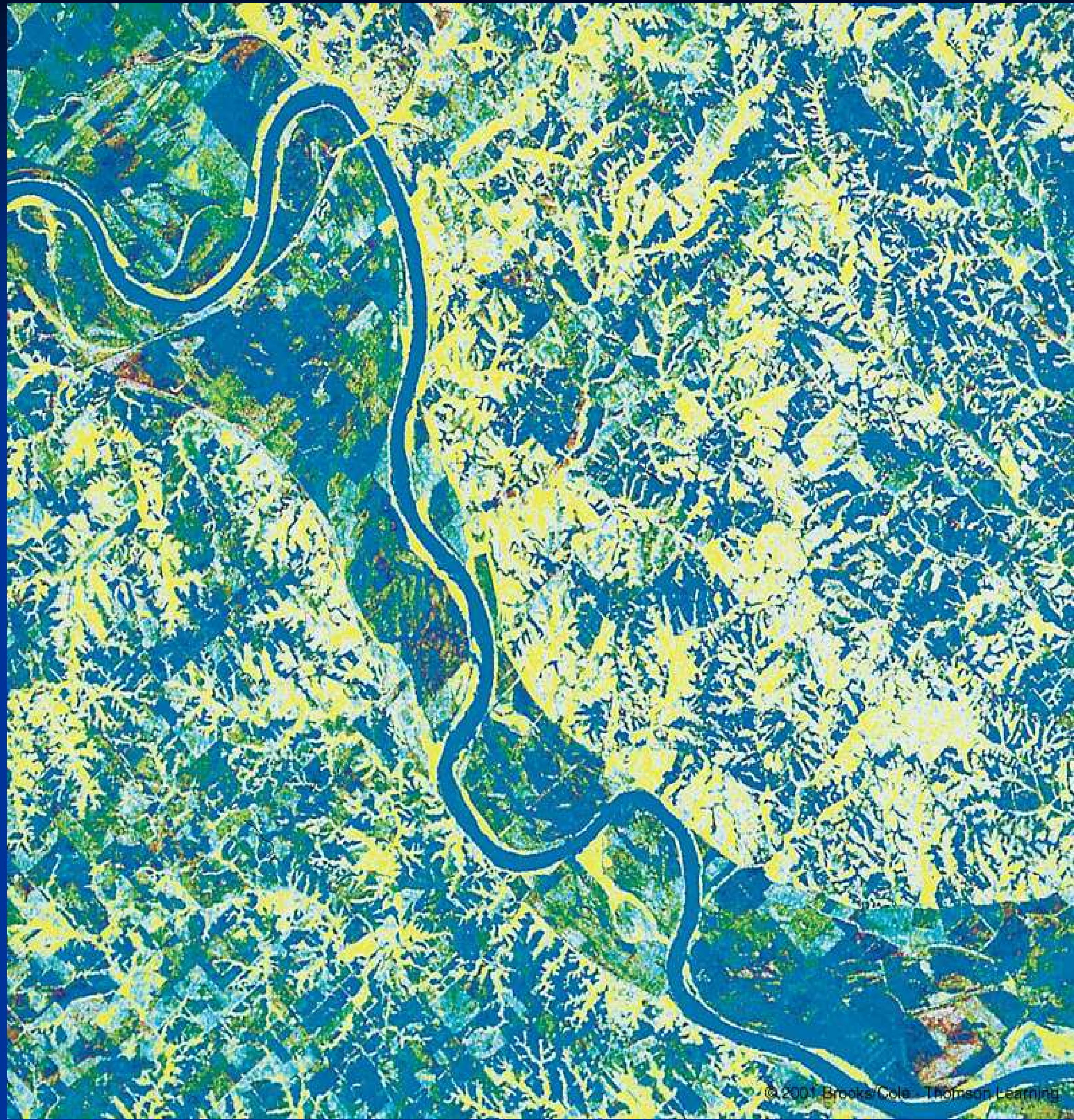

Sediment particles of many types and sizes are transported by streams.

Deltas are deposits of stream sediment that form where streams end at standing bodies of water, like oceans or lakes.

The MIssissippi River Delta shown here is an example.

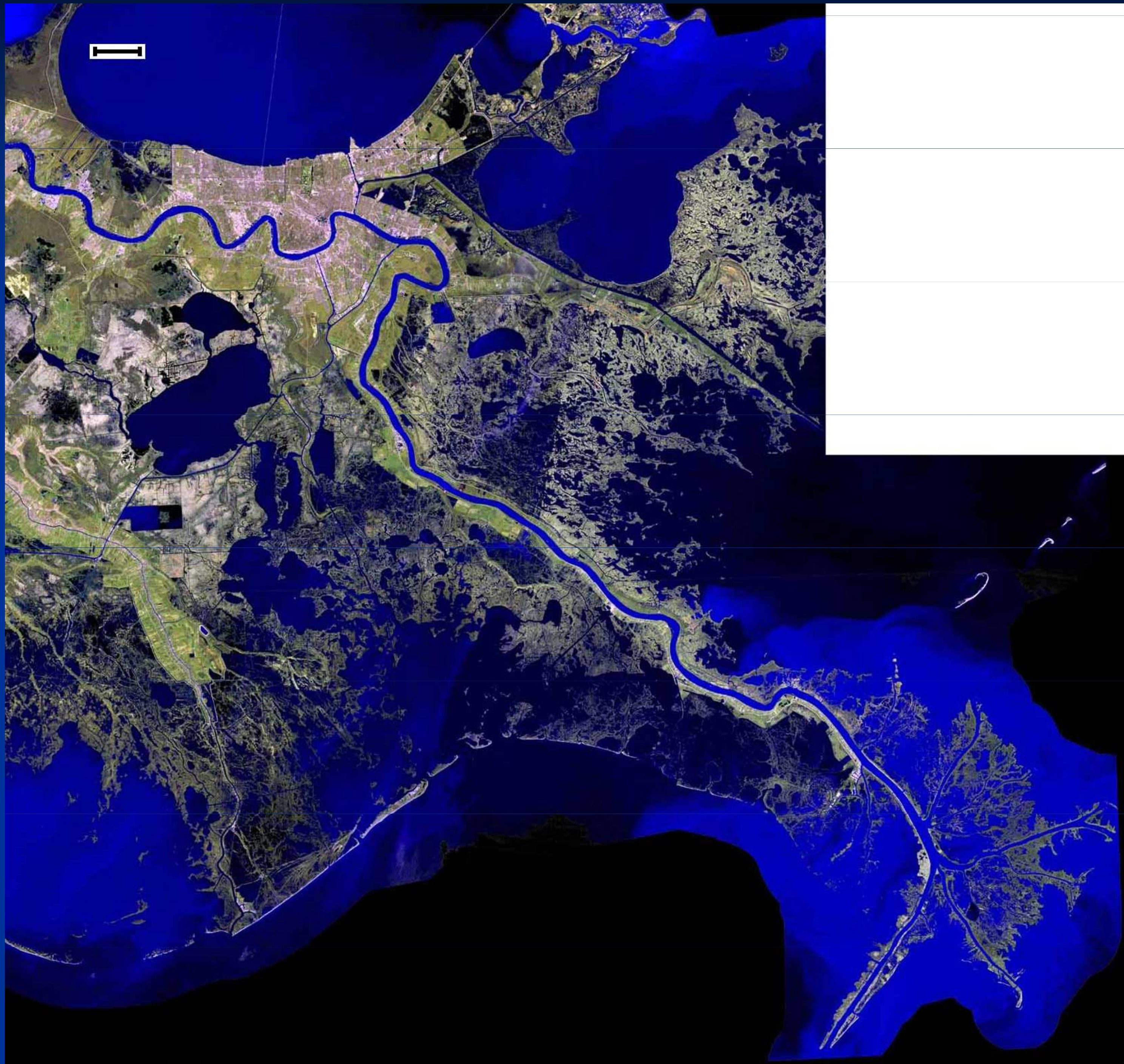

Fluviální eroze vs. sedimentace: estuarinní systémy → deltové systémy

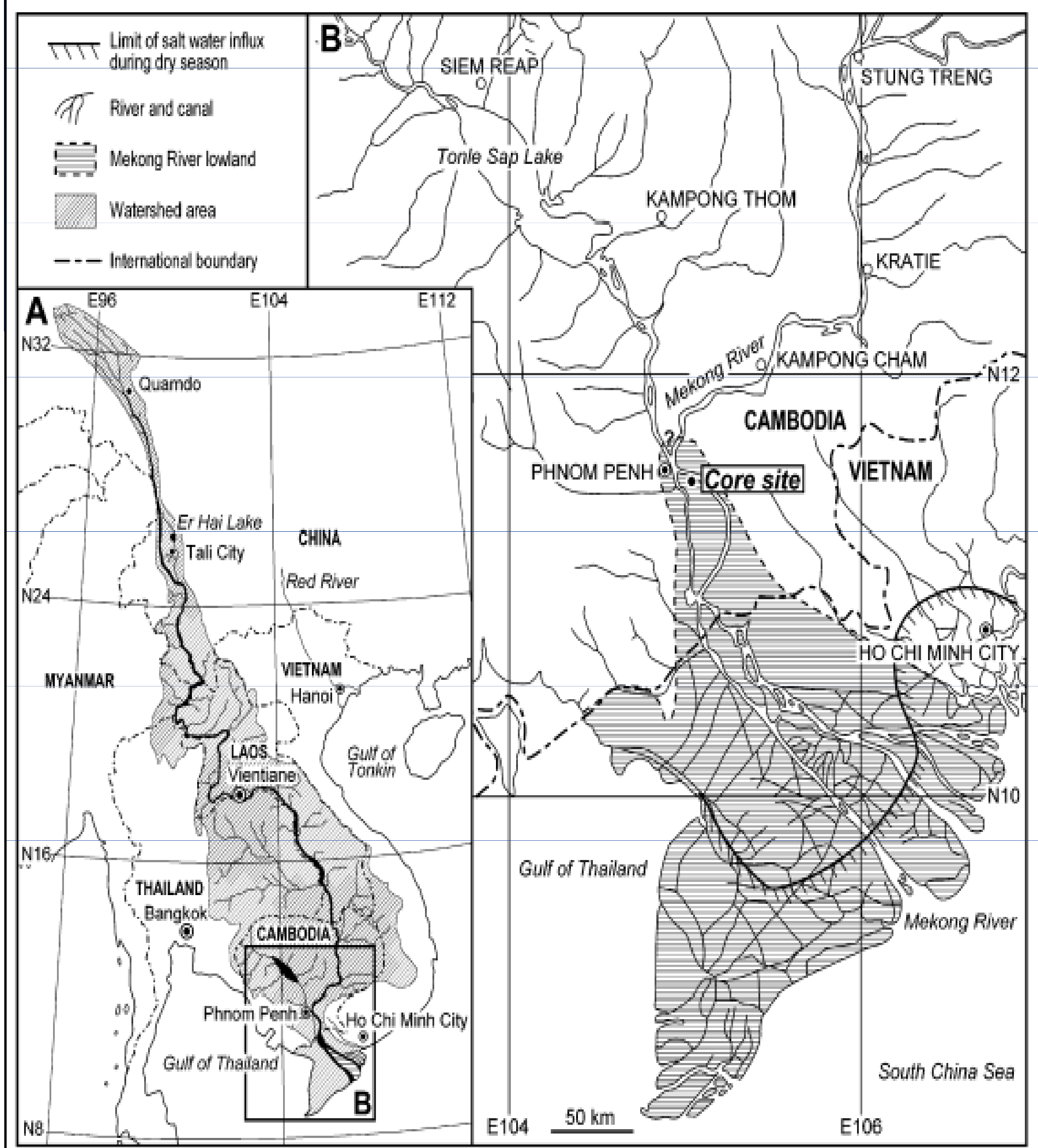

- Mekong River

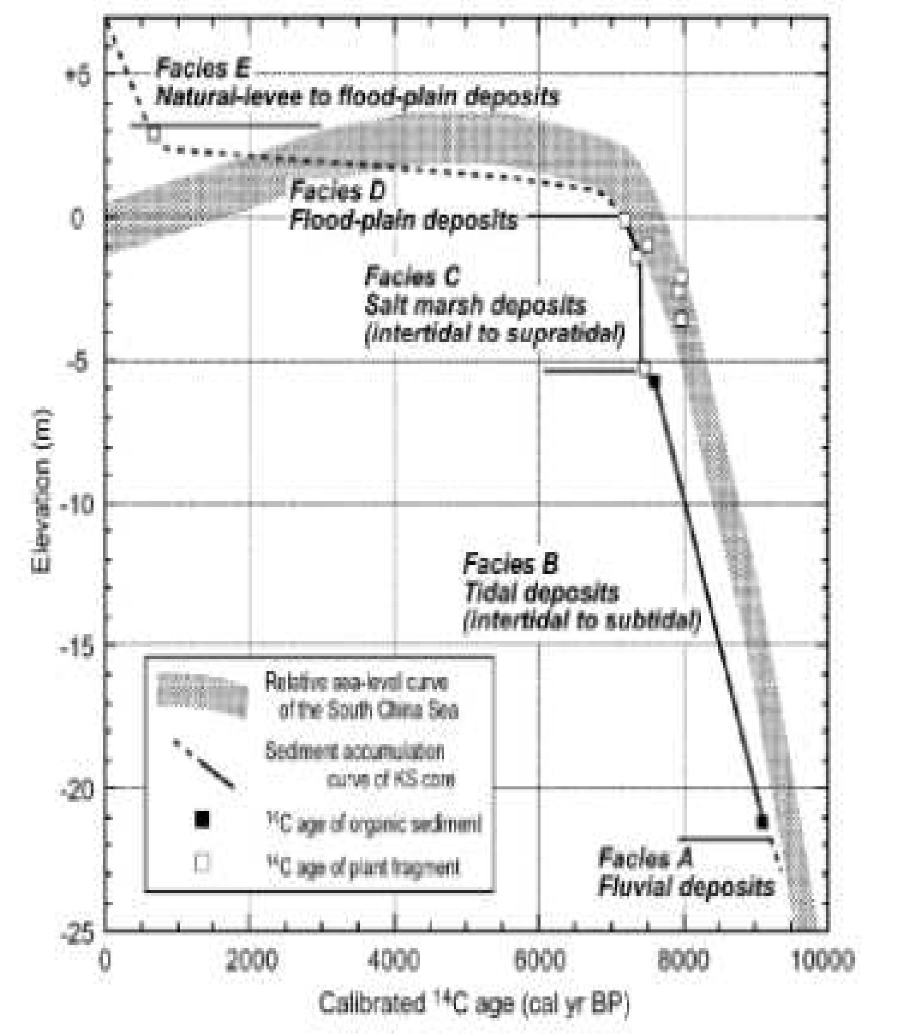

Hydrodynamika rozhraní kapalina – nesoudržný sediment
Jednosměrné proudění

- **Unidirectional flow** leads predominantly to asymmetric bedforms (two- or three-dimensional) or plane beds
  - Current ripples
  - Dunes
  - Plane beds
  - Antidunes

1. **Erosion in the trough of a bedform**

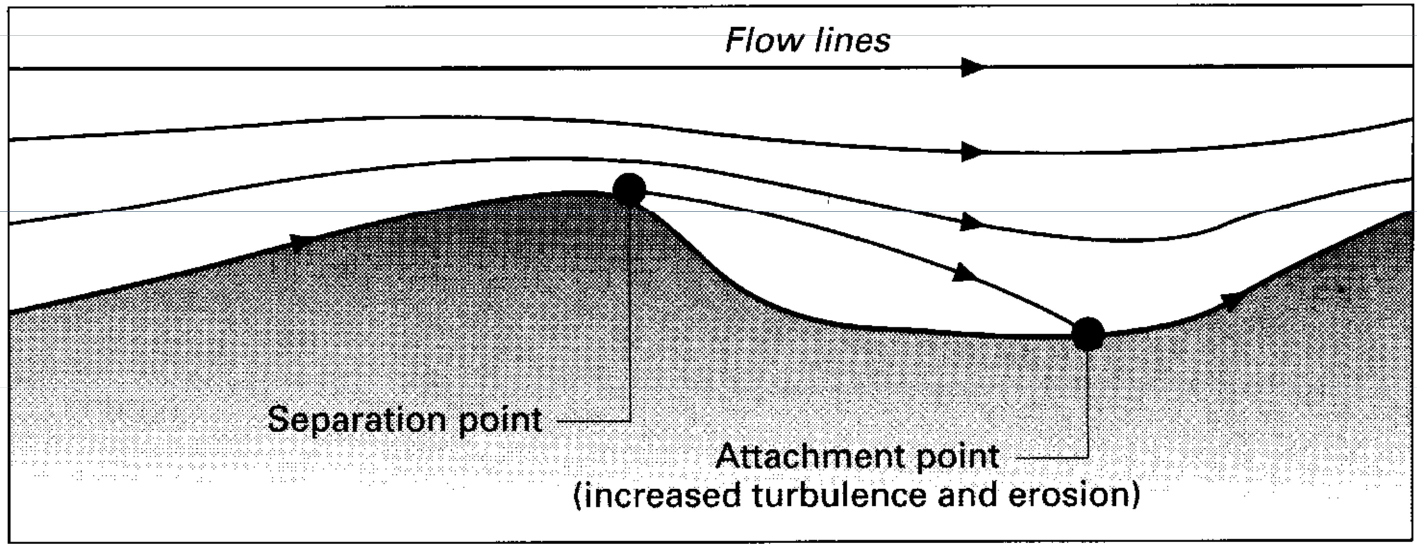

2. **Development of counter-currents in lee of bedform**

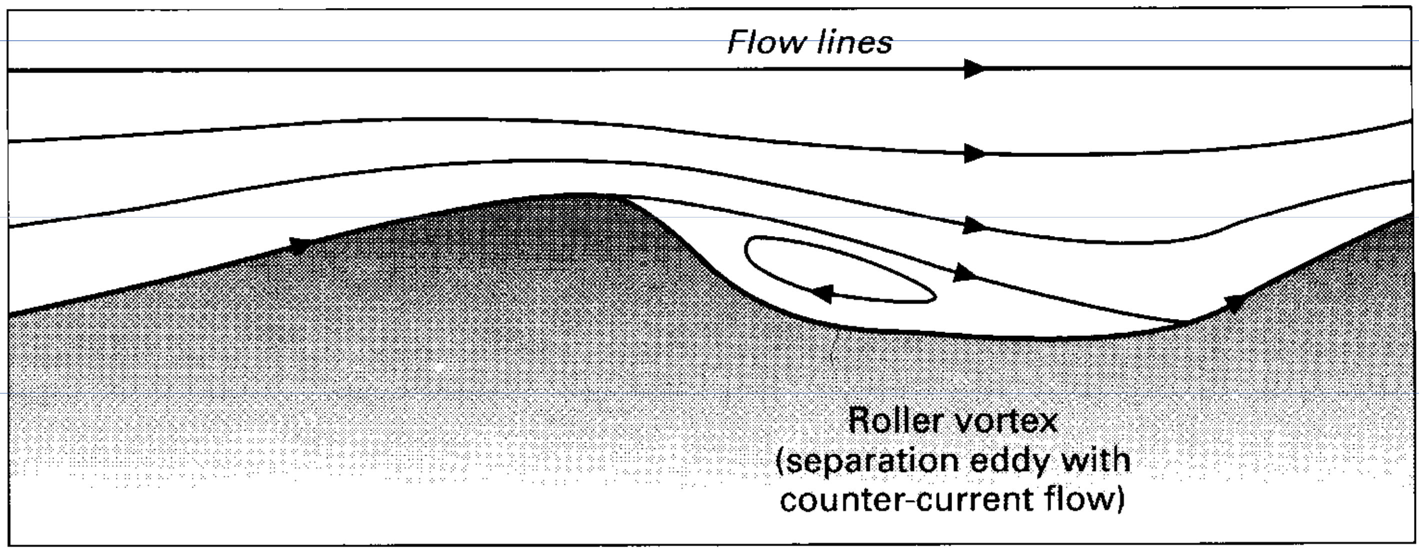

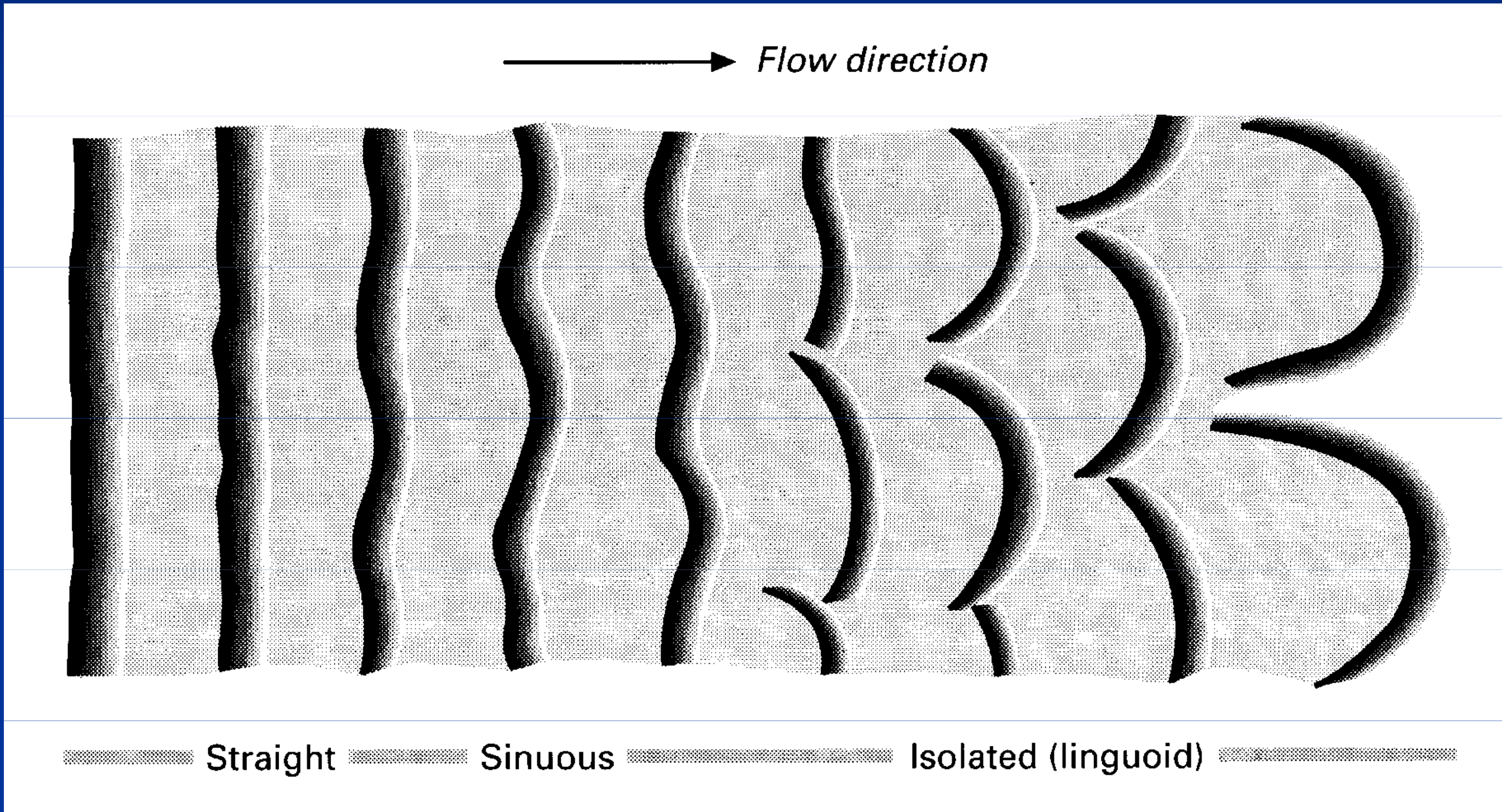
Flow direction
Straight
Sinuous
Isolated (linguoid)

Animation

Antiduny

- Jednosměrné vodní proudění s volným povrchem – ve fázi s povrchovým prouděním kapaliny
- Stacionární (nemigrují) nebo migrují proti směru proudění
- Sedimentace na návětrné straně, eroze na závětrné straně
- L <= 10m

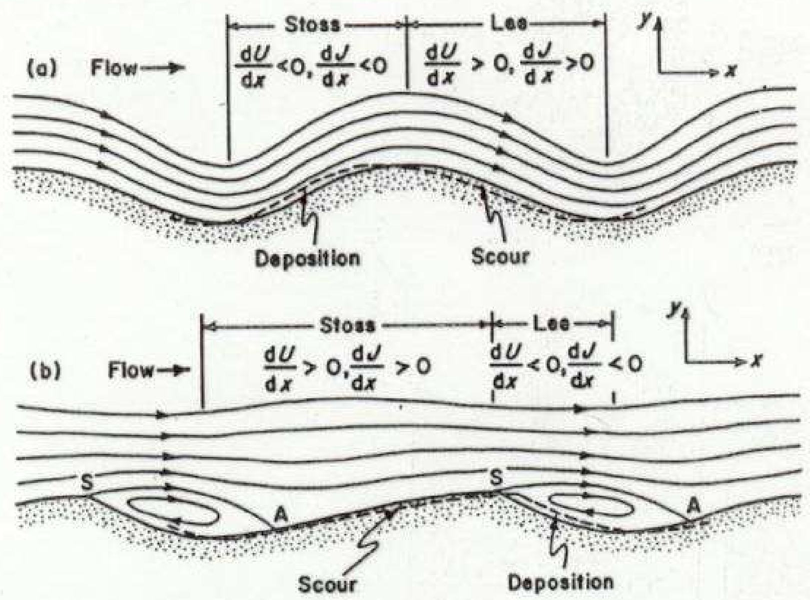

Fig. 7-2. Schematic representation of flow and sediment transport over (a) antidunes, and (b) current ripples and dunes. U=mean flow velocity; J=sediment transport rate.

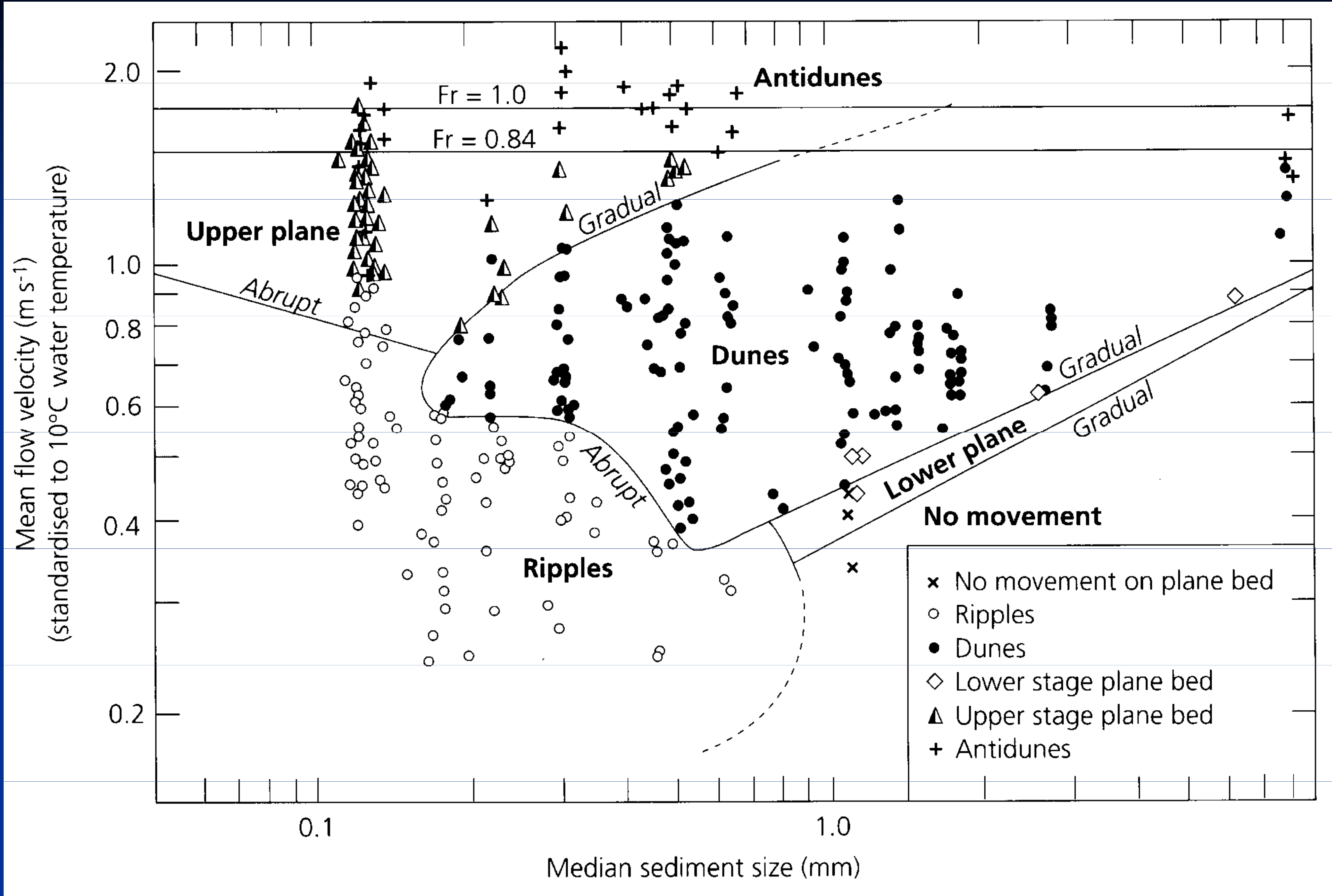

Antidunes
Fr = 1.0
Fr = 0.84
Upper plane
Gradual
Abrupt
Dunes
Abrupt
Gradual
Lower plane
Gradual
No movement
Ripples
× No movement on plane bed
○ Ripples
● Dunes
◇ Lower stage plane bed
Upper stage plane bed
+ Antidunes
2.0
1.0
0.8
0.6
0.4
0.2
0.1
1.0
Mean flow velocity (m s-1)
(standardised to 10°C water temperature)
Median sediment size (mm)

Oscilační proudění

- **Oscillatory flow** due to waves causes predominantly symmetric bedforms (wave ripples)

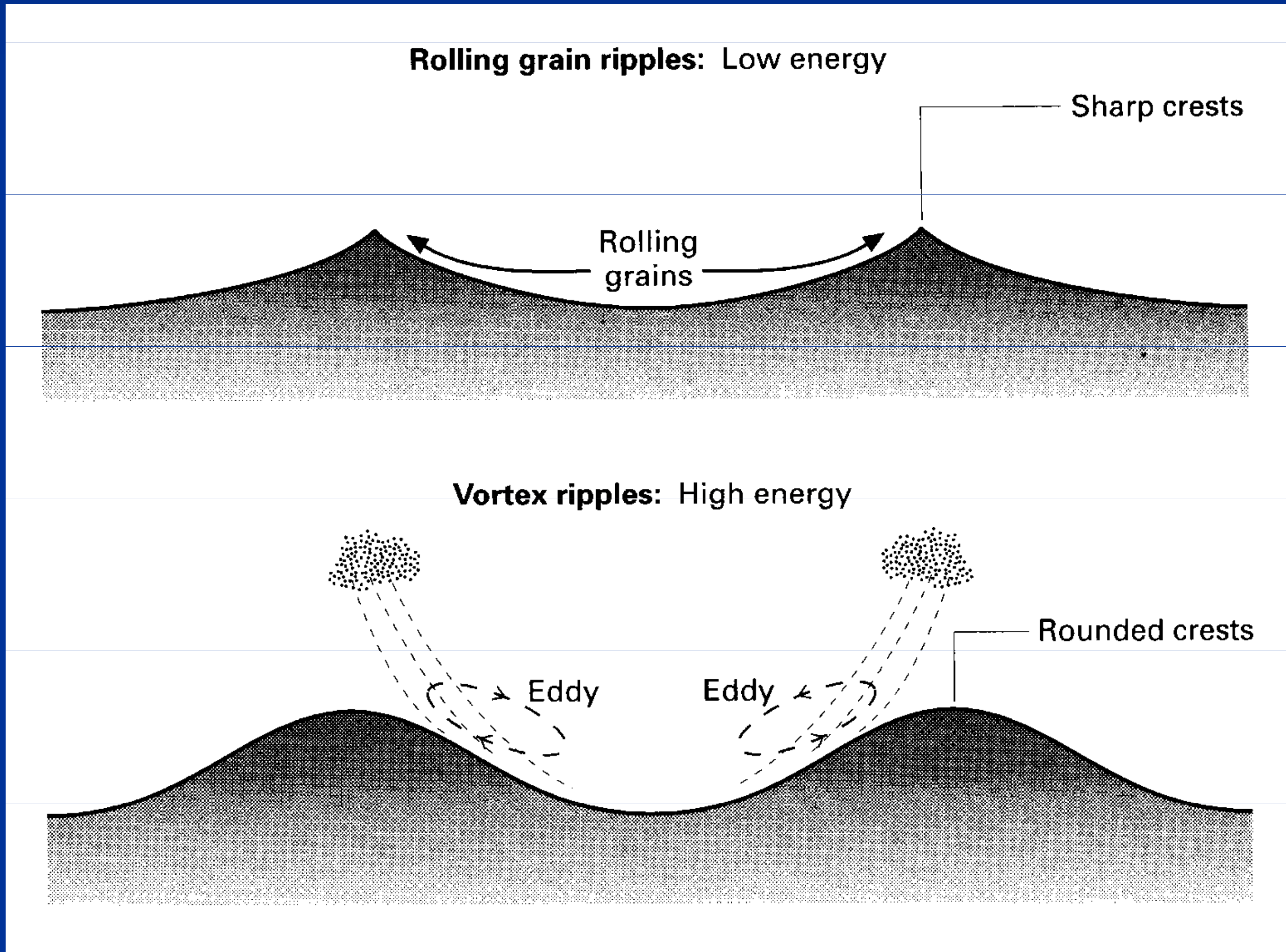

Rychlost proudění vs. velikost zrna

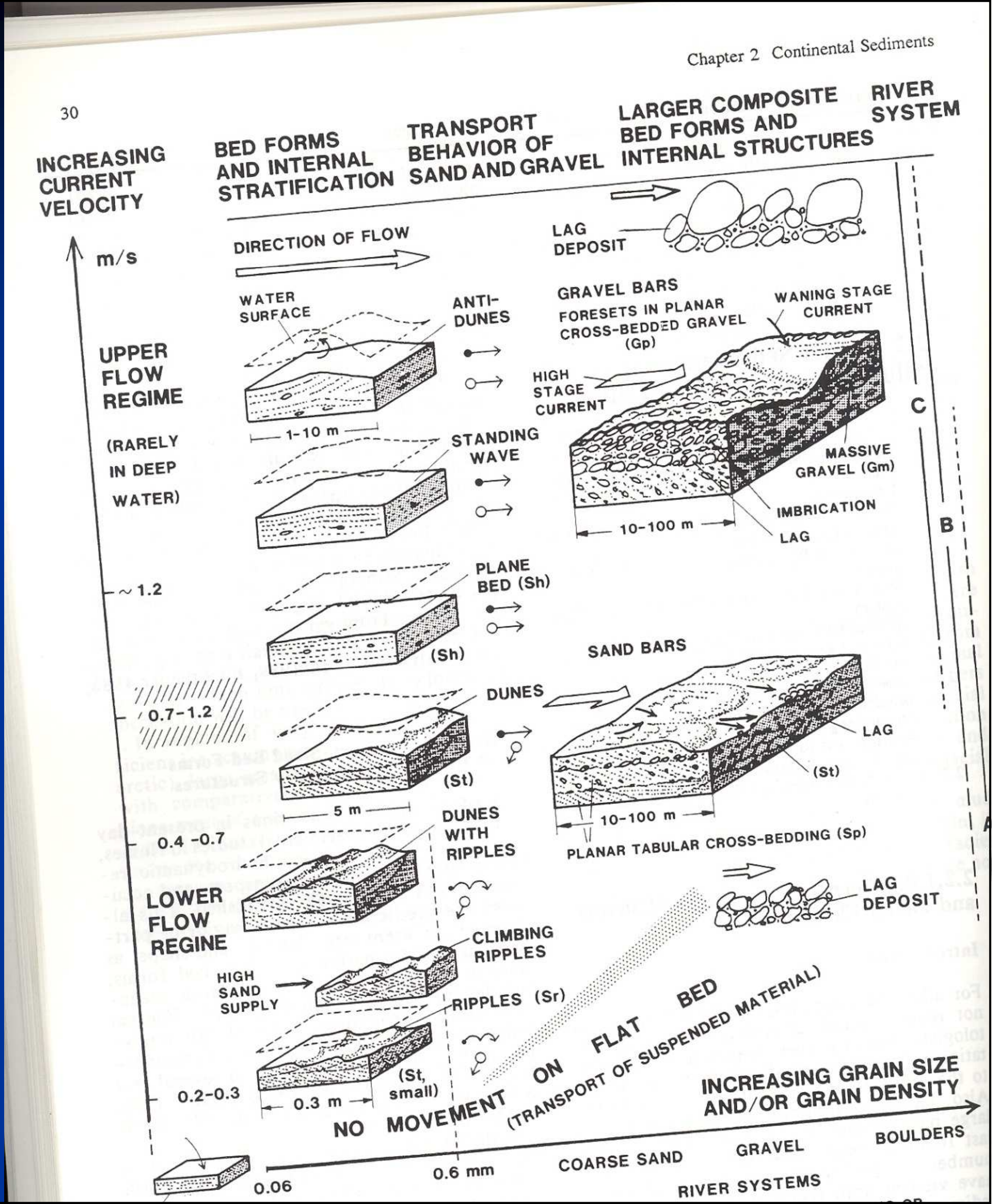

Textury:
Planární šikmé zvrstvení

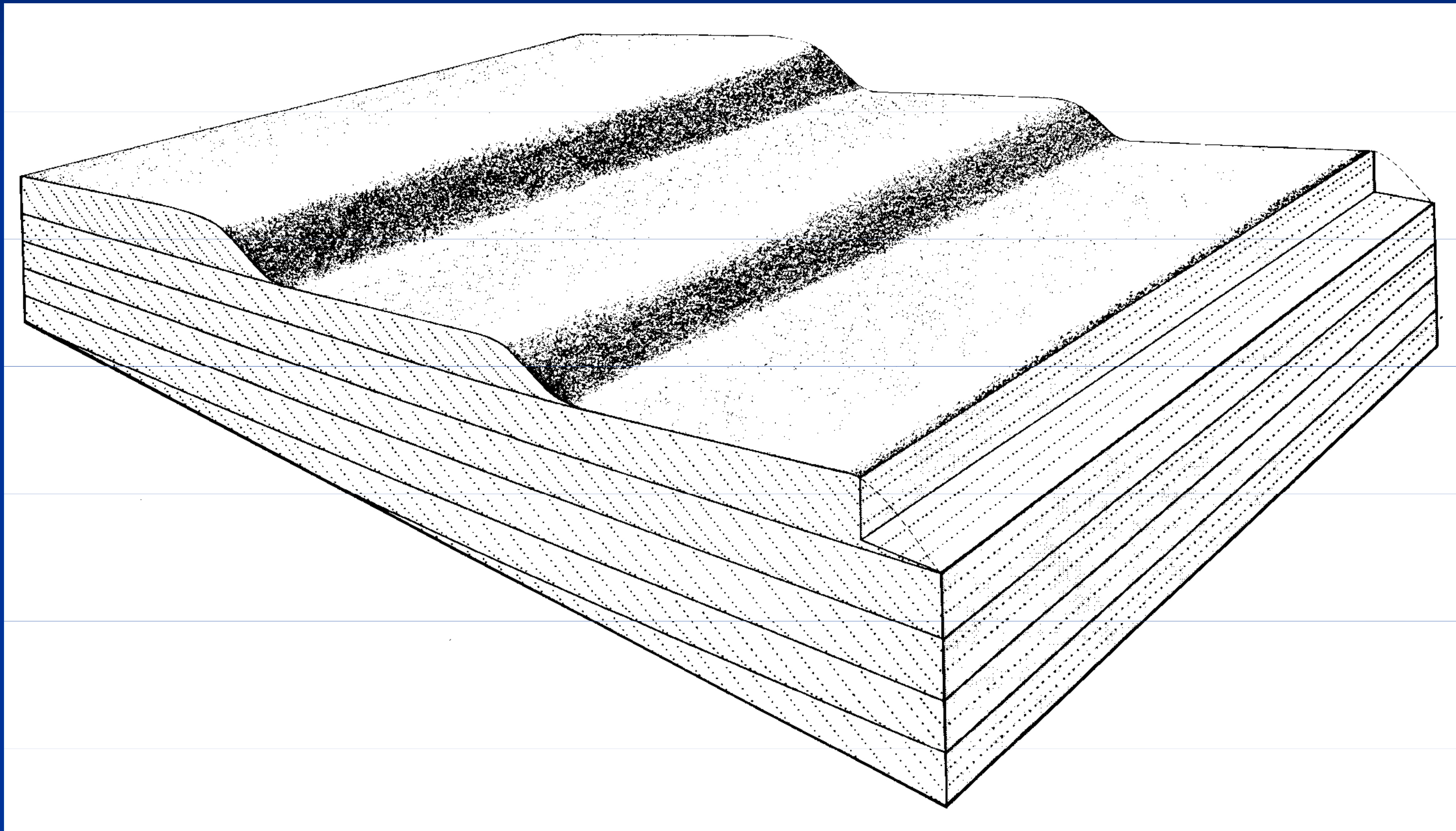

Textury:
Výmolové šikmé zvrstvení

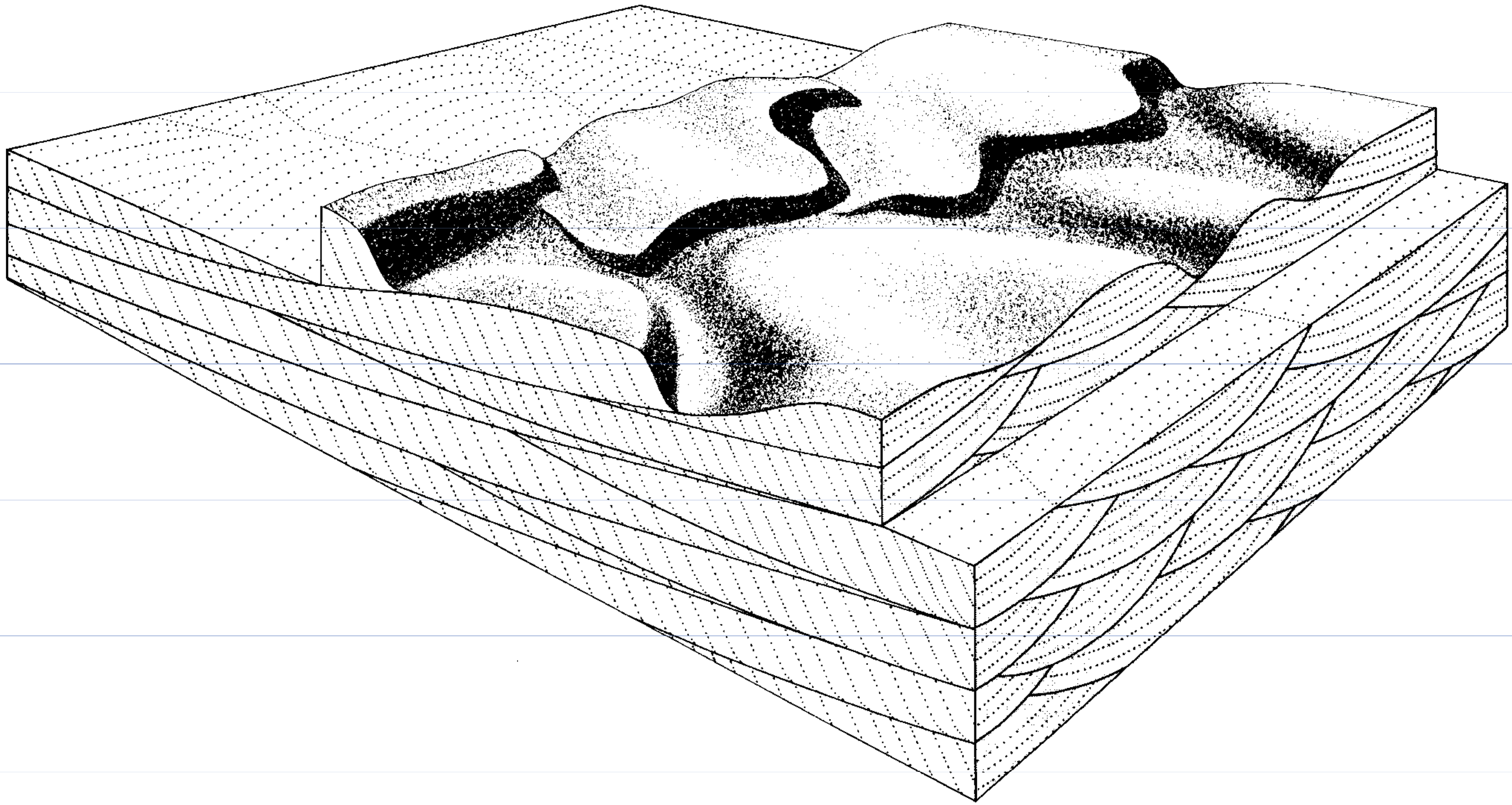

Fluviální prostředí

- Channel patterns (fluvial styles) of alluvial rivers are commonly classified as:
  - **Braided rivers**
  - **Meandering rivers**
  - **Straight rivers**
  - **Anastomosing rivers**
- Fluvial style is primarily controlled by specific stream power ω (W m^{-2}) and bed-load grain size, but also by bank stability and the amount of bed load (but **not** the proportion of suspended load!)

$$\omega = \frac{\rho g Q s}{w}$$

ρ=fluid density; Q=discharge, s (gradient); w=channel width

Stavební prvky fluviálních systémů

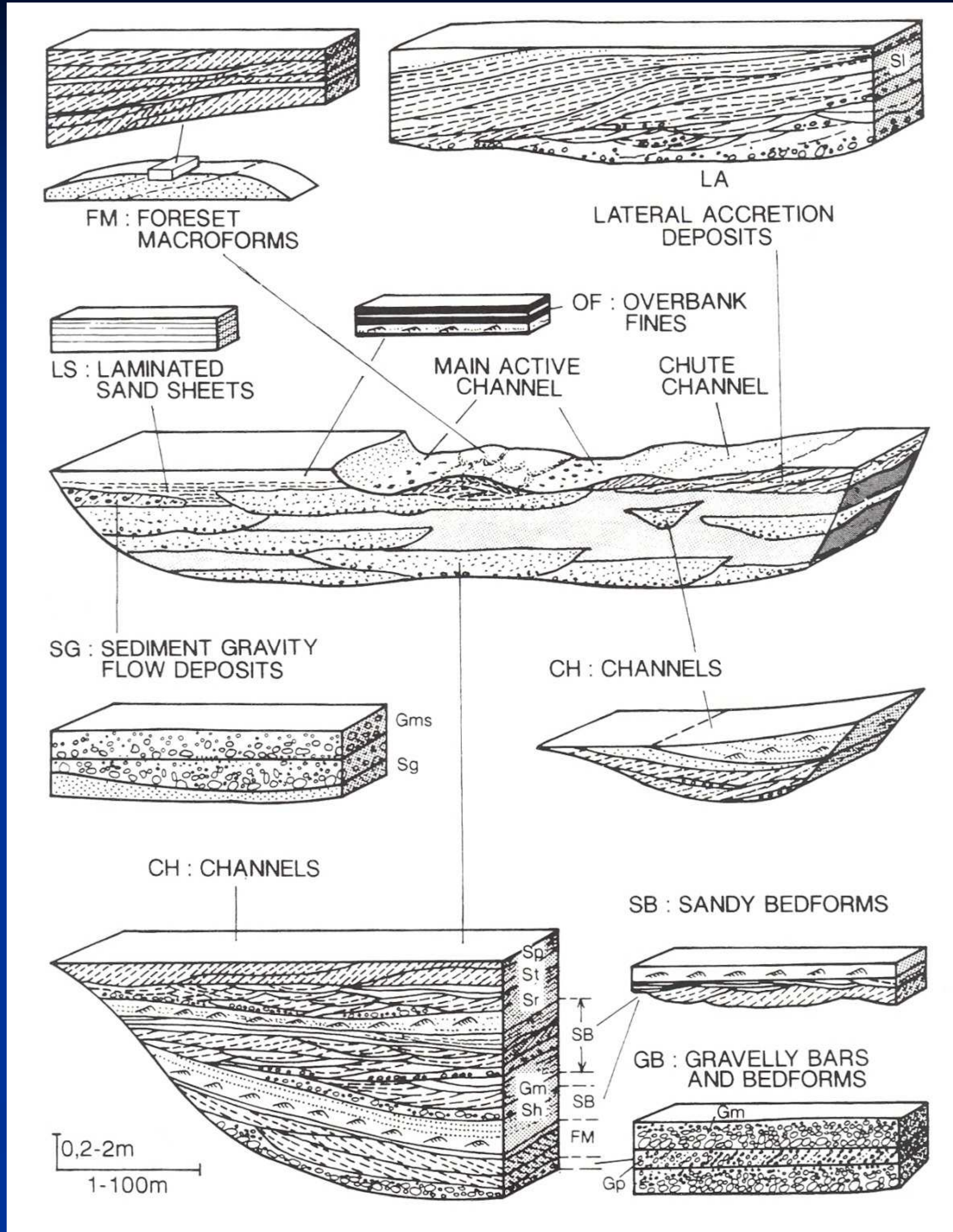

Aluviální vějíř

- **Lateral accretion** (boční akrece) involves higher-order bounding surfaces dipping perpendicular to paleoflow direction and associated lower-order bounding surfaces; in the case of **downstream accretion** higher-order bounding surfaces dip parallel to paleoflow direction
- Kanály
- Gravitační sedimenty (úlomkotoky)

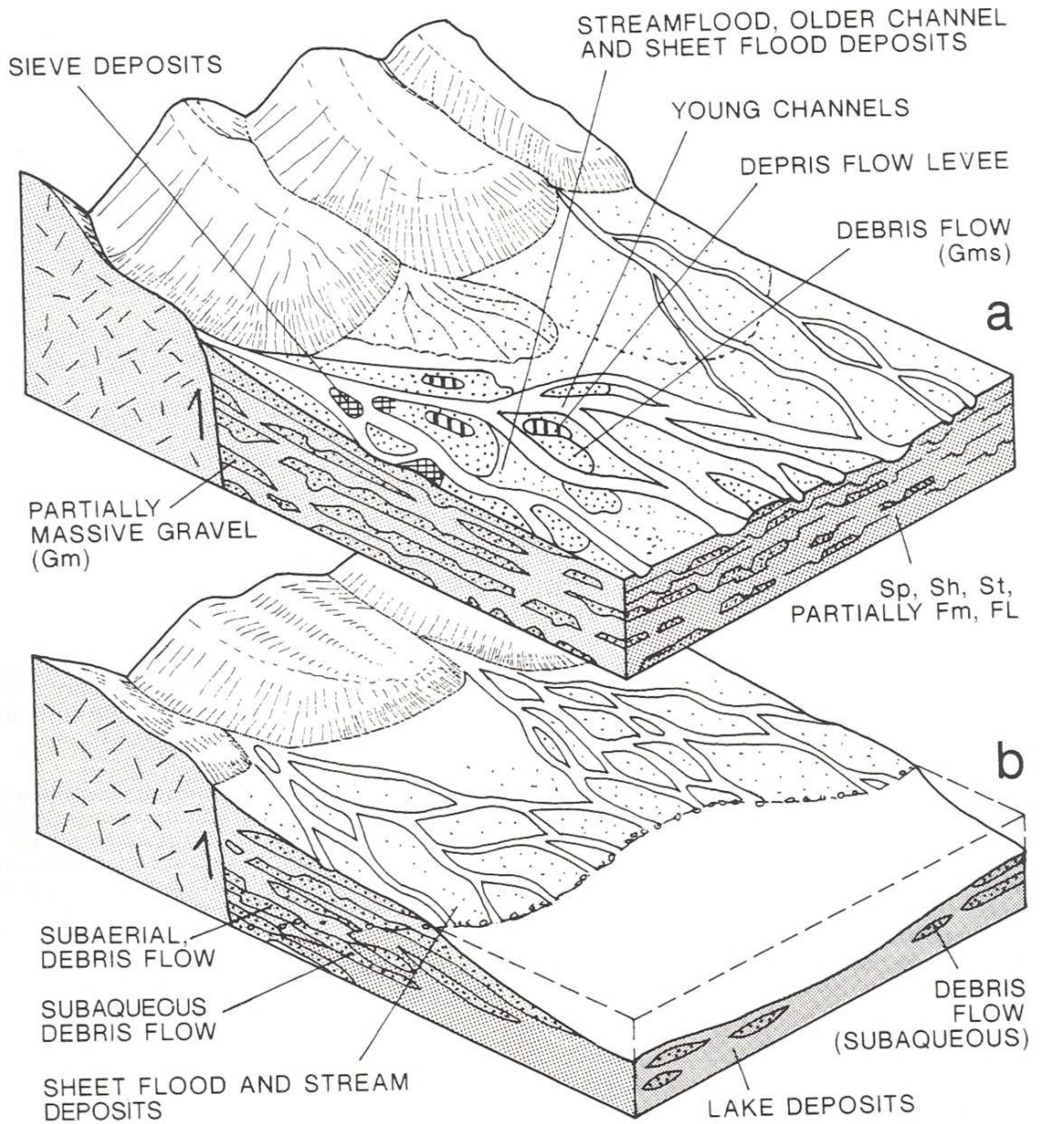

Fig. 2.11. Simplified facies models of **a** alluvial fan (proximal to mid fan region) and **b** fan delta. See Table 2.1 for explanation of symbols

Divočící řeky

- Braided rivers are characterized by a dominance of braid bars exhibiting both lateral and downstream accretion; meandering rivers primarily contain point bars with lateral accretion; in straight (and most anastomosing) rivers bars are commonly almost absent
- **Bars (valy)** are sandy or gravelly macroforms in channels that are emergent, mostly unvegetated features at low flow stage, and undergo submergence and rapid modification during high discharge

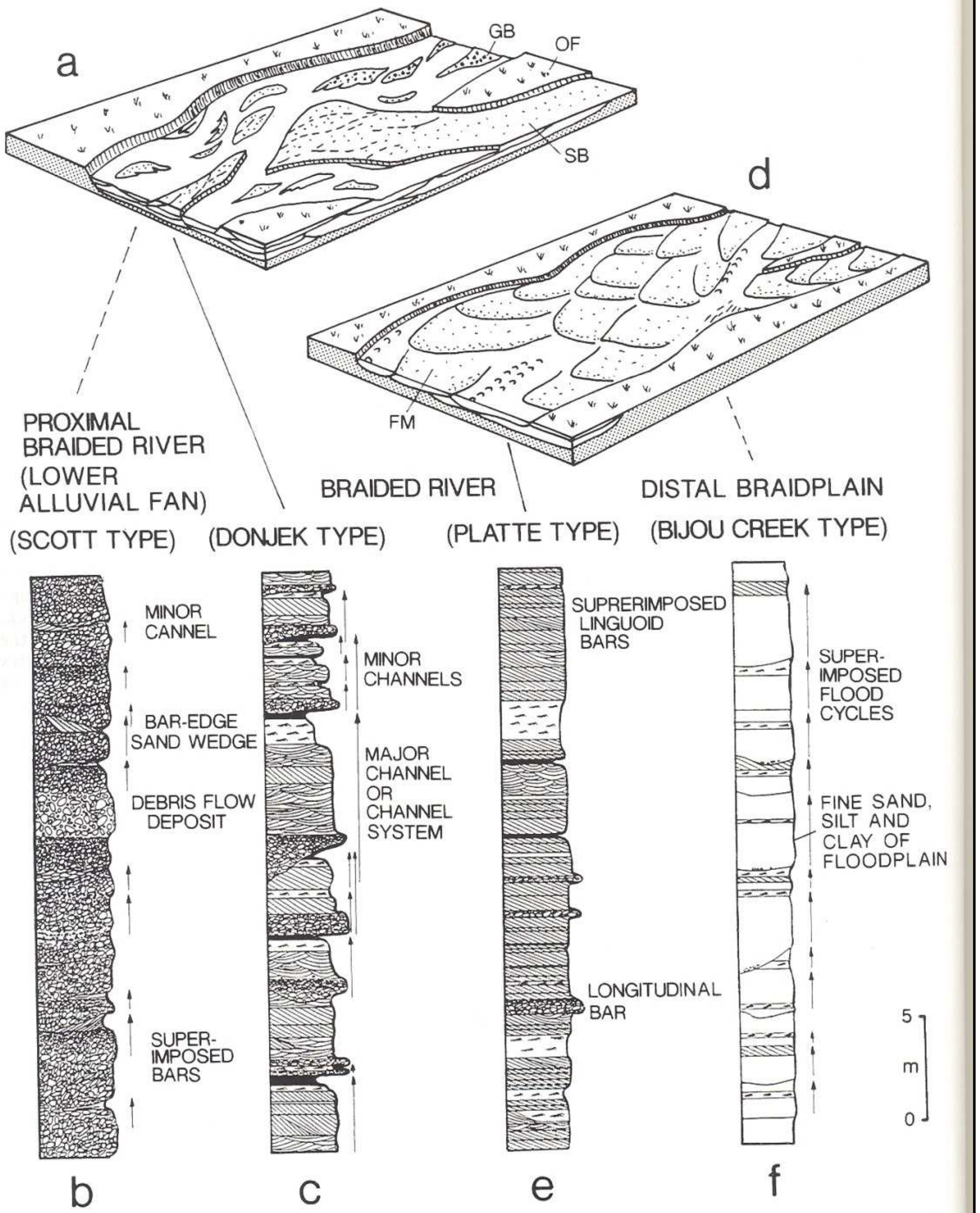

Fig. 2.15a-f. Braided river systems. **a-c** Proximal to middle reaches, gravel-dominated (**b**), or sand-dominated (**c**) with minor proportion of gravel. **d-f** Distal, sand-dominated system with wide channels and flat, linguoid sand bars (**d** and **e**), or wide floodplain rarely inundated by flash floods (**f**). (After Miall 1985)

Meandrující řeky

- **Point bars** (jesepní valy) form on inner banks and typically accrete laterally, commonly resulting in lateral-accretion surfaces; mid-channel or **braid bars** accrete both laterally and downstream
- Kanály, opuštěné kanály
- Přelivové sedimenty
- Povodňové roviny

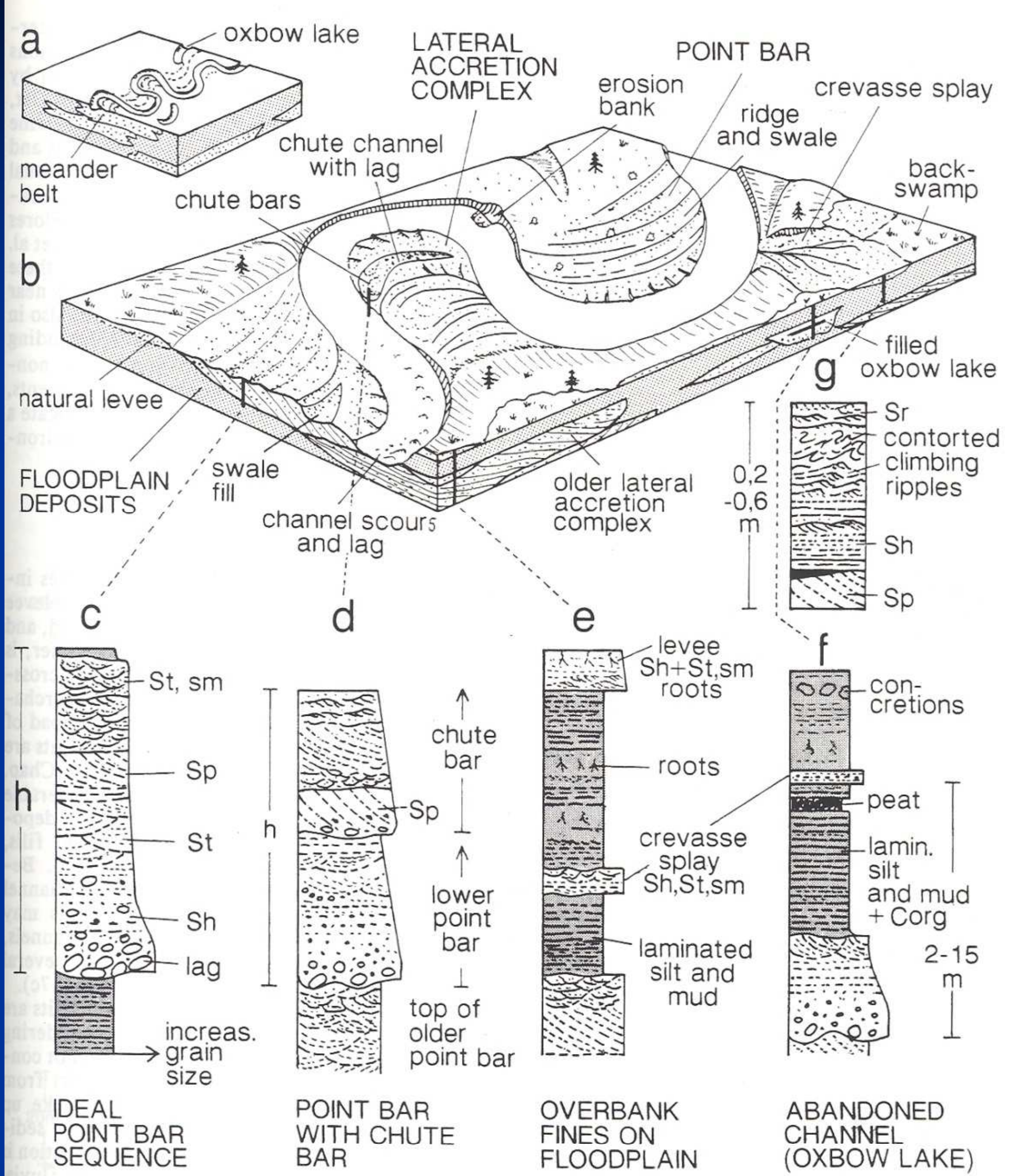

Fig. 2.16a-h. Meandering river system. **a** Formation of sandy meander belt within a flood basin. **b** Different sub-environments of meandering channel. **c-g** Characteristic vertical sections of the youngest sediments of the flood basin. **h** One fluvial cycle (autocyclic). See Table 2.1 for explanation of symbols; *sm* small-scale. (Based on different sources, e.g., Walker and Cant 1984; Galloway 1985; Miall 1985)

As shown by the photo in the previous slide, many streams naturally **meander** (form curving, S-shaped bends).

Stream channels tend to meander more and more over time. The reason is because **streams erode on the outsides of curves** (fastest water flow)**, and deposit sediment on the insides of curves** (slowest water flow).

The eroding outside part of the curve is called the **cut bank**. The inside part of the curve where sediment is deposited is called the **point bar**.

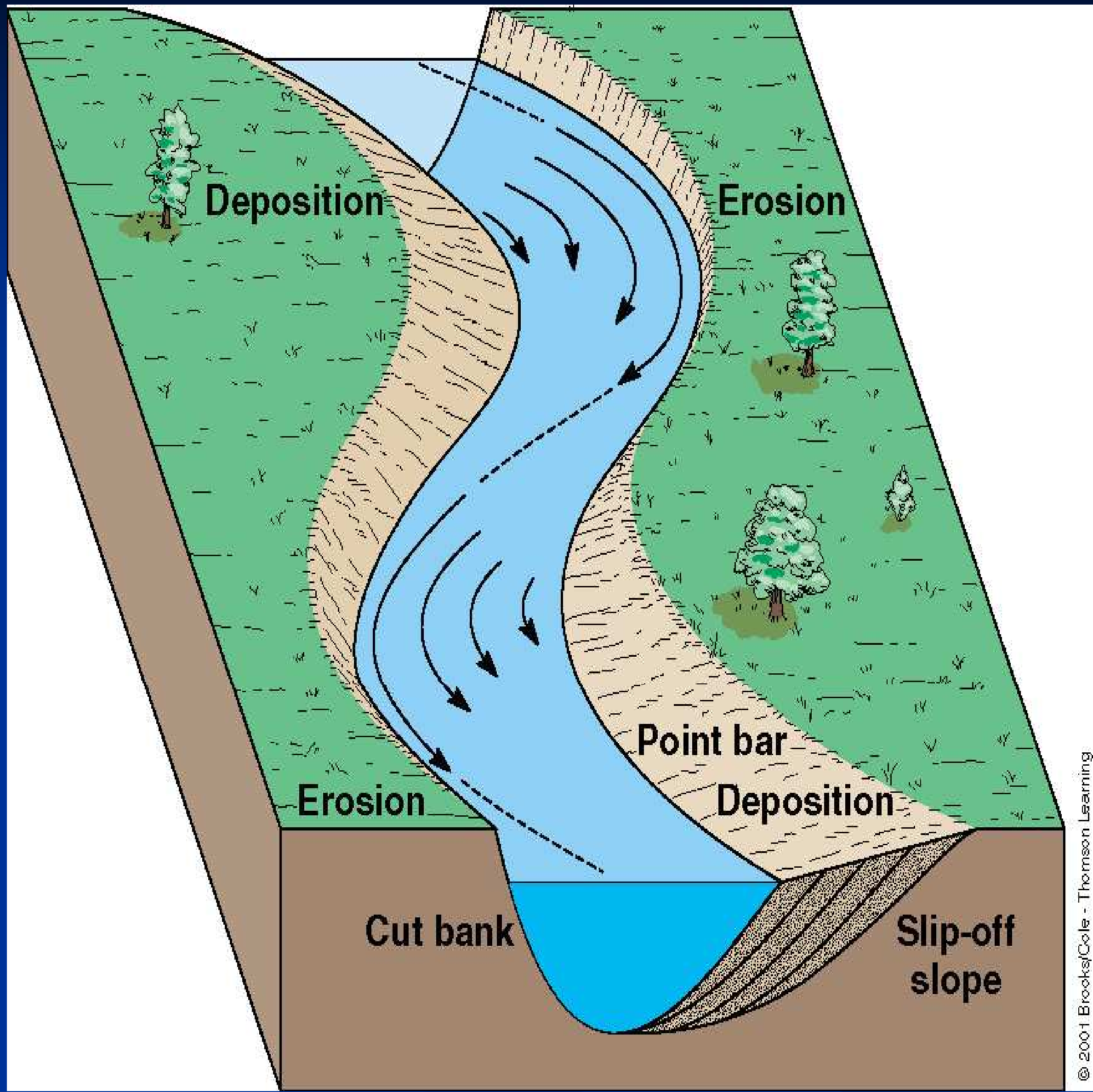

Mrtvé rameno
(Oxbow lake)

A long-term result of erosion of cut banks (outsides of bends) is that a stream may eventually cut through the neck of a tight meander, abandoning part of its channel, and forming a feature called an **oxbow lake**.

The figure here shows the steps in this process.

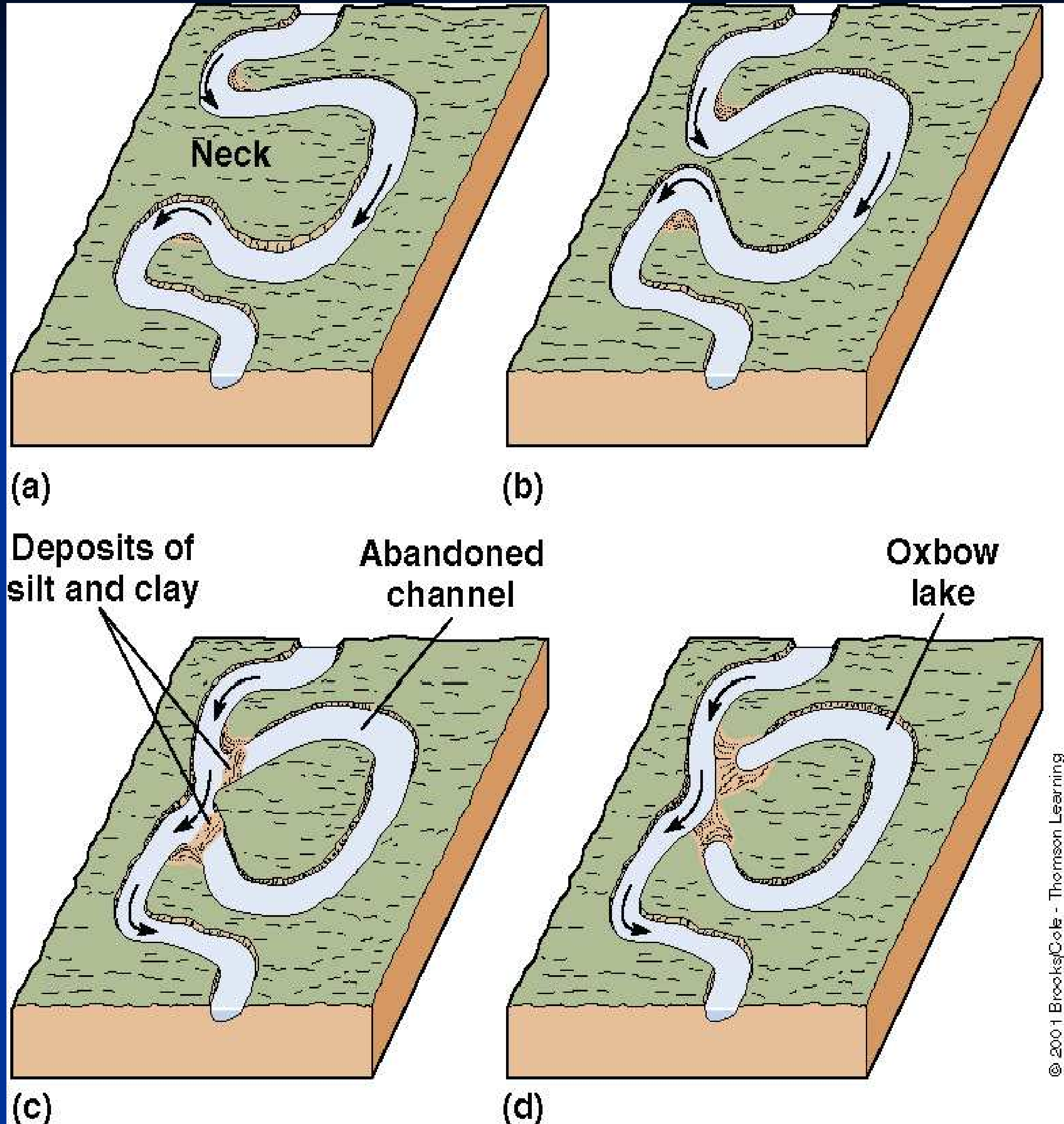

This air photo shows an **oxbow lake**. (The main channel is out of view to the right.) The curving "scars" on the land show the progressive migration of the meandering channel over time.

Litovelské Pomoraví

Note on this figure the locations of the **levees**.

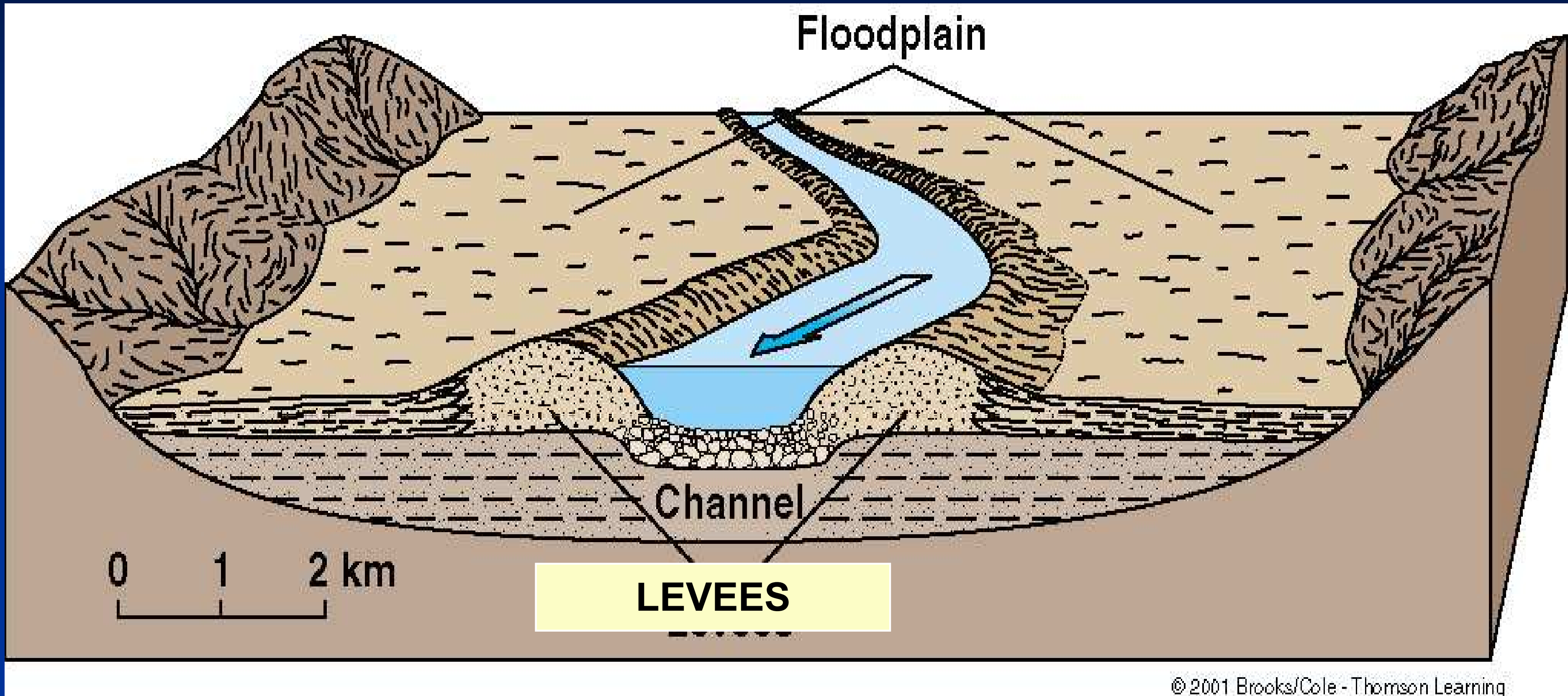

As a stream rises prior to flooding, its increased velocity and discharge allow it to carry more and more sediment. When the stream crests its banks and spills out onto the floodplain, the water slows down, depositing ridges of sediment along the banks called **levees**. The levees are often the highest places on the floodplain.

22. Large scale trough cross bedding (sandy bedforms)

Texture: sand with pebbles passing into sandy pebble gravel in the upper part of the section

Structure: trough cross bedding

Stratigraphy: Lower Pleistocene terrace of the River Vltava

Locality: Libčice (Praha Západ District)

Photo by: J. Kadlec 1997

11. River channel fill

Upper part of the section

Channel fill: **gravel bar** (GB) **overlain by lateral accretion deposits** (LA), channel fill **covered by gravelly and sandy bedforms** (SB)

Texture: medium grained sandy gravel (GB), medium to coarse sand (LA), intercalation of sand and sandy gravels (SB)

Structure: the sands filling the channel are cross bedded, gently dipping sand laminae are formed by lateral accretion in the inner part of the river meander, GB – planar cross bedding, SB – horizontal stratification

Lower part of the section

Sandy and gravelly bedforms

Texture: coarse sand with the occasional admixture of pebbles

Structure: faint planar cross-bedding

Stratigraphy: Middle Pleistocene terrace of the River Vltava

Locality: Hostín u Vojkovic (Mělník District)

Photo by: J. Kadlec 1997

3. River channel fill

Sandy and gravelly bedforms

Texture: alternation of medium to coarse sand and sandy pebble gravel

Structure: planar cross-bedding

Stratigraphy: Middle Pleistocene terrace of the River Vltava

Locality: Straškov (Litoměřice District)

Photo by: J. Kadlec 1997

8. Downstream accretion deposits
Texture: medium to coarse sand with an admixture of gravel
Structure: planar cross-bedding
Stratigraphy: Lower Pleistocene terrace of the River Vltava
Locality: Libčice nad Vltavou (Praha Západ District)
Photo by: J. Kadlec 1997

1. River channel fill
Upper part of the section
Sandy and gravelly bedforms
Texture: alternation of coarse sand and medium grained sandy gravel
Structure: trough cross-bedding
Middle part of the section
Downstream accretion deposits
Texture: coarse sand and gravelly sand
Structure: planar cross-bedding
Stratigraphy: Middle Pleistocene terrace of the River Labe
Locality: Tišice (Mělník District)
Photo by: J. Kadlec 1997

Říční terasy

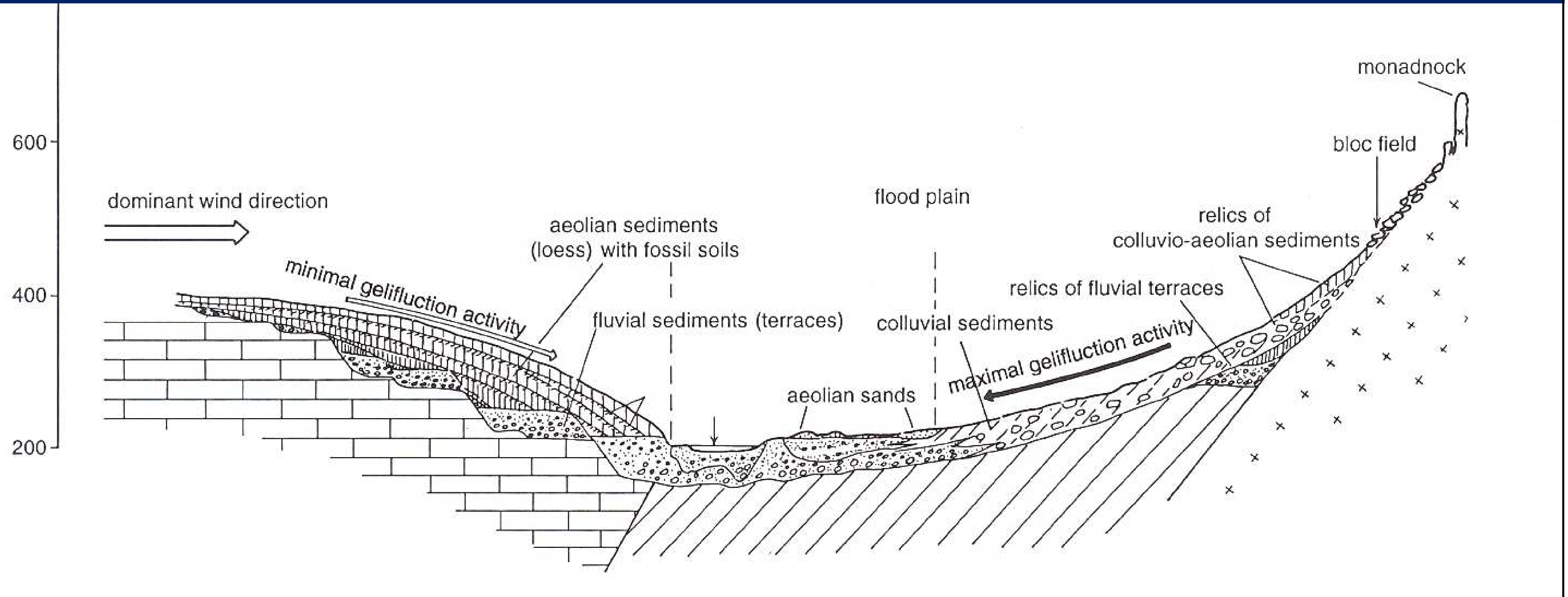

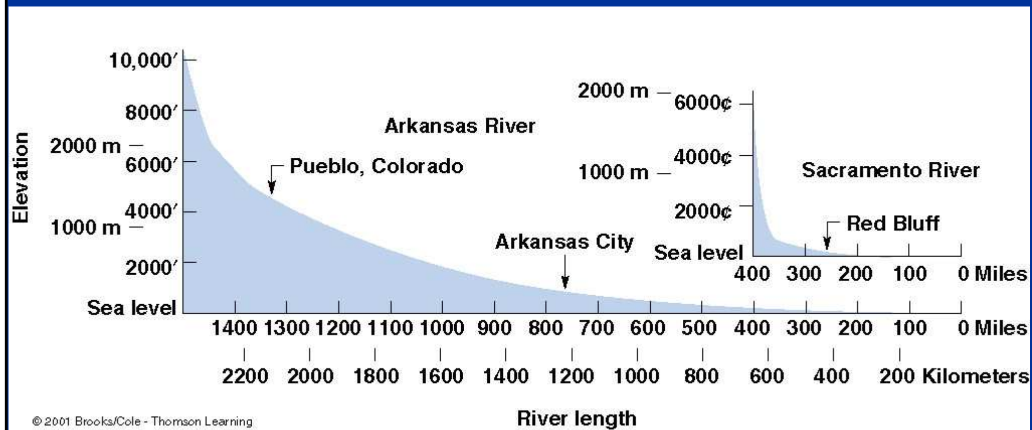

Holocenní sedimentační systémy řeky Moravy

HISTORICKÁ FAKTA / INTERPRETACE / TRADICE (.)

- **Niva Moravy osidlována od neolitu**
- **Přítomnost údolních svrchnopleistocenních teras v podloží aktivních holocenních niv (degradace → agradace)**
- **Změny v nivě v důsledku antropogenní činnosti – zvýšení rychlostí sedimentace (zahliňování) např. v době Velké Moravy**
- **Řeka Morava – anastomozující systém (holocenní změna meandrujícího systému na anastomozující)**

OTÁZKY (?)

- **Nastala skutečně holocenní změna režimu sedimentace Moravy (na bázi holocénu, během holocénu, antropogenní činností ?)**

CÍLE A METODY (!)

- **Mapování fluviálních facií pomocí mělkých geofyzikálních metod**
  - **Elektrická odporová tomografie (ERT) – měření měrného odporu hornin, který je závislý na zrnitosti, minerálním složení, obsahu vody**
  - **Dipólové elektromagnetické profilování (DEMP) – měření vodivosti hornin – převrácená hodnota odporu**
- **Stratigrafie vrtů**
- **Datování**
  - ^{14}C (AMS)

Aktivní niva Moravy:

- Hornomoravský úval
- Mohelnická brázda

Nízké sklony svahů (< 0,15º)
Zlomově omezená příkopová propadlina
Lokality v nivě Moravy a přítoků (Oslava)

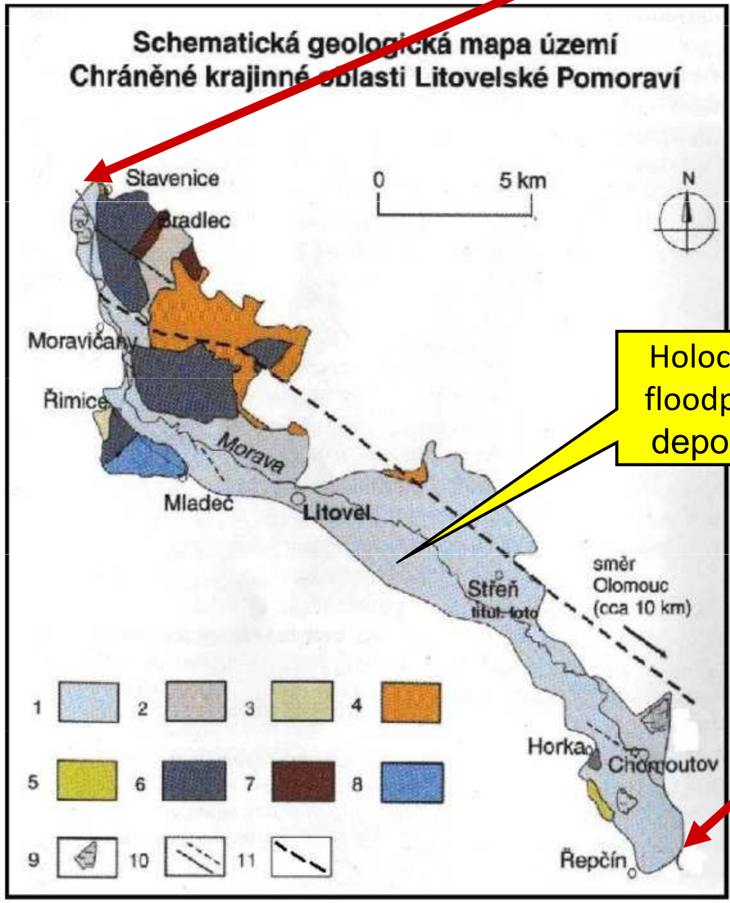

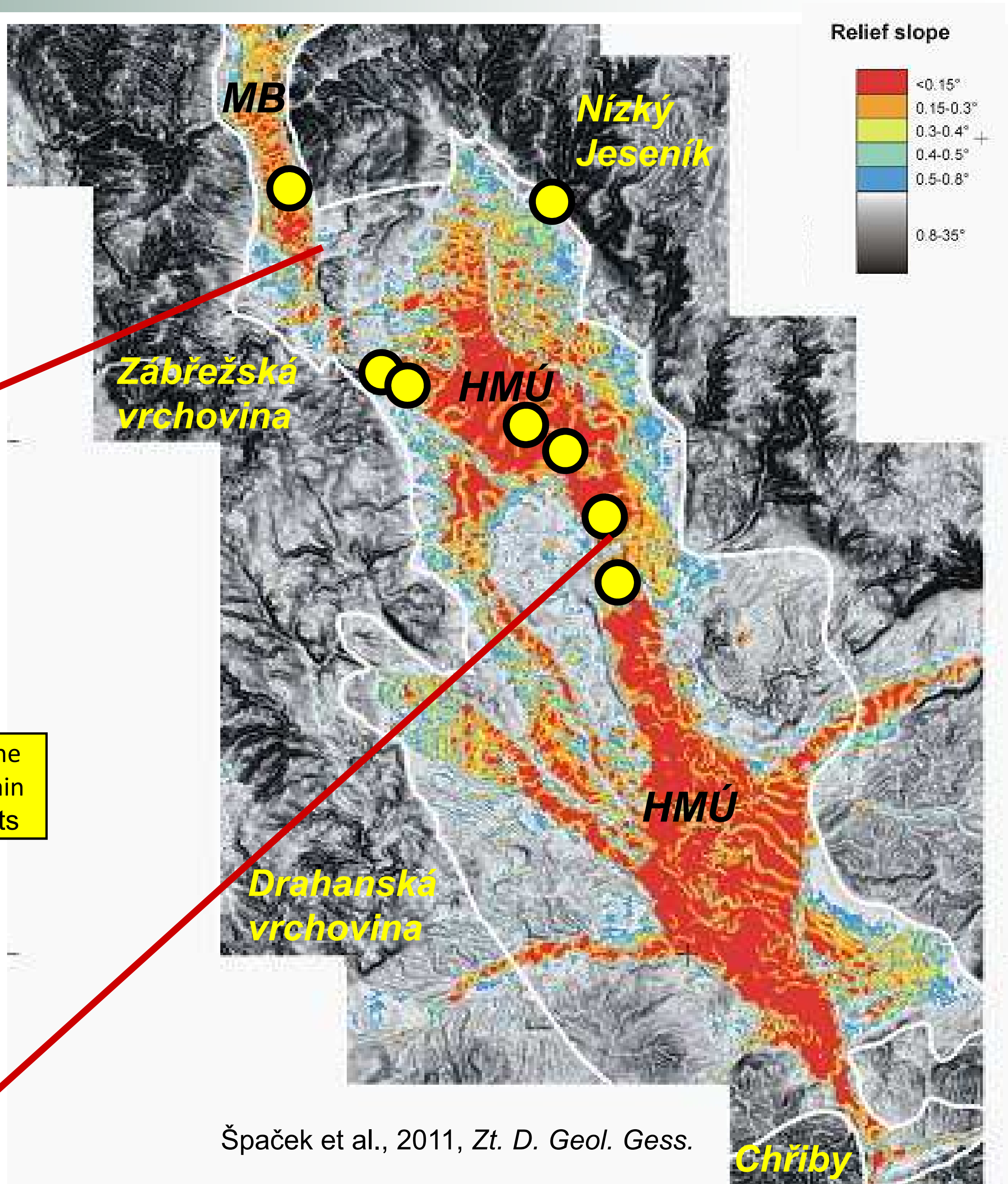

Špaček et al., 2011, *Zt. D. Geol. Gess.*

Stavební prvky fluviálního systému

- Vegetační příznaky
- Historické ortofotomapy

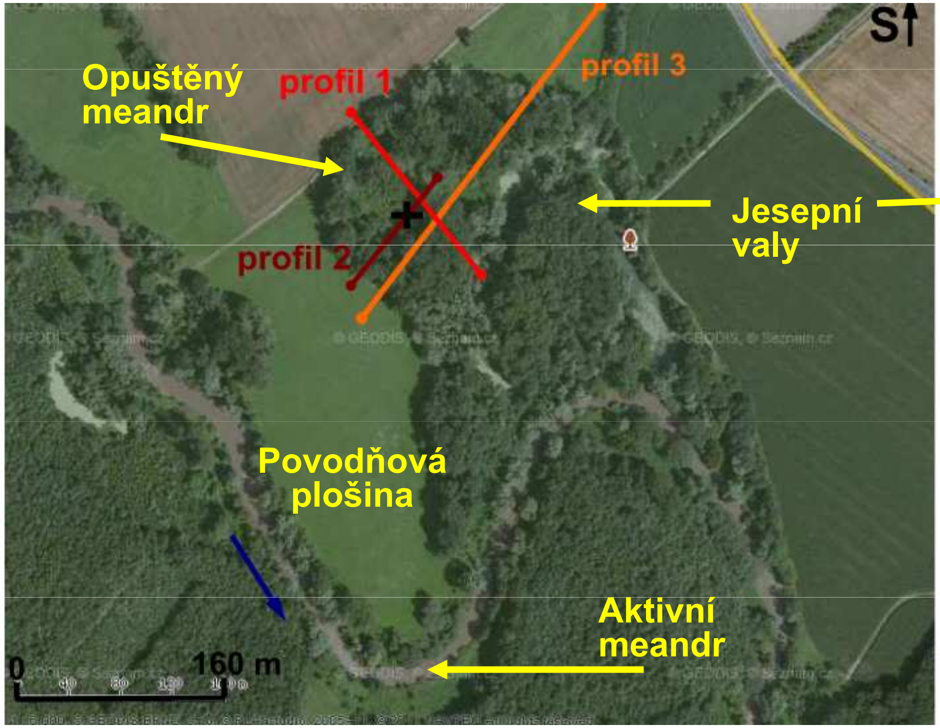

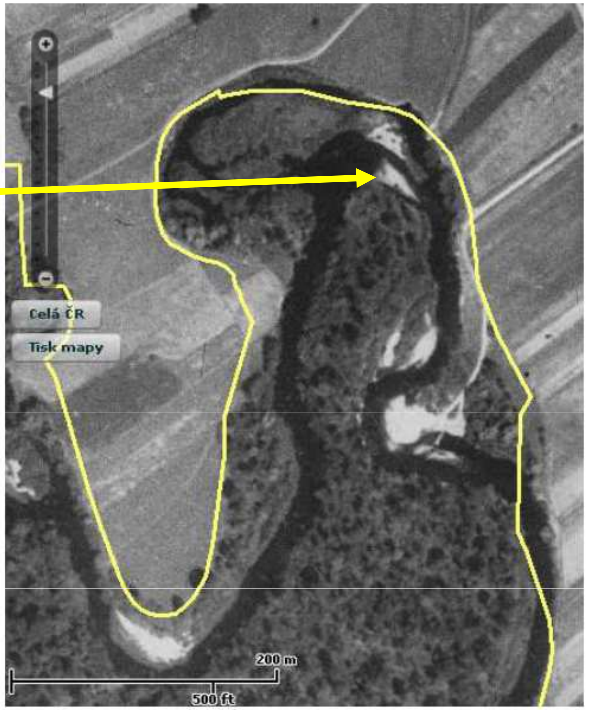

- opuštěné meandry
- aktivní meandry
- jesepní valy
- povodňové plošiny

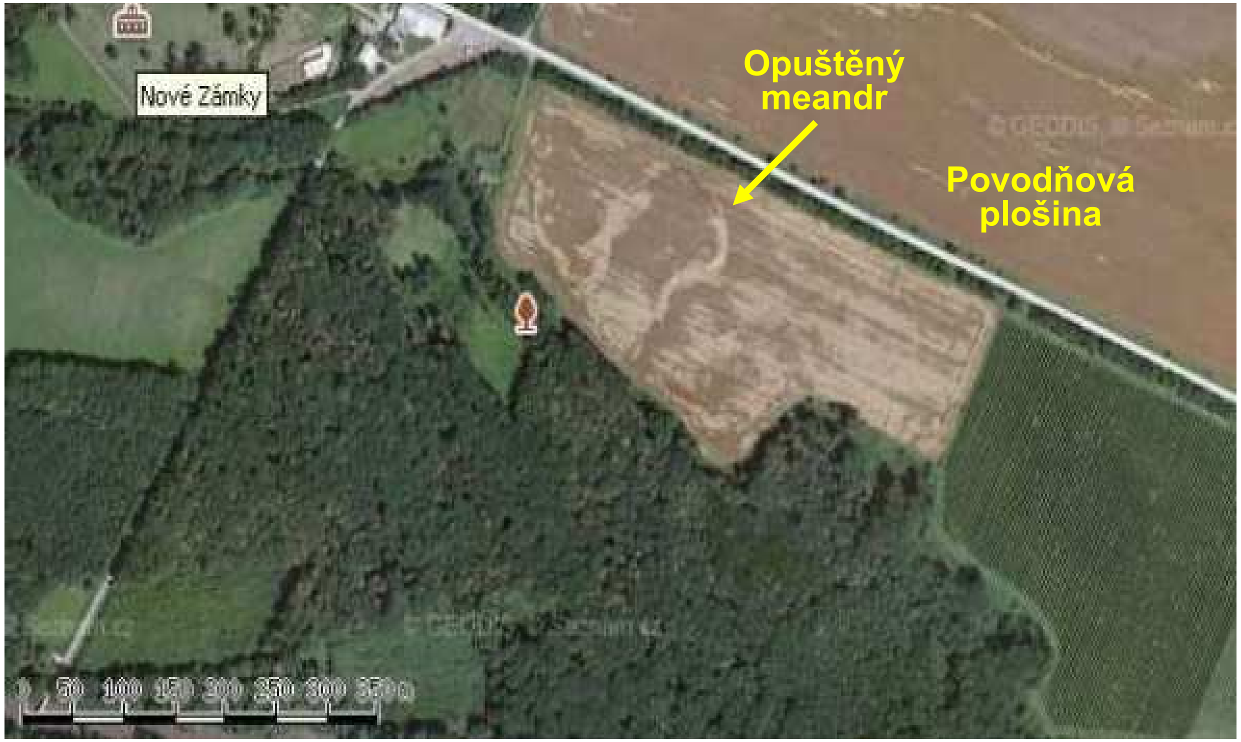

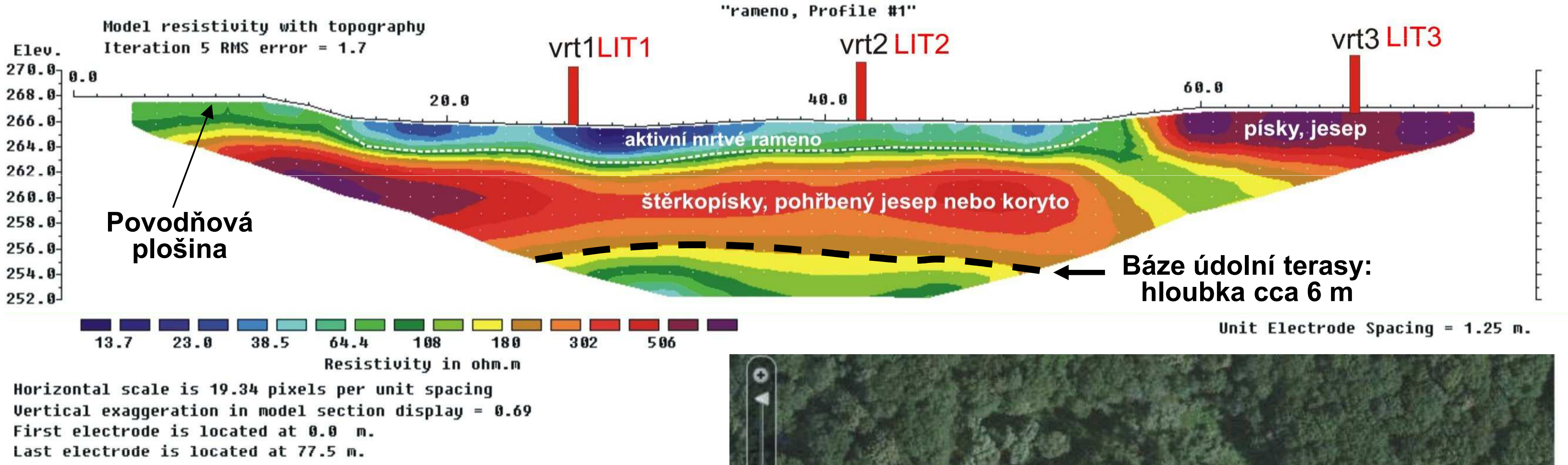

Litovelské luhy

- aktivní poloslepé rameno
- Jesepní val, štěrkopísky: resistivita 350 – 550 ohm.m
- Opuštěný meandr: silty, jíly: resistivita 10 – 50 ohm.m
- Povodňová plošina: silty, jíly: resistivita 60 – 80 ohm.m

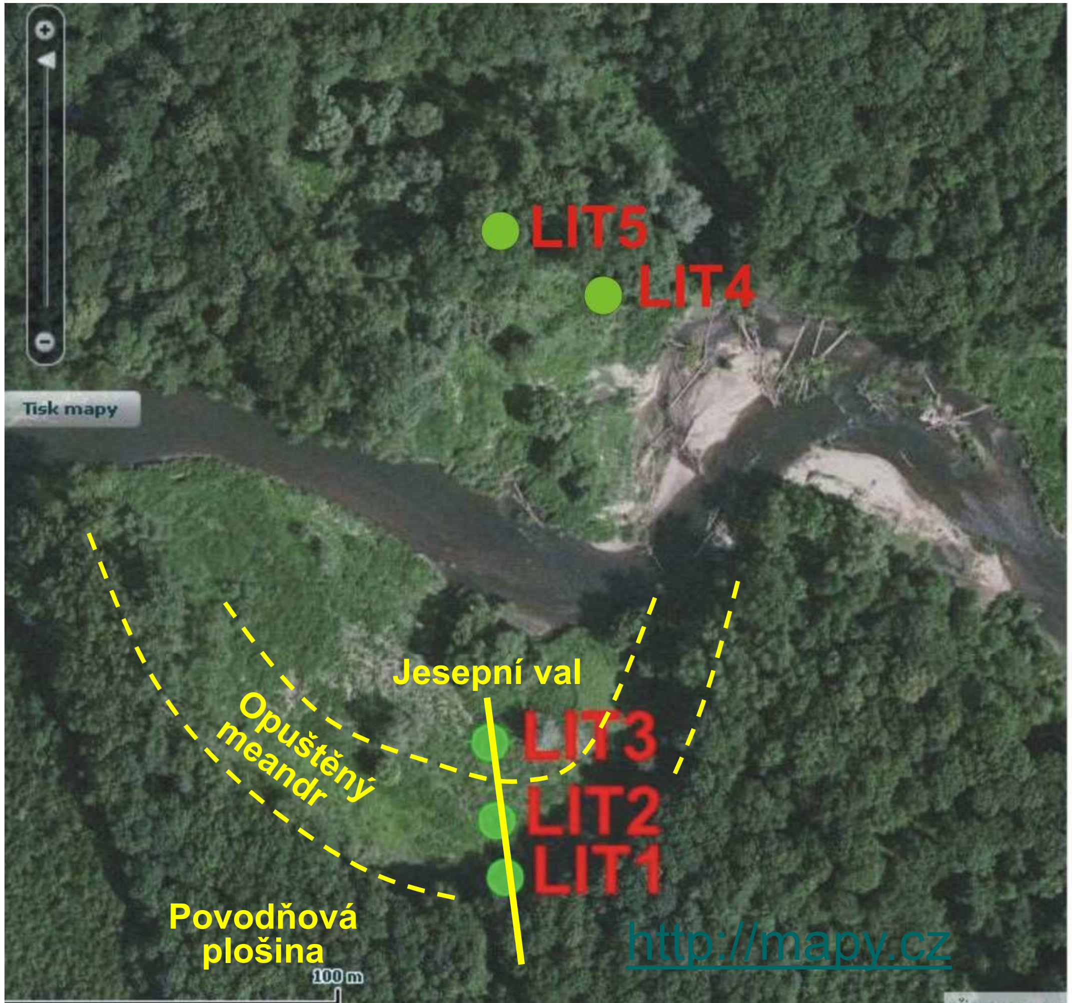

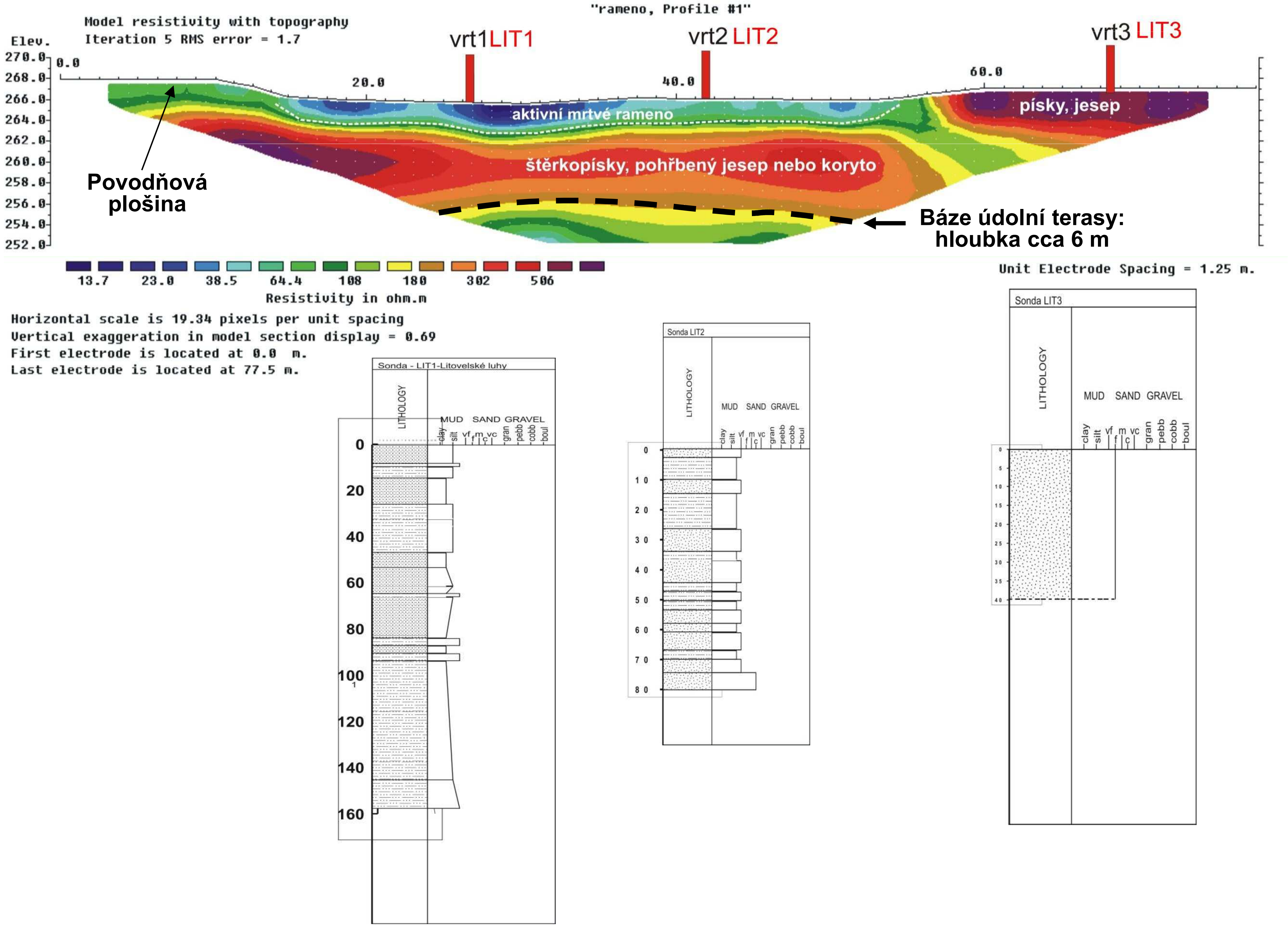
"rameno, Profile #1"
Model resistivity with topography
Iteration 5 RMS error = 1.7
Elev.
270.0
268.0
266.0
264.0
262.0
260.0
258.0
256.0
254.0
252.0
0.0
20.0
40.0
60.0
vrt1 LIT1
vrt2 LIT2
vrt3 LIT3
aktivní mrtvé rameno
písky, jesep
štěrkopísky, pohřbený jesep nebo koryto
Povodňová plošina
Báze údolní terasy: hloubka cca 6 m
13.7
23.0
38.5
64.4
108
180
302
506
Resistivity in ohm.m
Unit Electrode Spacing = 1.25 m.
Horizontal scale is 19.34 pixels per unit spacing
Vertical exaggeration in model section display = 0.69
First electrode is located at 0.0 m.
Last electrode is located at 77.5 m.
Sonda - LIT1-Litovelské luhy
LITHOLOGY
MUD SAND GRAVEL
clay silt vf f m c vc gran pebb cobb boul
0
20
40
60
80
100
120
140
160
Sonda LIT2
LITHOLOGY
MUD SAND GRAVEL
clay silt vf f m c vc gran pebb cobb boul
0
10
20
30
40
50
60
70
80
Sonda LIT3
LITHOLOGY
MUD SAND GRAVEL
clay silt vf f m c vc gran pebb cobb boul
0
5
10
15
20
25
30
35
40

Mapa vodivosti (DEMP)
Olomouc – Bázlerova pískovna
povodňová plošina

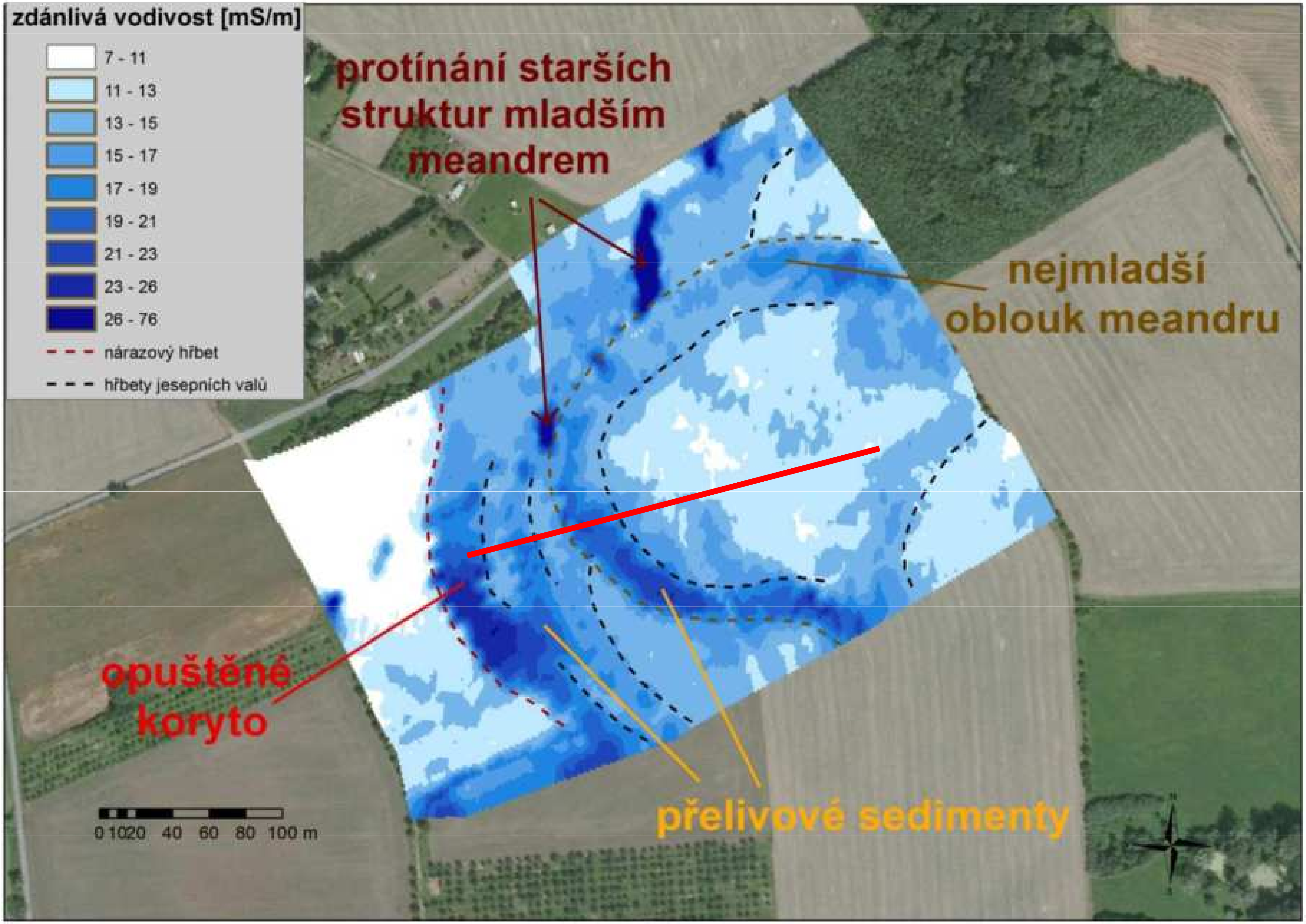

zdánlivá vodivost [mS/m]
7 - 11
11 - 13
13 - 15
15 - 17
17 - 19
19 - 21
21 - 23
23 - 26
26 - 76
nárazový hřbet
hřbety jesepních valů
protínání starších struktur mladším meandrem
nejmladší oblouk meandru
opuštěné koryto
přelivové sedimenty
0 10 20 40 60 80 100 m

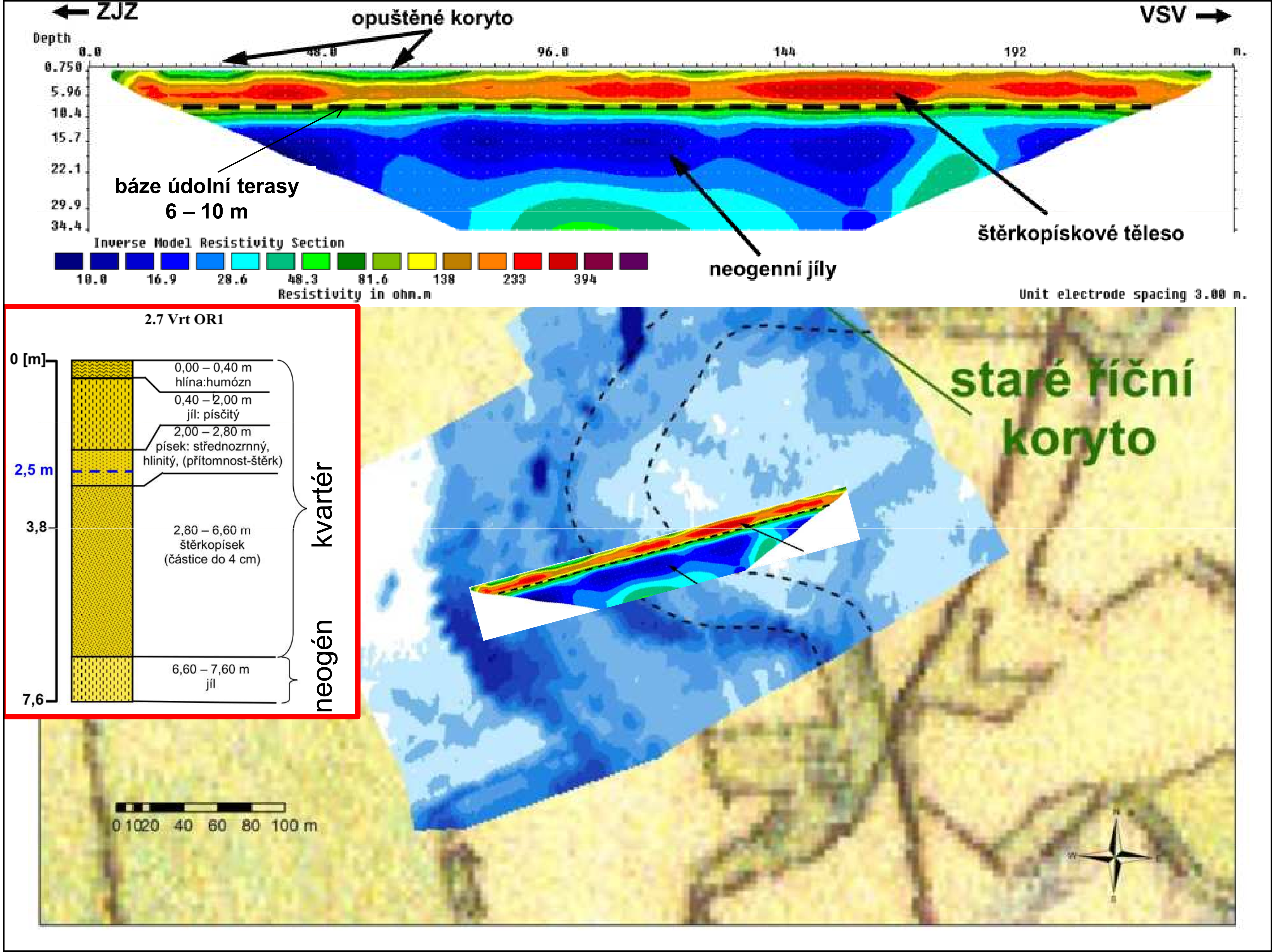

ZJZ
opuštěné koryto
VSV
Depth
0.0
48.0
96.0
144
192
m.
0.750
5.96
10.4
15.7
22.1
29.9
34.4
báze údolní terasy
6 – 10 m
neogenní jíly
štěrkopískové těleso
Inverse Model Resistivity Section
10.0
16.9
28.6
48.3
81.6
138
233
394
Resistivity in ohm.m
Unit electrode spacing 3.00 m.
2.7 Vrt OR1
0 [m]
0,00 – 0,40 m
hlína:humózn
0,40 – 2,00 m
jíl: písčitý
2,00 – 2,80 m
písek: střednozrnný,
hlinitý, (přítomnost-štěrk)
2,5 m
3,8
2,80 – 6,60 m
štěrkopísek
(částice do 4 cm)
6,60 – 7,60 m
jíl
7,6
kvartér
neogén
staré říční
koryto
0 10 20 40 60 80 100 m

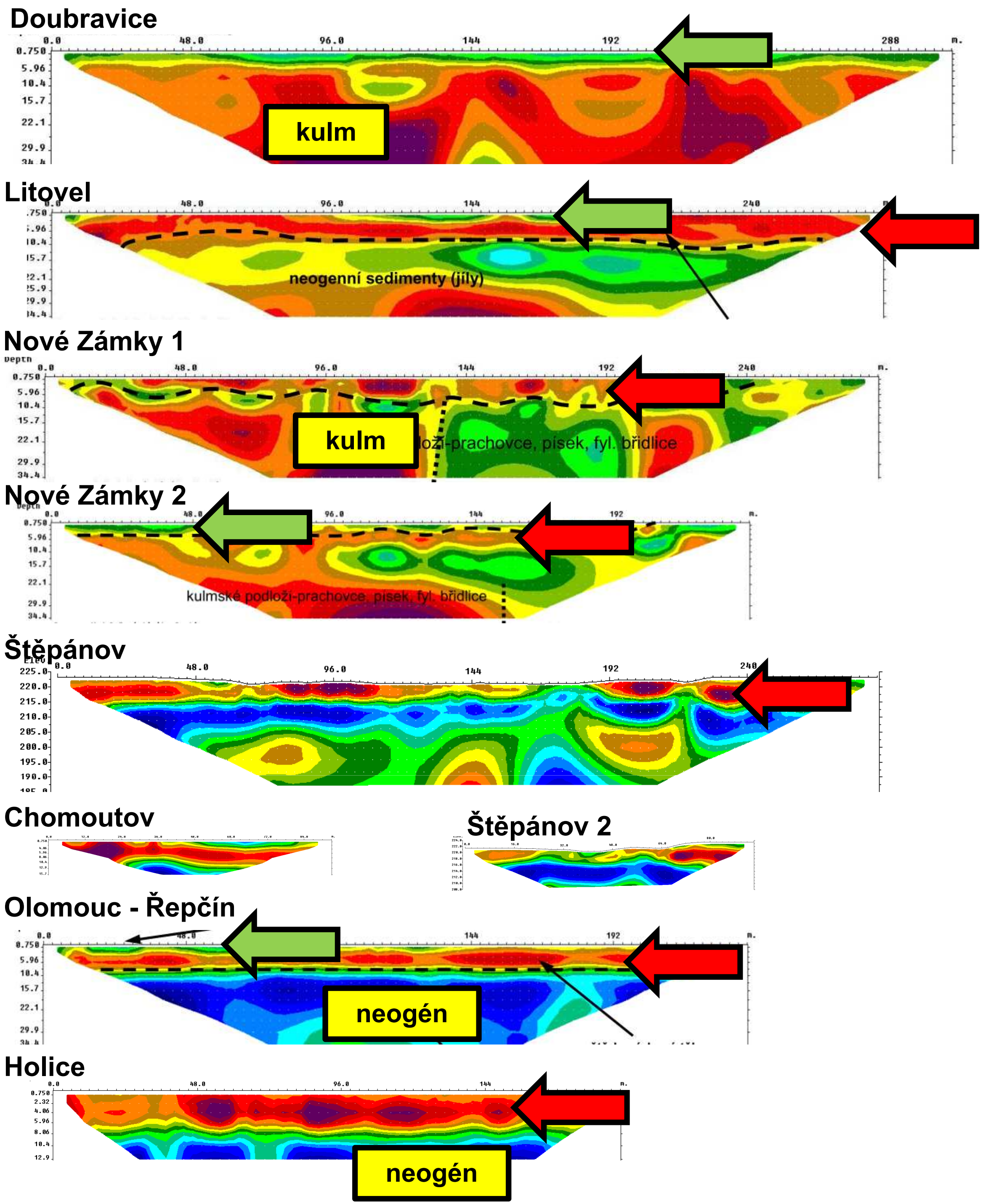

Jednotná stratigrafie

1. Předkvartérní podloží: různé rezistivity → neogén, kulm
2. Kvartér: vysoká rezistivita, štěrkopísková laterálně akreční tělesa = meandrování, horizontální báze těles → báze údolní terasy 6 – 10 m
3. Kvartér: nízká rezistivita, povodňové sedimenty, vertikální akrece
4. Stáří ??

Faciální modely fluviálních systémů

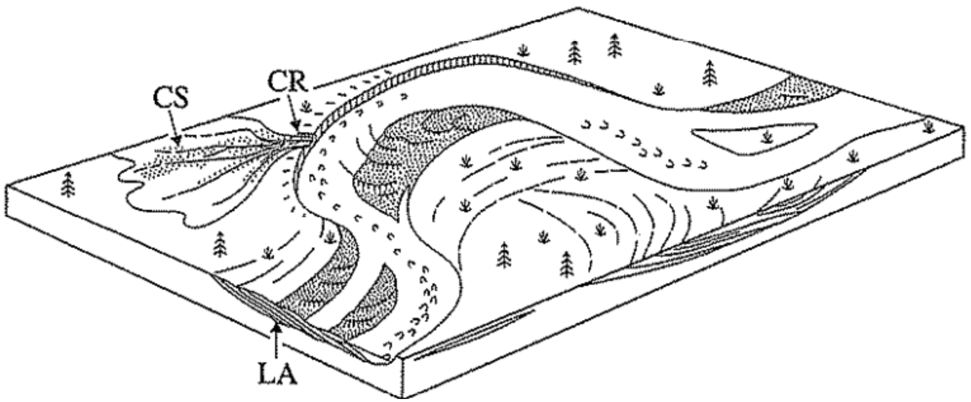

Písčité meandrující systémy

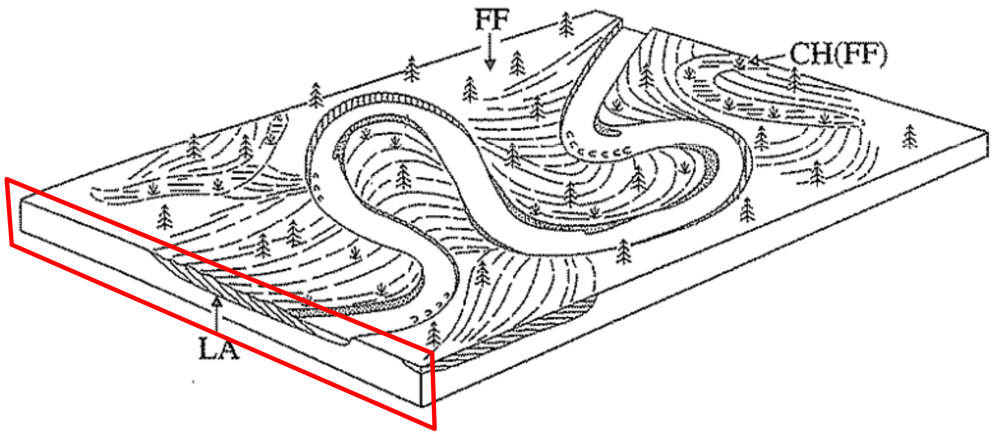

Jemnozrnné meandrující systémy

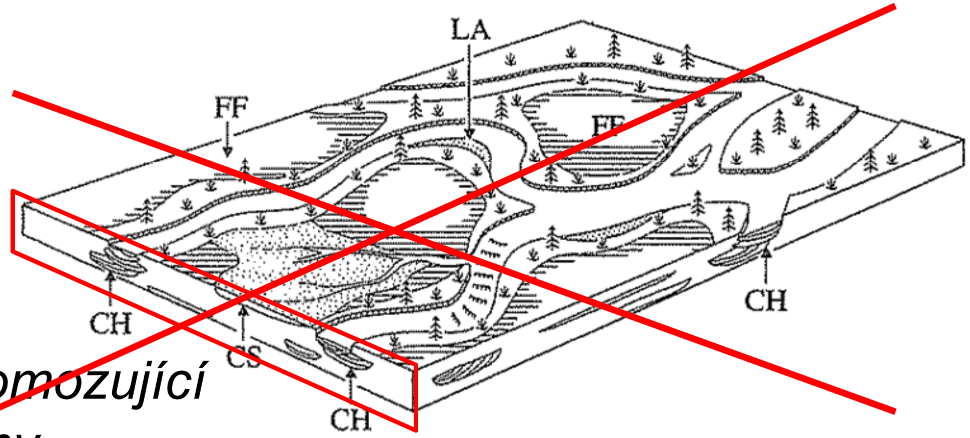

Anastomozující systémy

LA : laterálně akreční tělesa
CR : průvalová koryta
CS : průvalové sedimenty
FF : povodňové sedimenty
CH(FF) : výplně opuštěných koryt

Miall, 1996

^{14}C (AMS) datování

- Rozsah dat: 0,13 – 6,14 kyr BP
- Hloubkový rozsah: 0,76 – 3,3 m, neplatí superpozice
- Shluky dat: laterální pozice, nikoli hloubka
- → neustálá laterální akrece a recyklace holocenního materiálu (mladší atlantik – historická doba)

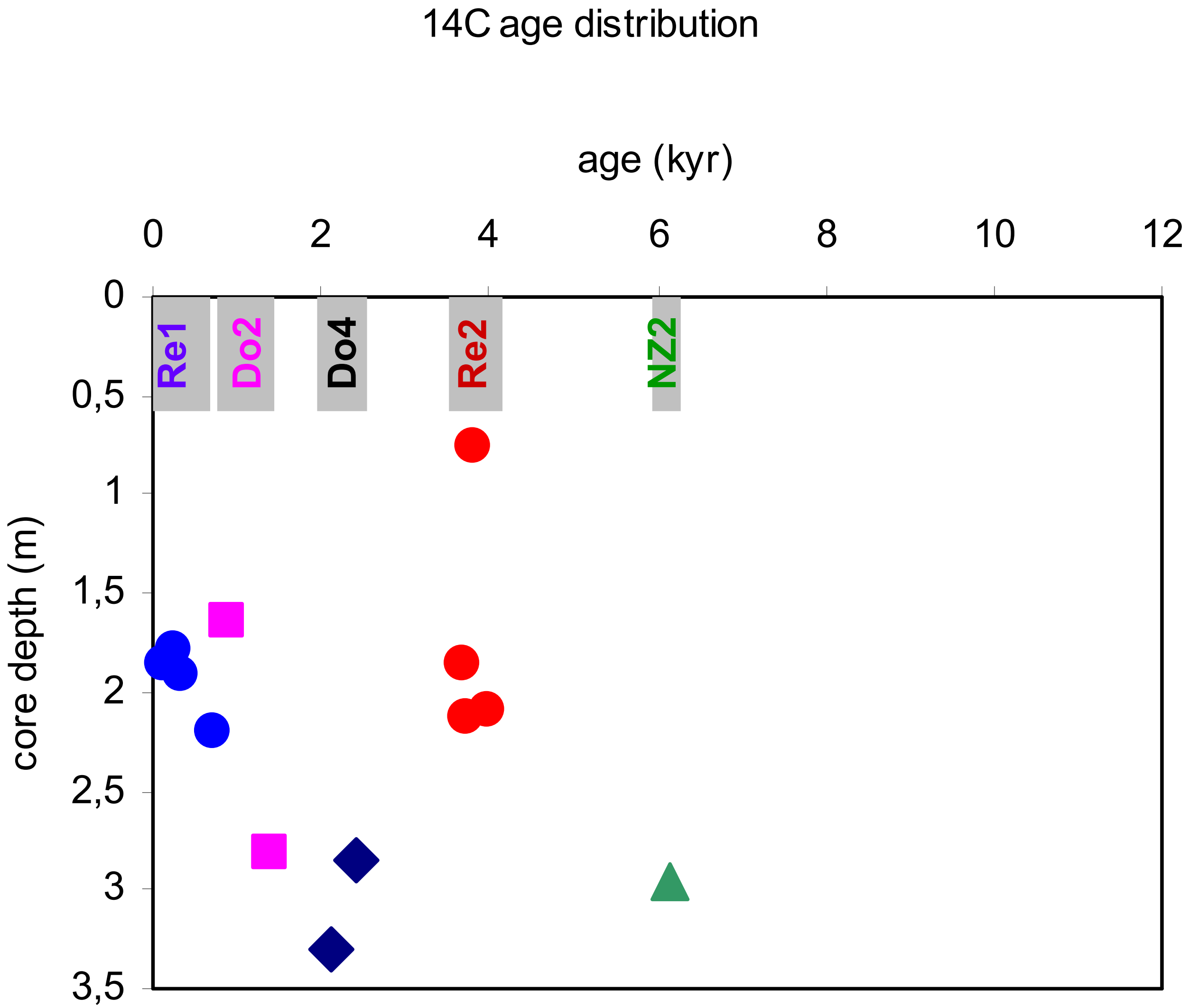

JESKYNNÍ SEDIMENTY

Kras

- Krasové jevy
  - Water reacts with carbon dioxide to form weak carbonic acid which then attacks limestone
    - $H_2O + CO_2 \Rightarrow H_2CO_3 + CaCO_3 \Rightarrow Ca^{++}\ HCO_3^{-}$
- Caves (jeskyně)- natural underground cavities and most common geological product of limestone dissolution
- Speleotémy - spelotherms are deposits on cave surfaces in a variety of forms: travertine, Stalactite, Stalagmite, banded draperies or drip curtains
- Růst speleotémů: depends on the solution and porosity of surface material, climate, topography, and vegetation

Světové rozšíření krasu

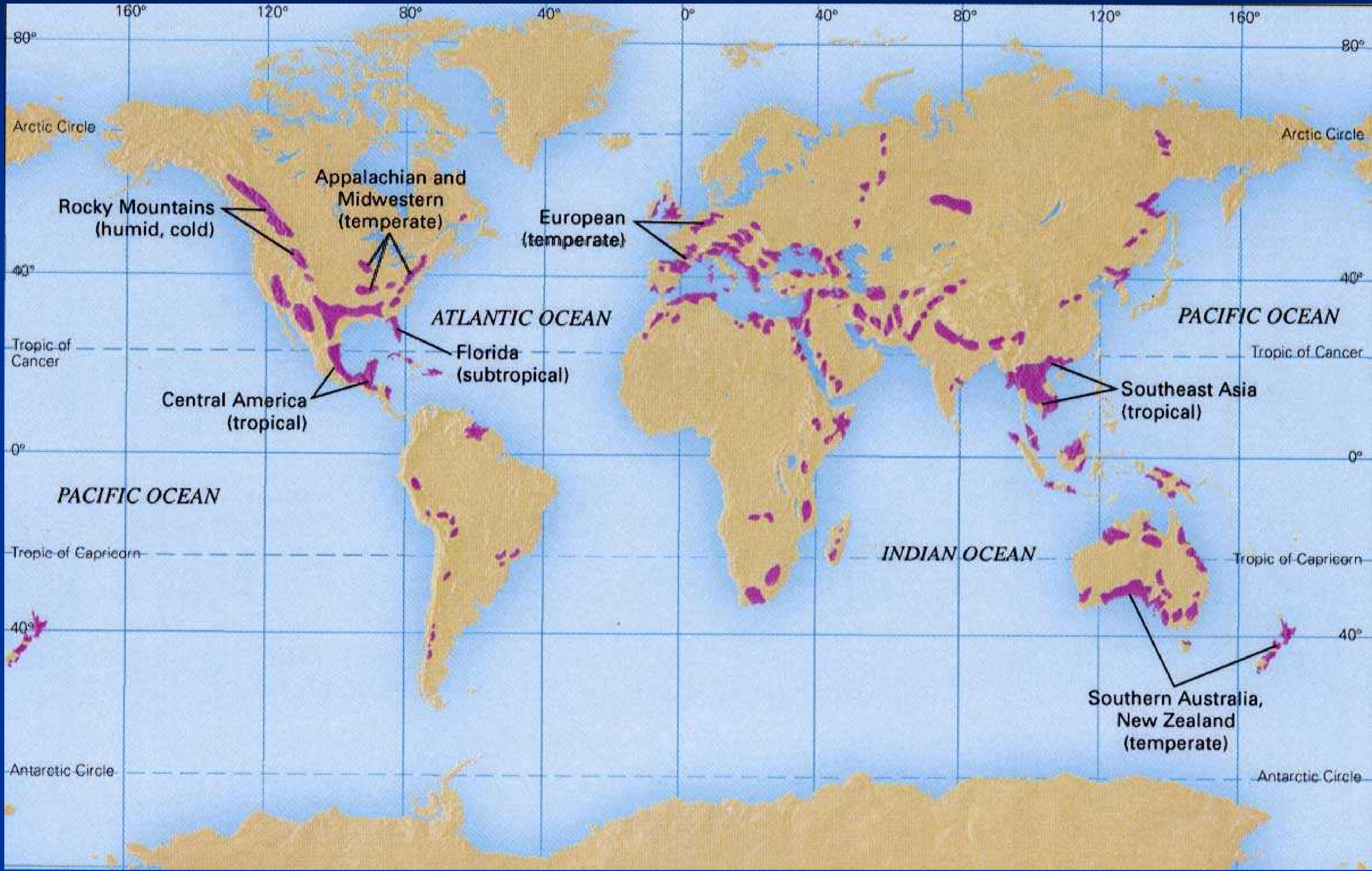

Topografie krasu

Surface expression of the geology of dissolved limestone and work of near surface water

- Cave and Karsts landscapes are extremely sensitive- so need to be protected
- Landform
  - Sinkholes (závrty) -circular surface depression
  - Disappearing Streams (ponory) - flow through sinkholes may emerge as spring several kilometers away
  - Natural Bridge (skalní mosty)- series of neighboring sinkholes expand and join together

Typical landforms associated with karst topography

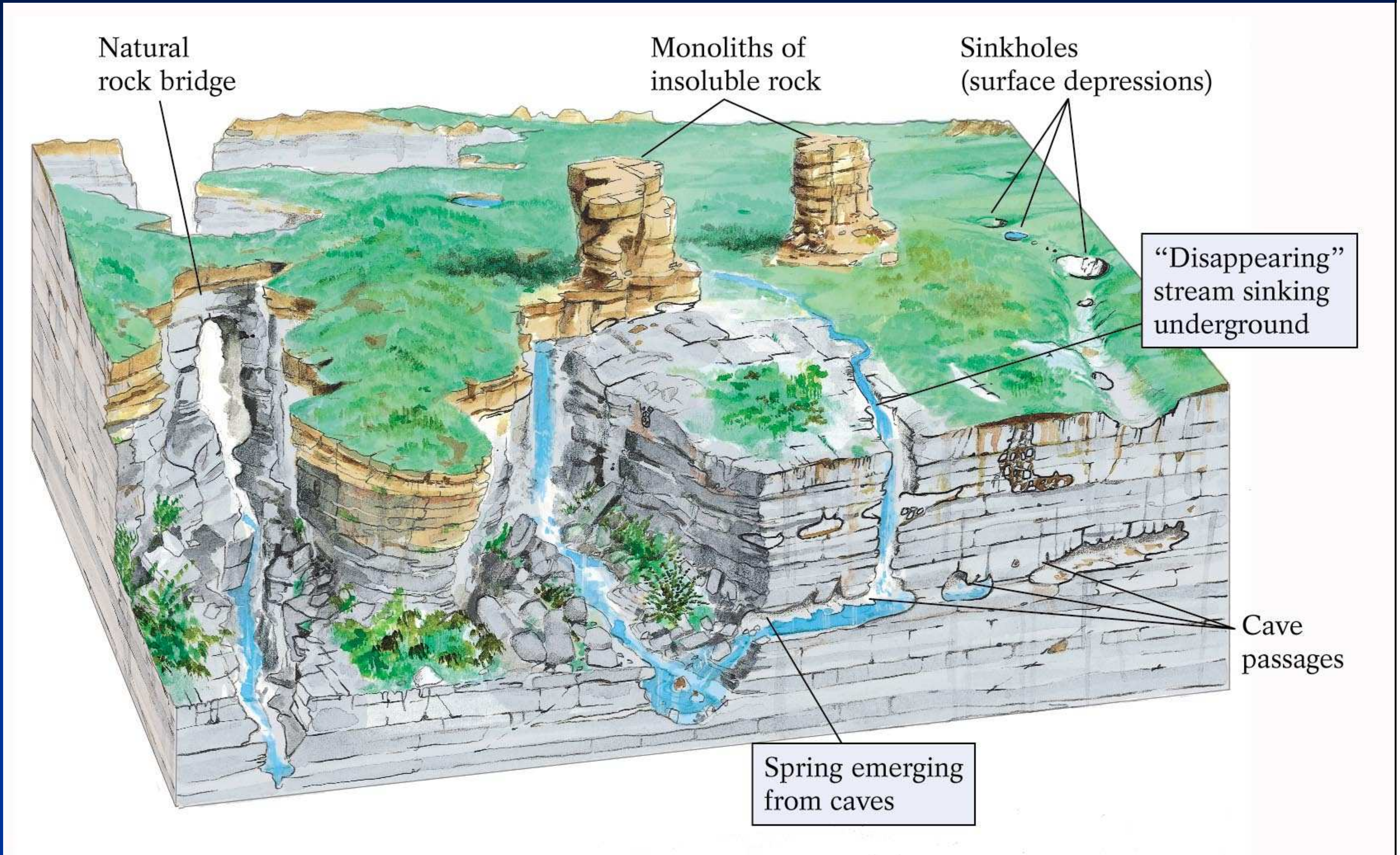

State 1 of cave formation

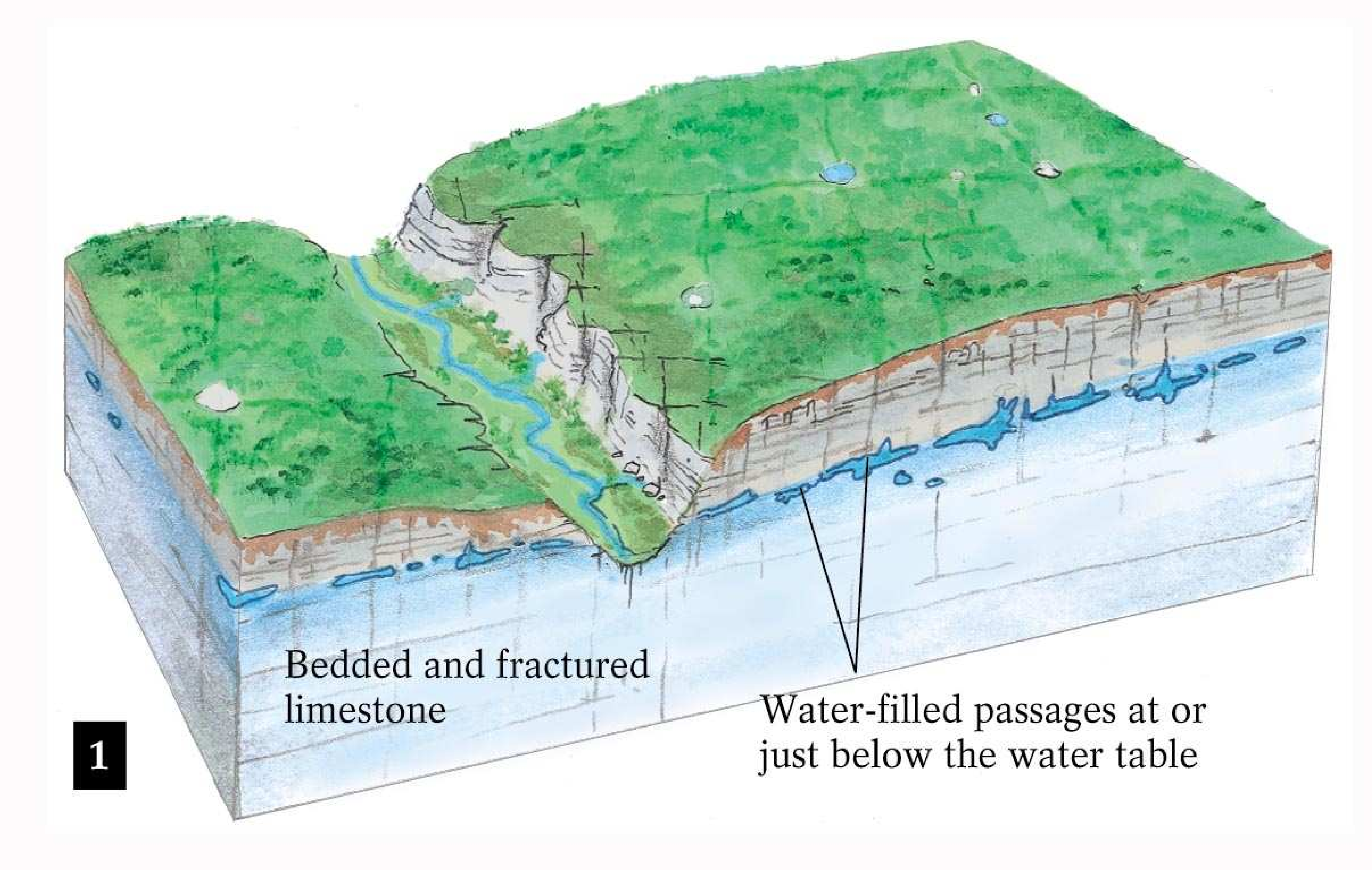

State 2 of Cave formation

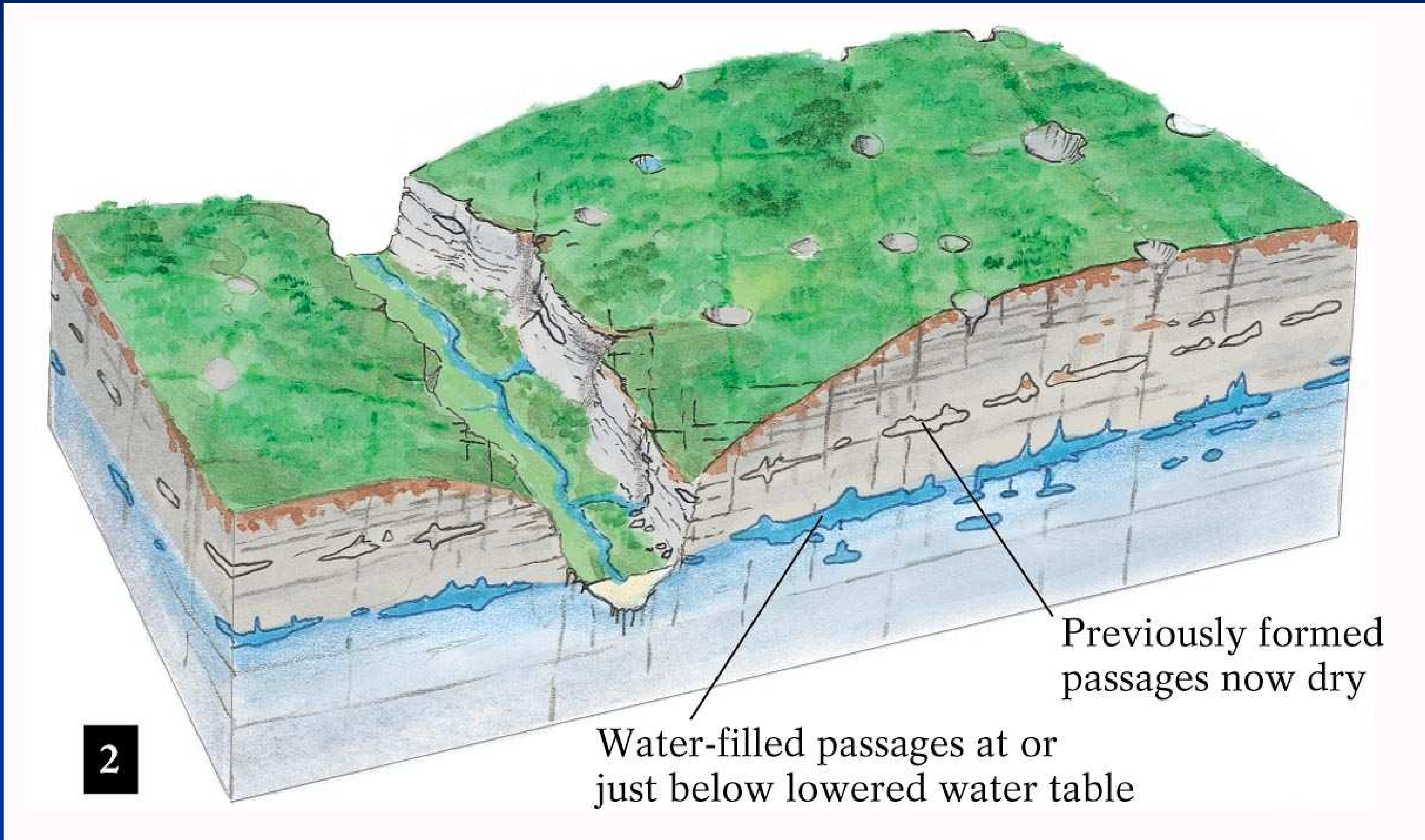

Cave morphology

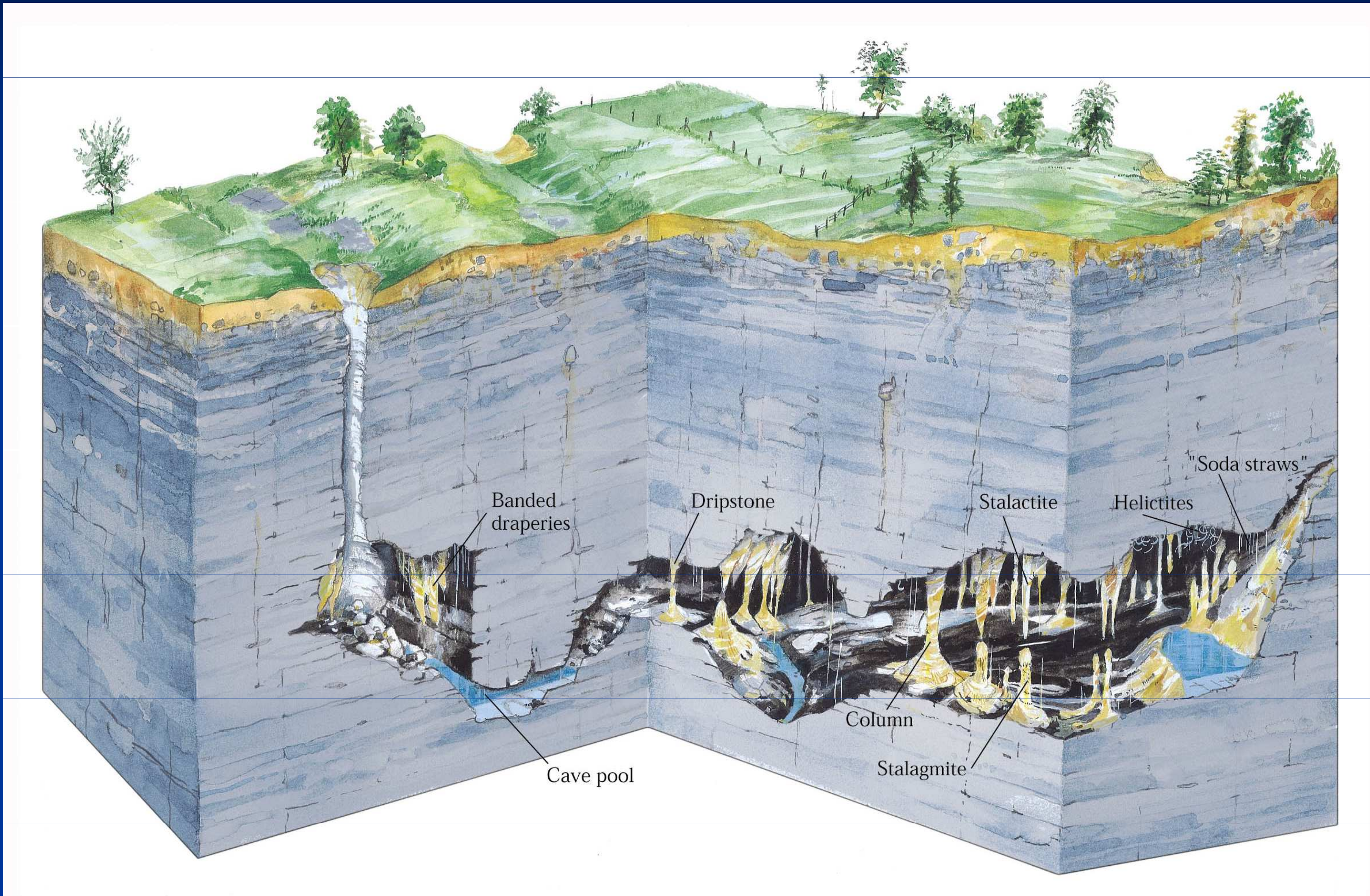

Speleotémy

- Commonly known as stalagmites and stalactites.
- Like trees, speleothems form growth rings that develop over hundreds or thousands of years.
- Growth rate depends on amount and rate of precipitation and on cave temperature and humidity.

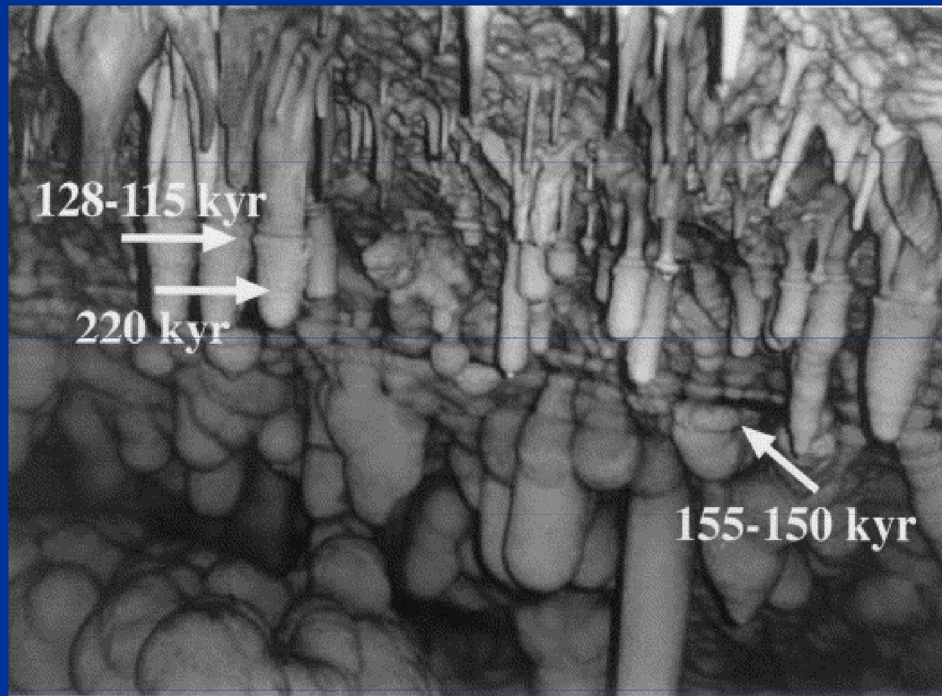

Růst speleotémů a klima

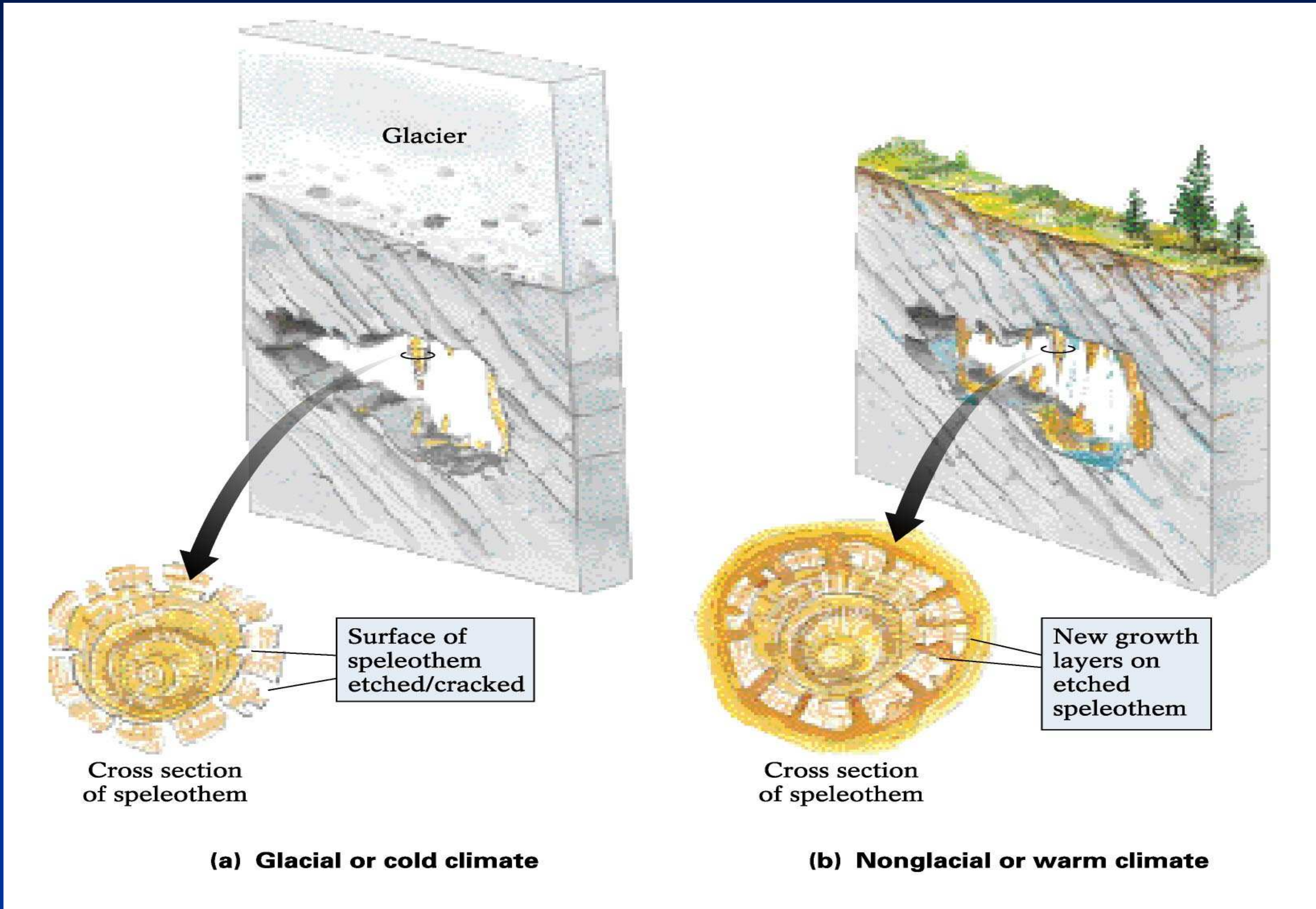

Vzestup a pád mořské hladiny

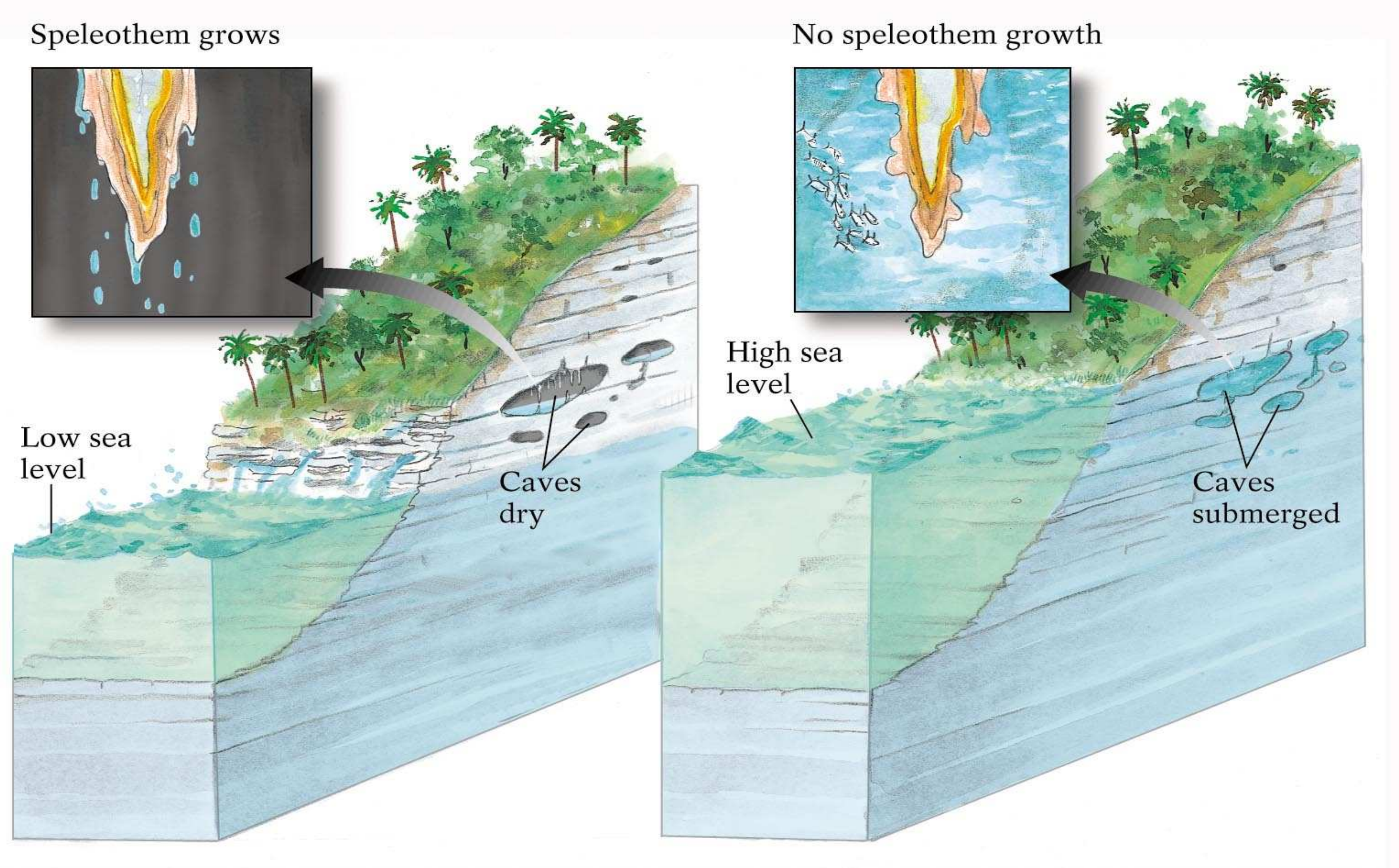

(a) Glacial period **(b) Warm period**

Datování speleotémů

- Dating of speleothems is based on U-Th series.
- Theoretical precision: <1‰ (10 yr in 10 kyr). Realistically, precision is better than 1% (100 yr in 10 kyr).

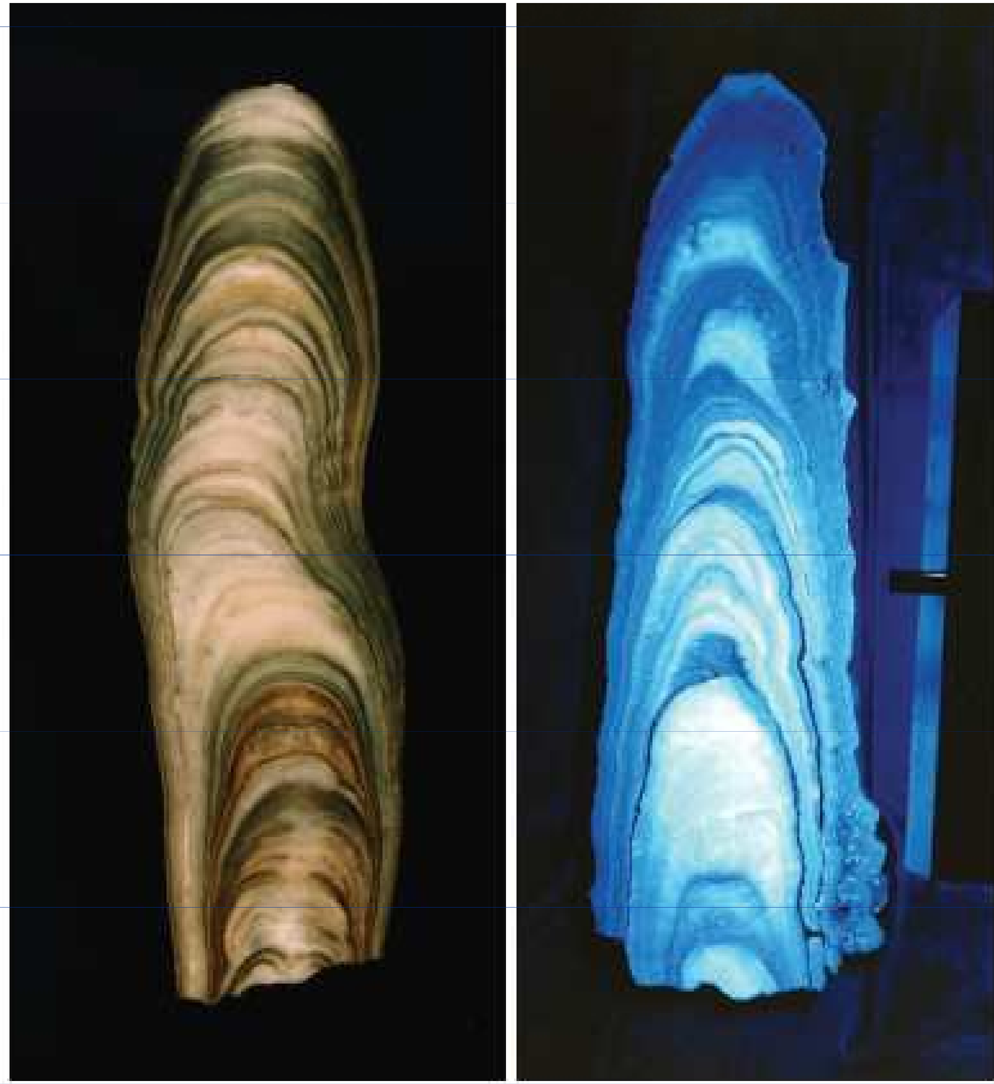

Cross-sections of two stalagmites. Ultra-violet light has been used to illuminate the growth rings in the photo on the right. The two stalagmites are approximately 50 cm long. (Photos: Paul Williams)

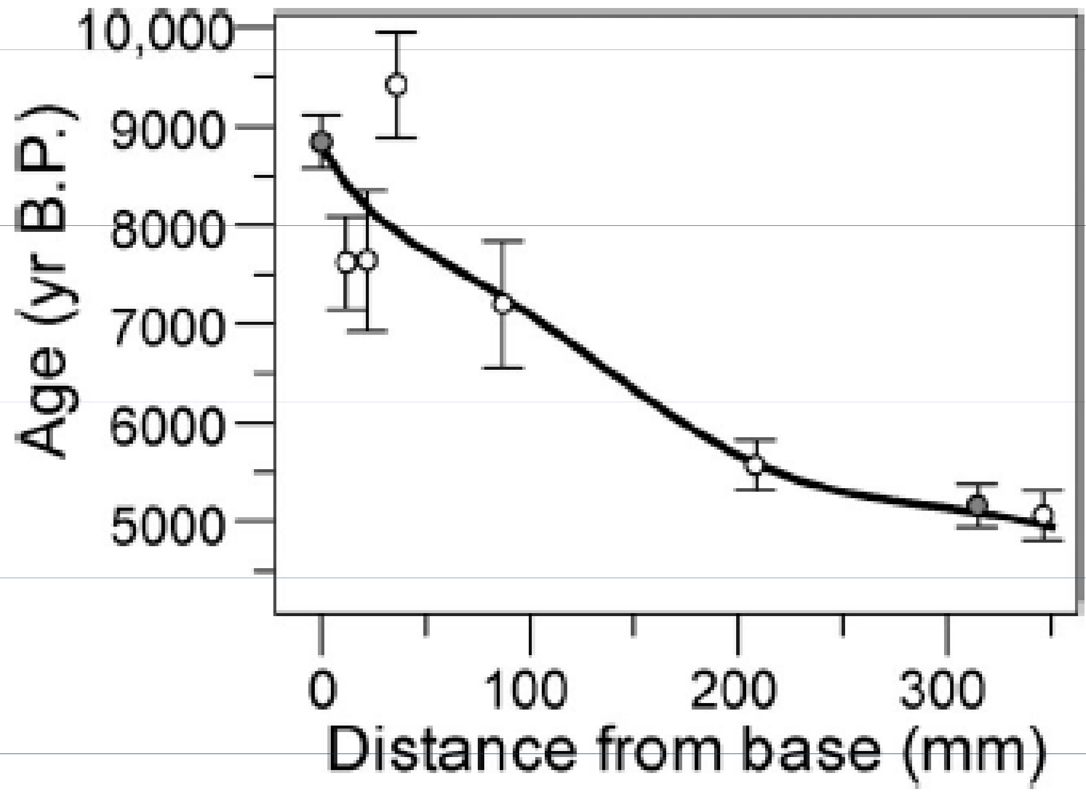

Figure 1. Age vs. depth plot for stalagmite V1. Filled circles are ages derived from three-point isochrons. Solid black line is fifth-order polynomial best-fit age model, visually weighted to most robust age determinations (isochron-based ages and those with smallest error bars).

Lachniet et al., 2004. Costa Rican speleothem.

Speleotémy: použití v paleoklimatologii

- Carbon and oxygen isotopes of calcite reflect vegetation and climate, respectively.
- Growth rate appears to reflect precipitation.
- Recent techniques: Mg/Ca, radiocarbon.

Speleotémy-izotopy kyslíku

- Oxygen isotopes in speleothem calcite ultimately come from rainwater.
- Some researchers argue that oxygen isotope ratios in rainwater depend on temperature.
- Others argue that the isotope ratios depend on rainfall amount, particularly in tropical regions.
- Also, some argue that the isotope ratios depend on evaporation taking place in soils or in the cave.

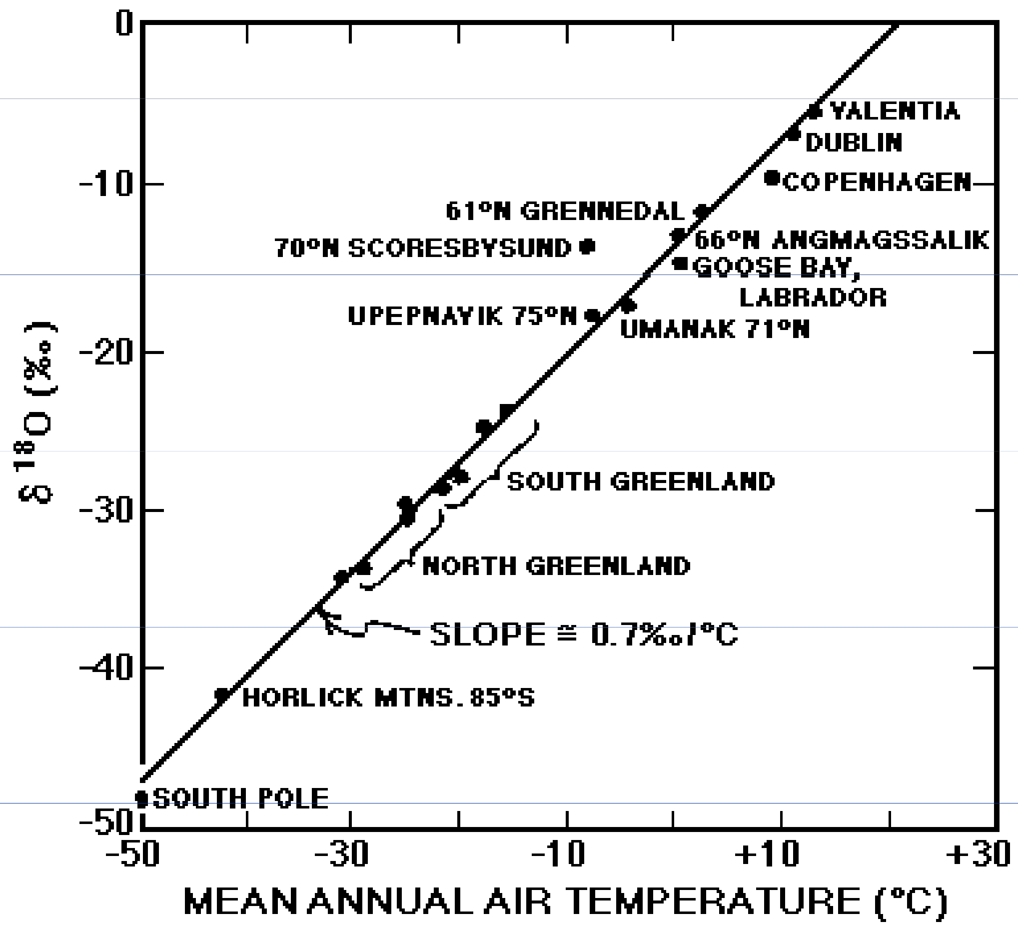

Observed $\delta^{18}O$ in average annual precipitation as a function of mean annual air tamperature (Dansgaard, 1964). Note that all the points on this graph are for high latitudes (>45°). The $\delta^{18}O$ values are calculated as follows:

$$\delta^{18}O = \frac{^{18}O/^{16}O \text{ sample} - {}^{18}O/^{16}O \text{ std.}}{^{18}O/^{16}O \text{ std.}} \times 1000$$

Broecker, W.S. The Glacial World According to Wally,

Speleotémy-izotopy kyslíku

- Colder climate = lower $\delta^{18}O$ values.
- Speleothem $\delta^{18}O$-MAT relationship is ~0.35 per mil/°C.

Coldest

Warmest

~4ºC

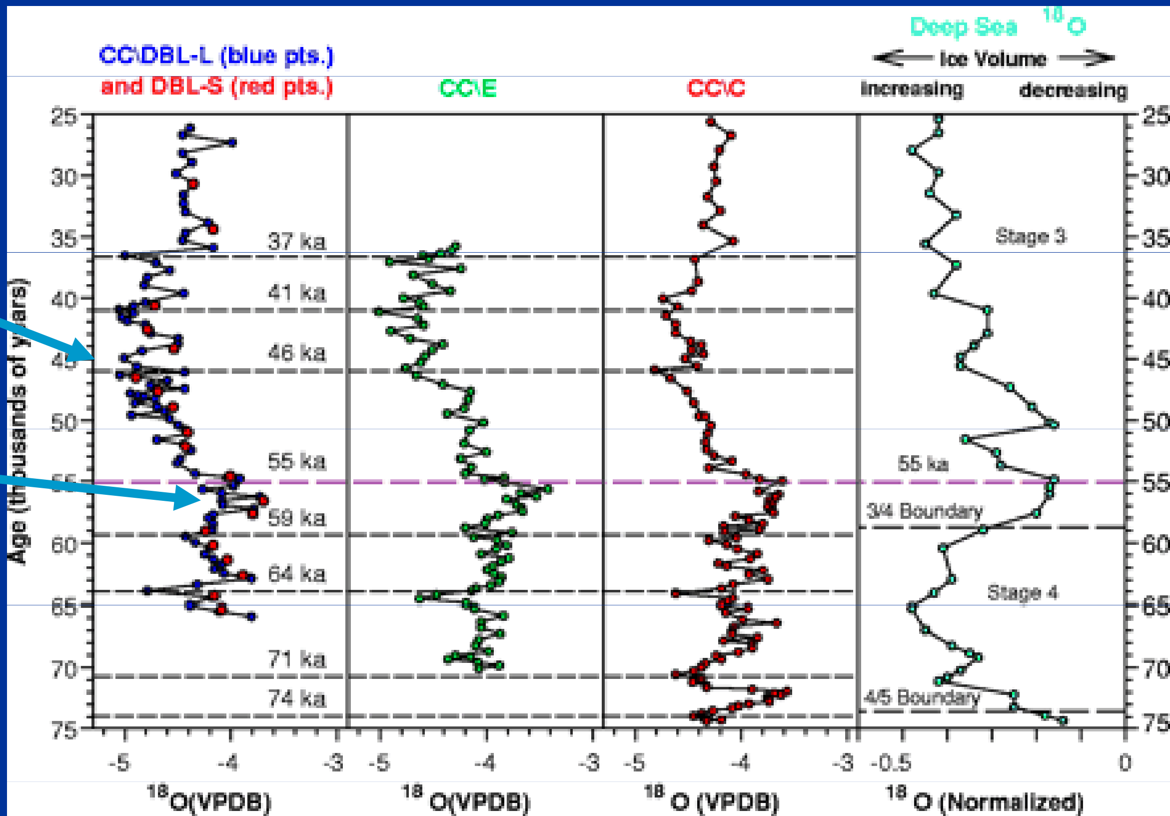

Dorale et al., 1998.

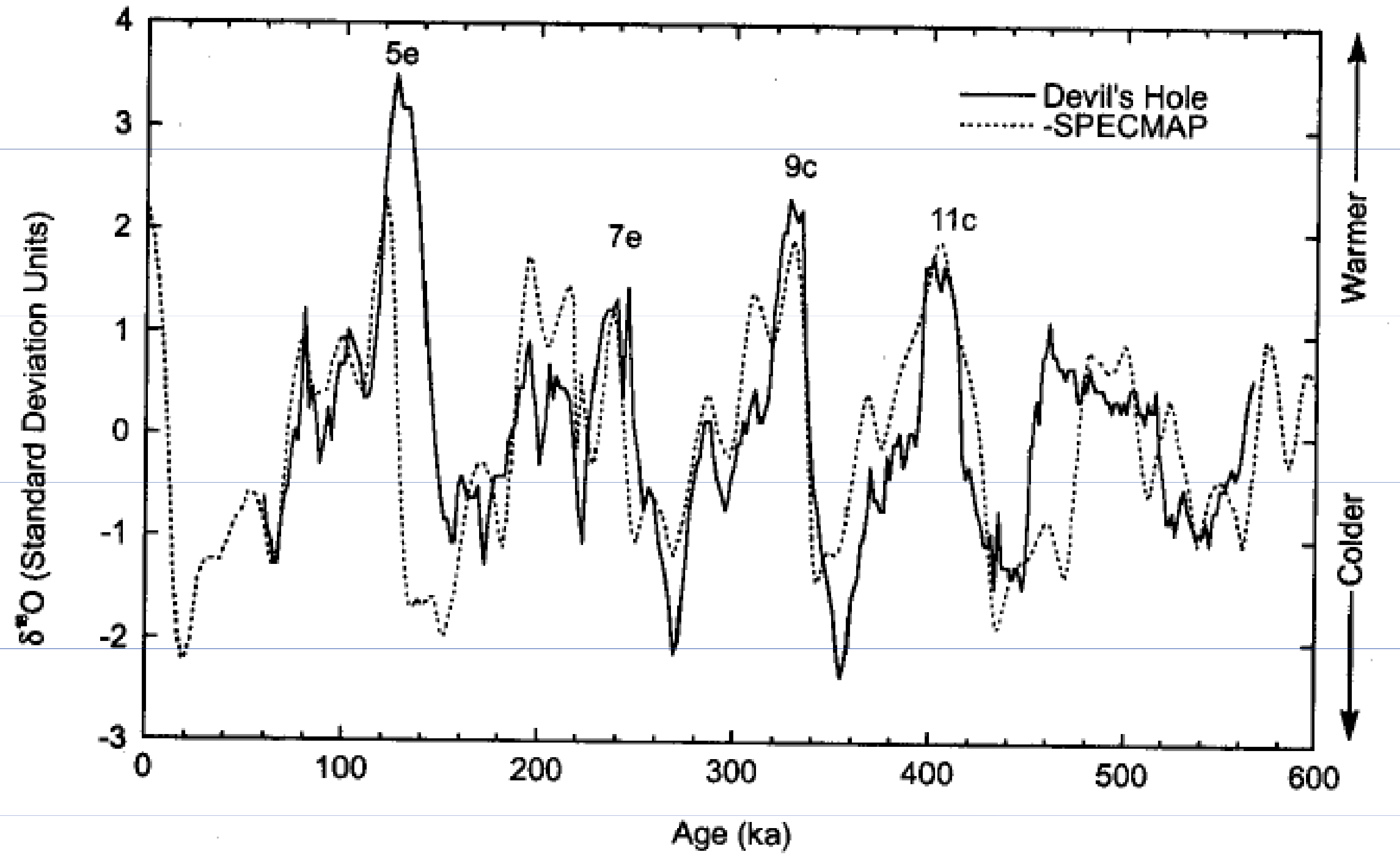

FIGURE 7.32 The $\delta^{18}O_c$ record in a calcite vein from Devil's Hole, Nevada compared to the SPECMAP marine isotope record. Selected marine isotope substages are numbered. Values are expressed as departures from the overall mean of each series, in standard deviation units (computed over the full record). The value of zero thus represents the mean for each record. Note that the sign of the SPECMAP time series has been reversed so that interglaciations appear as peaks (Winograd *et al.*, 1997).

Speleothem-carbon isotopes

- It appears that speleothem carbon isotopes primarily come from plants above the cave.
- Based on photosynthetic pathways, there are two major groups of land plants: C3 and C4 plants.
- **C4 plants**: warm season grasses adapted to high temperatures and relatively drier climates.
- **C3 plants**: Trees, shrubs, and cool season grasses.

Speleothem-carbon isotopes

- C4 grasses show high $\delta^{13}C$ values.
- C3 plants show low $\delta^{13}C$ values.
- Speleothem high $\delta^{13}C$ values are then interpreted to indicate more C4 grasses.

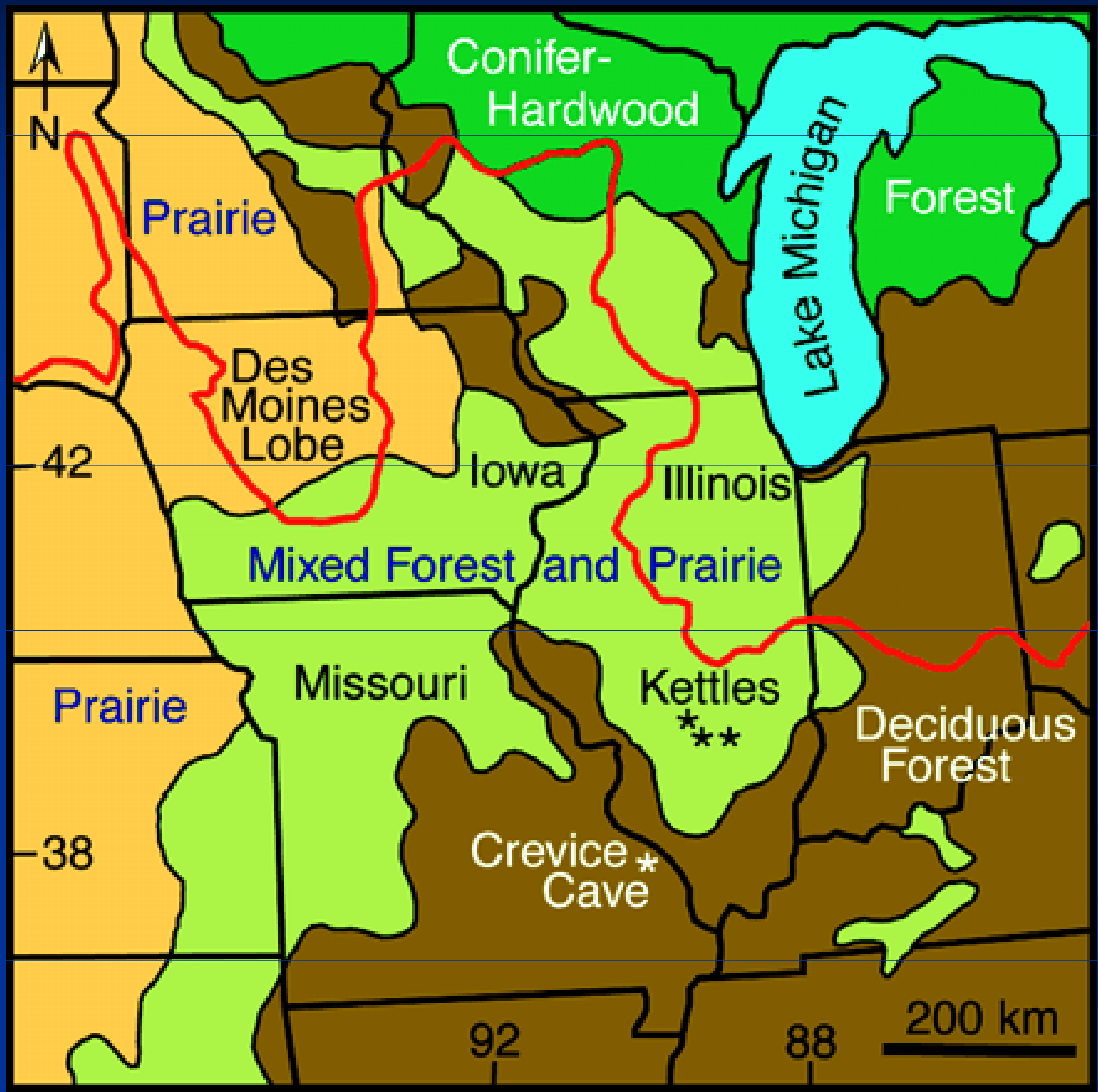

N
Conifer-
Hardwood
Forest
Lake Michigan
Prairie
Des
Moines
Lobe
-42
Iowa
Illinois
Mixed Forest and Prairie
Missouri
Kettles
Prairie
Deciduous
Forest
-38
Crevice
Cave
92
88
200 km

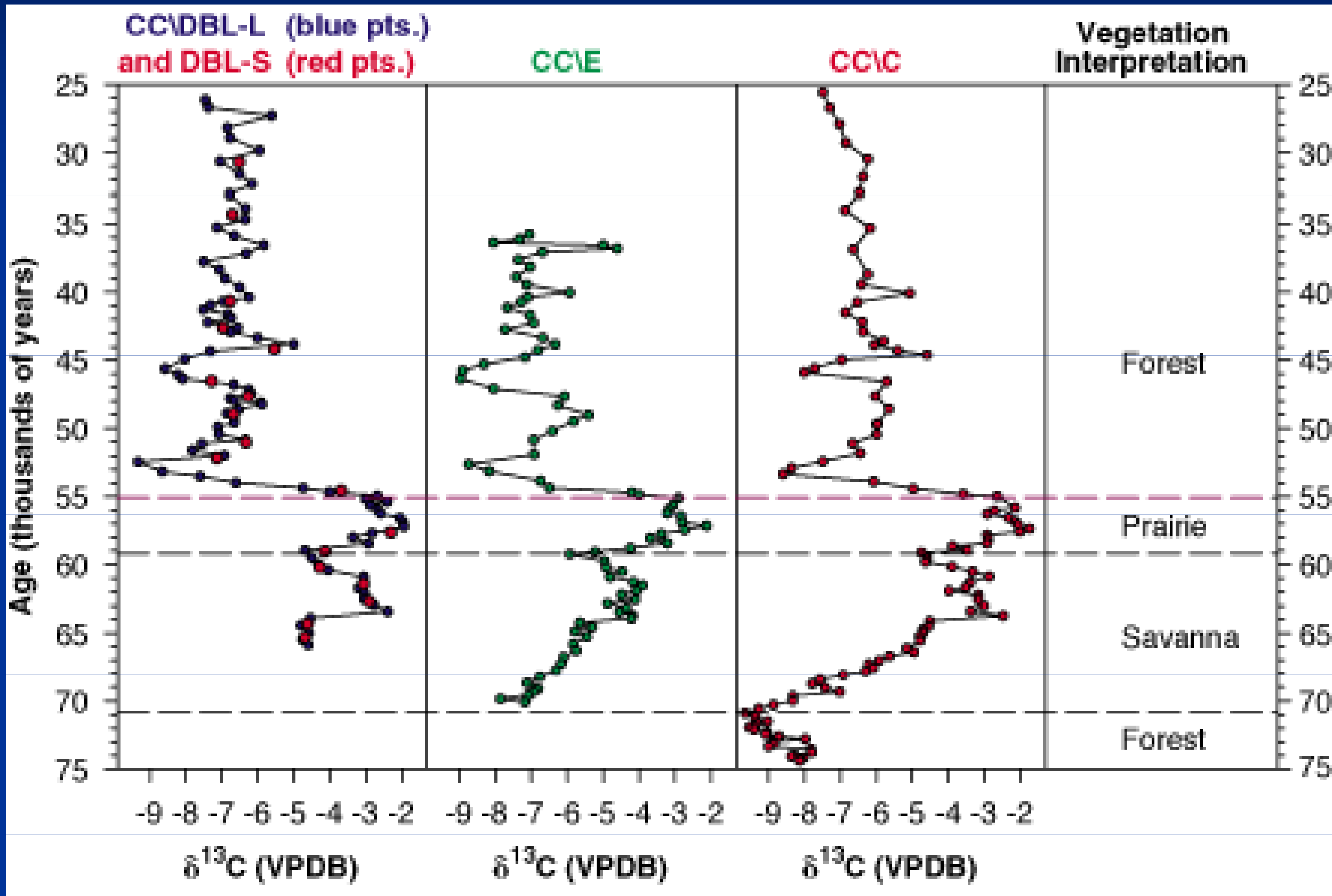

Crevice Cave, MO (Dorale et al., 1998)

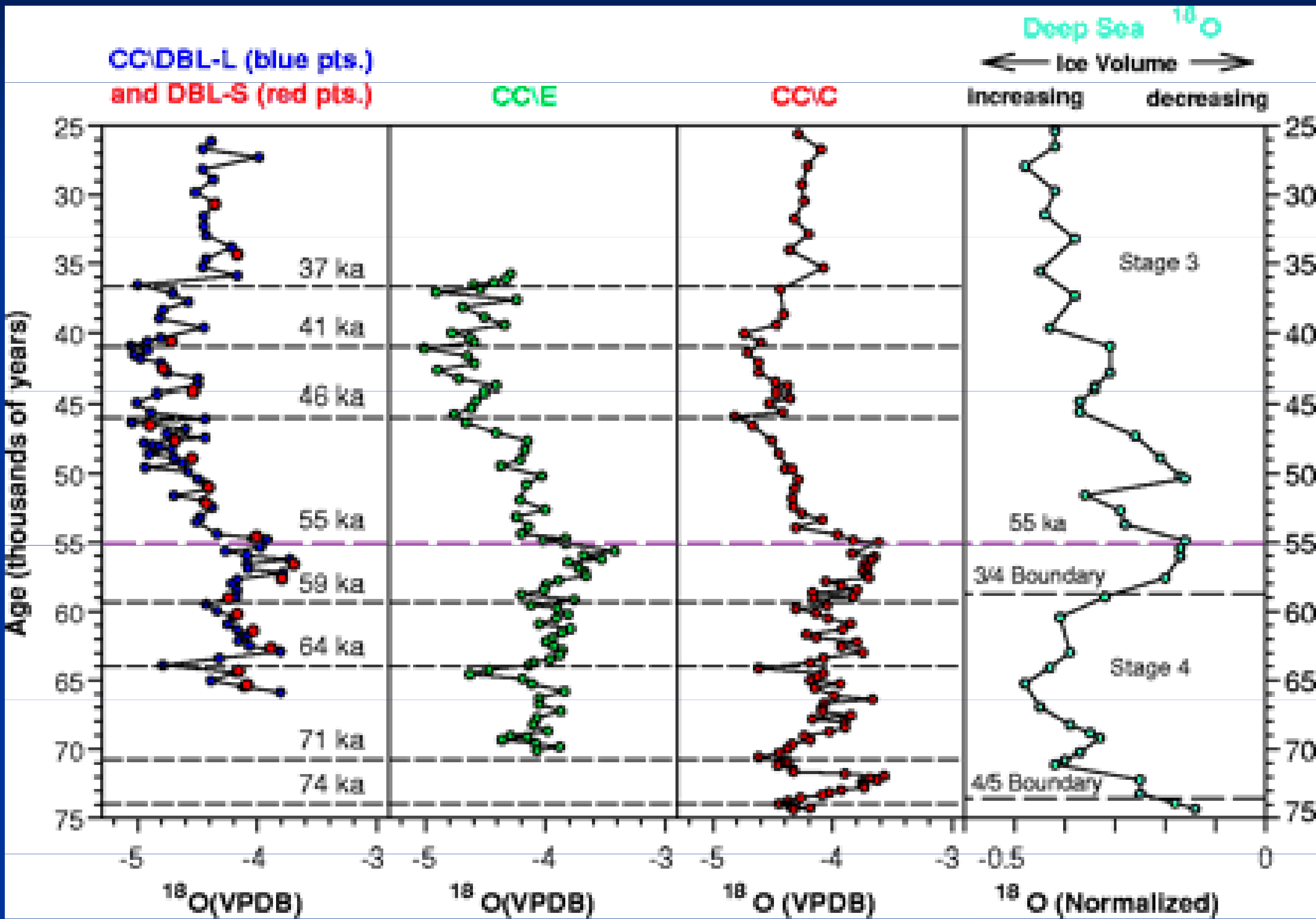

Crevice Cave, MO (Dorale et al., 1998)

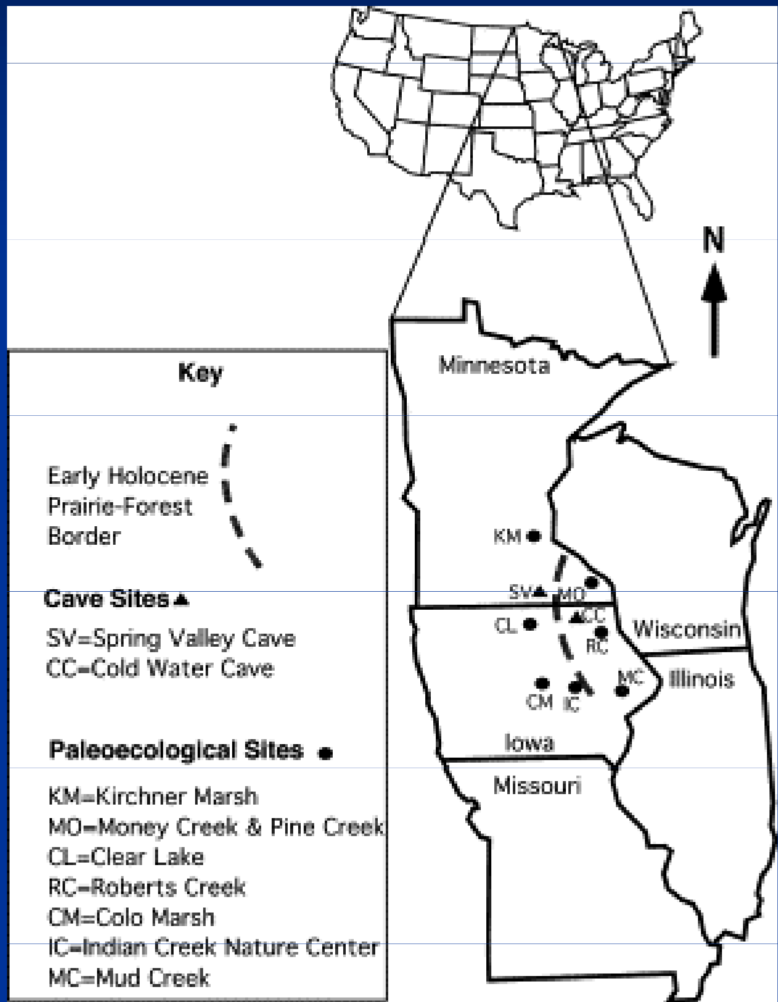
N
Minnesota
Key
Early Holocene
Prairie-Forest
Border
KM
SV
MO
CC
CL
RC
Wisconsin
Illinois
MC
CM
IC
Iowa
Missouri
Cave Sites
SV=Spring Valley Cave
CC=Cold Water Cave
Paleoecological Sites
KM=Kirchner Marsh
MO=Money Creek & Pine Creek
CL=Clear Lake
RC=Roberts Creek
CM=Colo Marsh
IC=Indian Creek Nature Center
MC=Mud Creek

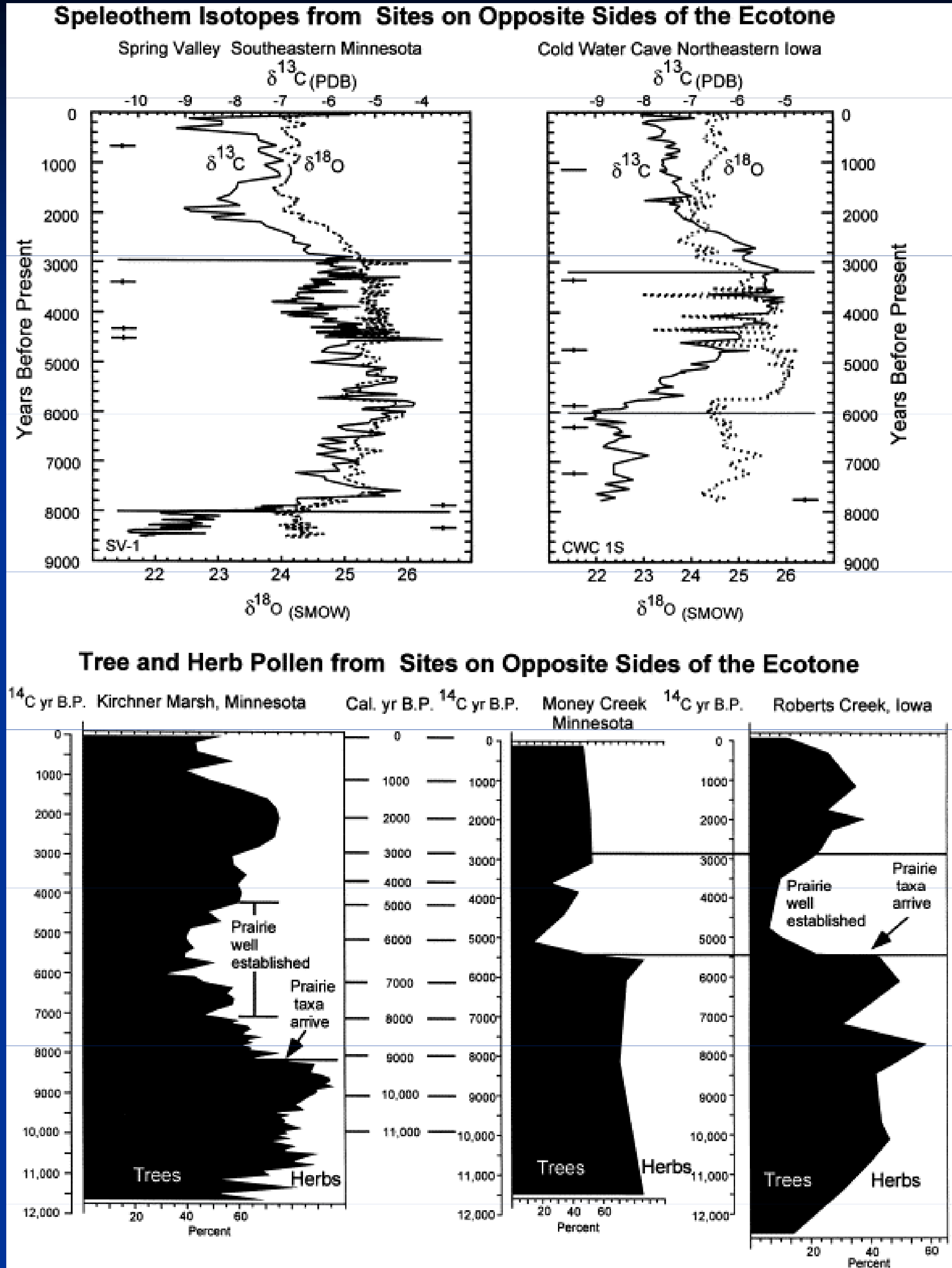

Speleothem Isotopes from Sites on Opposite Sides of the Ecotone
Spring Valley Southeastern Minnesota
Cold Water Cave Northeastern Iowa
δ13C (PDB)
δ13C
δ18O
Years Before Present
SV-1
CWC 1S
δ18O (SMOW)
Tree and Herb Pollen from Sites on Opposite Sides of the Ecotone
14C yr B.P.
Kirchner Marsh, Minnesota
Cal. yr B.P.
Money Creek Minnesota
Roberts Creek, Iowa
Prairie well established
Prairie taxa arrive
Trees
Herbs
Percent

SVAHOVÉ SEDIMENTY

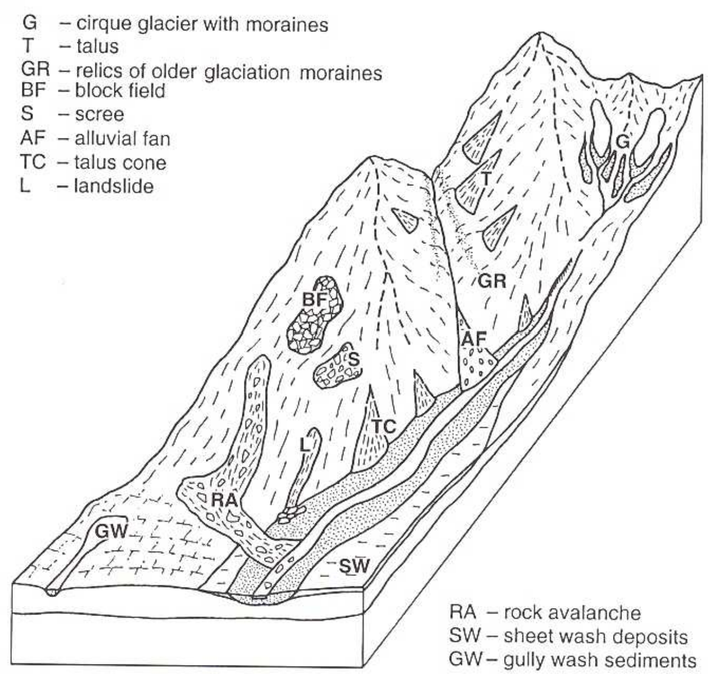

Figure 35. Types of deposits in mountain and hill landscape (SELBY 1994, modified).

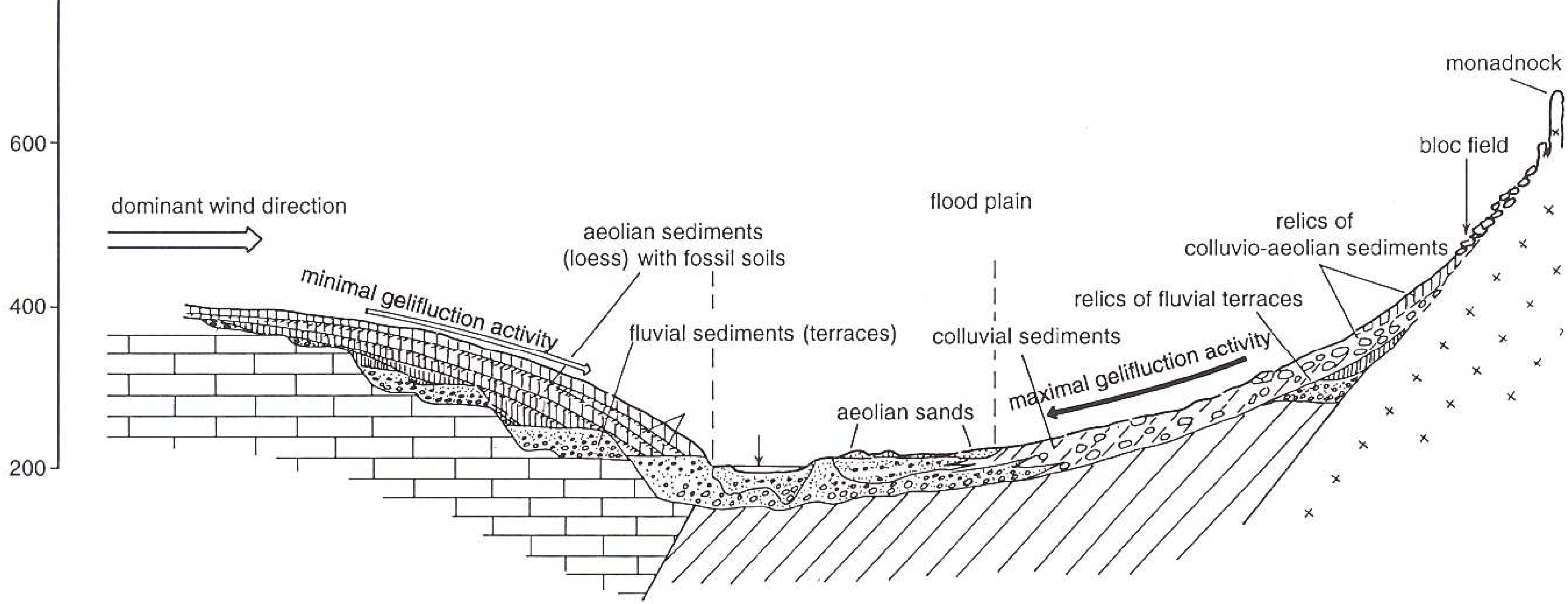

Kamenná moře

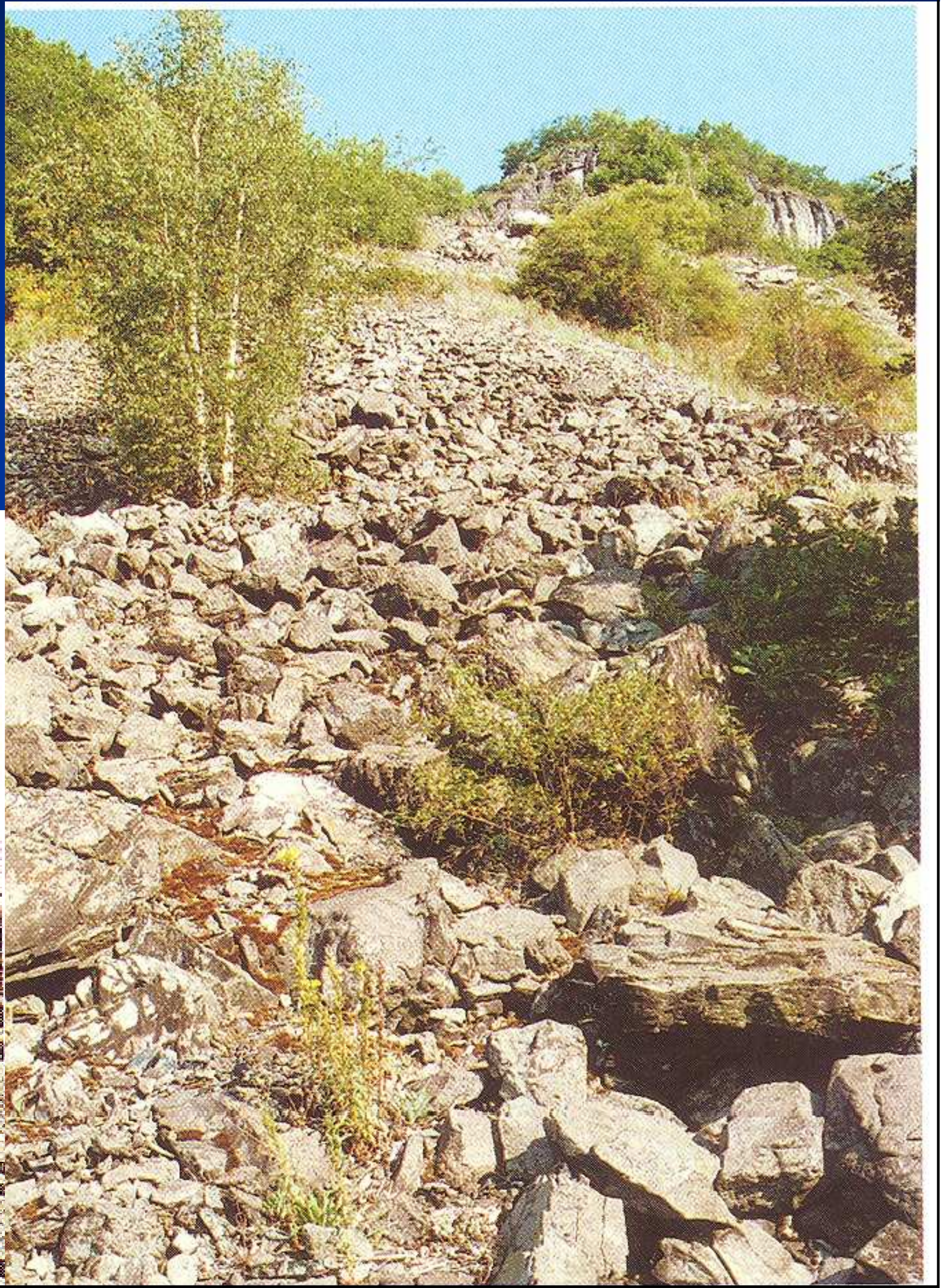

Sesuvy (debris flows), deluvia

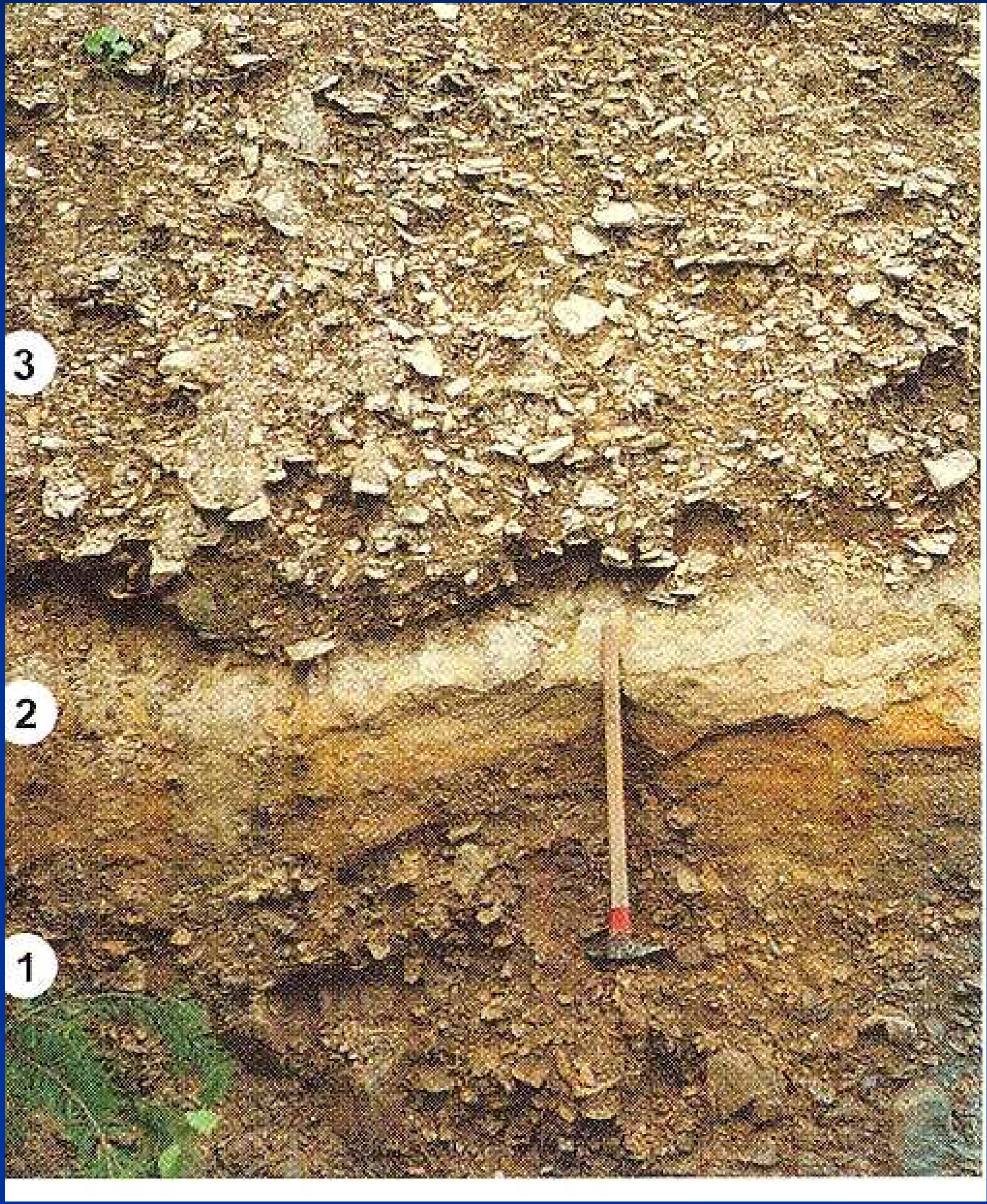

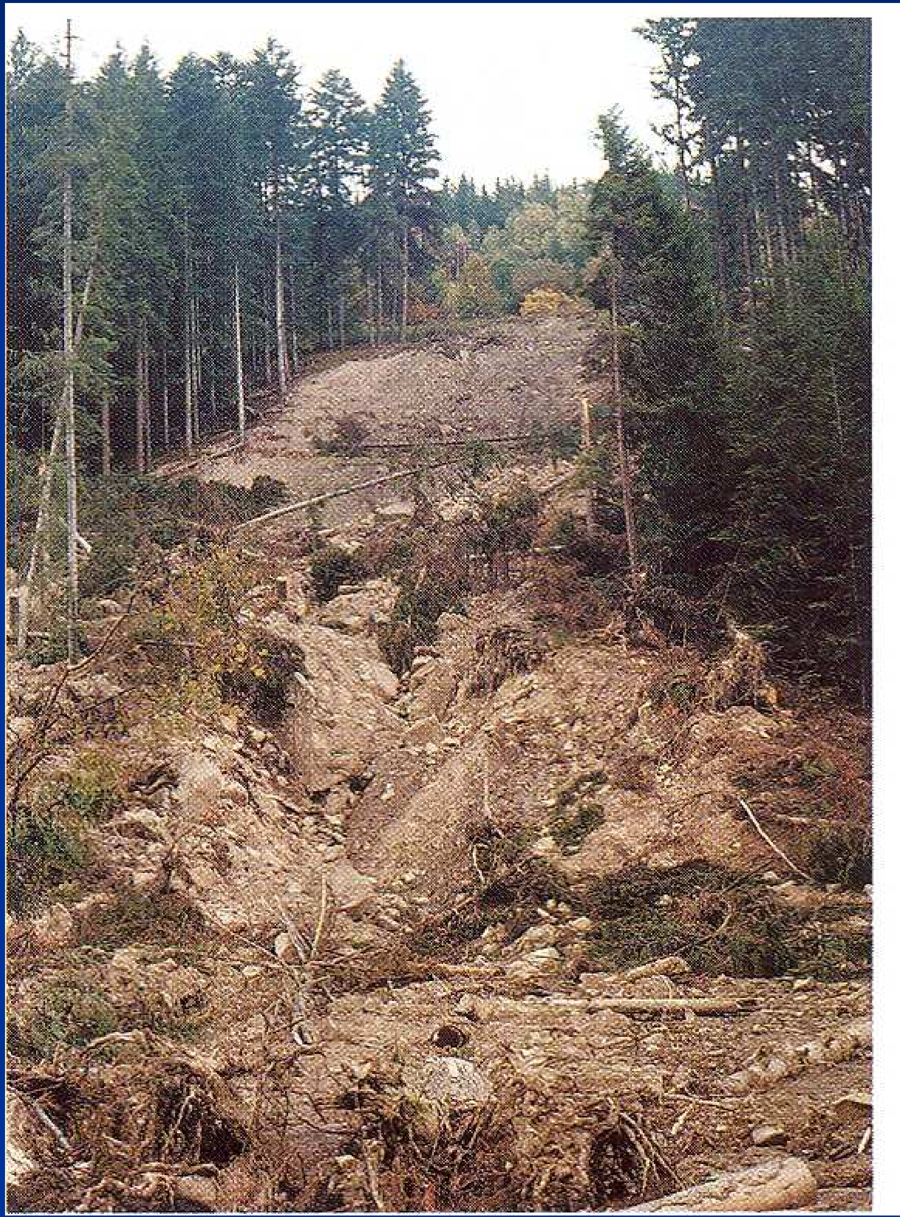

Soliflukce

254. Gravitational creep gelifluction sediment
Coarse sand (totally disintegrated syenite porphyry) with "floating" stones and blocks of less weathered parent rock; the gelifluction process is marked by stratification with distinct planes of discontinuity
Stratigraphy: Pleistocene
Locality: Bošice (Prachatice District)
Photo by: M. Růžička 1997

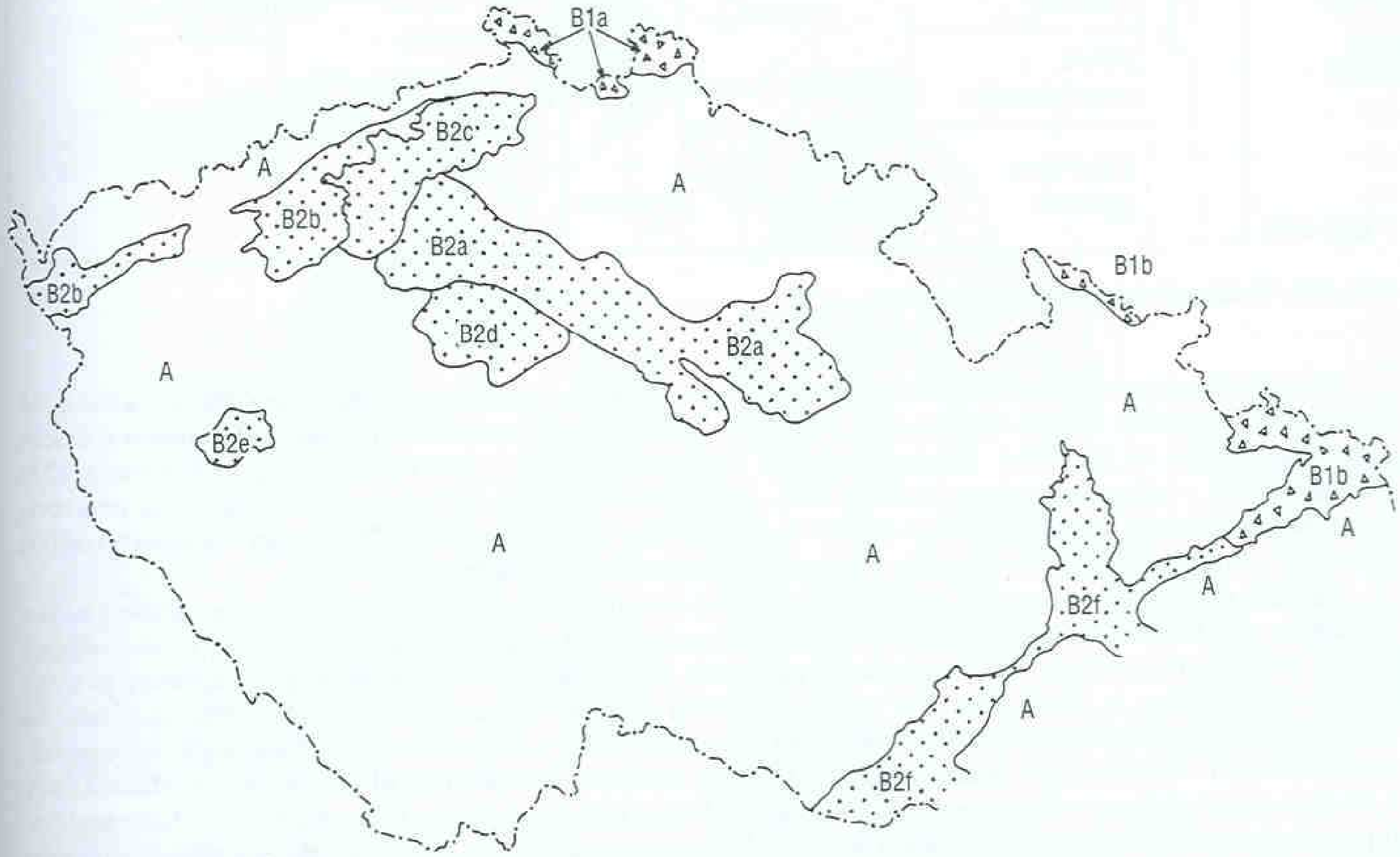

Obr. 262. Kvartér Českého masivu. A – denudační oblasti; B – akumulační oblasti: B1a – oblast kontinentálního zalednění severních Čech, B1b – oblast oderská. Extraglaciální oblasti: B2a – Polabí, B2b – podkrušnohorské pánve, B2c – České středohoří, B2d – Pražská plošina, B2e – Plzeňská kotlina, B2f – moravské úvaly (podle usnesení Čs. stratigrafické komise, J. Tyráček – M. Růžička 1992).